



Departament d'Enginyeria Química
Escola Tècnica Superior d'Enginyeria Química
Universitat Rovira i Virgili

**ELECTROCHEMICALLY CONTROLLED PATTERNING FOR
BIOSENSOR ARRAYS**

Dondapati Srujan Kumar
Tarragona, 2006

IOANNIS KATAKIS, Professor titular del Departament d'Enginyeria Química de la Universitat Rovira I Virgili

FAIG CONSTAR

que el present treball que porta el títol

ELECTROCHEMICALLY CONTROLLED PATTERNING FOR BIOSENSOR
ARRAYS

Que presenta en DONDAPATI SRUJAN KUMAR per optar al grau de Doctor en Enginyeria Química, ha estat realitzat sota la seva direcció en els laboratoris del Departament d'Enginyeria Química de la Universitat Rovira i Virgili, i que tots els resultats presentats i la seva anàlisi són fruit de la investigació realitzada per l'esmentada doctoranda.

I per a que se'n prengui coneixement i tingui els efectes que corpongui signo aquesta certificació.

Tarragona, 9 de Novembre de 2006

Dr. Ioannis Katakis
Professor Titular d'Universitat

Acknowledgements

I am pleased to take this opportunity to thank many people who made this thesis possible.

Firstly, and most importantly, I would like to thank Prof.Dr.Ioanis Katakis for giving me the opportunity to pursue my PhD thesis in his research group. His wide range of support, as well as his guidance, while giving me full responsibility of my research, was of invaluable significance to me. The many fruitful discussions, his critical suggestions, encouraging talks and ideas and his generous support during the course of my work here is greatly appreciated.

I would like to acknowledge my gratitude for the financial support provided by the European union quality of life and management of resources program DISSARM Project(QLK2-CT-2000-00765) and the European union competitive and sustainable growth program MICROPROTEIN project(G5RD-CT-2002-00744), without which this study has not been carried out.

Dr.Josep Maria Montornes for his support in the synthesis of polymers, electroactive substrates and other organic materials.

Dr.Pablo Lozano Sanchez for his valuable interesting discussions, scientific advisory.

A grateful acknowledgement to the Department of Chemical Engineering , Universitat Rovira i Virgili for financial support.

I would like to thank the people in Demokritos, NCSR for allowing to perform protein patterning experiments.

Thanks to Frank Jeyson, Guray Guven, Kelly Bricenko, Monica Mir, Mireia, Paula Pescador, Viviana Duarte for their support thorough out my work and also members of the past and present, for making our lab an enjoyable, multilingual, and interesting place to work.

Finally thanks to my family members especially my wife Mrs. Padmarupa Kothapalli and my mother for their moral support even during the tough times.

Table of contents

Chapter 1. Introduction	1
1.1. Biosensor arrays	1
1.1.1. Definition of biosensors	1
1.1.2. Types of biosensor arrays	2
1.2. Technologies involved in Array development	7
1.2.1. Probe immobilization	7
1.2.2 . Arraying	10
1.2.3. Methods of Detection	16
1.2.3.1. Label free methods	16
1.2.3.2. Using labelled analytes	19
1.3. Electrochemical and Electrophoretic patterning	21
1.3.1. Electrodeposition of colloidal gold	21
1.3.1.1 What is colloidal gold?	21
1.3.1.2. Why colloidal gold ?	21
1.3.1.3. Stability of Au nanoparticle suspensions	23
1.3.1.4. Electrophoretic deposition theory	25
1.3.1.5. Electrodeposition in biosensor development	27
1.3. 2. Electrochemically controlled patterning methods for biosensor arrays	30
1.3.2.1. Electrochemical switching for biomolecule patterning	30
1.3.2.2. Electrodesorption for biomolecule patterning	31
1.3.2.3. Electropolymerisation for selective protein and DNA conjugation	31
1.3.2.4. Electrochemical addressing for patterning of biomolecules	31
1.4. Organization of the thesis	33
1.5. Abbreviations	35
1.6. References	35
Chapter 2. Preparation and characterization of biofunctionalized gold nanoparticles	40
2.1. Abstract	40
2. 2. Introduction	40
2.3. Experimental	43
2.3.1. Apparatus	43
2.3.2. Materials	43
2.3.3. Synthesis of Au nanoparticles and characterization	43
2.3.4. Preparation of biofunctionalized nanoconjugates	44

2.3.4.1. Bionanoconjugates based on gold-thiol interactions.....	44
2.3.4.1.1. Thiolation of enzymes.....	45
2.3.4.1.1.1. SATA method of thiolation.....	45
2.3.4.1.1.2. Thiolation using carbodiimide chemistry.....	46
2.3.4.1.1.3. Thiolation of enzymes through bi-phase separation using DTSP.....	47
2.3.4.1.1.4. Assaying of thiolated enzyme activity.....	47
2.3.4.1.2. Preparation of enzyme conjugated gold nanoparticles.....	48
2.3.4.2. Bionanoconjugates based on steric interactions.....	48
2.3.4.2.1. Preparation of BSA modified Au nanoparticles.....	48
2.3.4.3. Bionanoconjugates based on electrostatic interactions.....	49
2.3.4.3.1. Layer-by-layer modification of the Au nanoparticles with redox polymer / enzyme / redox polymer.....	49
2.3.5. Characterization of gold colloids.....	50
2.3.6. Characterisation & stability studies of BSA modified Au nanoparticles.....	51
2.3.7. Characterization & stability studies of layer-by-layer modification of gold nanoparticles with redox polymer and enzymes.....	51
2.3.7.1. Characterization & stability of redox polymer modified Au nanoparticles.....	51
2.3.7.2. Characterisation of layer-by-layer modified redox polymer / enzyme / redox polymer Au nanoparticles.....	51
2.4. Results and Discussion.....	52
2.4.1. Synthesis of colloidal particles.....	52
2.4.2. Thiolation of enzymes.....	54
2.4.3. Characterisation of HRP-Au nanoconjugates.....	55
2.4.4. Effect of pH on the Zeta potential of BSA modified Au nanoparticles.....	56
2.4.5. Stability of redox polymer modified Au nanoparticles with pH.....	57
2.4.6. UV-Visible characterization of Layer-by-Layer modified Au / RP / GOX / RP particles.....	58
2.4.7. Zeta Potential Characterization of Au / RP 2 / GOX / RP 2 particles.....	59
2.5. Conclusions.....	61
2.6. Abbreviations.....	61
2.7. References.....	62
Chapter 3. Electrodeposition of functionalised Au nanoparticles.....	64
3.1. Abstract.....	64
3.2. Introduction.....	64
3.3. Experimental.....	66

3.3.1. Materials	66
3.3.2. Instrumentation	66
3.3.3. Electrodeposition of BSA modified Au nanoparticles	66
3.3.4. Electrodeposition of redox polymer modified Au nanoparticles.....	68
3.3.5. Electrodeposition of HRP-Au nanoparticles	68
3.3.6. Electrodeposition of GOX-Au nanoparticles	69
3.4. Results and Discussion	69
3.4.1. Effect of BSA on electrodeposition	69
3.4.2. Effect of potential on electrodeposition	70
3.4.3. Electrodeposition of redox polymer modified Au nanoparticles.....	78
3.4.4. Electrodeposition of enzyme-modified Au nanoparticles.....	84
3.5. Conclusions	87
3.6. Abbreviations	88
3.7. References	88

Chapter 4. Selective immobilization of biofunctionalized gold nanoparticles

through selective electrodeposition	89
4.1. Abstract.....	89
4.2. Introduction	89
4.3. Experimental	92
4.3.1. Materials	92
4.3.2. Instrumentation	93
4.3.2.1. Interdigitated microelectrodes	93
4.3.3. Methodology	93
4.3.3.1. Patterning of enzymes by site-selective electrodeposition through electrochemical desorption of thioctic acid esters	93
4.3.3.1.2. Selective electrodeposition of gold nanoparticles modified with enzyme and redox polymer on an interdigitated array.....	94
4.3.3.1.3. Electrochemical Characterisation of the IDE array.....	96
4.3.3.1.4. Amperometric measurements of the IDE array.....	96
4.3.3.2. Controlled electrodeposition of layer-by-layer modified gold nanoparticles with redox polymer and enzyme and redox polymer.....	96
4.3.3.2.1. Electrochemical conditions	97
4.3.3.2.2. Influence of electrodeposition potential on the glucose response	98
4.3.3.2.3. Influence of time on the glucose response	99
4.3.3.2.4. Influence of outer redox layering on the glucose response.....	99

4.3.3.2.5. Influence of type of potential on the glucose response	99
4.3.3.2.6. Influence of electrode geometry on glucose response	99
4.4. Results & Discussion	100
4.4.1. Patterning of enzymes by site-selective electrodeposition.....	100
4.4.2. Optimisation of electrode construction and transduction.....	107
4.5. Conclusions	116
4.6. Abbreviations	117
4.7. References	118
Chapter 5. Site-directed immobilization of proteins through electrochemical deprotection on electroactive self-assembled monolayers	120
5.1. Abstract.....	120
5.2. Introduction	120
5.3. Experimental	123
5.3.1. Materials	123
5.3.2. Instrumentation	123
5.3.3. Methods	124
5.3.3.1. Synthesis of electroactive thioctic acid esters.....	124
5.3.3.2. Preparation of the electrode.....	125
5.3.3.3. Characterisation of the benzo 1,3 dioxinol modified electrode	126
5.3.3.4. Electrochemical impedance spectroscopy	126
5.3.3.5. Electrochemical surface plasmon resonance (ESPR) measurements.....	127
5.4. Results and discussion	127
5.4.1. Electrochemical activation of SAMs	127
5.4.2. Electrochemical anodic desorption of TEG-thioctic acid esters.....	128
5.4.3. Electrochemical properties of modified electrodes	130
5.4.4. Patterning efficiency verification through surface plasmon resonance measurements	133
5.4.5. Functionality of patterned proteins.....	134
5.5. Conclusions	136
5.6. Abbreviations	137
5.7. References	137
Chapter 6 : Selective Electrodeposition of Viologen Functionalised Biomolecules	139
6.1. Abstract.....	139
6.2 . Introduction	139
6.3. Experimental	141

6.3.1. Instrumentation	141
6.3.2. Reagents	141
6.3.3. Preparation of the electrode	142
6.3.4. Synthesis of 4,4'-bipyridinium derivatives.....	142
6.3.4.1. N-methyl-4-(4'-pyridyl)pyridinium iodide (1).....	143
6.3.4.2. N-methyl-N'-(ω -carboxypentyl)-4,4'-bipyridinium salt (2).....	143
6.3.5. Electrochemical Characterisation of 4,4'-bipyridinium carboxylic acid.....	143
6.3.6. Conjugation of HRP conjugated 4,4'-bipyridinium carboxylic acid.....	144
6.3.7. UV-Vis and Electrochemical characterization of HRP functionalised 4,4'-bipyridinium carboxylic acid.....	144
6.3.8. Selectivity of HRP immobilization on on Au electrode electrodes.....	144
6.3.9. Electrochemical Quartz Crystal Microbalance (EQCM) studies	146
6.4. Results and Discussion	146
6.4.1. Characterisation of Electroactive immobilisation vehicles.....	146
6.4.2. Directed electrode modification of 4,4'-bipyridinium carboxylic acid and HRP patterning	150
6.4.3. EQCM measurement of the HRP-4,4'-bipyridinium deposition.....	153
6.5. Conclusions	155
6.6. Abbreviations	156
6.7. References	156
Chapter 7. Selective Microscale Protein Patterning through Photolithography	157
7.1. Abstract.....	157
7.2. Introduction	157
7.3. Experimental	160
7.3.1. Materials.....	160
7.3.2. Instrumentation	160
7.3.3. Methodology	161
7.3.3.1. Optimization of protein patterning method on macroelectrodes.....	161
7.3.3.2. Optimization of non-specific response	163
7.3.3.3. Patterning of proteins on interdigitated array	165
7.3.3.4. Electrochemical characterization of the IDE.....	167
7.3.3.5. Amperometric measurements of modified IDE.....	168
7.4. Results and Discussion	168
7.4.1. Optimisation of enzyme immobilization strategy Immobilization strategy	168

7.4.2. Optimisation of non-specific response.....	170
7.4.3. Electrochemical characterisation of the modified IDE array after GOX + RP immobilization on the IDE 1.....	172
7.4.4. Electrochemical characterization of the IDE after polyelectrolyte self-assembling on the IDE 1.....	174
7.4.5. Electrochemical Characterization of the IDE array after SOX + redox polymer immobilization on the IDE 2.....	176
7.4.6. Protein patterning with SOX + redox polymer on the IDE 1 and GOX + redox polymer on the IDE 2.....	178
7.4.6.1. Amperometric response from the IDE array after immobilization of the enzymes.....	178
7.4.7. Assessment of cross talk.....	180
7.5. Conclusions.....	182
7.6. Abbreviations.....	182
7.7. References.....	183
Chapter 8. Conclusions and Future work.....	186
Curriculum Vitae.....	190

Resumen

Existe una demanda creciente de dispositivos de análisis multianálisis, con aplicaciones potenciales en los campos de la biomedicina y biotecnología, así como en el ámbito industrial y ambiental. Para el desarrollo de estos dispositivos resulta esencial un buen control espacial durante la etapa de inmovilización de las biomoléculas de interés; cada una de ellas debe ser depositada de forma precisa sobre la superficie del sensor (por ejemplo, un transductor amperométrico), evitando solapamientos que puedan comprometer la especificidad del sistema.

El objetivo de esta tesis es desarrollar diferentes métodos de *patterning* para la inmovilización selectiva de biomoléculas. El primer método consiste en la electrodeposición selectiva de nanopartículas de oro biofuncionalizadas para el desarrollo de biochips. Se trata de un método de *patterning* controlado electroquímicamente, en el que las nanopartículas de oro se modifican en primer lugar recubriéndolas con diversos enzimas y a continuación se electrodepositan selectivamente sobre la superficie de un electrodo. Como parte de esta metodología, se prepararon nanopartículas de oro biofuncionalizadas utilizando tres estrategias diferentes: a través del enlace dativo oro-tiol, por adsorción directa o mediante interacción electrostática siguiendo la técnica *layer-by-layer* (capa por capa). Para la funcionalización de las nanopartículas de oro se emplearon distintas biomoléculas, como los enzimas peroxidasa de rábano (HRP), glucosa oxidasa (GOX) y albúmina de suero bovino (BSA), y finalmente oligonucleótidos modificados con moléculas fluorescentes y grupos tiol. Las nanopartículas biofuncionalizadas fueron caracterizadas mediante técnicas de espectroscopía UV-visible, microscopía electrónica de transmisión (TEM) y medida del potencial zeta. Mediante espectroscopía UV-visible se observó un pico de resonancia de plasmón característico de las nanopartículas modificadas, relacionado con la estabilidad de la preparación. La medida del potencial zeta permitió la caracterización de las nanopartículas de oro modificadas capa por capa con polímero redox y enzimas. También se estudiaron los cambios en el potencial zeta de nanopartículas modificadas con BSA a distintos valores de pH. Tras la preparación de las partículas biofuncionalizadas, se llevaron a cabo estudios fundamentales de electrodeposición de nanopartículas de oro modificadas con BSA y un polímero redox, con el fin de analizar el efecto de varios parámetros: potencial aplicado, tiempo de

deposición, distancia entre los electrodos, superficie del electrodo auxiliar y pH del medio. Para estudiar el comportamiento electrocatalítico de las nanopartículas modificadas una vez electrodepositadas, se llevaron a cabo experimentos utilizando coloides de oro modificados con HRP y GOX. A continuación se empleó esta metodología para el desarrollo de biochips, utilizando dos configuraciones diferentes. En la primera, se electrodepositaron nanopartículas de oro funcionalizadas con GOX y HRP y modificadas con un polímero redox sobre la superficie de un chip de electrodos interdigitados (IDE), consiguiendo eliminar por completo las repuestas no específicas. En la segunda configuración, las partículas se modificaron con una capa adicional de polímero redox, comprobando de nuevo la ausencia total de respuestas no específicas después de la electrodeposición. Este método de *patterning* es genérico y puede utilizarse para la producción de diversos biochips.

El segundo método de *patterning* también está basado en el control electroquímico, y consiste en la modificación de los electrodos con monocapas autoensambladas electroactivas cuya funcionalidad es modulable en función del potencial aplicado. En esta metodología, la monocapa electroactiva contiene grupos acetal que pueden ser desprotegidos selectivamente mediante la aplicación de un potencial en zonas específicas de la superficie del electrodo. De esta manera quedan expuestos en la superficie grupos aldehído activos, que pueden ser fácilmente conjugados con aminas primarias presentes en las biomoléculas de interés. Los enzimas GOX y HRP se usaron como proteínas modelo para comprobar la versatilidad de esta técnica. Su aplicabilidad para la fabricación de biochips se demostró con medidas amperométricas y medidas en tiempo real mediante resonancia de plasmón de superficie combinado con electroquímica (eSPR).

La tercera metodología es también un sistema de *patterning* controlado electroquímicamente, pero en este caso se utiliza la inmovilización del 4,4-bipiridil como base para la creación de biochips. Se sintetizaron moléculas de 4,4-bipiridil funcionalizadas con grupos carboxílicos, que fueron caracterizadas electroquímicamente y a continuación conjugadas con las biomoléculas de interés para la creación de biochips. La selectividad de estos sistemas se demostró colorimétricamente, obteniéndose niveles mínimos de respuesta inespecífica.

Por último, el cuarto de los métodos de *patterning* desarrollados está basado en la técnica de fotolitografía. Los enzimas glucosa oxidasa y sarcosina oxidasa se depositaron selectivamente junto con un polímero redox sobre la superficie de electrodos interdigitados utilizando un proceso de *lift off*, consiguiendo eliminar por completo las señales cruzadas o *cross-talk*. Como parte de esta metodología se optimizaron varios procedimientos de inmovilización de las biomoléculas, con el fin de seleccionar la estrategia más adecuada. También se llevaron a cabo ensayos con diferentes reactivos para eliminar la adsorción inespecífica. Finalmente, el sistema optimizado fue aplicado sobre IDEs fabricados mediante fotolitografía. Los sensores de glucosa y sarcosina respondieron de forma selectiva a sus respectivos sustratos, con ausencia total de *cross-talk*.

La presente tesis está estructurada en 7 capítulos. En el Capítulo I se exponen las bases del desarrollo de biochips, métodos de *patterning* con control electroquímico, otros métodos de *patterning* selectivo y las técnicas de fotolitografía, así como un resumen de la tesis. El Capítulo 2 y 3 describe la síntesis de coloides de oro, la modificación con biomoléculas, los estudios de estabilidad y los estudios fundamentales de electrodeposición de las nanopartículas de oro modificadas sobre la superficie de los electrodos. En el Capítulo 4 se muestra la aplicación de la electrodeposición de nanopartículas de oro biofuncionalizadas para la creación de biochips. El Capítulo 5 describe la inmovilización selectiva de biomoléculas mediante la desprotección electroquímica de monocapas autoensambladas electroactivas. En el Capítulo 6 se muestra la síntesis, caracterización e inmovilización selectiva de derivados de 4,4-bipiridil funcionalizados con HRP. El Capítulo 7 describe el *patterning* selectivo en la escala micrométrica de dos oxidasa sobre un chip de electrodos interdigitados mediante fotolitografía. Finalmente, el Capítulo 8 resume las conclusiones y el trabajo futuro.

Abstract

There is an increasing demand of multianalyte sensing devices having potential applications in biomedical, biotechnological, industrial and environmental fields. A good spatial control during biomolecule deposition step is strictly necessary; each biomolecule has to be precisely deposited on the surface of the relevant sensor (eg., an amperometric transducer), avoiding mixing that can compromise the biosensor specificity.

The aim of this thesis is to develop different patterning methods for the selective immobilization of biomolecules. The first method is selective electrodeposition of biofunctionalized Au nanoparticles for biosensor arrays. This is an electrochemically controlled patterning method where the Au nanoparticles modified by the enzymes initially and later the enzyme modified Au nanoparticles were electrodeposited selectively on the electrode surface. As a part of this methodology, initially biofunctionalized Au nanoparticles were prepared using three different approaches. One is Au-thiol dative bonding, the second is direct adsorption and finally electrostatic layer-by-layer approach. Different biomolecules like horse radish peroxidase(HRP), glucose oxidase (GOX), bovine serum albumin(BSA), and finally fluorescence labelled oligonucleotide thiols were used to attach to the Au nanoparticles. Biofunctionalized Au nanoparticles were characterized by different techniques like zeta sizer, UV-Vis spectroscopy, transmission electron microscopy (TEM). UV-Vis spectroscopy showed the successful modification of Au nanoparticles with a characteristic surface plasmon peak related to the stability. By using zeta sizer, layer-by-layer modification of the Au nanoparticles with redox polymer and enzymes were characterized successfully. Changes of the Au nanoparticles modified with BSA was characterized at different pH s by using the zeta sizer. After the preparation of biofunctionalized particles, some fundamental studies were done with electrodeposition of Au nanoparticles modified with medically important BSA, redox polymer to see how different parameters like potential, time of deposition, interelectrode distance, counter electrode sized, pH, effect the electrodeposition. As a part of these fundamental studies Au colloids modified with HRP and GOX were deposited for studying the electrocatalytic behaviour of the enzymes on the Au nanoparticles after electrodeposition. Later this methodology was applied for creating biosensor arrays by using two different approaches. In the first approach, GOX and HRP functionalized redox polymer modified Au nanoparticles were

electrodeposited successfully on an interdigitated electrode (IDE) array with complete absence of non-specific response. In the second approach the particles were modified with an extra redox polymer layer and proved that there is complete absence of non-specific response after electrodeposition. Moreover, this patterning methodology is generic and can be used for production of different biochips.

The second method is another electrochemically controlled patterning method where the electrodes were immobilized with self assembled monolayers with electroactive functionalities which can be tunable with potentials. In this methodology, electroactive self-assembled monolayer contains an active ligand aldehyde which can be readily conjugated to the primary amine group of the biomolecule is protected in the form of acetal. Later when a active potential was applied to the underlying electrode surface, the acetal functionality is deprotected to reveal the aldehyde functionality which was further conjugated to the biomolecule. Two enzymes GOX, HRP were used as model proteins to prove the versatility of this technique. Amperometric as well as real time measurements proved the selective applicability of this technique for creation of biosensor arrays.

The third methodology is also an electrochemically controlled patterning methodology where the special advantage of the electrochemically-controlled immobilization of the 4,4-bipyridyl was taken as base for the creation of biosensor arrays. In this methodology, carboxylic acid functionalised 4,4, bipyridyl molecules were synthesized and characterized by electrochemistry. Later the biomolecules were conjugated to these special molecules for the creation of sensor arrays. Proof of selectivity was shown using colourimetrically with minimal non-specific response.

Finally in the fourth method which is based on the photolithography technique, two different oxidases GOX & SOX were patterned along with redox polymer selectively on an IDE array using the lift off process with complete absence of cross-talk. As a part of this methodology, different immobilization methods were optimized initially for checking the best optimisation strategy. Later different reagents were tried to optimise the best reagent that prevents the non-specific adsorption. Later this optimised system was applied on the photolithographically created IDE array. Sarcosine and glucose sensors responded selectively to their substrates with complete absence of cross talk.

This thesis is structured in 7 chapters. Chapter 1 establishes the basics of the biosensor arrays, electrochemically controlled patterning methods, other selectively patterned methods, photolithography and summary of this thesis. Chapter 2 describes about the gold colloid synthesis, modification with the biomolecules, stability studies. Chapter 3 describes fundamental studies of the electrodeposition of the functionalised Au nanoparticles on the electrode surface. Chapter 4 describes the application of the electrodeposition of the protein functionalised Au nanoparticles for the creation of biosensor arrays. Chapter 5 describes the selective immobilization of biomolecules through electrochemical deprotection of electroactive self-assembled monolayers. Chapter 6 describes the synthesis, characterization and selective immobilization of HRP functionalized 4,4-bipyridyl derivatives. Chapter 7 describes the selective microscale protein patterning of two oxidases on an IDE array through photolithography. Finally chapter 8 summarizes the conclusions and the future work.

List of figures

Figure 2.1. Structure of redox polymers RP 1 (a) and RP 2 (b) used for modifying Au nanoparticles.....	49
Figure 2.2. UV-Vis spectroscopy of gold colloids	52
Figure 2.3. Zeta potential characterisation of the synthesized Au nanoparticles dissolved in distilled water (3×10^{11} particles)	53
Figure 2.4 . Typical TEM image of the 30nm Au nanoparticles (on a carbon coated copper grids).....	53
Figure 2.5 . Comparison of the two protocols of thiolation GOX residual enzymatic activity and number of thiols created permolecule as well as the number of thiols.....	54
Figure 2.6. UV-Visible spectra of HRP modified Au nanoparticles (curve a) in comparison with the unmodified Au colloid (curve b) and HRP (curve c) controls dissolved in distilled water. Concentrations: HRP control (200 mg mL^{-1}), Au nanoparticle control : 2×10^{11} particles mL^{-1}	55
Figure 2.7. Zeta Potential of 30-nm gold nanoparticles recorded as a function of the stabilizing BSA and pH. The average ζ -potentials are plotted with error bars representing the standard deviations for $n = 5$ measurements. Numer of particles : 3×10^{11} particles mL^{-1} , Buffers : 0.1M citrate-HCl pH 3.0, 0.1M PBS pH 6.0 and 8.0 and 0.1M Glycine-NaOH pH 10.0 and 12.0	56
Figure 2.8. UV-Visible spectroscopy of switching of redox polymer modified Au nanoparticles by changing pHs. Concentration of the particles : 3×10^{11} particles mL^{-1} , Buffers : 0.1M citrate-HCl pH 3.0, and 0.1M Glycine-NaOH pH 12.0	58
Figure 2.9. UV-visible spectroscopy of the Au colloids modified layer-by-layer with redox polymer / GOX / redox polymer.....	59
Figure 2.10. Zeta potential of Au nanoparticles modified with RP 2 followed by GOX and fuether by RP2. Concentration of the particles : 3×10^{11} particles mL^{-1}	60
Figure 2.11. Zeta potential of Au nanoparticles modified with RP 1 followed by HRP and further by RP1. Concentration of the particles : 3×10^{11} particles mL^{-1}	60

Figure 3.1. SEM images of glassy carbon electrode modified with Au nanoparticles (left) and BSA modified Au nanoparticles (right) at E = +1.2V for 30min. Conditions : Applied potential + 1.2 V for 30min. Distance between the working and counter electrodes 1mm. Particles are suspended in milli Q water (pH 6.7).....	70
Figure 3.2. SEM images of electrodeposited BSA modified Au nanoparticles on glassy carbon electrode at varying potentials with the same time of 15min. Images a-d corresponds to different potentials. Blank graphite (top left), +0.8V(top right), +1.2V(bottom left), +1.6V(bottom right). Conditions : Particles are suspended in milli Q water (pH 6.7). Distance between the working and counter electrodes 1mm.	71
Figure 3.3. SEM images of electrodeposited BSA modified Au nanoparticles on glassy carbon electrode at E = +1.2V. Images a-d corresponds to different periods of deposition time. (a) 5 (b) 15 (c) 30 (d) 45min. Applied potential + 1.2 V for 30min. Distance between the working and counter electrodes 1mm.. Particles are suspended in milli Q water (pH 6.7).	75
Figure 3.4. Effect of pH on the electrodeposition of BSA modified Au nanoparticles. Distance between the working and counter electrodes is 1mm. Concentration of the particles : 2×10^{11} particles mL ⁻¹	76
Figure 3.5. Current versus the deposition time for deposition of BSA modified gold nanoparticles for different inter electrode distances (a) 0.5mm (b) 1mm (c) 2mm (d) 3mm. Concentration of the particles : 2×10^{11} particles mL ⁻¹	77
Figure 3.6. Effect of interelectrode distance on the electrodeposition of BSA modified Au nanoparticles.....	77
Figure 3.7. Cyclic voltammogram of the gold electrode to EPD of RP 1-modified Au nanoparticles by applying potential of + 1.2 V for 30min with CE 1 (a) compared to a bare Au electrode (b) . Conditions of the electrolyte : 0.1M PBS pH 7.0 at a scan rate of 100 mV s ⁻¹	78
Figure 3.8. Charge calculated from the electrodes subjected to EPD of RP 1 modified gold nanoparticles after application of different electrodeposition potentials using CE 1. Electrolyte : 0.1M PBS pH 7.0 at a scan rate of 100 mV s ⁻¹	79

Figure 3.9. Charge calculated from the electrodes subjected to EPD of RP 1 modified gold nanoparticles after application of different times of electrodeposition with CE 1. Electrolyte : 0.1M PBS pH 7.0 at a scan rate of 100 mV s ⁻¹ . Applied potentials : + 0.8 V and + 1.2 V	80
Figure 3.10. Charge calculated from the electrodes subjected to EPD of RP 1 modified gold nanoparticles after application of different electrodeposition potentials using CE 2. Electrolyte: 0.1M PBS pH 7.0 at a scan rate of 100 mV s ⁻¹ ..	81
Figure 3.11. Charge under redox peaks obtained from the electrode subjected to EPD of RP 1 modified Au nanoparticles on the gold electrode by applying a potential of + 0.8 V and + 1.2 V for different time periods using CE 2.	82
Figure 3.12. Comparison of the charge calculated from the electrodes modified with redox polymer modified gold nanoparticles by applying electrodeposition potential + 1.2 V for 50 min using two different counter electrodes (1) 4 mm ² counter electrode and (2) 16 mm ² counter electrode.....	83
Figure 3.13. Scan rate dependence of the peak-to-peak separation ΔE_p (a) and peak current density j_p (b) of the RP1-Au films obtained at +0.8 V with CE 1 & CE 2 at several scan rates. Applied potential: +0.8V for 50min, Electrolyte : 0.1M PBS pH 7.0	84
Figure 3.14. Cyclic voltammogram showing the 5nm Au / GOX electrodeposited electrode. Electrolyte : 0.1M PBS pH 5.5.....	85
Figure 3.15. Plot of electrocatalytic current at +0.6 V (vs. Ag/AgCl) at different glucose concentrations with (a) 5nm Au colloid - GOX deposited electrode.(b) 20nm gold colloid - GOX deposited electrode. Electrolyte : 0.1M PBS at pH 7.0.	86
Figure 3.16. Plot of electrocatalytic current at +0.1 V (vs. Ag/AgCl) for HRP-Au colloid conjugate deposited electrode at different concentrations of peroxide. Electrolyte : 0.1M PBS pH 7.0.....	87
Figure 4.1. Electrodesorption of TEG-thioctic acid esters after applying a cathodic potential of - 1.2 V (vs. Ag/AgCl) for (1) 15min (2) 30min (3) 45min, 60min in the presence of 0.1M PBS pH 7.0 containing 10 mM K ₃ [Fe(CN) ₆] and 10 mM K ₄ [Fe(CN) ₆] a) E ₀ = 0.227 V and frequency range 0.1Hz to 100mHz., amplitude 5mV.	101
Figure 4.2. Cyclic voltammograms of the IDE array after the electrodeposition of 50 μ L of Au / RP1 / HRP particles (2 x 10 ¹¹ particles mL ⁻¹) Au / RP1 / HRP on the IDE 1 by applying +1.2V (vs Ag / AgCl) for 30min. Supporting electrolyte, 0.1M PBS pH 7.0, Scan rate, 50 mV s ⁻¹	103

Figure 4.3. Cyclic voltammograms of the IDE array after the electrodeposition of 50 μL of Au / RP2 / GOX particles (2×10^{11} particles mL^{-1}) on the IDE 2 by applying +1.2V (vs Ag / AgCl) for 30min. Supporting electrolyte , 0.1M PBS pH 7. Scan rate, 50 mV s^{-1}	104
Figure 4.4. Typical steady-state current response of the biosensor electrodeposited with the Au / RP 1 / HRP particles on the IDE 1 for successive injection of H_2O_2 into stirring PBS. Applied potential : 0V, supporting electrolyte : 0.1M PBS pH 7.0. Inset : Calibration plot of the currents produced due to the increasing H_2O_2 concentrations from the IDE array after immobilization of Au / RP 1 / HRP on the IDE 1.....	105
Figure 4.5. Typical steady-state current response of the biosensor electrodeposited with the Au / COPOs / GOX particles on the IDE 2 for successive injection of glucose into stirring PBS. Inset : Calibration plot of the currents produced due to the increasing glucose concentrations from the IDE array after immobilisation of Au / RP 2 / GOX on the IDE 2 . Applied potential : + 0.4V (vs. Ag / AgCl), supporting electrolyte: 0.1M PBS pH 7.0.....	107
Figure 4.6. Steady-state amperometric responses to the glucose from the electrode deposited with RP2/GOX/RP2/Au nanoparticles by applying different electrodeposition potentials. Applied Potential for amperometric response: + 0.4V (vs Ag / Ag Cl) ; supporting electrolyte: 2mL of 0.1M PBS pH 7.0 with stirring.....	108
Figure 4.7. (a) Current produced during the electrodeposition of RP 2 / GOX / RP 2 modified Au nanoparticles by applying electrodeposition potentials 0V (curve a), + 0.4 V (curve b), + 0.8 V (curve c) and +1.2V (curve d) for 15min. (b) Currents produced for +1.2 V (curve e) and +1.6 V (curve f) for 15min.....	109
Figure 4 .8. Steady-state amperometric responses of the biosensor with different electrodeposition at +1.2V for 15, 30, 60min to the oxidation of glucose in stirring PBS. Applied Potential for amperometric response +0.4V (vs Ag / Ag Cl); supporting electrolyte: 2mL of 0.1M PBS pH 7.0 with stirring.	111
Figure 4.9. Cyclic voltammogram of the electrodes deposited at different deposition times (15,30 and 60min) with gold nanoparticles modified L-b-L with RP 2 and GOX and RP 2. Electrodeposition conditions : + 1.2 V for 15, 30 and 60 min, Scan rate : 100 mV sec^{-1} . Supporting electrolyte : 2mL of 0.1M PBS pH 7.0... ..	112

Figure 4.10. Typical steady state chronoamperometric response of the biosensor on successive injections of glucose from the electrodes modified with Au / RP 2 / GOX / RP 2 & Au / RP 2 / GOX. Inset : currents plotted against the concentration of glucose. Applied Potential for amperometric response : + 0.4 V (vs Ag / Ag Cl) , supporting electrolyte : 2mL of 0.1M PBS pH 7.0 with stirring.....	113
Figure 4.11. Calibration curve of the currents produced from the biosensor on successive injections of glucose from the electrodes modified with Au / RP 2 / GOX / RP 2 & Au / RP 2 / GOX. Applied Potential for amperometric response: + 0.4V (vs Ag / Ag Cl) ; supporting electrolyte: 2mL of 0.1M PBS pH 7.0 with stirring.....	114
Figure 4.12. Typical steady state chronoamperometric response of the biosensor on successive injections of glucose from the electrodes modified with Au / RP 2 / GOX / RP 2 by the application of electrodeposition potential of + 1.2 V and - 1.2 V for 15 min. Applied Potential for amperometric response: + 0.4V (vs Ag / Ag Cl) ; supporting electrolyte: 2mL of 0.1M PBS pH 7.0 with stirring.....	115
Figure 4.13. Typical steady state chronoamperometric response of the biosensor on successive injections of glucose from the same electrode modified with Au / RP 2 / GOX / RP 2 by applying 0 V for 30 min first followed by + 1.2V for 30 min. Applied Potential for amperometric response: + 0.4V (vs Ag / Ag Cl) ; supporting electrolyte: 2mL of 0.1M PBS pH 7.0 with stirring.....	116
Figure 5.1. Cyclic voltammetry of benzo 1,3 dioxinol functionalised SAMs in 10 mM phosphate buffered with 0.15 M NaCl pH 7.0 at 0.1 V s ⁻¹	128
Figure 5.2. Nyquist Impedance response in 0.1M pH 7.0 PBS in the presence of 10 mM K ₃ [Fe(CN) ₆] and 10 mM K ₄ [Fe(CN) ₆] a) E ⁰ = 0.205 V and frequency range 0.1Hz to 100mHz., amplitude 5mV	129
Figure 5.3. Nyquist plot Impedance response in 0.1M pH 7.0 PBS in the presence of 10 mM K ₃ [Fe(CN) ₆] and 10 mM K ₄ [Fe(CN) ₆] a) E ₀ = 0.227 V and frequency range 0.1Hz to 100 mHz. b) 0.05 V s ⁻¹ . (a) Blank electrode, (b) non activated and (c) activated.....	130
Figure 5. 4. Cyclic voltammetry response in 0.1M pH 7.0 PBS in the presence of 10 mM K ₃ [Fe(CN) ₆] and 10 mM K ₄ [Fe(CN) ₆] at 0.05 V s ⁻¹ . (a) blank electrode, (b) non activated and (c) activated.....	131
Figure 5.5. Cyclic voltammetry response of the changes on the gold electrode in 0.1M pH 7.0 PBS in the presence of 10 mM Ru(NH ₃) ₆ ⁺ , scan rate 50 mV sec ⁻¹	132

Figure 5.6. ESPR measurement of the HRP immobilisation on electroactive SAM modified electrode after and before electrochemical activation. 10 mM pH 7.0 PBS with 0.15 M NaCl and 10 μ g mL ⁻¹ HRP.....	133
Figure 5.7. Amperometric response of electrodes exposed to GOX in 0.1 M pH 7.0 PBS, at a at 0.7 V vs Ag/AgCl showing the response 0, 10 and 20 mM concentrations of glucose on a) activated electrode b) non-activated electrode.....	135
Figure 5.8. (a) Comparison of amperometric response due to selective patterning vs. non-specific adsorption of GOX. (b) Comparison of HRP patterned vs. HRP non-specifically adsorbed as evidenced by ESPR. Data taken from Figures 5.7 and 5.8 respectively	136
Figure 6.1 Cyclic voltammogram of the carboxylic acid functionalised viologen derivative recorded . Background electrolyte solution composed of phosphate buffer 0.1M, pH 7.0, under argon. Scan rate 1V s ⁻¹ , working electrode area (16 mm ²), Reference electrode : Ag / AgCl.....	147
Figure 6.2. Cyclic voltammogram of the gold electrode in the presence of carboxylic acid functionalised viologen derivative dissolved in phosphate buffer 0.1M, pH 7.0, under argon recorded at different scan rates. Working electrode area : 4 mm ²	148
Figure 6.3. UV-Vis spectroscopy of HRP-conjugated 4,4'-bipyridinium derivative. Electrolyte : 0.1M PBS pH 7.0, concentrations : 4,4 dipyridyl carboxylic acid (20 μ g mL ⁻¹), HRP (500 μ g mL ⁻¹).....	149
Figure 6.4. Cyclic voltammogram of the HRP conjugated carboxylic acid functionalized viologen derivative recorded at different scan rates. Background electrolyte solution composed of phosphate buffer 0.1M, pH 7.0, under argon recorded at different scan rates. Working electrode area 4 mm ²	150
Figure 6.5. Absorbance at 650nm from the colourimetric reaction of the electrode immobilised with different concentrations of HRP on 4,4,'- bipyridine modified Au electrode at - 0.85 V for 10min. and 0V as control for 10min. Working electrode : gold electrodes (4mm ²).....	151
Figure 6.6. Colourimetric response of the electrode immobilised with HRP on 4,4,' bipyridine modified Au electrode at - 0.85 V and later applying - 0.4 V for 10min. Colorimetric detection was performed after 10min incubation with TMB and the colored product is detected at 650nm. Electrodeposition conditions : - 0.85V for 10min (experiment) and 0V for 10min (blank).....	152

Figure 6.7. Colourimetric assay response of the electrodes modified by HRP with and without conjugating to the carboxylic acid functionalised 4,4'-bipyridinium prior to the immobilization on the electrode. Colorimetric detection was performed after 10min incubation with TMB and the colored product is detected at 650nm. Electrodeposition conditions : - 0.85V for 10min (experiment) and 0V for 10min (blank).	153
Figure 6.8. Frequency variation during the immobilization of HRP functionalised viologen derivative dissolved in 0.1M PBS pH 7.0 by applying different potentials. Conditions : (a) Electrodeposition potentials - 0.85 V (vs Ag/AgCl) for 10 min (b) - 0.4 V (Ag/AgCl) for 10 min and (c) + 0.1V for 10min. Surface area of the quartz crystal 0.196 cm ² . Electrolyte : 0.1M PBS pH 7.0 under argon.	154
Figure 6.9. Variation in the frequency of the quartz crystal modified with HRP functionalized 4,4-bipyridyl molecules with switching the potential.. Conditions : Electrodeposition potentials - 0.85 V (vs Ag/AgCl) for 10 min followed by - 0.4 V (Ag/AgCl) for 10 min and finally + 0.1V for 10min. Surface area of the quartz crystal 0.196 cm ²). Electrolyte : 0.1M PBS pH 7.0 under argon.	155
Figure 7.1. Structure of osmium redox polymer used in the patterning of enzymes.	163
Figure 7.2. Gold interdigitated electrodes array image. Each set of electrodes consists 50 microelectrodes with a width of 20µm and a distance between electrodes of 20µm.	165
Figure 7.3. Scheme of patterning of enzymes (GOX, SOX) on two sets of electrodes within the IDA electrodes	167
Figure 7.4. (a) Dependence of the steady-state-D-glucose catalytic oxidation current density on electrode potential for a GOX / redox polymer immobilised on electrode through direct adsorption in 100 mM PBS buffer of pH 7.0, 50mM glucose at 2 mV s ⁻¹ ; (b) Dependence of the steady-state-D-sarcosine catalytic oxidation current density on electrode potential for a SOX / redox polymer immobilised on electrode through direct adsorption in 100 mM PBS buffer of pH 7.0, 50 mM sarcosine at 2 mV s ⁻¹ .	170
Figure 7.5. Current response to the glucose and sarcosine from the electrodes immobilised in the order GOX + redox polymer / spacer / SOX + redox polymer using different types of blocking agents as spacers	171
Figure 7.6. Current response to the glucose and sarcosine from the electrodes immobilized in the order SOX + redox polymer / spacer / GOX + redox polymer using different types of blocking agents as spacers.	172

Figure 7.7. Voltammetric response of the IDE array after GOX + redox polymer mixture immobilized on the IDE 1 (redox CV), before the exposure of photoresist polymer on the IDE 2 (noisy).....	173
Figure 7.8. Chronoamperometric response of IDE array after the deposition of GOX + redox polymer followed by polyelectrolyte multilayer on the IDE1 and before exposure of the photoresist on the IDE 2 at + 500mV (vs. Ag / Ag Cl) in 0.1M phosphate buffer pH 7 during successive injection of glucose.	173
Figure 7.9. Chronoamperometric response of IDE array after the deposition of SOX + redox polymer followed UV-Vis exposure on the IDE 2 at + 500mV (vs Ag / Ag Cl) in 0.1M phosphate buffer pH 7 during successive injection of glucose.....	174
Figure 7.10. Steady state response for glucose from the IDE after polyelectrolyte multilayer formation over the IDE 1 after GOX + redox polymer mixture immobilisation.....	175
Figure 7.11. Cyclic voltammetry of the IDE array after the exposure of the photoresist polymer and SOX + RP mixture immobilization on the IDE 2 (black).....	176
Figure 7.12. Chronoamperometric response of IDE array after the deposition of SOX + redox polymer followed UV-Vis exposure on the IDE 2 at + 500mV (vs. Ag / Ag Cl) in 0.1M phosphate buffer pH 7 during successive injection of sarcosine.	177
Figure 7.13. Chronoamperometric response of IDE array modified with SOX + redox polymer on the IDE 1 and GOX + redox polymer on the IDE 2 at + 500mV (vs Ag / Ag Cl) in 0.1M phosphate buffer pH 7 during successive injection of sarcosine.	178
Figure 7.14. Chronoamperometric response of IDE array modified with SOX + redox polymer on the IDE 1 and GOX + redox polymer on the IDE 2 at + 500mV (vs Ag / Ag Cl) in 0.1M phosphate buffer pH 7 during successive injection of glucose.....	179
Figure 7.15. The signal independence of the sarcosine and glucose sensors within the IDE microarray at + 500mV (vs Ag / Ag Cl) in 0.1M phosphate buffer pH 7.0 during successive injection of sarcosine followed by glucose.....	181

List of tables

Table 1.1 Types of Microarrays	3
Table 1.2 Biomolecule immobilization methods.....	8
Table 1.3. General techniques for the creation of microarrays	15
Table 1.4. Current detection methods used in protein microarray experiments.....	17
Table 4.1 . Kinetic parameters I_{\max} (maximum current) and K_m app (Michaelis Menten constant) from the glucose sensors made by EPD of RP 2/ GOX / RP 2 / Au nanoparticles by applying different potentials. Electrodeposition for 15min.....	109
Table 7.1. Summary of biosensor response using different strategies for the immobilization of the GOx + redox polymer & SOx + redox polymer on the gold electrode	183

List of Schemes

Scheme I.1. Schematic representation of the signalling of the nose.....	1
Scheme 1.2.2. Schematic diagram of the variation of free energy with particle separation according to DLVO theory. The net energy is given by the sum of the double layer repulsion and the van der Waals attractive forces that the particles experience as they approach one another.....	23
Scheme 1.2.3. Schematic diagram of the variation of free energy with particle separation at higher salt concentrations showing the possibility of a secondary free energy.....	24
Scheme 1. 2. 4. Preparation and electrodeposition of biofunctionalized gold nanoparticles on an electrode array.....	29
Scheme 2.1. Flow chart of the thiolation of GOX using carbodiimide reaction.....	46
Scheme 2.2. Thiolation of enzymes through bi-phase separation using DTSP.....	47
Scheme 2.3. Scheme of step by step modification of Au nanoparticles with redox polymer (RP 2) first followed by GOX and finally again with redox polymer (RP 2).....	50
Scheme 4.1. Scheme of the selective electrodeposition of enzyme / redox polymer modified Au nanoparticles on an interdigitated array.....	95
Scheme 4.2. Schematic representation of the electrodeposition of Au nanoparticles modified layer-by-layer with RP 2 followed by GOX and finally with RP 2.....	98

Scheme 5.1. Schematic representation of the generation of the aldehyde group by electrochemical deprotection of SAM containing thioctic esters presenting benzo1,3 dioxinol substrate and subsequent covalent coupling of aldehyde with amine containing enzymes.....	122
Scheme 5. 2. Steps for the synthesis of benzo (1,3) dioxinol thioctic ester.....	124
Scheme 6.1. Steps in synthesis of a) CH ₃ I, benzene, room Temperature, 48h; b) methyl 5-bromovalerate, DMF, 110°C, 20h; c) H ₂ O, 16 % HCl	142
Scheme 6.2. Double step immobilisation of HRPfunctionalized viologen derivative.....	145
Scheme 6.3. Single step immobilisation of HRP on the gold electrode.....	145
Scheme 7.1. Lithographic scheme for the patterning of proteins	166

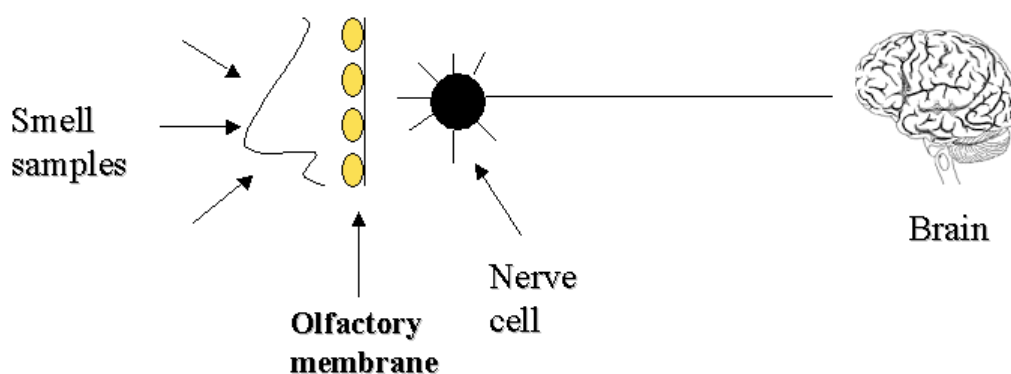
Chapter 1. Introduction

1.1. Biosensor arrays

1.1.1. Definition of biosensors

A biosensor is a compact analytical device that consists of a biological recognition element like an enzyme, antibody, nucleic acid, aptamer and chemoreceptor in intimate contact with a signal transducer. The interaction of the analyte with the biorecognition element produces an effect that can be detected by the transducer. Next the transducer converts this biorecognition event into a measurable signal that can be detected by the detector element (works in a electrochemical, piezoelectric, optical or thermometric mode).

Biosensor arrays can be defined as devices that integrate several biosensors. In making the step from biosensors to arrays the immobilisation of distinct biomolecules needs to be directed and addressed spatially. In nature biosensor arrays have evolved with receptors that have a broad specificity. The human nose for example uses only a limited number of odour receptors for a sensitive detection at the parts per trillion level in combination with the discrimination of thousands of different odours.



Scheme 1.1. Schematic representation of the signalling of the nose

Upon binding of odour molecules with olfactory ligands a signal cascade and neural transmission is started, which amplifies and processes the response leading to a neural activity reflecting the smelled odour. The olfactory pathway achieves its goal by using large arrays of cross-reactive receptors instead of using highly compound specific

sensors. Based on the principle of olfactory recognition, various concepts for pattern recognition and multisensing with chemosensors have been described. In general, a biosensor array is constructed with a large set of capture ligands (DNA, antibodies, proteins, carbohydrates, peptides and aptamers) arrayed on a solid support. After washing and blocking the surface of unreacted sites, the array is probed with a sample mixture containing the counterparts of the molecular recognition events under study. If an interaction occurs, a signal is detected on the surface. By scanning the entire array, a large number of binding events are detected in parallel. The challenge of signal processing and signal transduction in parallel have converted multianalyte detection to an emerging area of interest in the last decade.

1.1.2. Types of biosensor arrays

Biosensor arrays or biochips can be classified either by their bioreceptor (biorecognition element) or their type of transducer. Based on the biorecognition element to be immobilised on the substrate, biochips can be classified into protein arrays, antibody arrays, DNA arrays, aptamer arrays, and cell arrays. Different types of biosensor arrays are listed in Table 1.1.

DNA Arrays

Detection of specific DNA sequences through hybridization with a complementary DNA probe has many potential applications. With the results of the Human Genome Project at hand creating a massive amount of DNA sequence information, scientists have developed new techniques and tools for conducting research. DNA microarrays are an example of a tool that uses genome sequence information to analyse the structure and function of tens of thousands of genes at a time[1-4]. DNA arrays or chips can be defined as the integration of several DNA sensors (oligonucleotide sequences) in the same device. The recognition event is the hybridization of the probe with its complementary sequence present in the sample mixture. There are several applications of these arrays especially in medical diagnosis, gene expression analysis, single nucleotide polymorphisms (SNPs) typing, pharmacogenomic research, and forensic applications.

Table 1.1 Types of Microarrays, Developers and companies

	Target	Recognition event	Applications	Ref
DNA arrays	Complementary DNA sequence	Hybridization	Medical diagnostics, gene expression analysis, single nucleotide polymorphism (SNP) typing, pharmacogenomics, forensic applications,	[1-4]
Immunoarrays	Protein	Affinity interactions	Antibody assays, monitoring of protein expression, detection of proteins, drug development, medical diagnostics, cell signaling	[5,6]
Peptide arrays	Protein	Affinity interactions	Epitope mapping, Pathogen detection, Cell adhesion studies,	[13-15]
Carbohydrate arrays	Glycoproteins especially lectins	Affinity interactions	Lectin-carbohydrate interactions, Medical diagnostics, Pathogen detection	[18,19]
Aptamer arrays	Protein	Affinity interactions	Medical diagnostics, Targeting cancer cells	[8,9]
Cell arrays	Antibodies during immunocytochemistry	Affinity interactions	Drug screening, drug discovery, gene expression studies, cellular profiling , cellular immune response	[16,17]
Small molecule arrays	Biomolecule	Affinity interactions	Drug screening and drug discovery, Chemical genetics	
Enzyme microarrays	Substrate	Conversion of substrate to product	Clinical diagnostics, Food analysis Toxicology, carbohydrate analysis	[20]

These high-throughput analysis tools are easier to use, do not require large-scale DNA sequencing, and allow the parallel quantification of thousands of genes from multiple samples. Some of the leading companies in the field of DNA microarrays are Synteni pharmaceuticals, Hyseq, Affymetrix, Clinical Microsensors, Nanogen, Combimatrix, Telechem international, Nimblegen, Zymomyx and they use different strategies to immobilize biomolecules on to the substrate along with different detection methods.

Protein arrays

Though DNA microarrays are proven to be successful in the analysis of whole genome and profiling of gene expression, in order to have in depth understanding about the how the gene function of the gene and the mechanisms or the biological processes in which these genes are involved, analysis of the gene products i.e proteins should be performed. Therefore, protein microarrays are emerging as a possible tool based on protein-ligand interactions. In producing protein microarrays, many challenges have to be overcome such as the detection of protein functionality which depends on the state of proteins, the discrimination of post-translational modifications, partnership with other proteins, protein subcellular localization, and reversible covalent modifications (e.g. phosphorylation). Challenges to the development of protein arrays include non – specific adsorption, retaining of the native activity, selective arraying, and detection. Some of the leading companies in the field of protein arrays and proteomics includes Invitrogen, Biomax, Genomic solutions, Abnova, Telechem international, Eppendorf, Zymomyx etc.

Immunoarrays can be defined as the integration of several immunosensors in the same device which contains an ordered set of known antibodies or antigen probes immobilized on precisely defined locations of a solid substrate. Immunoarrays are one sub set of protein arrays. Antibody microarrays have the potential of allowing the researcher to monitor cell signaling [5]. As proteins are the common targets for the drugs, antibody microarray technology can be used to identify potential candidates for drug development. Antibody arrays can be used to detect how drugs and growth factors affect the post-translational modification of specific proteins [6]. Autoantigen microarrays for multiplex characterization of autoantibody responses has been developed. Recently, Clontech has produced antibody array BD Clontech Ab Microarray 500 for detecting human proteins. Biochip.net has commercialised several antibody microarrays made up of hundreds of antibodies. Panomics has produced antibody arrays for detecting multiple angiogenesis. Hypromatrix, Inc [7] has commercialised antibody arrays for signal transduction, apoptosis. Lab Vision Corporation has commercialised antibody arrays for following signal transduction, cell cycle, discovering cancer markers, following apoptosis etc.

Enzyme arrays

The development of assays that measure the enzyme activities has wide range of applications in the field of clinical diagnosis, food analysis and toxicology studies. The most important parameter to be considered while designing electrochemical enzyme biosensor is the cross talk. Cross talk occurs when there are freely diffusing species detectable at adjacent (enzyme) microelectrodes. In order to avoid this problem, enzymes should be patterned with higher specificity and selectivity, and the transduction should be contained at the spot where biorecognition occurs.

Aptamer arrays

Aptamers are single-stranded DNA or RNA molecules that, like antibodies, can bind target molecules with extraordinary affinity and specificity [8,9]. Although single-stranded nucleic acids are commonly thought of as linear molecules, they actually assume complex, sequence-dependent, three-dimensional shapes. When the resulting shapes interact well with a target protein, the result is a tightly bound complex analogous to an antibody-antigen interaction. Usually aptamers are selected using a process called SELEX (Systematic Evolution of Ligands by Exponential enrichment) [10]. In this procedure, a combinatorial library of single stranded nucleic acid molecules is allowed to interact with a purified protein, cells, peptides, small molecules or nucleic acids. The members of the library that have successfully bound their targets are separated from the rest of the nucleic acids. After separation, the functional nucleic acid molecules are amplified using the polymerase chain reaction (PCR). Since these RNA and DNA molecules bind their targets with similar affinities as antibodies, and are able to distinguish between isotypes of an enzyme, aptamers have been also called synthetic antibodies. Although aptamers mimic the protein recognition properties of antibodies, aptamer research is still in its infancy compared with antibody technology.

Aptamer based arrays have been reported recently for the human IgG aptamer [11], and other analytical purposes [8,9,12]. Some of the leading companies in the field of aptamer array are LC Sciences, and Somalogic. LC Sciences is able to produce an aptamer array with almost 1000 oligonucleotide sequences ready to detect proteins by using μ Paraflo microfluidics technology.

Peptide arrays

Peptide array is a rapidly growing tool that provides both large-scale and high-throughput capabilities for protein detection and activity studies [13-15]. An important difference between peptide arrays and the oligonucleotide arrays is found in the range of applications they can be used to address. DNA arrays are used almost entirely to profile mRNA populations in cells and rely exclusively on the hybridization principle. Peptide arrays, by contrast, are based on multiple interactions including protein binding, enzyme action, the adhesion of cells, the binding of metals, and many others. Peptide arrays have also been used in diagnostic applications. Some of the leading companies in the field of peptide arrays are LC Sciences, New England Peptide Inc., JPT Peptide Technologies, Eurogentec etc. New England Peptide Inc was able to synthesize 96 peptides used for epitope mapping.

Cell Microarrays

There is an increasing need for high throughput cell-based assays for the functional exploration of genomes, drug screening and toxicology testings [16,17]. Especially drug screening is extremely useful to evaluate potential drug targets by functionally characterizing their effect on cells, assessing specificity and efficacy of drug leads, and identifying the targets for drugs of unknown mechanism of action. Compared to microtiter plates, cell microarrays increase throughput while reducing the overall cost of screening by reducing the amount of expensive reagents and materials, the time and the number of cells used in each assay.

1.2. Technologies involved in Array Development

Microarray is taking place at the interface of multidisciplinary technologies. Several steps are necessary to create reliable arrays that meet the requirements as state of art tools for the applications mentioned. These steps are

- Probe immobilization
- Arraying
- Detection of the biorecognition
- Interpretation of the data

The three first of these are of special relevance to the contents of this work and are examined in same detail in what follows

1.2.1. Probe immobilization

Immobilization of the capture probes plays a key role for establishing reproducible and reliable protein-detecting systems. They should be placed in such a way that they retain thier native activity and are accessible to the interacting partner. Summarized in table 1.2 are the general methodologies widely used for immobilisation in biosensor arrays.

Adsorption

This approach has been routinely used in standard ELISA and Western blot and is based on adsorption of the macromolecules either by electrostatic forces on charged surfaces or by hydrophobic interactions. The most convenient method is the coating of glass slides with the nitrocellulose membrane or poly lysine and the subsequent use of these slides for passive adsorption of the probes. In spite of its simplicity, the adsorption method presents several drawbacks. Non-specific binding can be a significant problem, proteins are oriented in a random fashion, which might act as a barrier for the complimentary biomolecule, the attached proteins can be removed by stringent washing conditions, background level is usually high due to non-specific

protein adsorption–desorption and also proteins adsorbed on hydrophobic surfaces tend to denature.

Table 1.2 Summary of Biomolecule Immobilization Methods

Method	Technique	Specificity	Advantages	Disadvantages	References
Adsorption	Interaction with substrate, Electrostatic or hydrophobic	Random	Simplicity, reagentless	Cannot resist stringent washing steps, high background signal due to non-specific adsorption, denaturation	[21,22]
Covalent binding	EDC reaction, schiffs base, Gold-thiol interactions	Reactive groups, random	Strong, high density and low background	Random orientation of the surface attached proteins	[23-25]
Affinity	Via protein G, A / Biotin interactions /	Uniform orientation	Strong, Specific, High density	Biomolecules have to be labelled	[26]
Physical entrapment	Entrapment in polymer matrices	Random	Flexibility, simplicity, enzyme loadings with high activity	Gel structure may prevent diffusion of the substrate,	[27]

Covalent linkage

Proteins and other biomolecules are bound normally through their primary amine groups or other reactive aminoacid, or glycoprotein groups [23,24]. The primary amine groups can react readily with aldehyde or epoxide groups or through the

carbodiimide reaction to the carboxylic acid groups on the surface. Substrate surfaces are usually glass or gold and an additional step is required to create reactive groups. Silanisation is the most common procedure for the modification of glass surfaces. Amino groups are introduced by aminopropyl-triethoxy- (or trimethoxy) silane. These amino groups can, for example be crosslinked with glutaraldehyde, to the proteins via schiff's base formation [25]. In the case of gold coated glass surfaces used widely in SPR and mass spectrometry, functional thiols have been used for self assembling since they interact specifically with the gold surface presenting a second functional group like carboxylic or boronic acid to the solution which can be used for linking to the capture biomolecules. This type of chemistry helps in the monitoring of the interactions in real time and has great potential in drug discovery and biomedical research.

Retention in a polymeric matrix

Entrapment of the biomolecule in a three-dimensional polymer matrix has been widely used for higher density sensors . The polymer might be an inert support or it may perform some function essential to the transduction of the analyte-dependent signal. Recently electrochemically polymerised matrices have been deposited selectively for the immobilization of wide variety of biomolecules [28]. The major disadvantage of this strategy is the random orientation of the probes.

Affinity binding

Immobilizing proteins and other biomolecules through covalent linkage or adsorption, results in random orientation, which might reduce the availability of the functionally active part of the molecule [26]. Therefore there is a necessity to develop methods that can achieve uniform orientation. Such methods depend on the biochemical properties of the biomolecules. Usually affinity interactions are used to such end: examples include immobilization of antibodies via protein A or protein G, immobilization through biotin-streptavidin interactions, or immobilization of recombinant proteins via tags. Protein A or protein G bind specifically the Fc portion of antibodies so that they orient themselves in a way that makes them accessible to the analytes. As a result higher signals for the analyte detection can be obtained.

Proteins avidin and streptavidin have high affinity towards biotin. Biotin has a carboxylic acid, which can be used for conjugating to a wide range of biomolecules. Later the biotin-conjugated biomolecules can be tightly bound to the avidin and streptavidin coated surfaces.

1.2.2. Arraying

Although immobilisation is important for developing biosensors, biosensor arrays require the directed addressing of specific recognition sites for the directed immobilisation of biomolecules. Summarized in Table 1.3 are the general methods widely used for arraying for the creation of biosensor arrays.

Electronic addressing

This is an electrochemically controlled arraying method. The directed immobilization of the biomolecules on to the surface of the electrodes in an array can be controlled by controlling their potentials.

Nanogen's technology uses this electronically addressing technique for the immobilisation as well as the detection. Electronic addressing of the biotinylated samples was done through the electrodeposition by taking advantage of negative charge of the sample probe and there by applying positive potentials. After addressing, fluorescently labeled probes or samples are hybridized to bound complementary biotinylated strands. The core technology is an automated programmable electronics matrix (APEX), which has the ability to transport, bind and separate charged molecules in an electric field generated on the surface of the device. This technology is not only limited to DNA but also applied to immunoassays, receptor-binding assays, cell typing assays, enzyme assays. The biggest advantage of this technology is that even the hybridization of the probe with the complimentary DNA is also controlled by electrochemistry which provides stringency to remove unbound and nonspecifically bound strands after hybridization which makes this technique more versatile when compared to other techniques.

Combimatrix technology is based on specially modified semiconductor circuitry which uses localized electrochemistry to fabricate DNA microarrays [29-31]. These integrated circuits contain arrays of microelectrodes that are individually addressable using embedded logic circuitry on the chip. The semiconductor logic circuitry directs digitally controlled simultaneous synthesis of different oligonucleotides at thousands of electrodes in response to a computer software program. To perform a synthetic step, a microelectrode is activated to selectively generate acid by means of an electrochemical reaction. The generated acid in turn deprotects the growing oligonucleotide chain activating it for binding of the next nucleotide. Since a different oligonucleotide can be synthesized at each microelectrode, this technology enables one to design a microarray of any desired configuration. The advantage of this technology is that electrochemistry is used both for synthesis as well as the detection by utilizing the underlying electronics employed for the oligonucleotide synthesis for electrochemical detection of target molecules bound to the microarray which helps in lowering the cost of production. The ElectraSense is one of the products from the combimatrix which uses this digitally controlled electrochemical arraying technique combined with electrochemical detection.

Photolithography

This is an optically controlled method of arraying. Photolithography is the process of activating geometric platforms on a surface through a mask that selectively allows light to penetrate through it. Photolithographic techniques are well established for mass production of silicon chips with a pattern resolution and alignment precision of better than 1 μm . The pattern in the photoresist, which is generated by light exposure through a mask followed by chemical development, can be transferred to thin films of molecules immobilised on a surface. Affymetrix manufactures its genomic microarrays by a light-directed chemical synthesis process, which combines solid-phase chemical synthesis with photolithographic fabrication techniques. It is able to synthesize short single stranded oligonucleotides of about 20-25 bases in length. In this case, chromium photomasks are used while along with the UV exposure. Nimblegen, Xeotron and Febit use maskless array synthesizers to fabricate microarrays. Maskless photolithography is more flexible but a principle advantage of

maskless method is that a significant amount of design work and cost is associated with the mask design is reduced. Apart from this, stability problems for functional proteins due to the organic solvents and alkaline solutions can be avoided.

Soft lithography

Soft lithography is a high resolution patterning technique in which a "stamp" is made from an elastomeric material called polydimethylsiloxane (PDMS). Microcontact printing (μ CP), is perhaps most attractive among soft lithography due to its exceptional versatility, ease of application, and low cost. In μ CP, a PDMS stamp is inked with the biomolecules of interest and transferred to the substrate surface by direct contact. A key requirement for a successful soft lithography process to pattern protein molecules is surface chemistry. The surface chemistry involved should allow high spatial resolution, low background adsorption, and high selectivity for protein immobilization. Self-assembled monolayers (SAMs) of oligo(ethylene glycol) (OEG) terminated thiols on Au surfaces have been proved to be the most successful in patterning a variety of biomolecules on gold surfaces due to their ability to prevent non-specific adsorption. In addition, the OEG terminal groups can be capped with other functional groups, such as carboxylic acids, for further activation and protein attachment. Using soft lithography, proteins and cells have been patterned successfully for biosensor and tissue engineering applications [32]. Although this technique is versatile, there are several drawbacks for protein patterning. For example, time consuming in the complex and serial patterning may lower the activity of previously attached proteins under ambient conditions. Apart from this, the patternable area in soft lithography is limited by the size of the PDMS stamps, therefore affecting its application in large-scale pattern production. This methodology has the high-resolution capability to create features with 2–500 μ m resolution.

Dip pen nanolithography

Dip-Pen Nanolithography (DPN) is the first commercially available technology based on Atomic Force Microscopy (AFM). Dip-Pen Nanolithography (DPN) is a scanning probe nanopatterning technique in which an AFM tip is used to deliver molecules to a surface via a solvent meniscus, which naturally forms in the ambient atmosphere.

This technique is a simple and powerful method of transporting molecules from AFM tips to substrates with spatial resolutions of 5nm. Using this technique, nanoarrays of enzymes, antibodies and oligonucleotides have been created with high selectivity [33]. Biofunctionalized nanoarrays of inorganic structures have been generated using the DPN technology [34]. Nanoink Inc has commercialised this technique for application towards biosensor arrays. The biggest advantage of this methodology is time reduction and ease of fabrication. Structures smaller than 10nm can be built using this technology.

Ink-jet Printing

Inkjet printing mechanism is an in-situ non-contact method to deliver the biomolecules onto the detection site. The inkjet-head movement is computer-controlled to ensure the accuracy of the nucleotide deposition process. Companies producing inkjet printed DNA microarrays includes Agilent (SurePrint)[Rosetta Inpharmatics], Perkin-Elmer (PiezoTip), Canon (Bubble Jet), Arrayjet, Biodot / Cartesian, Protogene Laboratories, Pamgene. Inkjet printable biomolecules includes DNA, Proteins, Cells and Other biomolecules. There are many technical problems with the protein arrays produced by this methodology due to the complex nature of proteins. **Arrayjet** inkjet technology overcomes these challenges, enabling high quality protein microarray production. The use of ink jet technology promises reduced spot sizes down to 25 μm . This technology can potentially eliminate the irregular spots, reproducibility and hybridization quality issues associated with pin-tool technologies [35]. This technique is simple and is commercially used in production of microarrays.

In general, a disadvantage of ink-jet arraying is that air bubbles may reduce the repeatability and the reliability of the system. Other disadvantages include the difficulty associated with changing samples, maintenance problems related to the obstruction of the inlet tubing and capillaries or syringes, excessive splashing, clogging of the nozzle, and poor uniformity of the deposit, which can cause cross-over contamination between probes. Based on this technique, Rosetta Inpharmatics, Inc has developed Flex Jet inkjet-based microarrays. The flex jet system was able to print tiny arrays of thousands of different gene sequences onto a single glass slide by using ink jet synthesizer. Recently, ITRI's Phalanx Microarray Technology which

employs bubble jet printer technology to precisely dispense micro-volume liquids t very high density has been reported.

Pin deposition

Pin deposition is a contact printing technique, where pin tools are immersed in the probe pool, so that small volumes adhere to the tips of the pins [36-39]. When the pin touches the substrate surface, a drop is transferred onto the surface. Although pin deposition also suffers from splashing, evaporation problems or poor uniformity of the deposit, it is more robust, simpler, cheaper, and easier to maintain than the non-contact printing techniques. One versatile technique based on this principle is the mechanical microspotting. This is a contact printing method, which prints small quantities of premade biochemical substances onto solid surfaces. Printing is accomplished by direct surface contact between the printing substrate and a delivery mechanism that contains an array of tweezers, pins or capillaries that serve to transfer the biochemical samples to the surface. Advantages of this technology includes ease of prototyping, low cost and versatility. Based on this principle, Synteni manufactured 1000 gene fragments per square centimeter. Although this system is versatile, the biggest drawback of this methodology is that each sample should be synthesized, purified and stored separately.

Laser-induced forward transfer

This is a non-contact technique and an alternative arraying technique recently reported for the production of functional DNA microarrays [40-42]. The advantage of this methodology is that it does not need an expensive photolithographic processes. The high focusing power of the laser used while arraying was reported to present high integration scales when compared to pin deposition and ink jetting. The basic principle behind this methodology is that a laser pulse impinges on the thin film of material to be deposited. The focussed laser beam has sufficient intensity to vaporize a portion of the metal film and as a result the portion exposed to the laser is transferred to the substrate opposite to this thin film of material.

Table 1.3. General techniques for the creation of microarrays

Arraying Technique	Advantages	Disadvantages	Specifications
Photolithography with masks	Sub-micron resolution High density arraying	In situ synthesis Expensive Rigorous laboratory procedures Limited flexibility	1) Affymetrix 20-25mer oligonucleotides, 12,000 genes/cm ²
Maskless Photolithography	Reduction of the cost Time reduction Accommodates substrates of various shapes, materials, and sizes.	In situ synthesis Lack of sufficient resolution	1) Nimblegen 17,000 genes/cm ² Require 1 - 3µg isolated gDNA test sample
Non contact printing (Ink-jet technology)	High throughput Low cost Automation Flexibility No Surface contact Maintainence No masks Capable of depositing small volumes	Repeatability and the reliability Difficulty associated with changing samples Poor uniformity of the deposit Maintenance problems	1) Agilent 60,000 genes/cm ² 60mer oligos,
Contact printing Technology (Pin deposition)	Quick and simple pattern formation	Poor uniformity of the deposit Splashing , reliability	1) Array it 6400 genes/cm ²
Electronic addressing	Stringency Electric field for addressing as well as for hybridization Reduction of time Requires lower concentrations	Limited to oligonucleotides	1) Combimatrix Range of sensitivity is 0.1 to 200 nA. 1,700,000 targets / cm ²
Microfluidics technology	No spotting needed Can be used with multiple samples Fast hybridization rates Cost effective	Influenced by environmental factors(especially temperature fluctuations) More complex to fabricate Require pressure balancing to control flow across the membrane	1) LC Sciences uses µParafluo Microfluidic Chip Technology Sample requirement : 10 µg Total RNA Detection limit : 100 attomole 1500 sequences / cm ²

1.2.3. Methods of Detection

After the probe immobilization and arraying, the next important step is the detection. Depending on the usage of labels, detection methods are classified into two types. One is label free methods like surface plasmon resonance, quartz crystal microbalance, atomic force microscopy, mass spectrometry, nanowires and some label free electrochemical measurements like impedance spectroscopy. Table 1.4 summarizes different detection methods widely used in the field of biosensor arrays.

1.2.3.1. Label free methods

Surface plasmon resonance (SPR) detection method

Surface plasmon resonance (SPR) is an optical biosensor technique that measures molecular binding events at a metal surface by detecting changes in the local refractive index. SPR offers several advantages over conventional techniques such as fluorescence or ELISA (enzyme-linked immunosorbent assay). These includes

Label free and direct (based on refractive index changes), measurements can be performed in real time, and versatility (capable of detecting analytes over a wide range of molecular weights and binding affinities). Due to the above unique features, SPR has become a powerful tool for studying biomolecular interactions [43,44]. Recently, up to 400 real-time antibody-target bindings could be measured simultaneously within a single hour using antibody microarrays combined with SPR technology [45].

Lumera has developed a proteomic processor for detecting and quantifying binding interactions in a label-free format utilizing surface plasmon resonance (SPR) technology.

Table 1.4. Current detection methods used in protein microarray experiments

Detection	Labelling	Data requirement	Real-time measurement	Resolution	References
ELISA	Enzyme linked antibodies	CCD imaging	No	Low	[46-48]
Radio labelling	Radio isotope labeled analyte	Autoradiography	No	High	[49-51]
Sandwich immunoassay	Fluorescence and enzyme labelled antibodies	Laser scanning, colourimetric	No	High	[52]
AFM	Not needed	Surface topological change	No	High	[53]
QCM	Not needed	Change in the frequency	Yes	Low	[54]
Grating-coupled SPR	Not needed	Change in the refractive index	Yes	Low	[45,55-57]
Electrochemical	Metal coupled analyte	Measurement of conductivity	Yes	High	
SELDI TOF MS	Not needed	Mass spectrometry	No	Low	[58-61]

Mass spectrometry

Mass spectrometry is another alternative label free technique. In mixtures, it can detect low abundance proteins because it measures protein molecular mass. Mass spectrometry (MS) and, in particular, surface-enhanced laser desorption-ionization (SELDI) MS, are helping to form a new generation of protein chip. Protein microarrays based on Surface-enhanced laser desorption/ionization (SELDI) TOF MS, employ an “on chip” selection of the proteins of interest from a complex mixture

and subsequent ionization of the retained molecules to a detector for a classification based on the mass/charge ratio [58-61]. Analysis using mass spectrometry data is then performed in order to reveal the identities of these proteins. The advantages of this detection is the increased sensitivity due to the mass spectrometry detection and the relative ease of production of SELDI matrices. Ciphergen has already started marketing protein arrays coupled with mass spectrometry commercially. Sequome (SanDiego,CA) has already developed a high-throuput resequencing array which uses MALDI-TOF mass spectrometer for subsequent detection and identification of DNA fragments, used for SNP and genotyping.

Quartz crystal microbalance (QCM)

QCM is a sensitive mass-measuring system at the nanogram level which can be used to monitor biological events such as molecular interactions in real-time [54].

Atomic force microscopy (AFM)

The atomic force microscopy (AFM) method uses surface topological changes to identify the captured proteins on an antibody array. The basic concept of AFM operation involves the movement of a sharp , nanometer-scale tip in a ordered pattern over a surface. As surface features are encountered by the AFM tip, the deflection of the cantilever is recorded and used to create a force-based map of the sample. This method allows the intermolecular forces between individual ligand-receptor pairs, complementary DNA strands, cell adhesion proteoglycans, and the specific antigen-antibody interaction to be determined [64,65]. For example, in the case of immunosensors, AFM detects the increase in height, due to the proten-protein interactions and thus is able to measure binding interactions.

Nanowires

Carbon nanowires and nanotubes, have been proven to have potential application in the field of label free detection in protein arrays [66]. They consist in a wire with a mean diameter of 30–100 nm and lengths of 5–10 nm. Once the protein binds to the functionalized nanowires connecting two electrodes, the change in the conductance

can be used for sensing. The multiplexed electrical detection of cancer markers using silicon-nanowire was demonstrated [67]. In this work protein markers were detected at femtomolar concentrations with high selectivity.

All label-free detection methods are promising tools to characterize binding events on surfaces. They do not require labelling of molecules that may affect protein activity. The major drawbacks of label-free detection principles are their limited sensitivity and the need for specialised equipment, which is not easily available in all the clinical laboratories.

Electrochemical impedance spectroscopy

Although not widely used in bioarrays detecting the biointeractions, this technique is low cost and promising. There are few reports in the detection of aptamer-protein interactions using this impedance.

1.2.3.2. Using labelled analytes

Fluorescence

Fluorescent dye labelling is the method of choice for labelling and detection of molecules in microarray applications especially for DNA hybridisation[1-3] [68-70]. This method is simple, safe, highly sensitive. Recently proteins to be probed were expressed with a green and red fluorescence protein tag and later used for performing protein interaction studies [70].

Colourimetric detection

Colourimetric detection is performed by using chromogens that are substrates for an enzymatic label. The most common microarray application of immunoenzymatic reactions involves labeling an antibody with an enzyme. The enzyme acts on a colourless substrate generating a colored precipitate. Commonly used enzymes for chromogenic reactions are horseradish peroxidase (HRP) and alkaline phosphatase

(AP). These enzymes act on a variety of colorless chemical substrates, each generating a different colored product.

Radio isotope assaying

Radioisotope labeling is used to study protein–protein, protein–DNA, protein–drug interactions on filter arrays [50,71]. Due to safety concerns and waste issues, it's not widely used anymore. Moreover it's not fully compatible with high throughput screening methodologies.

ELISA

Enzyme Linked Immunosorbent Assay was first used to detect proteins for both filter arrays and glass arrays. ELISA based detection methods have the disadvantage of non-specificity of protein-antibody interactions, leading to many false positives.

Electrochemistry

Electrochemical biosensor arrays are attractive analytical tools because they are robust, economical, easily quantifiable and can achieve excellent detection limits with small analyte samples. Furthermore electrochemical transduction needs low instrumentation with higher sensitivity and can be compatible with microfabrication technology. Recently, based on the electrochemical transduction, researchers were able to measure seven important tumor markers good accuracy and precision [72]. Based on the electrochemical detection, DNA sensor in an array was able to discriminate a 4 mutation sequence [73,74]. Electroactive diffusional mediators like $\text{Ru}(\text{bpy})_3^{3+}$, $\text{Co}(\text{bpy})_3^{3+}$ etc have been used for widely for the detection of biorecognition. Potentiometric stripping analysis was used for directly monitoring guanine oxidation at the target DNA. Recently impedance spectroscopy has been used for the labelless detection of the protein-protein interactions and DNA-protein interactions.

1.3. Electrochemical and Electrophoretic patterning

1.3.1. Electrodeposition of Colloidal gold

1.3.1.1. What is colloidal gold?

In this work, with the term “Colloidal gold” reference is made to nanoparticles of pure gold suspended in water. Colloidal gold consists of an elemental gold core with adsorbed ions on its surface, such as citrate or borate ions depending on its synthesis. These surface adsorbed ions play a key role in maintaining the suspension stable without aggregation. The size of the gold nanoparticles range from 2nm to 150nm in diameter, depending on the synthesis procedure. In general, gold nanoparticles are synthesized by the reduction of Au^{3+} , usually in the form of gold trichloride, using different reducing agents such as sodium citrate, sodium borohydride depending on the size of the nanoparticle. Citrate reduction methods produce a larger sized nanoparticles ranging from 20 nm to 100 nm and the borohydride reduction method produces smaller sized nanoparticles ranging from 3 to 20 nm. The size of the gold nanoparticles depends on the concentration of gold trichloride, the reducing agents used, their concentration, and the reaction time.

1.3.1.2 Why colloidal gold ?

Recently nanoparticles have found numerous applications in biological and chemical research. Nanoscale particles offer a variety of interesting properties, and there is growing interest in their usage for constructing biosensor platforms. Metal and semiconductor nanocrystals have tunable properties (e.g., optical, electronic, and magnetic) that depend on particle size. There are some free electrons on the surface of metallic nanoparticles. When light is shone to the nanoparticles, it interacts with the surface plasmons present on the surface of the particle and causes the free-electrons in the metal to oscillate by polarisation. This phenomenon is referred to as the surface plasmon resonance.

Depending on the size, shape of the nanoparticle, type of metal and its dielectric constant the resonance condition varies. As the shape or size of the nanoparticle

changes, the surface geometry changes causing a shift in the electric field density on the surface. Changing the dielectric constant of the surrounding material will have an effect on the surface plasmon resonance. Chemically bonded molecules can be detected by the observed change they induce in the electron density on the surface, which results in a shift in the surface plasmon absorption maximum. This is the basis for the use of noble metal nanoparticles as sensitive sensors, and can be used also to characterize the modification of the particles.

For nanoparticles, localized surface plasmon oscillations can give rise to the intense colors of solutions of nanoparticles and/or very intense scattering. Nanoparticles of noble metals exhibit strong Ultraviolet-Visible absorption bands that are not present in the bulk metal. Shifts in this resonance due to changes in the local index of refraction upon adsorption of biopolymers to the nanoparticles can also be used to detect biopolymers such as DNA or proteins.

Surface plasmon resonance is used by biochemists to detect the presence of a molecule on a surface, interparticle spacing, and higher order structure.

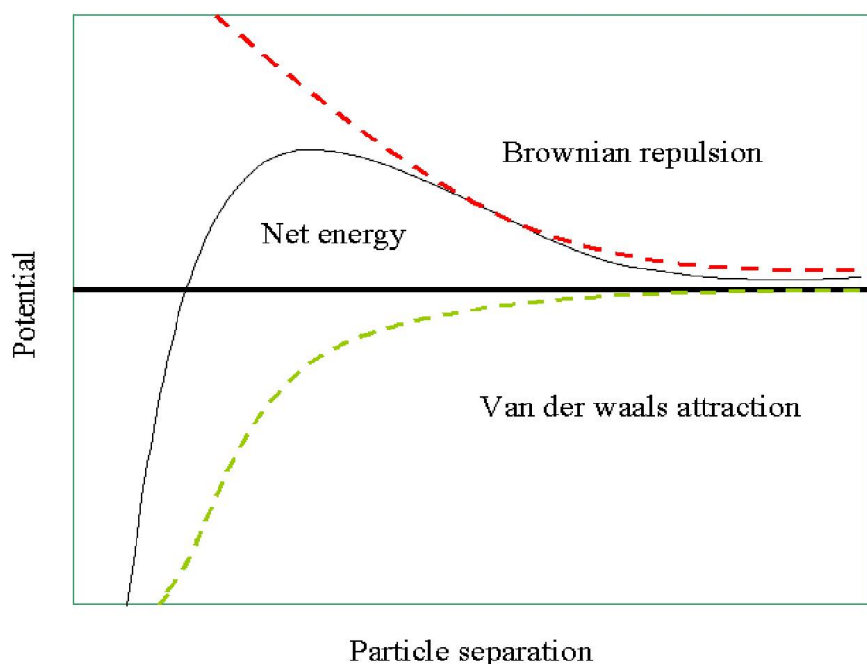
Nanoparticles can display four unique advantages over macroelectrodes when used for electroanalysis: enhancement of mass transport, catalytic efficiency, high effective surface area and control over electrode microenvironment. Among them, colloidal Au has gained much attention in biological studies because of its easy preparation, good biocompatibility, and relatively large surface. Colloidal Au is an extensively used metal colloid, which has been applied in the study of direct electrochemistry of proteins. It provides an environment similar to that of redox proteins in native systems and gives the protein molecules more freedom in orientation, thus reducing the insulating property of the protein shell for the direct electron transfer through the conducting tunnels of colloidal Au [76]. The gold nanoparticles were proven as an electron relay or “electrical nanoplug” for the alignment of the enzyme on the conductive support and for the electrical wiring of its redox - active centre.

Hence colloidal Au has been used widely in the fields of biochemistry as a modifier for antibodies (immunogold) and a protein label. Three types of interactions are possible with the gold nanoparticles. One is the well known gold-thiol bonding, the

second is direct adsorption and finally electrostatic interactions. These give versatility to Au nanoparticles as carriers of biochemical and biorecognition properties

1.3.1.3. Stability of Au nanoparticle suspensions

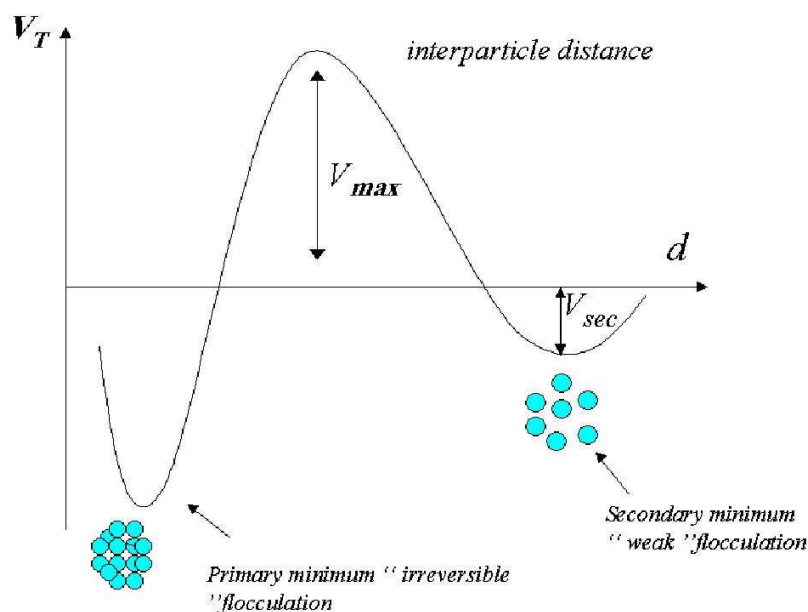
Stability of Au colloid suspensions is very important in the field of nanotechnology. One of the major problems encountered during the direct electrodeposition of colloidal gold is the interparticle interaction leading to aggregation. Upon aggregation particles lose their ability to deposit as well as the surface plasmon resonance characteristic of individual gold nanoparticles. Generally the Derjaguin-Landau-Verwey-Overbeek (DLVO) theory explains the stability of colloids in terms of a repulsive (double-layer) force and an attractive (van der Waals) one. DLVO theory suggests that the stability of a colloidal system is determined by the sum of these van der Waals attractive (V_A) and electrical double layer repulsive (V_R) forces that exist between particles as they approach each other due to Brownian motion.



Scheme 1.2.2. Schematic diagram of the variation of free energy with particle separation according to DLVO theory. The net energy is given by the sum of the double layer repulsion and the van der Waals attractive forces that the particles experience as they approach one another

As observed from the scheme 1.2.2, this theory explains that there exists an energy due to the repulsive force between the particles preventing the two adjacent particles from aggregation. If the particles have sufficient energy to break that barrier, then repulsive forces will be replaced by vanderWaals attractive forces and thus leading to aggregation.

From the figure 1.2.3, it can be observed that there exists a secondary minimum in certain conditions like higher salt concentrations where particles are coagulated but not aggregated completely. In this case the coagulation is not strong enough and can be reversible. Reduction in the rate of coagulation is due to the formation of an electrical double layer at the particle-fluid interface. When two particles approach one another their double layers interact giving rise to repulsive forces, which oppose coagulation.



Scheme 1.2.3. Schematic diagram of the variation of free energy with particle separation at higher salt concentrations showing the possibility of a secondary free energy.

Electrostatic repulsive forces are the main source of stabilization of the suspension, due to common surface charge on the particles. However, the colloidal stability, which is governed by the total interparticle energy V_T , can be mathematically expressed as follows

$$V_T = V_A + V_R \quad \text{Eq 1.1}$$

where V_A is the attractive potential energy due to long van der Waals interactions between the particles, V_R the repulsive potential energy resulting from electrostatic interactions between like charged particles surfaces.

$$V_A = - \frac{A\alpha}{12S} \quad (\text{Eq 1.2})$$

$$V_R = 2\pi \epsilon_0 \epsilon_b \alpha \psi_0^2 \ln(1 + e^{-ks}) \quad (\text{Eq 1.3})$$

A is the Hamaker constant, S is the interparticle distance, α is the particle radius, ϵ_0 is the permittivity of free space, ϵ_b is the dielectric constant of the medium, ψ_0 is the surface potential and k is the Debye–Huckel constant.

In order to deposit Au nanoparticles on an electrode surface electrophoretically (which is an objective of this work), the particles must be highly stable in the solution. For the suspension to be stable there must be an interparticle repulsive force preventing the particles from Vander Waals attractive forces. Therefore to maintain the stability of the colloidal system, the repulsive forces must be dominant.

1.3.1.4. Electrophoretic deposition theory

Electrophoretic particle deposition (EPD), is a process in which stable charged colloidal particles suspended in a liquid medium migrate under the influence of an electric field (electrophoresis) and are deposited onto an electrode.

Since colloidal metals are usually charged , a promising approach is to utilize an external driving force which makes the particles move towards the electrode surface. This process known as electrophoretic particle deposition (EPD), permits external regulation of surface nanoparticle density and film growth. There are very few cases where gold nanoparticles have been employed for the formation of metallic thin films, especially selectively (i.e for arraying).

In order to perform electrophoretic deposition, an applied force that drives the colloidal particles towards the substrate must overcome the natural forces of gravitation, buoyance and friction [3].

The natural force on the particles is given by the equation

$$F_N = v 3\pi \eta d \quad (\text{Eq 1.4})$$

Where v is the velocity of the colloid, η is the viscosity of the medium , and d is the diameter of the colloid .

The velocity at which colloid moves in the absence of an electric field is described by the following equation

$$v = [d^2 (\rho_s - \rho_w) g] / 18 \eta \quad (\text{Eq 1.5})$$

where ρ_s is the density of the colloid, ρ_w is the density of the medium and g is the acceleration due to gravity.

The magnitude of the force that a colloid experiences in the presence of an electric field is given by

$$F_E = Q_E E \quad (\text{Eq 1.6})$$

Where Q_E is the surface charge, which is given by

$$Q_E = u_E 3\pi \eta d \quad (\text{Eq 1.7})$$

Where μ_E is the electrophoretic mobility of the colloid and E is the applied voltage. The electrophoretic mobility can be estimated from the zeta potential of the particles which can be determined experimentally. When the magnitude of the force that a colloid experiences in the presence of electric field is greater than the natural forces on the particles then the particles can be manipulated by the field.

Sometimes, the term electrodeposition is referred to as electrochemical deposition or electroplating where an ionic solution of the metal is reduced to a metal by electrochemistry. There can be two types of electrophoretic deposition depending on which electrode the deposition occurs. When the particles are positively charged, the deposition happens on the cathode and the process is called cathodic electrophoretic deposition. The deposition of negatively charged particles on positive electrode (anode) is termed as anodic electrophoretic deposition. Depending on the surface charge of the particle any of the two types of deposition is possible.

1.3.1.5. Electrodeposition in biosensor development

Application of the electrodeposition technique allows preparation of colloidal Au-based enzyme electrode array easily and simply, because the negatively charged colloidal Au could be deposited on an electrode surface by applying positive potentials. Colloidal Au modified on a solid electrode behaves as an ensemble of closely spaced but isolated microelectrodes. Thus it is a suitable material for fabrication of nano-scale biosensors.

Despic and Pavlovic first introduced the electrophoretic deposition technique for the deposition of Au nanoparticles on the electrode surface. Since then, this technique has been used for the creation of biosensors by modifying the Au nanoparticles with redox enzymes and later electrophoretically depositing them on the electrode surfaces. Crumbliss et al [75] have developed biosensors for peroxide, glucose and other analytes based on this technique (i.e. never using the technique for arraying (i.e. directed electrode position)).

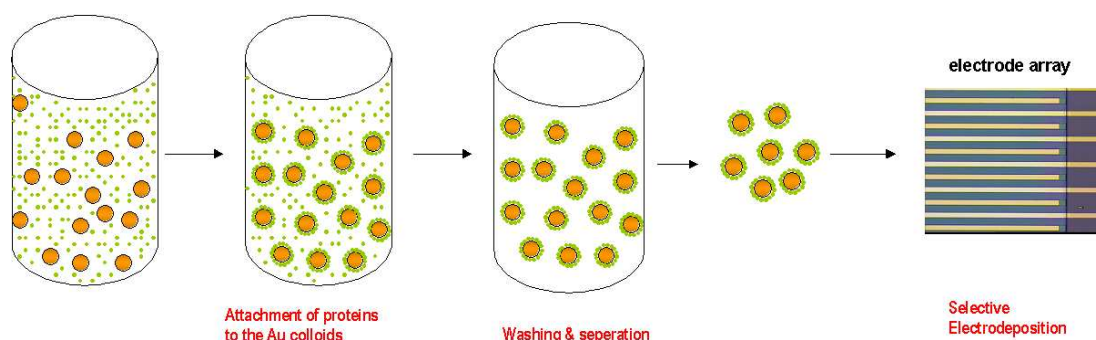
Electrodeposition of redox polymers and glucose oxidase has been reported with excellent catalytic activity based on crosslinking. Though these reports are used for creating single molecule biosensors this technique has not been used to address and immobilize these bionanomodules to specific locations of an array for the development of biosensor arrays. For the first time, selective electrodeposition of oligonucleotide modified Au nanoparticles for the detection of hybridization event successfully using electrochemistry by differentiating the mutated DNA from the experimental DNA has been reported by campas et al [74].

Over the years, a large number of methods have been used for the electrochemical deposition of enzymes on electrodes as part of the fabrication of electrochemically based biosensors. Electrochemically controlled co-deposition of enzymes with other proteins such as collagen and bovine serum albumin (BSA) has been reported [78,79]. Co-deposition of enzyme glucose oxidase (GOx) with a Pt salt to form a Pt black surface has been reported where GOX sensors were prepared by first electrodeposition of GOX / BSA (bovine serum albumin) mixture on platinized Pt and subsequent crosslinking with glutaraldehyde[80]. Using this electrophoretic deposition approach, controlled immobilization of glucose oxidase (GOX) on a platinum electrode has been achieved in the presence of a nonionic detergent, Triton X-100 producing a multilayer films [81]. A procedure is described that provides for electrochemically mediated deposition of enzyme and a polymer layer permselective for endogenous electroactive species where electrodeposition was first employed for the direct immobilization of glucose oxidase to produce a uniform, thin, and compact film on a Pt electrode followed by the electropolymerization of phenol to form an anti-interference and protective polyphenol film within the enzyme layer [82]. Layer-by-layer electrodeposition of redox polymer/enzyme composition films on screen-printed carbon electrodes for fabrication of reagentless enzyme biosensors has been used for producing very stable and rigid films [83]. Glucose biosensors based on the one-step co-electrodeposition of a poly(vinylimidazole) complex of [Os(bpy)₂Cl]^(+/2+) (PVI-Os) and glucose oxidase (GOX) on a gold electrode surface has been developed [84]. Electrodeposition of hydrated redox polymers and co-electrodeposition of enzymes through coordinate crosslinking has been proved to produce a stable enzymes films with excellent catalytic activity [84]. All these efforts were directed towards using the electrophoretic deposition to achieve maximum enzyme loading as well as higher

activity. Though all the research work done by using electrophoretic deposition was used for creating single molecule biosensors, this technique has not been used to address and immobilize these bionanomodules to specific locations of an array for the development of biosensor arrays. This is probably due to the non-specific deposition or aggregation due to vanderWaals forces already discussed.

Selective electrodeposition of biofunctional gold nanoparticles for electrochemical biosensor array

In this work, for the first time, a novel way of patterning enzymes was done by modifying the gold nanoparticles with the enzymes as shown in the scheme 1.2.4. First gold nanoparticles were added to the enzyme mixture. After mixing, the enzyme modified gold nanoparticles were washed and separated from the unmodified particles. Later these stable enzyme gold nanoparticles were electrodeposited by electric potential control.



Scheme 1.2.4. Preparation and electrodeposition of biofunctionalized gold nanoparticles on an electrode array

In order to have higher catalytic response, these gold nanoparticles were modified with a redox polymer for better electron transfer and later modified with the enzymes to have multifunctional nanomodules. After electrodeposition the sensors showed a very high substrate specific response with minimal non-specificity.

1.3.2. Electrochemically controlled patterning methods for biosensor arrays

1.3.2.1. Electrochemical switching for biomolecule patterning

Recently surfaces with switchable properties, which can be controlled by electrochemical potential, have been developed for the immobilisation of biomolecules and cells. These surfaces could be electrically switched from a state that prevents the attachment of the cells or biomolecules to a state that promoted cell or biomolecule attachment which in turn provides a strategy for the selective immobilisation of the biomolecules. These surfaces offer a new dimension in the design of advanced materials providing an electrochemical route to turn on the presentation of immobilized ligands. Dynamic substrates based on a SAM presenting hydroquinone groups on a background of ethylene glycol groups has been developed for the immobilisation of cells [7,84,85]. In this case, hydroquinone groups has been oxidised when an electric potential is applied to the underlying gold film to give the corresponding quinone, which then undergoes a selective and efficient Diels-Alder reaction with cyclopentadine functionality forming a covalent adduct. Based on hydroquinone to quinone conversion and Diels Alder reaction, patterning of two different types of cells has been achieved.

As a part of this, surfaces formed by the electroactive self-assembled monolayers have been developed. These electroactive substrates mask the active group essential for the binding of the selective biomolecule. Kim and Kawk have developed an electroactive hydroquinone monoester which masks the carboxylic acid functionality essential for binding to the amine containing biomolecules [87-89]. Upon electrochemical oxidation of the hydroquinone, quinone is released and the carboxylic acid functionality is deprotected. Later with the help of EDC + NHS, the amine containing biomolecules were attached to the active group over the electrode surface. The advantage of this strategy is that is very quantitative, rapid and that it generated specific binding sites under mild conditions.

Dynamic surface formed by the self-assembly of thiolated electroactive acetal substrate which reveals an aldehyde group upon electrochemical oxidation have been reported. This technique is based on the protection of the aldehyde moiety in the form of an acetal mask. Upon application of electrochemical potential, the acetal functionality can be activated very rapidly by electrochemistry to reveal an aldehyde

group, which can be used for the immobilisation of amine-containing ligands. The advantage of this strategy compared to the previously mentioned strategies is that the label is directly reactive and the interaction can be monitored in real time. This substrate has been used for cell migration studies [90]. Strategies for controlling the interface between a cell and a material have been developed for cell based sensing technologies.

1.3.2.2. Electrodesorption for biomolecule patterning

Based on the electrodesorption, a simple, integrated patterning technique based on the electrochemical control called “Locally Addressable Electrochemical Patterning Technique” (LAEPT) has been developed [91]. In this methodology specific adsorption / desorption of biomolecules onto selected regions has been achieved while simultaneously preventing non-specific adsorption on the surrounding areas. Using the electrochemical desorption technique, proteins were adsorbed after desorption of the ethylene glycol self assembled surfaces by applying a potential of $> -1.2V$ (vs Ag/AgCl) [92].

1.3.2.3. Electropolymerisation for selective protein and DNA conjugation

Based on the polyphenol free radical electropolymerisation, insulating films are formed on specific electrodes with multiple reactive functionalities (aldehyde, amine and carboxylic acid groups) capable of conjugating small molecules, proteins and DNA oligonucleotide [28]. The most significant advantage of this methodology is that it offers multiple conjugation chemistries, is not surface specific and is stable in aqueous solutions. All the chemicals used for the synthesis are available commercially.

1.3.2.4. Electrochemical addressing for patterning of biomolecules

The basic principle behind this technique is the attachment of free radical to the electrode surface. Diazonium salts have been widely used for the selective patterning of biomolecules. In this case, the aniline derivative is diazotized to form an aryl diazonium. Later the reduction of aryl diazonium gives an aryl radical which can be

attached to the electrode surface selectively by a free radical – electrode bonding. Using this approach, the biomolecules can be conjugated to the aniline derivatives and further deposited on the electrode surfaces. Electrochemically directed addressing of proteins on to graphite electrodes has been reported by linking the proteins to the diazonium derivatives [93,94].

Electrochemical addressing through electrochemical reduction of nitro groups to amine groups and further covalent linkage covalently to DNA using heterofunctional cross-linker sulfo-succinimidyl 4-(N-maleimidomethyl)cyclohexan-1-carboxylate (SSMCC) has been demonstrated [95]. In this approach, nitrogroup functionalized groups were immobilised on the electrode surface using diazonium chemistry. Later the amine groups are reduced for the immobilization of biomolecules.

Recently “click” chemistry which is a 1,3-dipolar cycloaddition between an azide and a terminal alkyne to a 1,2,3-triazole in the presence of copper (I) catalyst has been used to independently address microelectrodes [96]. 1,2,3-triazole formation between terminal acetylenes and the organic azides is efficiently catalyzed by copper (I) complexes, since the oxidized copper (II) complexes are inactive. Using the switching of the redox state by electroactivating and deactivating the catalyst the above reaction can be controlled electrochemically.

Very recently, selective electrodeposition of oligonucleotide modified Au nanoparticles on an IDE array for the detection of the hybridisation event using electrochemistry by differentiating the mutated DNA from the control DNA has been reported [74]. Controlling the surface functionality by electric signals in order to electrically address the fabrication of biosensor arrays has been reported [95,97].

The objective of all the above methods is to control the patterning of biomolecules electrochemically.

In this thesis, three different electrochemically controlled patterning methods have been used for the selective patterning of biomolecules. The first method is the selective electrodeposition of biofunctionalized gold nanoparticles just by controlling potentials. The second is the selective electrochemical deprotection of aldehyde for the selective immobilization of the enzymes. The third is selective electrodeposition of the viologen functionalised biomolecules through radical-electrode interactions. All three methods have shown excellent selectivity with minimal non-specific adsorption.

1.4. ORGANIZATION OF THE THESIS

The overall objective of this thesis is to develop new methods of patterning biomolecules for creating biosensor arrays with a special focus on the simplicity and versatility. Proteins especially enzymes were used as model biomolecules for these studies. If successful, these patterning methods should make a substantial contribution in the field of low cost biosensor arrays. The whole work describes four different types of patterning methods. In all the cases extensive patterning was not attempted, but rather an effort was made to optimise selectivity on a pair of electrodes, one used as the study electrode and the other as control to quantify non-specific events.

Overview of the thesis chapters:

Chapter 1 introduces an overall view of biosensor arrays, different methods for arraying with focus on the recent developments in the field of biosensor arrays, fundamentals of electrodeposition which includes theory of electrophoretic deposition and its applications towards biosensors and finally electrochemical addressing methods available in the literature. One of the main conclusions is that despite the great progress made in deciphering selective patterning, there is a lack of understanding at the microscopic level.

The next three chapters present an electrochemically controlled patterning of biomolecules through addressed electrodeposition of functionalised gold nanoparticles for producing biosensor arrays. Chapter 2 presents the methods to produce stable biofunctionalised Au nanoparticles. There are many obstacles while preparing enzyme modified Au nanoparticles, mainly in the form of aggregation, due to presence of multiple functional moieties essential for attachment to the Au nanoparticle. In order to avoid this problem, proteins were immobilised on the Au nanoparticle by using different Au colloid interactions such as gold-thiol dative bonding, steric interactions and electrostatic interactions. Biofunctionalised gold colloids were characterized using different colloidal characterization techniques. The main conclusion from this chapter is that stable biofunctionalised gold nanoparticles have been prepared and characterized which can be further used for producing

biosensor arrays. Chapter 3 presents the fundamental studies on the electrodeposition of biofunctionalised gold nanoparticles by studying the effect of various parameters during the electrodeposition process. As a result of these studies, the behaviour of the electrodes after electrodeposition of the biofunctionalised gold nanoparticles can be understood. Chapter 4 deals with the selective electrodeposition of the biofunctionalised gold nanoparticles for producing electrochemical biosensor arrays. Two different methods were used for achieving this. The first method is based on the selective electrophoretic deposition of biomolecule functionalised Au nanoparticles by just controlling potentials. The advantage of this technique is, increase in the surface area due to the use of nanometer sized gold particles, excellent catalytic activity, biocompatibility due to the retention of the enzyme activity. The second method is the controlled electrodeposition of multifunctional nanoparticles formed by layer-by-layer modification of gold nanoparticles with redox polymer and glucose oxidase for application towards biosensors. Both these methods showed good selectivity and acceptable amperometric response.

Chapter 5 presents an electrochemically controlled patterning method for biosensor where an acetal functionality self assembled on the gold electrode is activated to produce an aldehyde functionality, which was further used for conjugation to the biomolecules. This method showed good selectivity by simply controlling the potentials of the electrodes for the immobilization of the required biomolecules.

Chapter 6 presents an electrochemically controlled patterning method where biomolecule was selectively immobilised on the 4,4'-bipyridinium functionalised surfaces, again by simply controlling the electrode potential.

Chapter 7 presents the selective protein patterning at the microscale level on an interdigitated array through photolithography. Proteins were photolithographed with higher selectivity due to the use of biocompatible photoresist and can be used for producing biosensor arrays.

Chapter 8 reaches the conclusions of the work and provide an outlook on different methods explained for the controlled patterning of biomolecules along with the future extensions possible.

It should be noted that throughout the thesis the term “arraying” refers to the proof of principle of patterning by demonstrating and quantifying the non-specific events between the study electrode and a control.

1.5. Abbreviations

AP-Alkaline phosphatase

AFM-Atomic force microscopy

DPN-Dip pen nanolithography

DNA – Deoxyribonucleic acid

ELISA- Enzyme Linked Immunosorbent Assay

HRP-Horse radish peroxidase

QCM-Quartz crystal microbalance

PDMS- polydimethylsiloxane

SPR-Surface plasmon resonance

1.6. References

1. Campas, M., Katakis, I., *TrAC*, 2004. 23: p. 49-62.
2. Fodor, S.P., Read, J.L., Pirrung, M.C., Stryer, L., Lu, A.T., Solas, D, *Science*, 1991. 251: p. 767-773.
3. Lucas, S.W., and Harding, M.M, *Anal. Biochem*, 2000. 282: p. 70-79.
4. Millan, K.M., Mikkelsen, S.R, *Anal. Chem*, 1993. 65: p. 2317-2323.
5. Nielsen, U.B., Cardone, M. H., Sinskey, A. J., MacBeath, G., Sorger, P. K, *Proc. Natl. Acad. Sci. U.S.A.*, 2003. 100: p. 9330-9335.
6. Ivanov, S.S., Chung, A. S., Yuan, Z. L., Guan, Y. J., Sachs, K. V., Reichner, J. S., Chin, Y. E, *Mol. Cell. Proteomics*, 2004. 3: p. 788-795.
7. Yousaf, M.N., Houseman, B.T., Mrksich, M, *Angew. Chem. Int. Ed*, 2001. 40: p. 1093-1096.
8. Cho, E.J., Collett, J.R., Szafranska, A.E., Ellington, A.D, *Anal. Chim. Acta*, 2006. 564: p. 82-90.
9. McCauley, T.G., Hamaguchi, N., Stanton, M, *Anal. Biochem*, 2003. 319: p. 244-250.

10. Brody, E.N., Willis, M.C., Smith, J.D., Jayasena, S., Zichi, D., Gold, L., *Mol. Diagn.*, 1999. 4: p. 381-388.
11. Xu, D., Han, H., He, W., Liu, Z., Xu, D., Liu, X., *Electroanalysis*, 2006. 18: p. 1815-1820.
12. Liu, Y., Lin, C., Li, H., Yan, H., *Angew. Chem. Intl. Ed.*, 2005. 44: p. 4333-4338.
13. Cretich, M., Damina, F., Pirria, G., Chiari, M., *Biomol. Eng.*, 2006. 23: p. 77-88.
14. Liu, R., Enstrom, A.M., Lam, K.S., *Exp. Hem.*, 2003. 31: p. 11-30.
15. Min, D.H., Mrksich, M., *Curr. Opin. in Chem. Bio.*, 2004. 8: p. 554-558.
16. Gu, M.B., Mitchell, R.J., Kim, B.C., *Adv. Biochem. Eng. Biotechnol.*, 2004. 87: p. 269-305.
17. Hinde, P., Meadows, J., Saunders, J., Edwards, C., *Adv. Appl. Microbiol.*, 2003. 52: p. 29-74.
18. Feizi, T., Fazio, F., Chai, W., Wong, C.H., *Curr. Opin. Struct. Biol.*, 2003. 13: p. 637-645.
19. Wang, D., Liu, S., Trummer, B.J., Deng, C., Wang, A., *Nat. Biotechnol.*, 2002. 20: p. 275-281.
20. Lange, J., Wittmann, C., *Anal. Bioanal. Chem.*, 2002. 372: p. 276-283.
21. Kusnezow, W., Hoheisel, J.D., *J. Mol. Recognit.*, 2003. 16: p. 165-176.
22. Bussow, K., Cahill, D., Nietfield, W., Bancroft, D., Scherzinger, E., Lehrach, H., Walter, G., *Nucleic Acids Res.*, 1998. 26: p. 5007-5008.
23. Oh, B.K., Kim, Y.K., Park, K.W., Lee, W.H., Choi, J.W., *Biosens. Bioelectron.*, 2004. 19: p. 1497-1504.
24. Martin, K., Steinberg, T.H., Cooley, L.A., Gee, K.R., Beechem, J.M., Patton, W.F., *Proteomics*, 2003. 3: p. 1244-1255.
25. Dondapati, S.K., Montornes, J.M., Sanchez, P.L., Sanchez, J.L.A., Sullivan, C.O., Katakis, I., *Electroanalysis*, 2006. 18: p. 1879-1884.
26. Zhu, H., Bilgin, M., Bangham, R., Hall, D., Casamayor, A., Bertone, P., Lan, N., Jansen, R., Bidlingmaier, S., Houfek, T., Mitchell, T., Miller, P., Dean, R.A., Gerstein, M., Snyder, M., *Science*, 2001. 293: p. 2101-2105.
27. Arenkov, P., Kukhtin, A., Gemmell, A., Voloshchuk, S., Chupeeva, V., Mirzabekov, A., *Anal. Biochem.*, 2000. 278: p. 123-131.
28. Stern, E., Jay, S., Bertram, J., Boese, B., Kretzschmar, I., Evans, D.T., Dietz, C., LaVan, D.A., Malinski, T., Fahmy, T., Reed, M., *Anal. Chem.*, 2006. 78: p. 6340-6346.
29. Ghindilis, A.L., Smith, M.W., Schwarzkopf, K.R., Roth, K.M., Peyvan, K., Munro, S.B., Lodes, M.J., Stover, A.G., Bernards, K., Dill, K., McShea, A., *Biosens. Bioelectron.*, 2006: p. Article in press.
30. Dill, K., Ghindilis, A., Schwarzkopf, K., *Lab. Chip*, 2006. 6: p. 1052-1055.

31. Tesfu, E., Maurer, K., Ragsdale, S.R., Moeller, K.D, *J. Am. Chem. Soc.*, 2004. 126: p. 6212-6213.
32. Kane, R.S., T.S., Ostuni, E., Ingber, D.E., Whitesides, G.M., *Biomaterials*, 1999. 20: p. 2363-2376.
33. Lee, K.B., Park, S.J., Mirkin, C.A., Smith, J.C., Mirkin, M., *Science*, 2002. 295: p. 1702-1705.
34. Zhang, H., L.K., Li, Z., Mirkin, C.A., *Nanotechnology*, 2003. 14: p. 1113-1117.
35. Okamoto, T., Suzuki, T., Yamamoto, N., *Nat. Biotechnol.*, 2000: p. 438-441.
36. Tsai, J.G.F., Chen, Z., Nelson, S.F., Kim, C.-J., *App. Phys. Lett.*, 2006, 89, 083901(1-3)
37. McQuain, M.K., Seale, K., Peek, J., Levy, S., Haselton, F.R., *Anal. Biochem.*, 2003, 320, 281-291
38. Mossoba, M.M., Al-Khalidi, S.F., Kirkwood, J., Fry, F.S., Sedman, J., Ismail, A.A., *Vibr. Spectr.*, 2005, 38, 229-235
39. Barbulovic-Nad, I., Lucente, M., Sun, Y., Zhang, M., Wheeler, A.R., Bussmann, M., *Crit Rev Biotech.*, 2006, 26, 237-259
40. Colina, M., Duocastella, M., Fernández-Pradas, J.M., Serra, P., Morenza, J.L., *J. App. Phys.*, 2006, 99, 084909 (1-7)
41. Serra, P., Fernández-Pradas, J.M., Berthet, F.X., Colina, M., Elvira, J., Morenza, J.L., *App. Phys A: Mat. Sci. Proc.*, 79, 949-952
42. Colina, M., Serra, P., Fernández-Pradas, J.M., Sevilla, L., Morenza, J.L., *Biosens Bioelectron.*, 2005. 6: p. 1638-1642.
43. McDonnell, J.M., *Curr. Opin. Chem. Biol.*, 2001. 5: p. 572-577.
44. Peterlinz, K.A., Georgiadis, R.M., *J. Am. Chem. Soc.*, 1997. 119: p. 3401-3402.
45. Usui-Aoki, K., Shimada, K., Nagano, M., Kawai, M., Koga, H., *Proteomics*, 2005. 5: p. 2396-2440.
46. Sreekumar, A., Nyati, M.K., Varambally, S., Barrette, T.R., Ghosh, D., Lawrence, T.S., Chinnaiyan, A.M., *Cancer Res.*, 2001. 61: p. 7583-7593.
47. Knezevic, V., Leethanakul, C., Bichsel, V.E., Worth, J.M., Prabhu, V.V., Gutkind, J.S., Liotta, L.A., Munson, P.J., Petricoin III, E.F., Krizman, D.B., *Proteomics*, 2001. 1: p. 1271-1278.
48. Fall, B.I., Eberlein-Konig, B., Behrendt, H., Niessner, R., Ring, J. and Weller, M.G., *Anal. Chem.*, 2003. 75: p. 556-562.
49. Falsey, J.R., Renil, M., Park, S., Li, S., Lam, K.S., *Bioconj. Chem.*, 2001. 12: p. 346-353.
50. Ge, H., *Nucleic Acids Res.*, 2000. 28: p. e3.
51. Weng, S., Gu, K., Hammond, P.W., Lohse, P., Rise, C., Wagner, R.W., Wright, M.C., Kuimelis, R.G., *Proteomics*, 2002. 2: p. 48-57.

52. Rissin, D.M., Walt,D.R, *Anal.Chim.Acta*, 2006. 564: p. 34-39.
 53. Lee, Y., Lee,E.K., Cho,Y.W., Matsui,T., Kang,I.C., Kim,T.S., Han,M.H, *Proteomics*, 2003. 3: p. 2289–2304.
 54. Matsuno, H., Niikura,K., Okahata,Y, *Biochemistry*, 2001. 40: p. 3615-3622.
 55. Johnsson, B., Lofas,S., Lindquist,G, *Anal.Biochem*, 1991. 198: p. 268-277.
 56. Ramachandran, N., Larson,D.N., Stark,P.R., Hainsworth,E., LaBaer,J, *FEBS. J*, 2005. 272: p. 5412-5425.
 57. Unfricht, D.W., Colpitts,S.L., Fernandez,S.M., Lynes,M.A, *Proteomics*, 2005. 5: p. 4432-4442.
 58. Batorfi, J., Ye, B., Mok, S.C., Cseh, I., Berkowitz, R.S., Fulop, V, *Gynecol. Oncol*, 2003. 88: p. 424-428.
 59. Figeys, D., *Proteomics*, 2002. 2: p. 373-382.
 60. Liotta, L., Petricoin, E, *Nat. Rev. Genet*, 2000. 1: p. 48-56.
 61. Liotta, L.A., Kohn, E.C., Petricoin, E.F, *JAMA*, 2001. 286: p. 2211-2214.
 62. Merchant, M., Weinberger,S.R, *Electrophoresis*, 2000. 21: p. 1164-1177.
 63. Bischoff, R., Luider,T.M, *J. Chromatogr. B Anal. Technol. Biomed. Life Sci*, 2004. 803: p. 27-40.
 64. Dammer, U., Popescu, O., Wagner, P., Anselmetti, D., Güntherodt, H.-J., Misevic, G.N, *Science*, 1995. 267: p. 1173-1175.
 65. Lee, G.U., Chrisey, L.A., Colton, R.J., *Science*, 1994. 266: p. 771-773.
 66. Ramachandran, N., Larson,D.N., Stark,P.R., Hainsworth,E., LaBaer,J, *FEBS. J*, 2005. 272: p. 5412–5425.
 67. Zheng, G., Patolsky,F., Cui,Y., Wang,W.U., Lieber,C.M, *Nat. Biotechnol*, 2005. 23: p. 1294-1301.
 68. Coleman, M.A., Lao,V.H., Segelke,B.W., Beernink,P.T, *J. Proteome Res*, 2004. 3: p. 1024-1032.
 69. Houseman, B.T., Huh,J.H., Kron,S.J.,Mrksich,M, *Nat. Biotechnol*, 2002. 20: p. 270-274.
 70. Kukar, T., Eckenrode,S., Gu,Y., Lian,W.,Megginson,M., She,J.X., Wu,D, *Anal.Biochem*, 2002. 306: p. 50-54.
 71. Falsey, J.R., Renil,M., Park,S., Li,S., Lam,K.S, *Bioconjug .Chem*, 2001. 12: p. 346–353.
 72. Wilson, M.S., Nie,W, *Anal.Chem*, 2006. 78: p. 6476-6483.
 73. Campàs, M., Katakis,I, *Sens.Act.B*, 2006. 114: p. 897-902.
 74. Campàs,M., Katakis,I, *Anal.Chim.Acta*, 2006. 556: p. 306-312.
 75. Crumbliss, A. L., Perine, S.C., Stonehuerner.J., Tubergen, K.R., Zhao, J., Henkens, R.W., O'Daly,J.P, 1992, *Biotech. Bioeng*, 40, 483 - 490.
-

76. Li, H., Rothberg, L., 2004, *Proc. Natl. Acad. Sci. U S A*, 101, 14036-14039.
77. Bailey, R. C., Stevenson, K.J., Hupp, J.T., 2000, *Adv. Mat.*, 12, 1930-1934.
78. Wang, S. S., Vieth, W.R., 1973, *Biotechnol. Bioeng.*, 15, 93-115.
79. Johnson, K. W., Allen, D.J., Mastrototaro, J.J., Morff, R.J., Nevin, R.S., 1994, *ACSSymp. Ser.*, 556, 84-95.
80. Kim, C. S., Oh, S.M., 1996, *Electrochim. Acta*, 41, 2433-2439.
81. Matsumoto, N., Chen, X., Wilson, G.S., 2002, *Anal. Chem.*, 74, 362-367.
82. Chen, X., Matsumoto, N., Hu, Y., Wilson, G.S., 2002, *Anal. Chem.*, 74, 368-372.
83. Gao, Q., Yang, X., 2004, *Chem. Comm.*, 7, 30-31.
84. Gao, Z., Binyamin, G., Kim, H.H., Barton, S.C., Zhang, Y., Heller, A., 2002, *Angew. Chem. Int. Ed.*, 41, 810-813.
85. Yeo, W.S., Hodneland, C.D., Mrksich, M., *ChemBioChem*, 2001. 7: p. 590-593.
86. Yousaf, M.N., Houseman, B.T., Mrksich, M., *Proc. Natl. Acad. Sci.*, 2001. 98: p. 5992-5996.
87. Kim, K., Yang, H., Kim, E., Han, Y.B., Kim, Y.T., Kang, S.H., Kwak, J., *Langmuir*, 2002. 18: p. 1460-1462.
88. Kim, K., Yang, H., Jon, S., Kim, E., Kwak, J., *J. Am. Chem. Soc.*, 2004. 126: p. 15368-15369.
89. Kim, K., Jang, M., Yang, H., Kim, E., Kim, Y.T., Kwak, J., *Langmuir*, 2004. 20: p. 3821-3823.
90. Yeo, W., S., Mrksich, M., *Adv. Mater.*, 2004. 16: p. 1352-1356.
91. Tang, C.S., Schmutz, P., Petronis, S., Textor, M., Keller, B., Voros, J., *Biotechnol. Bioeng.*, 2005. 91: p. 285-295.
92. Jiang, X., Ferrigno, R., Mrksich, M., Whitesides, G.M., *J. Am. Chem. Soc.*, 2003. 125: p. 2366-2367.
93. Corgier, B.P., Marquette, C.A., Blum, L.J., *J. Am. Chem. Soc.*, 2005. 127: p. 18328-18332.
94. Corgier, B.P., Marquette, C.A., Blum, L.J., *Biosens. Bioelectron.*, 2006: p. in press.
95. Lee, C.S., Baker, S.E., Marcus, M.S., Yang, W., Eriksson, M.A., *Nano. Lett.*, 2004. 4: p. 1713-1716.
96. Devaraj, N.K., Dinolfo, P.H., Chidsey, C.E.D., Collman, J.P., *J. Am. Chem. Soc.*, 2006. 128: p. 1794-1795.
97. Yang, W., Baker, S.E., Butler, J.E., Lee, C.S., Russell, J.N., Shang, L., Sun, B., Hamers, R.J., *Chem. Mater.*, 2005. 17: p. 938-940

Chapter 2. Preparation and characterisation of biofunctionalised gold nanoparticles

2.1. Abstract

The aim of this work is to prepare and characterise biomolecule functionalised gold nanoparticles. Stable suspensions of such bionanomodules can be used for their application in biosensors. Gold nanoparticles were synthesized and characterised. Biomolecules were attached to the surface of gold nanoparticles using three different approaches: gold-thiol dative bonding, direct adsorption and electrostatic layer-by-layer modification.

For the preparation of bionanoconjugates using gold-thiol dative bonding, native enzymes were modified by incorporating sulfhydryl groups on their surfaces using different thiolation protocols. The thiolated enzymes were conjugated with the gold nanoparticles and characterised. Bovine serum albumin (BSA) modified gold nanoparticles prepared based on the second approach showed a high stability at different pH. Finally using the third approach, negatively charged gold nanoparticles were modified with cationic osmium redox polymer (RP) to achieve higher electron transfer rates. In a second step, RP modified gold nanoparticles were further modified with anionic enzymes.

Biofunctionalized gold nanoparticles were characterised by measurement of their zeta potential, UV-Visible spectroscopy and transmission electron microscopy (TEM).

2.2. Introduction

Surface functionalisation of gold nanoparticles is a focus of current research interest in understanding their physical chemistry and receptor- based sensor applications.

The adsorption and conformation of proteins on metal surfaces is critical to many bioanalytical techniques involving transduction of protein-based signals for detection including electrochemistry, SERS, surface plasmon resonance and quartz crystal microgravimetry [1,2]. Unfortunately proteins adsorbed directly on metallic

surfaces suffer from denaturation. To address this problem, Au nanoparticles were used to modify the metallic surfaces. Proteins bound to gold colloids are known to retain biological activity [3,4]. Metal particle bionanoconjugates are important structures for biosensing, therapeutic delivery and cellular imaging where Au nanoparticles can be used delivery agents for biomolecules [5-13]. Cell-targeting peptides were conjugated to bovine serum albumin (BSA) where peptide-BSA conjugates were subsequently adsorbed onto gold nanoparticles, microinjected into cell lines for transmission electron microscopy applications [14-16]. Stability of the BSA modified Au nanoparticles studied at different pH and proved that steric interactions play a major role for the surface modification of Au nanoparticles by BSA [17].

In the area of metal nanoparticle-enzyme conjugate materials, Crumbliss, Stonehuerner and coworkers have studied the formation and enzymatic activity of gold nanoparticles complexed with horse radish peroxidase (HRP) and xanthine oxidase (XOD) as well as glucose oxidase (GOX) and carbonic anhydrase molecules [18]. A significant feature of their work is the demonstration that enzyme molecules are bound tightly to gold colloidal particles and retain significant biocatalytic activity in the conjugated form. Layer-by-layer(L-b-L) self assembly technique has been used as an alternative method for the construction of protein multilayer films[19]. The L-b-L method has been widely employed for the formation of multilayer films of a wide array of water soluble proteins, alternately assembled with oppositely charged polyelectrolytes [20-22]. As an extension to this work, in this chapter Au nanoparticles were modified by enzymes through electrostatic interactions by combining advantages of mediator adsorption on the Au nanoparticle surface for better electron transfer and enzyme for biorecognition.

There are two key requirements while preparing biofunctionalized Au nanoparticles.

a) The suspension of the biofunctionalized Au nanoparticles should be highly stable

Preparation of a stable dispersion of biofunctionalized Au nanoparticles is a necessary requirement for successful electrophoretic deposition (EPD). A well-dispersed stable suspension will result in better deposition during the EPD process compared to an unstable or agglomerated particle suspension [23,24]. In the present

work, utmost importance is given towards maintaining the stability of the bionanoconjugates. The best conditions for maintaining the stability of the biofunctionalized Au nanoparticles are presented. In this chapter, bionanoconjugates were prepared using different methods. In this chapter, stability of the particles was monitored by zeta potential measurements. The magnitude of the zeta potential gives an indication of the potential stability of the colloidal system [25]. If all the particles in suspension have a large negative or positive zeta potential they will tend to repel each other and there is no tendency to flocculate. Zeta potential determination gives valuable information about the surface charge of the particles so that depending on that the particles can be modified with opposite charges.

UV-Visible spectroscopy was used for monitoring the changes on the surface of gold colloids while modification with biomolecules. In the case of UV-visible spectroscopy gold nanoparticles were characterised by observing localised surface plasmon resonance peak characteristic of gold colloids, which is absent in the case of bulk metals and gives information about the stability of the Au nanoparticles. By using this technique, valuable information regarding the surface modification when the Au nanoparticles are modified by proteins and polymers due to the changes in the surface plasmon peak can be obtained.

b) The biomolecule should retain its native activity

Direct adsorption of proteins onto naked metal surfaces can frequently result in their denaturation and the loss of bioactivity. Hence the biomolecule after attachment with the Au nanoparticles should retain its native activity which is essential for the functionality of the biosensors. As a part of this, multifunctional Au nanoparticles were prepared by modifying the Au nanoparticles with redox polymer in order to have better electron transfer capability for biosensing.

2.3. Experimental

2.3.1. Apparatus

Absorption spectra were measured with an HP 8453 UV-Visible spectrophotometer. Zeta potential measurements were done using zeta sizer (MALVERN, UK). All solutions were made with purified distilled water obtained from a Milli-Q water system. Centrifugation of the Au particles was performed by Mikro22R (Hettich). Optical images of the Au nanoparticles were obtained by Transmission Electron Microscope (Zeiss 10 CA).

2.3.2. Materials

Tetrachloroauric [III] acid (HAuCl_4), Sodium citrate, Horseradish peroxidase (HRP), Bovine serum albumin (BSA) (A-7888), mercaptoethanolN-Succinimidyl S-acetylthioacetate (SATA), Dithiobis-N-succinimidyl propionate (DTSP), 1-Ethyl-3-(3-dimethylaminopropyl)-carbodiimide (EDC), and 3,3',5,5'-tetramethyl-benzidine (TMB) liquid substrate system for colour development (containing TMB and H_2O_2 in a slightly acidic buffer) (T-0440) were purchased from Sigma-Aldrich, Spain. Glucose oxidase (GOX) was purchased from Biozymes, UK. The polycationic redox polymer, poly [vinylpyridine Os (bis-bipyridine) 2Cl]-co-allylamine (PVP-Os-AA)(RP 1) and the redox co-polymer (RP 2) as shown in the Figure 2.1 were synthesized as reported in the literature [26]. Aqueous solutions were prepared with Milli Q water (Milli Q system, Millipore). 20nm and 5nm gold colloids were purchased from Sigma-Aldrich, Spain. Fluorescence label FITC labelled 3' FITC-(C) 12(T) 20(C) 12-SH 5' and digoxigenin labelled PROBE, 3'dig-ACTTAACCGAGTCGACCGA-SH 5' were purchased from Genosys.

2.3.3. Synthesis of Au nanoparticles and characterisation

All glassware used in the procedures was cleaned in a bath of freshly prepared solution (3:1 HNO_3 -HCl), thoroughly washed with water. Gold nanoparticles were synthesized by using the well known Frens method [27]. In this case, 100 μl of 10

% HAuCl_4 was dissolved in 98.5 mL-distilled water. The mixture was left stirring with continuous boiling. To this boiling mixture, 1.5 mL of Sodium citrate was added and left to react for 20 min until a wine red colour solution formed. Later the heater was turned off and the stirring was continued for the next 30 min. Gold colloids were characterised and stored at 4°C.

2.3.4. Preparation of biofunctionalized nanoconjugates

As outlined before, three different methodologies were tried for modifying gold nanoparticles with biomolecules. The first one take advantage of the well known gold-thiol interactions. The second one is the direct adsorption of proteins on the gold nanoparticle surface. The third one is the layer-by-layer modification of gold nanoparticles with redox polymer and enzymes through electrostatic interactions.

2.3.4.1. Bionanoconjugates based on Au-thiol interactions

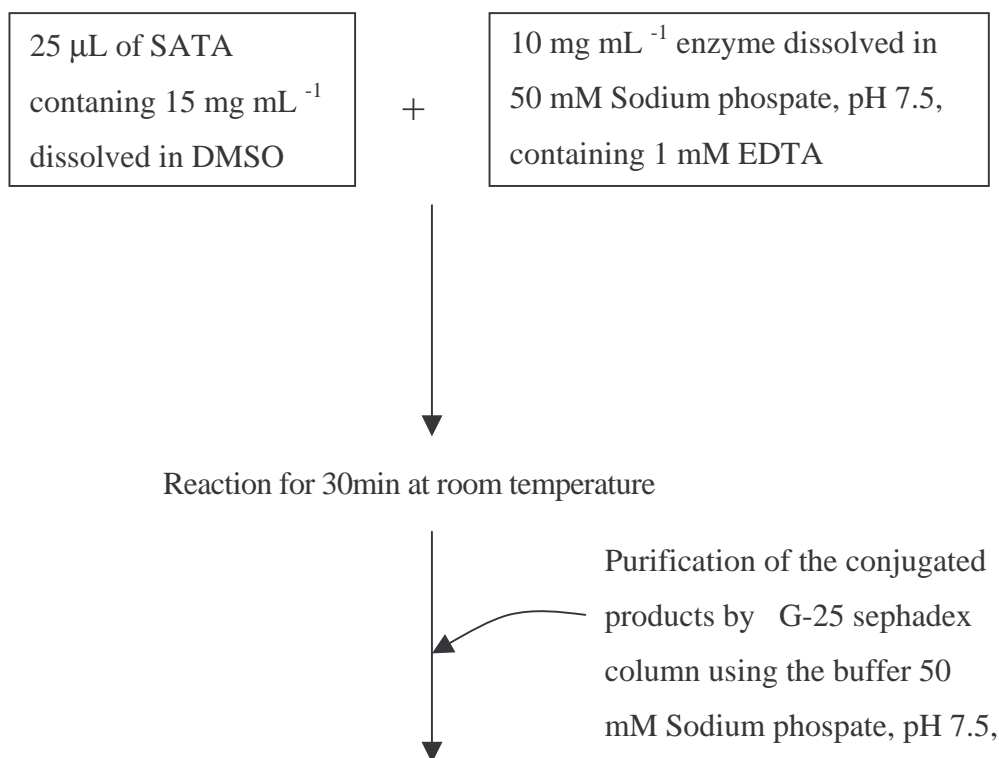
Redox enzymes (HRP, GOX) were modified in order to create thiols externally by using different thiolation protocols. This modification should be done according to the structural properties and properties of the active centre of the redox enzymes.

Three different protocols were used for thiolation of enzymes

2.3.4.1.1. Thiolation of enzymes

2.3.4.1.1.1. SATA method of thiolation

SATA method of thiolation is followed according to the protocol modified from that explained[28] .

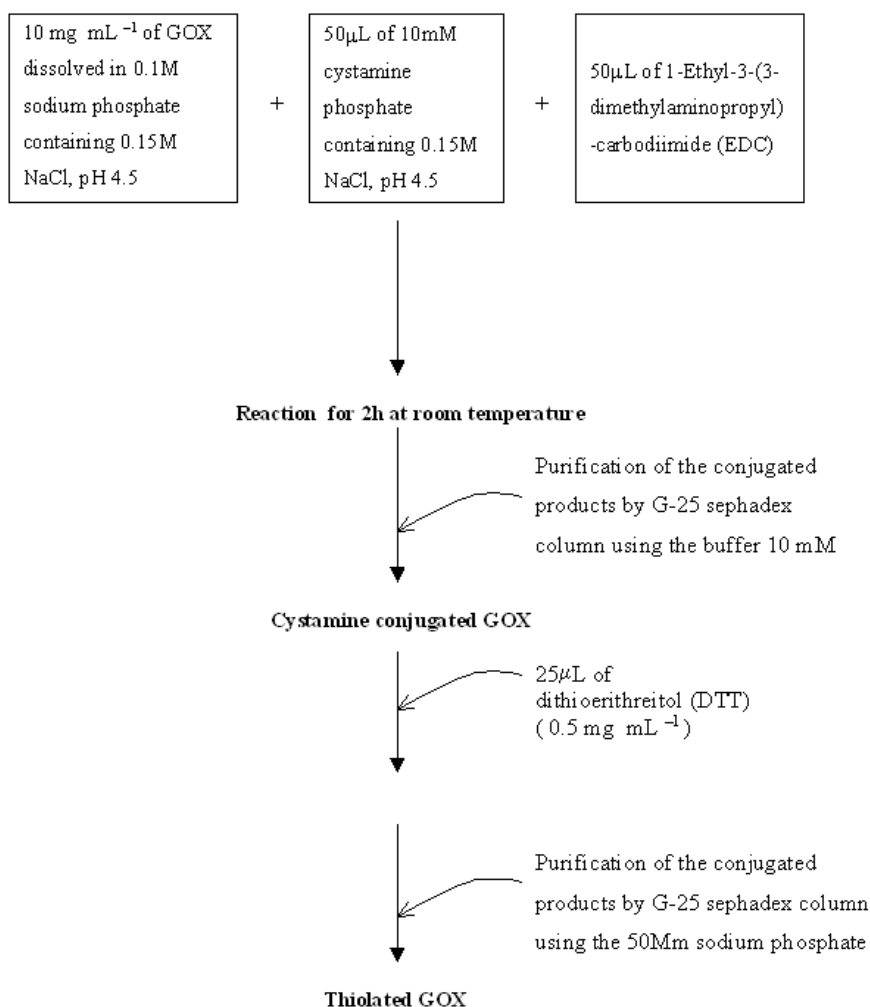


500 μL of the fractions containing the modified enzyme which contains the thiols in the protected stage are collected and tested with Ellmans reagent for the presence of SH groups

Next, the acetylated –SH groups were deprotected using 100 μL of 0.5 M hydroxylamine hydrochloride (NH₂-OH) in 50mM Sodium phosphate, pH 7.5, containing 25 mM EDTA added to 1mL of SATA modified protein solution. After reacting for 2 h, the mixture was purified by using G-25 sephadex column with 50mM Sodium phosphate, pH 7.5, containing 1mM EDTA. The protein fractions collected were checked by Ellmans assay for the presence of –SH groups. Later the fractions were concentrated using ultrafiltration microcons depending on the size of the enzyme with the 0.1M PBS pH 7.0.

2.3.4.1.1.2. Thiolation using carbodiimide chemistry

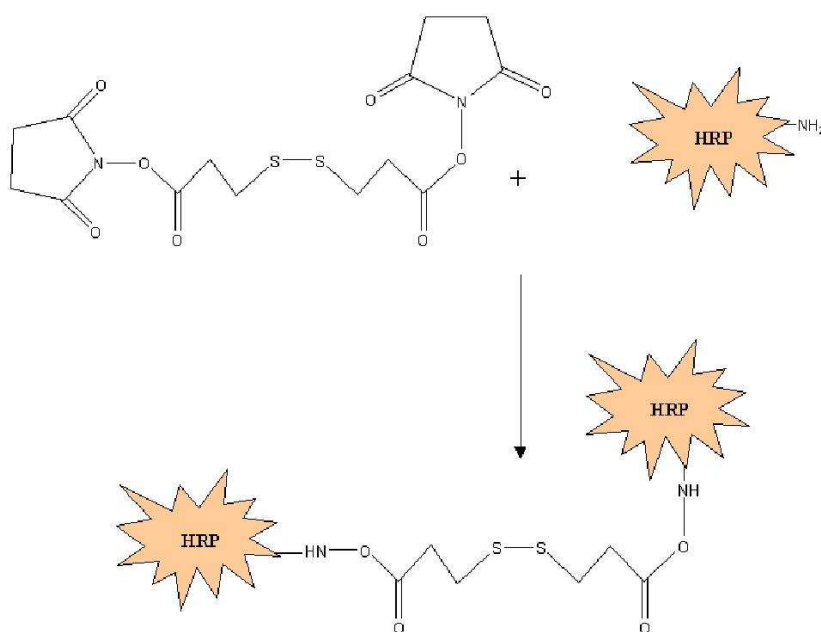
The scheme 2.1 represents the protocol for obtaining the thiolated GOX using the 1-Ethyl-3-(3-dimethylaminopropyl)-carbodiimide (EDC) as a thiolation reagent to conjugate the amine groups of the cystamine to the carboxylic acid groups of the protein.



Scheme 2.1. Flow chart of the thiolation of GOX using carbodiimide reaction

2.3.4.1.1.3. Thiolation of enzymes through bi-phase separation using DTSP

The scheme showing the reaction between the DTSP and HRP is shown in the scheme 2.2. First, 1 mg HRP was dissolved in 1 mL of water and mixed with 3.1mg DTSP dissolved in 1mL THF and left to react with stirring for 5 h at room temperature. Next the unattached DTSP was extracted by 10 mL of THF + benzene.



Scheme 2.2 . Schematic representaion of DTSP thiolation protocol

Later the separated modified enzyme was concentrated using microcon and dissolved in 0.01M phosphate buffer, pH 7.0. Activity of the thiolated HRP was compared with the native enzyme by incubating the gold electrode with 1mg mL⁻¹ with both thiolated and native HRP for 5h.

2.3.4.1.1.4. Assaying of thiolated GOX enzyme activity

Enzyme activity assay of the thiolated GOX was done using the available protocol outlined in the biozyme laboratories, UK [30] and compared with the activity of the unmodified enzyme. Quantification of the thiols for the thiolated enzymes is done by using the Ellmans assay [31].

2.3.4.1.2. Preparation of enzyme conjugated gold nanoparticles

Enzymes thiolated by using SATA method were used for conjugation experiments. 20nm Au nanoparticles were added into eppendorfs containing thiolated HRP solution in 0.1M phosphate buffered saline pH 7.0 and mixed well. The final colloidal gold concentrations were 2.3×10^{12} particles mL^{-1} and the final enzyme concentration was $250\mu\text{M}$ (10 mg mL^{-1}) to make sure an excess enzyme molecules so that the problem of aggregation due to the multiple moieties of the HRP can be avoided and the particles can be stable. Mixtures were left to react for 40 h at room temperature protected from light. Afterwards, they were centrifuged twice at 5000 rpm and 4°C for 30 min. The supernatants were removed, and the pellets were resuspended in 0.1M phosphate buffered saline, pH 7.0. Finally HRP-Au colloids were used for further experiments. For the preparation of GOX modified Au nanoparticles, the same above mentioned protocol was repeated using $62.5 \mu\text{M}$ (10 mg mL^{-1}) with 5nm and 20nm Au nanoparticles.

2.3.4.2. Bionanoconjugates based on steric interactions

2.3.4.2.1. Preparation of BSA modified Au nanoparticles

BSA binds to the Au nanoparticle surface due to electrostatic as well as the steric interactions [32]. Some fundamental studies have been done using BSA as a model protein for modifying Au nanoparticles. Initially the effect of BSA on the electrodeposition of Au nanoparticles was studied. In order to prepare these, initially citrate stabilised Au colloids were washed three times through centrifugation at 5000 rpm for 30min with distilled water to concentrate the Au sol and to remove the impurities. Later $100\mu\text{L}$ of the pellet containing concentrated Au sol was added to 1% BSA and mixed for 30min. Later the mixture was centrifuged at 5000 rpm for 30min thrice to remove the unadsorbed BSA. Finally $100\mu\text{L}$ of the pellet containing BSA modified nano Au was used for electrodeposition studies.

2.3.4.3. Bionanoconjugates based on electrostatic interactions

2.3.4.3.1. Layer-by-layer modification of the Au nanoparticles with redox polymer / enzyme / redox polymer

Layer-by-layer formation of the RP 2 / GOX / RP 2 on the gold nanoparticles was done in a step by step manner starting with the modification of gold colloids with cationic osmium redox polymer followed by the modification with the glucose oxidase and finally again with the redox polymer as shown in the scheme 2.3.

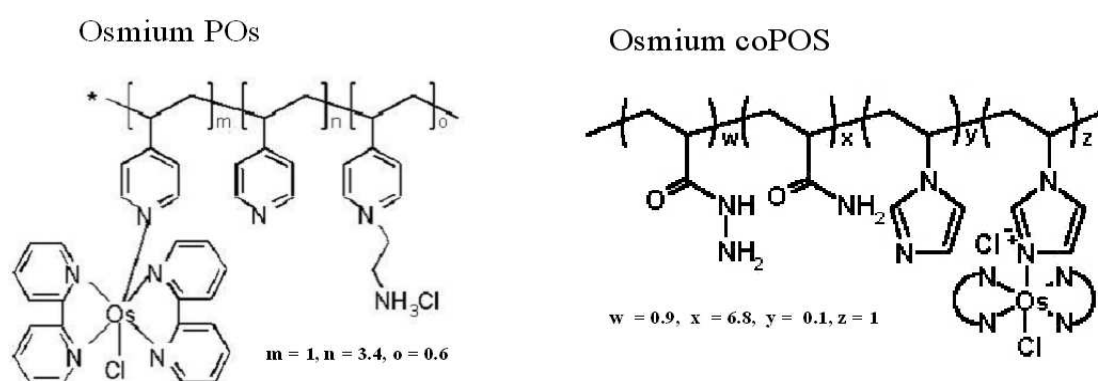
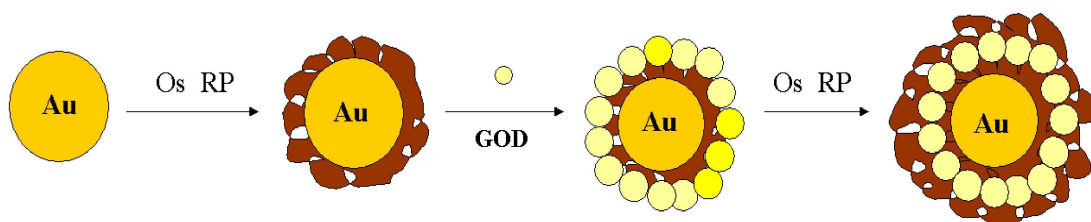


Figure 2.1. Structure of redox polymers RP 1 (osmium POs) and RP 2 (osmium coPOs) used for modifying Au nanoparticles.

In the first step, several aliquots of 30 nm gold colloids containing 1mL each were centrifuged at 5000 rpm for 30 min in order to concentrate the gold sol as well as for reducing the citrate concentration present in the solution. 950 μL of the supernatant was removed from each eppendorf and replaced with the same amount of water. This step was repeated total three times to completely remove the impurities. In the second step, 50 μL of the concentrated pellet collected after centrifugation was added drop by drop to the 950 μL of 10 mg mL^{-1} cationic redox polymer solution while stirring. The mixture was left overnight to react at room temperature away from light with continuous stirring. Next the mixture was washed three times by centrifugation at 5000 rpm for 30 min with distilled water removing 950 μL of the supernatant and replacing it by the same amount of distilled water. This washing was carried out to separate the redox polymer modified nanoparticles and the

unmodified particles. After the modification with RP, 50 μ L of the concentrated pellet was added drop by drop to the 950 μ L of 10 mg mL⁻¹ of glucose oxidase dissolved in milli Q distilled water while stirring. The mixture was left overnight to react at room temperature away from light with continuous stirring. As the isoelectric point (pI) of GOX is 4.2, the enzyme should have negative charge at higher pH which is essential for the attachment to the redox polymer modified nanoparticles. Again the RP-GOX modified gold nanoparticles mixture was washed three times by centrifugation at 5000 rpm for 30 min with distilled water removing 950 μ L of the supernatant and replacing it by the same amount of distilled water. The modification with the outer RP layer was achieved by repeating the addition of RP-GOX modified gold nanoparticles to the cationic redox polymer solution, leaving under stirring overnight in darkness and three consecutive washing steps with distilled water.



Scheme 2.3. Scheme of step by step modification of Au nanoparticles with redox polymer (RP 2) first followed by GOX and finally again with redox polymer (RP 2).

In the case of HRP, the same protocol used for the GOX was used for the modification of nano Au with change in the redox polymer. In this modification protocol, RP1 was used instead of RP2. HRP was dissolved in the 0.1M PBS pH 7.8 to have a negatively charge surface.

2.3.5. Characterisation of gold colloids

UV-Visible absorption spectroscopy was used for measuring the characteristic surface plasmon resonance of the Au colloids. TEM was used to characterise the particles optically. Size measurements of the gold nanoparticles were taken with the

help of the zeta sizer. Combination of all these methods gives accurate information about the particle characteristics.

2.3.6. Characterisation & stability studies of BSA modified Au nanoparticles

100 μL pellets containing the concentrated Au sol (3×10^{12} particles per mL^{-1}) were dissolved in 900 μL of various buffers like 0.1M citrate-HCl at pH 3.0, 0.1 M Phosphate Buffered Saline at pH 6.0 and 8.0, and 0.1M Glycine-NaOH at pH 10.0 and 12.0 to check the stability of Au nanoparticles so that the final concentration of the particles were 3×10^{11} particles mL^{-1}). Zeta potential measurements were compared in order to see how effective is the protein in preventing gold nanoparticles from aggregation.

2.3.7. Characterisation of layer-by-layer modification of gold nanoparticles with redox polymer and enzymes

2.3.7.1. Characterisation & stability of redox polymer modified Au nanoparticles

Redox polymer modified Au nanoparticles prepared as explained was used to study the stability by dissolving in buffers with various pH 3.0, 6.0, 8.0, 10.0 & 12.0. Monitoring of the colour changes along with the UV-Visible measurements for the surface plasmon resonance peak of the Au nanoparticles was done for studying the aggregation behaviour of the Au nanoparticles.

2.3.7.2. Characterisation of layer-by-layer modified redox polymer / enzyme / redox polymer Au nanoparticles

The Zeta potential measurements were used to monitor the adsorption of redox polymer and enzymes (GOX, HRP) onto the surfaces of Au nanoparticles by observing the changes of charge sign on the particle surface with the successive layer modifications. This approach provides indirect and fairly qualitative information about the adsorption of species onto oppositely charged particles. UV-visible absorption spectroscopy was used for measuring the changes on the surface plasmon resonance of the Au colloids due to the modification with redox polymer and

enzymes that demonstrate the stability of gold colloids as well as the changes occurring on the Au colloid surface.

2.4. Results and Discussion

2.4.1. Synthesis of colloidal particles

The change of colour from light yellow to red colour was due to the reduction of Au[4] to Au (0) started instantaneously. The diameter of the Au nanoparticles prepared by the second protocol was 30 nm. Figure 2.2 shows UV-vis measurements with a maximum absorbance peak around 525 nm, which clearly shows the presence of nano Au. In Figure 2.3, Zeta sizer measurements show the size of Au nanoparticles is around 30 nm with a zeta potential of -45mV . The zeta potential combined with the UV-Visible spectroscopy data proved the stability of Au nanoparticles.

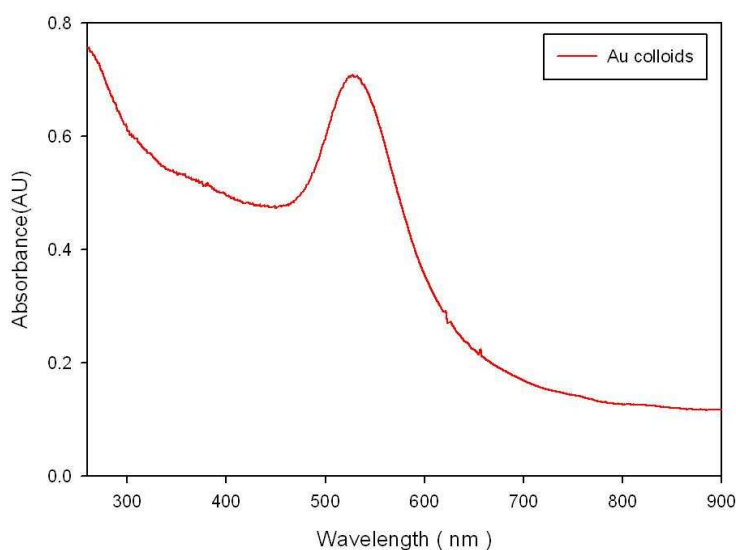


Figure 2.2. UV-Visible spectroscopy of 30nm gold colloids dissolved in distilled water (2×10^{11} particles)

Figure 2.4 shows the typical TEM image of the synthesized 30nm Au nanoparticles. From the Figures 2.3 and 2.4, it can be confirmed that the particles are homogenous and the size of the particles is 30nm.

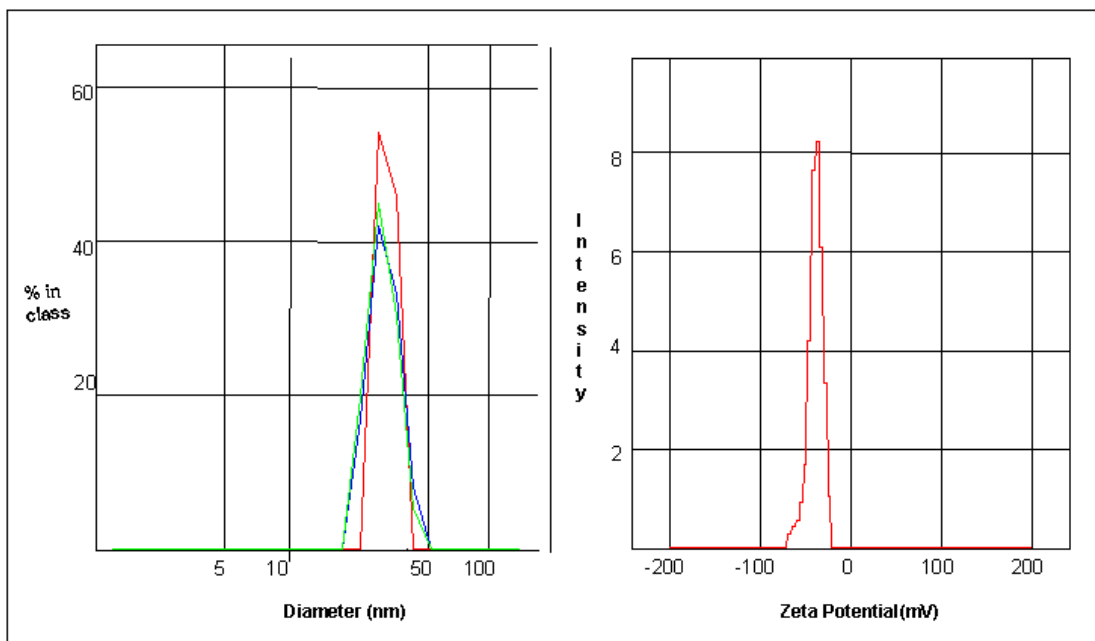


Figure 2.3. Zeta size and zeta potential measurements of the synthesized Au nanoparticles dissolved in distilled water (3×10^{11} particles)

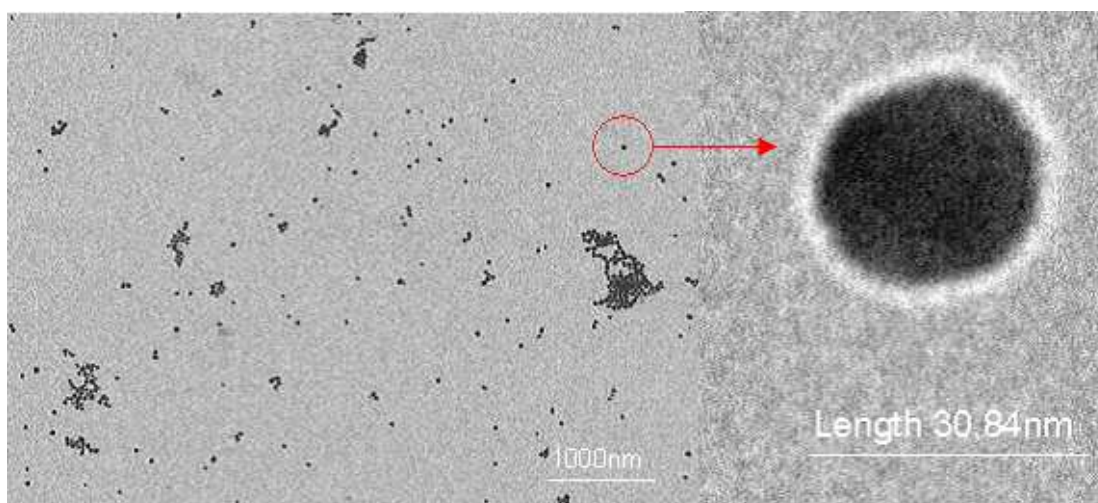


Figure 2.4. Typical TEM image of the 30nm spherical Au nanoparticles (on a carbon coated copper grids)

2.4.2. Thiolation of enzymes

In order to determine the best method of thiolation of GOX, the residual activity of the enzyme after thiolation and the number of thiol groups per enzyme were determined. From Figure 2.5, it can be observed that the activity of the thiolated enzyme (GOX) was retained almost completely when using the SATA method of modification as compared with the EDC method.

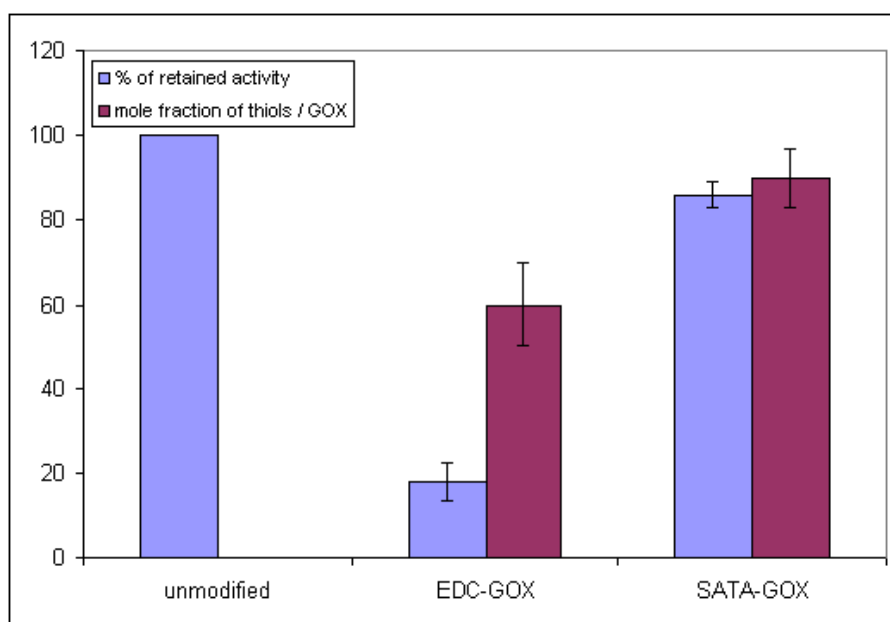


Figure 2.5. Comparison of the two protocols of thiolation. GOX residual enzymatic activity and number of thiols created per molecule.

It can also be seen that there were more thiols created by the SATA method as compared with the EDC method of modification. Based on these observations the SATA method of thiolation was chosen as the most appropriate.

In the case of HRP, the DTSP protocol was used because, in this case success of thiolation and retention of activity was validated by adsorbing native HRP and later DTSP modified HRP on gold electrodes and assaying them for enzymatic activity. It was found that DTSP-HRP modified electrodes resulted in five fold increase of activity after incubation of the electrodes clearly demonstrate that thiolation was successful and presented an advantage with respect to achieving modified electrodes with higher activity.

2.4.3. Characterisation of HRP-Au nanoconjugates

Figure 2.6 shows the effect of HRP-modification on UV-Visible spectroscopy of Au nanoparticles. It can be observed that HRP modified Au nanoparticles showed two peaks at 535 nm characteristic of Au nanoparticles as well as at 405 nm characteristic of heme group of HRP. The results are compared to the unmodified HRP and Au nanoparticle controls, and demonstrate that UV-Vis spectrophotometry carries useful information for the characterisation of bioconjugates. Independent experiments showed that in order to achieve saturation, modification of Au colloids with model thiolated molecules, a 40 h interaction was necessary and for this reason this time was used for subsequent experiments.

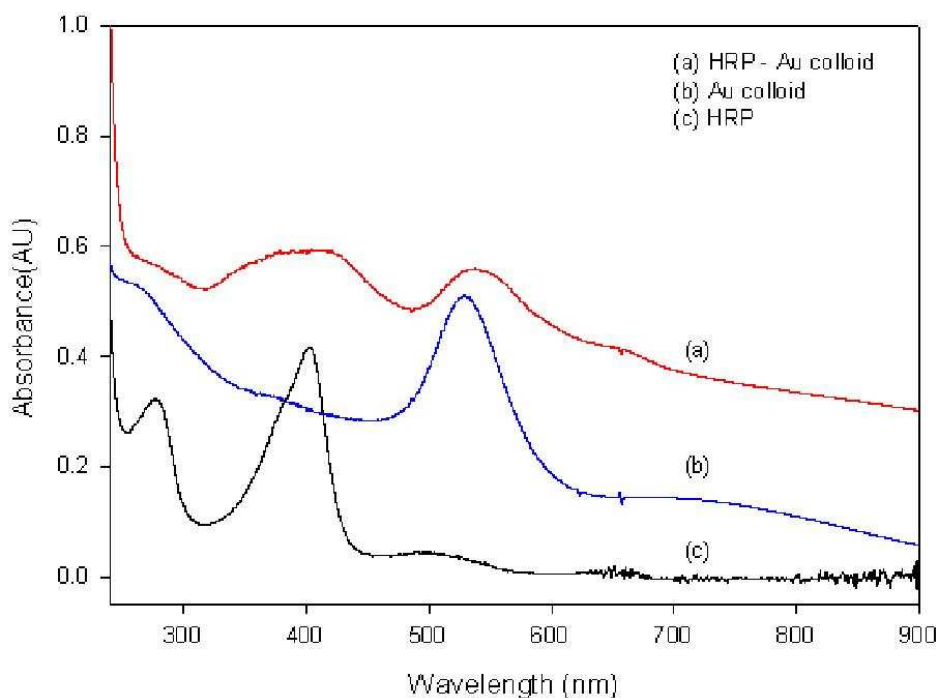


Figure 2.6. UV-Visible spectra of HRP modified Au nanoparticles (curve a) in comparison with the unmodified Au colloid (curve b) and HRP (curve c) controls dissolved in distilled water (pH 6.7). Concentrations: HRP control ($200 \mu\text{g mL}^{-1}$), Au nanoparticles control: 2×10^{11} particles mL^{-1}

2.4.4. Effect of pH on the Zeta potential of BSA modified Au nanoparticles

When working with the colloidal particle for EPD is crucial to establish the operational window in which nanoparticle solution is stable. Figure 2.7 shows the zeta potential measurements from a pH titration of 30nm nanoparticles stabilized by BSA. The BSA modified particles exhibited a pI around 5. The unmodified nanoparticle suspension is least stable at the isoelectric point because electrostatic repulsion is at a minimum and attractive van der Waals interaction lead to particle flocculation. The pH titration of the unmodified Au nanoparticles is not shown here as the particles are not stable enough below pH 7.0. This clearly proves that even though there is a change in the charge of the BSA modified Au nanoparticles, they are stable enough not to aggregate. The zeta - potential data show that BSA imparts stability to the gold nanoparticles with respect to aggregation by both electrostatic (depending on the pH) forces and steric interactions.

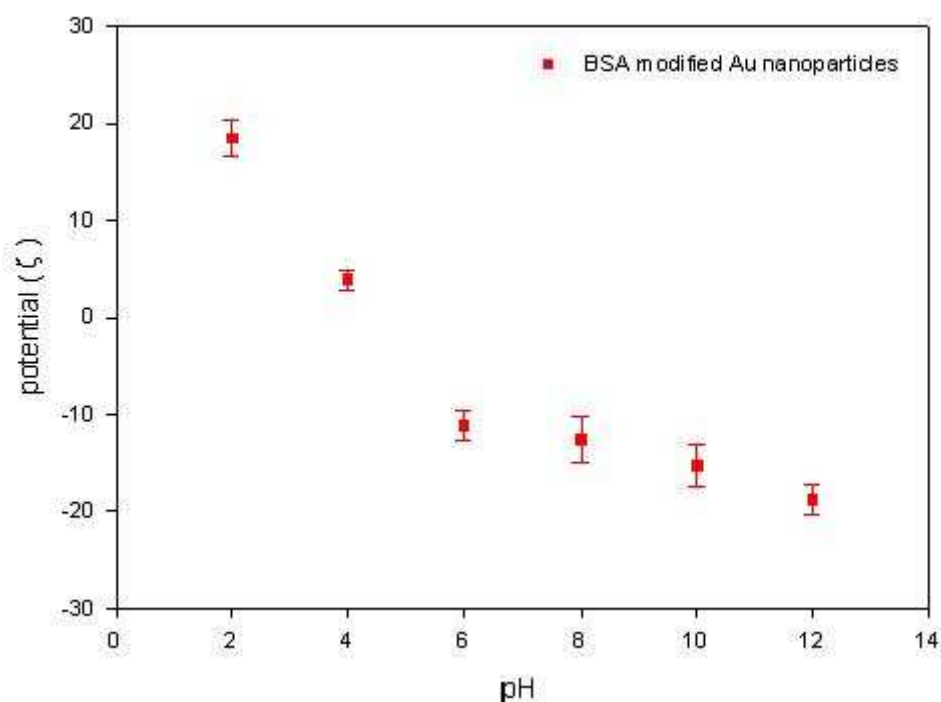


Figure 2.7. Zeta Potential (ζ) in mV of BSA modified 30-nm gold nanoparticles recorded as a function of pH. The average -potentials are plotted with error bars representing the standard deviations for $n = 5$ measurements. Number of particles: 3×10^{11} particles mL^{-1} , Buffers: 0.1 M citrate-HCl pH 3.0, 0.1M PBS pH 6.0 and 8.0, and 0.1 M Glycine-NaOH pH 10.0 and 12.0.

Stability imparted by steric interactions (bulky proteins on the surface preventing neighboring gold nanoparticles from getting in close enough proximity to interact and aggregate) is demonstrated by the fact that BSA-coated gold nanoparticles remain stable even at the pI of the colloid.

2.4.5. Stability of redox polymer modified Au nanoparticles with pH

Unmodified Au nanoparticles are highly stable at pH 12.0 and aggregate completely at pH 3.0. This might be due to the increase in the concentration of hydrogen (H^+) ions at low pH and decrease in the hydroxyl (OH^-) ions, which cause the particles to aggregate. After modifying with redox polymer (RP 2), the stability behaviour of the modified particles changed completely.

At pH 3.0, redox polymer modified Au nanoparticles are highly stable. It can be observed from the Figure 2.8 that there is the presence of sharp peak at 535nm and the ratio of absorbance between 530 and 650 is higher. Visually the particles have a wine red colour. At pH 12.0 there is violet colour formation visually and the particles are aggregated with a very low ratio of the absorbance between 530 and 650.

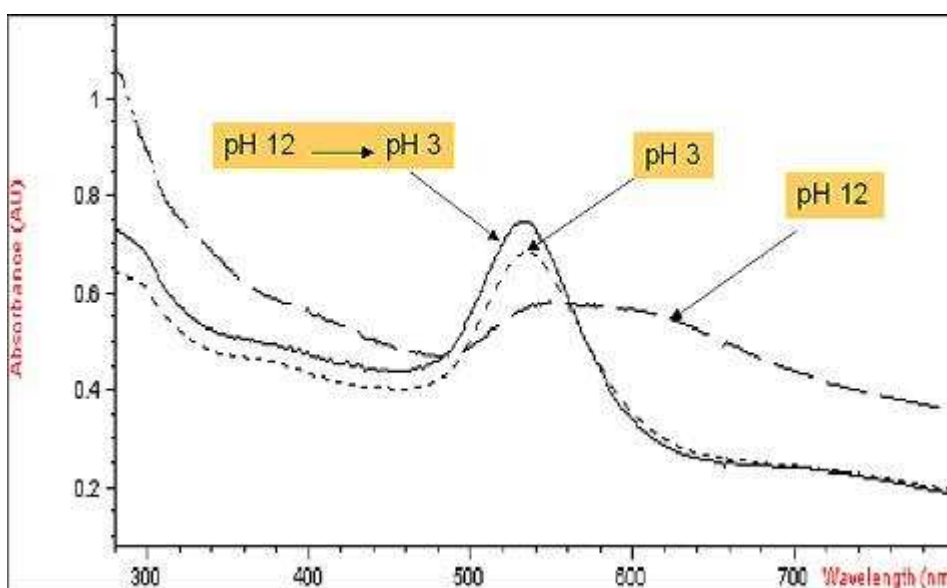


Figure 2.8. UV-Visible spectroscopy of RP 2 modified Au nanoparticles at different pH conditions. Concentration of the particles: 3×10^{11} particles mL^{-1} , Buffers: 0.1 M citrate-HCl pH 3.0 and 0.1 M Glycine-NaOH pH 12.0

When the modified particles dissolved in pH 12.0 buffer were centrifuged, the aggregated particles settled as a black pellet. After removing the supernatant and replacing with the same amount of solution at pH 3.0, all the particles that were aggregated dissolved resulting in a red coloured solution. UV-visible spectra clearly showed the increase in the ratio of the absorbance values between 530 nm and 630 nm as the pH was changed from 12.0 to 3.0. The broad absorbance peak observed due to the aggregation of the particles at pH 12.0 became narrow with a sharp peak characteristic of the stable Au sol. This shows that the Au nanoparticles are modified with the redox polymer successfully and the modified particles showed rarely observed reversible pH dependent aggregation behaviour.

2.4.6. UV-Visible characterisation of Layer-by-Layer modified Au / RP 2 / GOX / RP 2 particles

Figure 2.9 shows UV-Vis absorbance spectra of the first and second layers of RP 2 modified Au nanoparticles. Initially gold colloids gave a characteristic surface plasmon resonance absorption peak at $\lambda = 523$ nm.

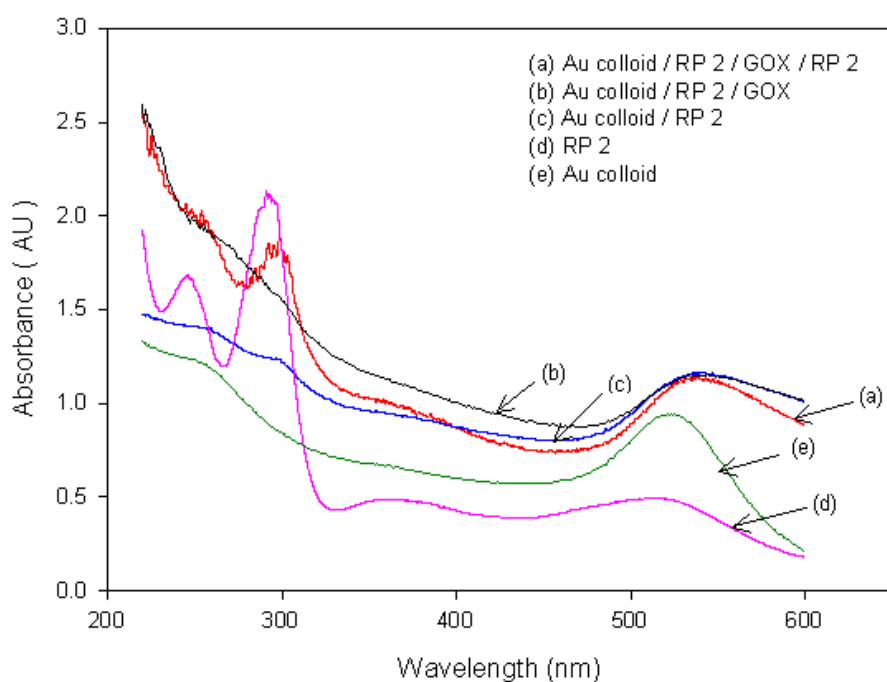


Figure 2.9. UV-visible spectroscopy of the Au colloids modified layer-by-layer with redox polymer / GOX / redox polymer.

After modification with the successive layers the peak shifted to 538 nm upon RP modification, then to 544 nm after GOX modification and back to 538 nm after modifying with the outer RP 2 layer. The modified gold nanoparticles also showed characteristic absorbance peaks due to the redox polymer at 300 nm as well as at 260 nm. There is an increase in the peak intensity after modifying with the second redox polymer.

2.4.7. Zeta Potential Characterisation of Au / RP 2 / GOX / RP 2 particles

From Figure 2.10, it can be observed that bare gold nanoparticles showed a zeta-potential of - 0.45 V, while the same nanoparticles modified with the first layer of RP 2 showed a change to + 0.28 V. After modification with GOX, a charge reversal was observed to -0.23 V. Finally after the second layer of RP 2 modification, the surface charge changed to + 0.26 V. This observations verifies qualitatively the efficiency of modification of the surface of the Au nanoparticles with the redox polymer and GOX.

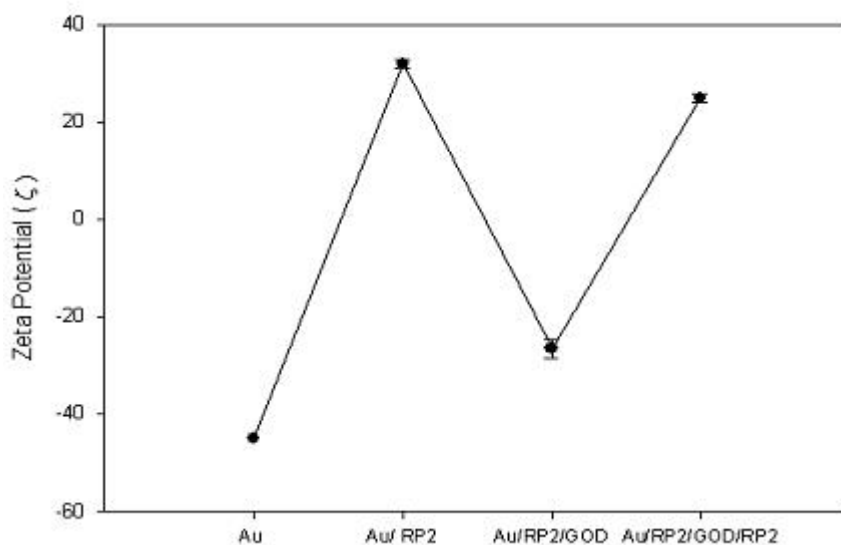


Figure 2.10. Zeta potential of Au nanoparticles modified with RP 2 followed by GOX and further by RP 2. Concentration of the particles: 3×10^{11} particles mL^{-1}

Figure 2.11 shows the zeta potential curve of the HRP / RP 1 modified Au nanoparticles. From this figure, it can be observed that the zeta potential changes from -45 mV of the bare Au nanoparticles to $+26$ mV after modifying the gold nanoparticles with RP1. When the RP 1-modified Au nanoparticles were modified with HRP the zeta potential value changed to $+10$ mV.

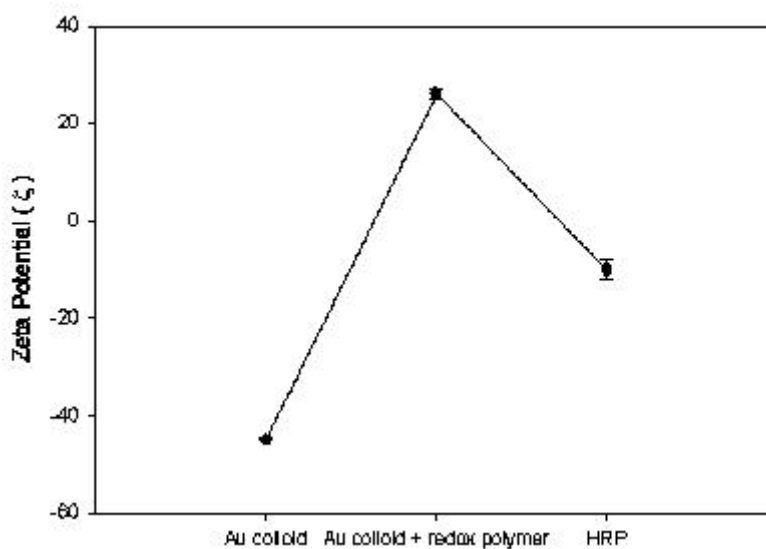


Figure 2.11. Zeta potential of Au nanoparticles modified with RP 1 followed by HRP and further by RP1. Concentration of the particles: 3×10^{11} particles mL^{-1}

2.5. Conclusions

In this chapter, biofunctionalized Au nanoparticles were prepared and characterised. Initially Au nanoparticles were synthesized and characterised successfully. Later the Au nanoparticles were modified with biomolecules through different approaches. In the first approach where biomolecules were conjugated through Au-thiol interactions, enzymes were thiolated and immobilized on the surface of Au nanoparticles successfully. Biofunctionalised nanoparticles formed using Au-thiol interactions are stable enough and well characterised. Au nanoparticles were modified with BSA through steric interactions. Study of the effect of pH on the BSA modified Au nanoparticles showed that the particles are stable at all pH s with a variation in the surface charge. In the third approach, multifunctional nanoparticles were prepared by modifying Au nanoparticles with redox polymer and the enzymes using L-b-L approach. Zeta potential values demonstrated the successful modification of Au nanoparticles with redox functionality followed by the enzymes. Effect of pH on the redox polymer modified Au nanoparticles proved that there was a pH based switching of redox polymer modified nanoparticles from aggregation to non-aggregation. This effect is rarely observed and it serves as an additional proof of successful modification of the Au colloids.

2.6. Abbreviations

BSA – Bovine serum albumin

DTSP-Dithiobis-N-succinimidyl propionate (DTSP)

EDC-1-Ethyl-3- (3-dimethylaminopropyl)-carbodiimide

EPD – Electrophoretic deposition

FITC - Fluorescein iso thiocyanate

GOX – Glucose oxidase

HRP – Horse radish peroxidase

L-b-L – Layer by Layer

PBS – Phosphate buffered saline

RP – redox polymer

SATA- N-Succinimidyl S-acetylthioacetate

TEM – Transmission electron microscopy

TMB – 3,3', 5,5'-tetramethyl-benzidine liquid substrate

UV-Vis – Ultraviolet Visible

2.7. References

1. Mignani, A., Scavetta, E., Tonelli, D, 2006, *Anal.Chim.Acta*, 577, 98-106.
2. Kotzian, P., Brazdilova, P., Rezkova,S., Kalcher,K., Vytras, K, 2006, *Electroanalysis*, 18, 1499-1504.
3. Xiao, Y., Ju,H-X., Chen,H. Y, 1999, *Anal.Chem.Acta*, 391, 73-82.
4. Patolsky, F., Gabriel,T., Willner,I, 1999, *J. Electroanal. Chem*, 479, 69-73.
5. Jena, B. K., Raj,C.R, 2006, *Anal.Chem*, 78, 6332-6339.
6. Endo, T., Kerman,K., Nagatani,N., Hiepa,H.M., Kim,D.K., Yonezawa,Y., Nakano,K., Tamiya , E, 2006, *Anal.Chem*, 78, 6465-6475.
7. Peng, H., Soeller,C., Cannell,M.B., Bowmaker,G.A., Cooney,R.P., Travas-Sejdic,J, 2005, *Biosens.Bioelectron*, 21, 1727-1736.
8. Liu, G. L., Rodriguez,V.B., Lee,L.P, 2005, *J.Nanosci.Nanotech*, 5, 1933-1937.
9. Liu, S. F., Li,Y.F., Li,J.R., Jiang,L, 2006, *Biosens.Bioelectron*, 21, 1727-1736.
10. Chu, X., Fu,X., Chen,K., Shen,G.L., Yu,R.Q, 2005, *Biosens.Bioelectron*, 20, 1805-1812.
11. Li, M., Lin,Y.C., Su,K.C., Wang,Y.T., Chang,T.C., Lin,H.P, 2006, *Biosens.Bioelectron*, 117, 451-456.
12. Luo, X. L., Killard,A.J., Smyth,M.R, 2006, *Electroanalysis*, 18, 1131-1134.
13. Agui, L., Manso,J., Yanez-Sedeno,P., Pingarron,J.M, 2006, *Sens.Act.B*, 113, 272-280.
14. Dykman, L. A., Sumaroka,M.V., Staroverov,S.A., Zaitseva, I.S., Bogatyrev.V.A, 2004, *Biology Bulletin*, 31, 75-79.
15. Xie, H., Tkachenko,A.G., Glomm,W.R., Ryan,J.A., Brennaman,M.K., Papanikolas,J.M., Franzen,S., Feldheim,D.L, 2003, *Anal.Chem*, 75, 5797 - 5805.
16. Tkachenko, A. G., Xie,H., Coleman,D., Glomm,W., Ryan,J., Anderson,M.F., Franzen, S., Feldheim, D.L, 2003, *J.Am.Chem.Soc*, 125, 4700 - 4701.
17. Brewer, S. H., Glomm, W.R., Johnson, M. C., Knag, M.K., 2005, *Langmuir*, 21, 9303-9307.
18. Crumbliss, A. L., Perine, S.C., Stonehuerner.J., Tubergen, K.R., Zhao, J., Henkens, R.W., O'Daly,J.P, 1992, *Biotech. Bioeng*, 40, 483 - 490.

19. Caruso, F., Möhwald, H, 1999, *J.Am.Chem.Soc*, 121, 6039-6046.
20. Calvo, E. J., Etchenique, R., Pietrasanta, L., Wolosiuk, A., Danilowicz, C, 2001, *Anal. Chem*, 73, 1161-1168.
21. Shen, L., Hu,N, 2005, *J. Am. Chem. Soc*, 6, 1475-1483.
22. Zhang, H., Lu, H., Hu, N, 2006, *J. Phys. Chem. B*, 110, 2171-2179.
23. Yang, Y., Wu,X.D., Weng,D, 2006, *J. Coll. Interfc. Sci*, 287, 16-23.
24. Besra, L., Liu,M, 2006, *Prog. Mat. Sci*, 52, 1-61.
25. Van der Biest, O. O., Vandeperre.L.J, 1999, *Mater. Sci*, 29, 327-352.
26. Gregg, B. A., Heller, A, 1991, *J. Phys. Chem*, 95, 5970-5975.
27. Frens, G., *Nature*, 241, 1972.
28. Hermanson, T. G., 1996, *Bioconjugate techniques*, Academic Press, San Diego California.
29. M.Campàs, I. K., 2006, *Anal.Chim.Acta*, 556, 306-312.
30. Enzymatic activity assay of glucose oxidase with abts. Biozymes protocol, available from www.biozyme.com.
31. Ellman,G.L, 1959, *Arch. Biochem .Biophysics*, 82, 70-77.
32. Brewer.SH, G. W., Johnson. MC, Knag.MK, Franzen.S, 2005, *Langmuir*, 21, 9303-9307.

Chapter 3. Electrodeposition of functionalised Au nanoparticles

3.1. Abstract

The aim of this chapter is to establish the operating conditions for controlled electrodeposition of functionalised Au nanoparticles on electrode surfaces. For this reason the effects of BSA presence on the surface of Au nanoparticles, of applied potential, of duration of applied field, of interelectrode distance and size of counter electrode (field intensity and distribution) were studied on the efficiency of the deposition. This efficiency was determined by electrochemistry and observation of the electrode under SEM. It was found that both field intensity and distribution and colloidal suspension properties are important for a controlled and efficient electrodeposition. The requirement to retain biological activity of the deposited biofunctionalised particles imposes limits to the field intensity used for deposition. In general, fields not higher than 16 V cm^{-1} should be applied for electrodeposition but pH and total potential should always be optimised to retain biological and electrochemical activity of the bionanomolecules.

3.2. Introduction

Electrophoretic deposition (EPD) has been gaining increasing interest in the field of biomedical applications [1,2]. EPD is essentially a two-step process. In the first step, charged nanoparticles suspended in a liquid move towards an oppositely charged electrode by applying an electric field to the suspension (electrophoresis). In the second step, the particles collect at the electrode and coagulate to form a dense mass. Over the years, a number of methods have been used for the electrodeposition of enzymes on electrodes as part of the fabrication of electrochemically based biosensors. Electrochemically controlled co-deposition of enzymes with other proteins such as collagen and bovine serum albumin (BSA) has been reported [3,4]. Co-deposition of enzyme (glucose oxidase, GOX) with a Pt salt to form a Pt black surface has been reported where GOX sensors were prepared by first electrodeposition of GOX / BSA (bovine serum albumin) mixture on platinized Pt and subsequent crosslinking with glutaraldehyde [5]. Using this electrophoretic

deposition approach, controlled immobilization of glucose oxidase (GOX) on a platinum electrode has been achieved in the presence of a non-ionic detergent, Triton X-100 producing multilayer films [6]. A procedure was described that provides for electrochemically mediated deposition of enzyme and a polymer layer permselective for endogenous electroactive species where electrodeposition was first employed for the direct immobilization of glucose oxidase to produce a uniform, thin and compact film on a Pt electrode followed by the electropolymerization of phenol to form an anti-interference and protective polyphenol film within the enzyme layer [7]. Layer-by-layer electrodeposition of redox polymer/enzyme composition films on screen-printed carbon electrodes for fabrication of reagentless enzyme biosensors has been used for producing very stable and rigid films [8]. Glucose biosensor based on the one-step co-electrodeposition of a poly (vinylimidazole) complex of $[\text{Os}(\text{bpy})_2\text{Cl}]^{+/2+}$ (PVI-Os) and glucose oxidase (GOX) on a gold electrode surface has been developed [9]. Electrodeposition of hydrated redox polymers and co-electrodeposition of enzymes through coordinate crosslinking has been proven to produce stable enzyme films with excellent catalytic activity [10]. In all cases, the purpose of these strategies is to immobilize enzyme in a highly active state.

The mechanism of EPD involves charged particles in a suspension being deposited onto an electrode under the influence of an applied electric field. In order to obtain reproducible films, control of the deposition parameters is very important, especially when using aqueous media. Two groups of parameters determine the characteristics of this process; (i) those related to the suspension (pH, ionic strength, Zeta potential) and (ii) those related to the process including the electric field intensity and distribution and the nature of the electrodes (electrode geometry, interelectrode distance, applied potential relationship, deposition time)

In this chapter, the effects of these operating parameters on the electrodeposition of functionalized Au nanoparticles were studied. These parameters include the applied electrodeposition potential, time of electrodeposition, effect of protein coating, inter electrode distance, electrode geometry, pH and ionic strength. In order to characterise the resulting films, the electrocatalytic behaviour of the thiolated enzyme molecules conjugated to the gold colloids after electrodeposition was

studied, and scanning electron microscopy (SEM) was used to corroborate the electrochemical behaviour. In all cases, a criterion for optimisation was the minimisation of deposition on control electrodes not exposed to an electric field.

3.3. Experimental

3.3.1. Materials

NaH₂PO₄ was purchased from Aldrich. 3,3', 5,5'-tetramethyl-benzidine (TMB) liquid substrate system for colour development (containing TMB and H₂O₂ in a slightly acidic buffer) (T-0440), glucose and hydrogen peroxide was purchased from Sigma-Aldrich, Spain. Aqueous solutions were prepared with Milli Q water (Milli Q system, Millipore).

3.3.2. Instrumentation

Electrochemical measurements were carried out using an Autolab PGSTAT10 electrochemical analysis system running GPE management software from Eco Chemie with a conventional three-electrode cell. A Ag/AgCl electrode (BAS, UK) was used as reference electrode and platinum as counter. All solutions were made with purified distilled water obtained from a Milli-Q water system. Interdigitated arrays were purchased from ABtech Scientific, Inc. (Richmond, VA). 0.5mm gold wire (Advent, Oxford, UK) was resin-sealed (Mercurapex M 42, PRESI, France) within a glass capillary and used as a working electrode. 1mm glassy carbon rods was resin-sealed (Mercurapex M 42, PRESI, France) within a glass capillary and used as a working electrode. Optical measurements were performed using Environmental scanning electron microscope (ESEM) Philips XL30 model, FEI company ,USA.

3.3.3. Electrodeposition of BSA modified Au nanoparticles

In general the concentration of the BSA modified Au nanoparticles were 2×10^{11} particles. The electrochemical cell is a two electrode system with gold as both

working and counter electrodes. The electrodes are placed exactly opposite to each other while deposition.

In this experiment, the behaviour of the electrode after the electrodeposition of the gold nanoparticles modified with and without BSA was studied. Initially BSA modified gold nanoparticles as described in 2.3.4.2 were electrodeposited using potentiostatic method of electrodeposition by applying + 1.2 V for 30min. Next the modified glassy carbon electrode was washed with distilled water and dried with argon. Later image analysis of the modified glassy carbon electrodes was done by examining under scanning electron microscopy (SEM). Results were compared with those from electrodes deposited with unmodified gold nanoparticles. Image analysis was taken from the multiple locations of the same sample to verify the particle distribution. This experiment produces a qualitative analysis of the number of particles on the electrode surface.

The dependence of potential on the electrodeposition of the gold nanoparticles modified with BSA was studied by applying different potentials 0 V, + 0.8 V, + 1.2 V, + 1.6 V for 15 min. Next the modified glassy carbon electrodes were washed with distilled water and dried with argon. Later image analysis of the modified glassy carbon electrodes was done using scanning electron microscopy (SEM).

The effect of time on electrodeposition was studied by applying + 1.2 V for 5, 15, 30, 45 min in the same cell and the electrodes were subjected to the same analysis as before.

The same setup was used to examine the effect of pH. BSA modified Au nanoparticles were dissolved in buffers of pH 2, 4, 6, 8, 10 & 12 and used for performing electrodeposition studies. Electrodeposition was performed by applying + 1.2 V for 30 min. Electrochemical characterisation of the modified electrodes was done by cyclic voltammetry scanning from -0.2 V to + 1.8 V at a scan rate of 100 mV s⁻¹. The integration of the charge under the AuO reduction peak was used to estimate the coverage of nanoparticles on the electrode surface.

Finally the effect of interelectrode distance on the electrodeposition was studied by applying + 1.2 V for 30 min on electrodes immersed in BSA-modified Au

nanoparticles and changing the distance between the counter and working electrode. Interelectrode distances of 0.5mm, 1mm, 2mm & 3mm were used for characterization of the electrodeposition in a cell where the distance was controlled. The resulting films were characterized as before.

3.3.4. Electrodeposition of redox polymer modified Au nanoparticles

Redox polymer (RP 1) modified Au colloids prepared as explained in the 2.3.4.3 were used for electrodeposition under the same experimental conditions as described (pH, concentration of the particles etc) these experiments. In these experiments, 0.785 mm² gold electrodes were used as working electrodes. Two different sizes of gold counter electrodes (4 mm² & 16 mm²) were used . Electrodeposition was performed by applying different potentials + 0.4 V, + 0.8 V, + 1.2 V and + 1.6 V for 10, 20, 30, 40, 50 & 60min. After the electrodeposition, the modified electrodes were washed with water, dried with argon, and CVs of the modified electrodes were taken in the presence of 0.1 M PBS pH 7.0 scanning from 0 V to + 0.6 V at different scan rates. The increase in the charge detected on the surface was estimated by integrating the voltammetric peaks characteristic of the presence of the redox polymer modified nanoparticles after electrodeposition.

3.3.5. Electrodeposition of HRP-Au nanoparticles

HRP-Au nanoconjugates prepared as explained in section 2.3.4.1 has been used for the electrodeposition. A potential of + 1.2 V for 30 min was used for electrodeposition. After electrodeposition, the modified electrodes were washed and later the response to different concentrations of H₂O₂ was measured. Control experiments were performed with Au colloid deposited electrode, blank Au electrode and also HRP-Au modified electrode. Response to peroxide from the controls was measured at different potentials from - 0.2 to + 0.1V (vs. Ag/AgCl) with continuous stirring in the presence of argon. The potential where the response is minimum from the controls was selected for measuring response from the bionanoconjugate-modified electrode.

3.3.6. Electrodeposition of GOX-Au nanoparticles

5nm and 20nm gold nanoparticles were modified by the thiolated GOX as explained in section 2.3.4.1 and used for electrodeposition on Au electrodes. A potential of + 1.2 V (vs./AgCl) for 10 min was applied for electrodeposition of GOX-Au particles in a similar electrochemical cell. After the electrodeposition, modified gold electrodes were washed with distilled water and dried under argon. Next, the modified Au electrode was washed and dried under argon. Finally CVs were taken in the presence of 0.1M sodium phosphate buffer pH 5.5 at different scan rates from - 0.1 V to - 0.7 V. The modified Au electrodes were tested for the electrocatalytic response to glucose using chronoamperometry by applying a potential of + 0.6V (vs. Ag/AgCl) and injecting different concentrations of glucose.

3.4. Results and Discussion

3.4.1. Effect of BSA on electrodeposition

The modification of Au nanoparticles with BSA has a marked effect on zeta potential which might influence the efficiency of electrodeposition. In figure 3.1, a typical SEM image is shown demonstrating that in the presence of BSA, the gold nanoparticles in the deposited film are well dispersed laterally with more number of particles when compared to the electrode deposited with unmodified Au nanoparticles, when deposition is performed under the same conditions. Such influence was not observed since BSA modified Au nanoparticles formed a more stable suspension probably due to steric interactions. This led to higher density forming homogenous depositions under all conditions tested.

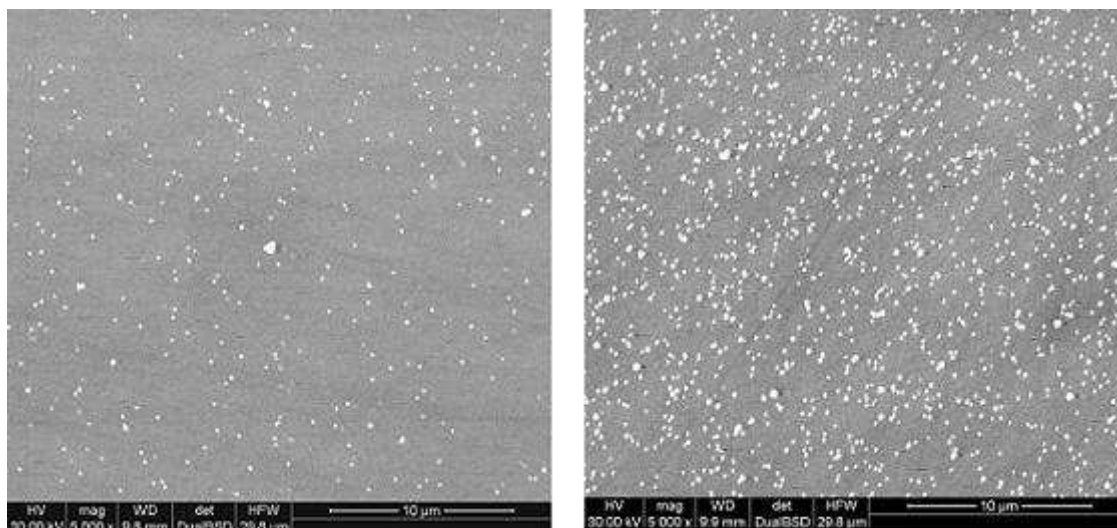


Figure 3.1. SEM images of glassy carbon electrode deposited with unmodified Au nanoparticles (left) and BSA modified Au nanoparticles (right). Conditions : Applied potential + 1.2 V for 30min. Distance between the working and counter electrodes 1mm. Particles are suspended in milli Q water (pH 6.7).

During the electrodeposition of unmodified Au nanoparticles, the particles aggregated on the surface of the electrode. This aggregation might cause less deposition of the particles. In the case of BSA modified Au nanoparticles, the particles are highly stable through out the experiment which leads to the deposition of the particles on the electrode surface.

3.4.2. Effect of potential on electrodeposition

The effect of deposition potential on the electrodeposition of the protein modified gold nanoparticles is expected to follow the hamacker equation

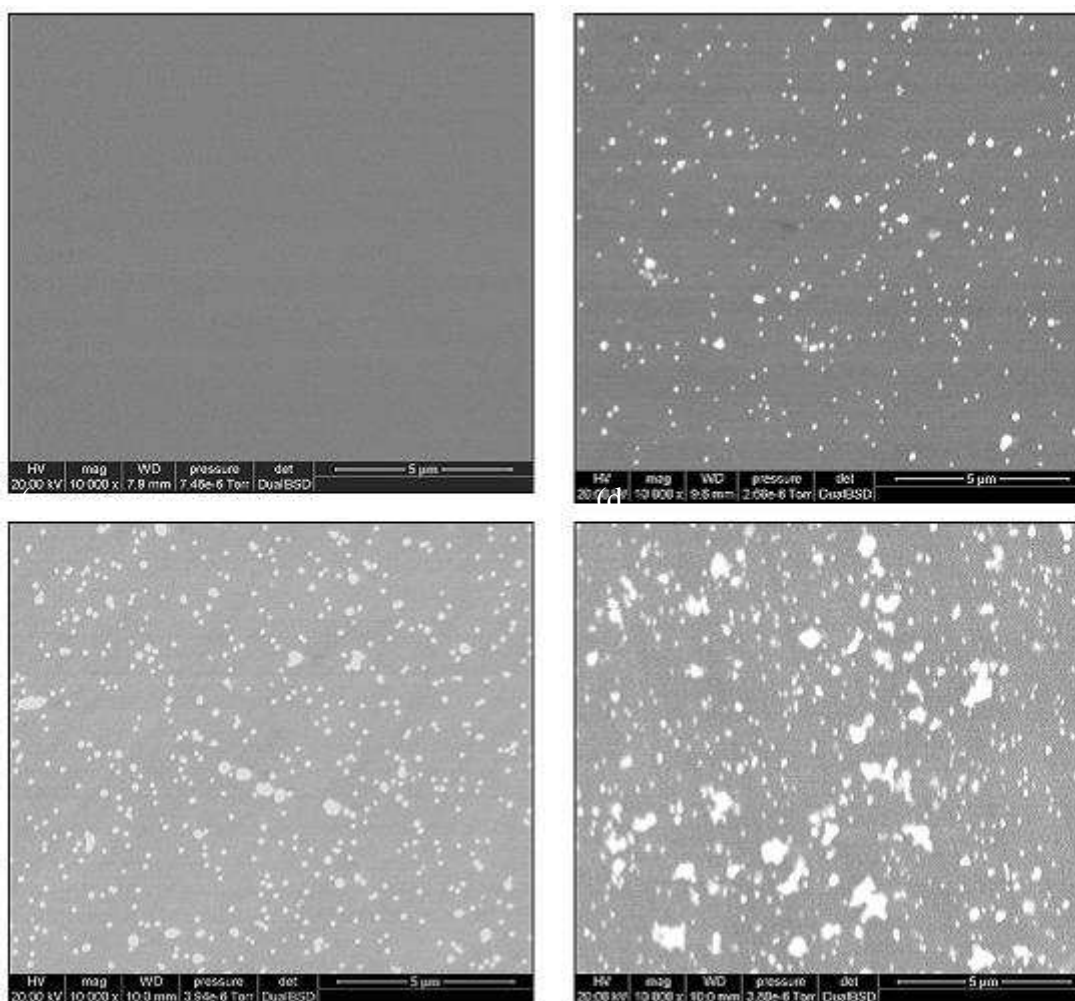


Figure 3.2. SEM images of electrodeposited BSA modified Au nanoparticles on glassy carbon electrode at varying potentials with the same time of 15min. Images a-d corresponds to different potentials. Blank graphite (a), +0.8 V (b), + 1.2 V (c), + 1.6 V (d). Particles are suspended in milli Q water (pH 6.7). Distance between the working and counter electrodes 1mm

Figure 3.2 shows the SEM pictures of electrodes subjected at different applied potentials in the presence of protein modified gold colloids. As shown, with increasing potential, the number of BSA modified particles deposited on the glassy carbon electrode surface increases as expected by equation 3.1. At a potential of + 1.6 V, the particles started to aggregate and form clusters.

At these high potentials, several processes can be responsible for the observing clustering : electrolysis or accumulation of counterions locally can cause connective or electrohydrodynamic flows that disturb locally the particles distribution. As will be discussed later these higher particles also affect the

electrochemical behaviour of modified particles. For these reasons more moderate potentials are used for electrodeposition (0.8-1.2V).

Electrophoretic deposition is the process where charged colloidal suspensions in a liquid medium are attracted and then deposited on a conductive substrate of opposite charge under the effect of an applied DC field. The modelling of the process is quite straight forward but one has to keep in mind the assumptions made in order to achieve a reasonable interpretation of the results. First of all, it should be noted that EPD analysis usually is made for particles in the range of 1-20 μ m. In these sizes, particles tend to flocculate and precipitate under the effect of gravity. At smaller sizes, Brownian motion maintains the suspensions stable and colloidal stability depends on the interplay between vanderWaals and electrostatic forces, generally accounted for by the DLVO theory as explained before. When sub-micrometer particles are modified however by adsorption or dative bonding as attempted in this thesis work, a third type of forces, generally termed “steric” interactions comes into play. Modification of nanoparticles with such surface groups leads to complex behaviour. Since there is an one bond modification of the electric double layer (which in turn affects both the range of electrostatic and vanderWaals interactions) and on other an introduction of osmotic and electrokinetic phenomenon at shorter range that can only be completely probed through microscopic theories and molecular modelling. Still, macroscopically, what is observed is an unexpected stabilisation of such sub micron colloidal suspensions (that is termed steric stabilisation in the literature) and the need of application of higher intensity electric fields for EPD because the particles even when they are in vicinity of the electrode, are still under strong effect of Brownian motion. This explains the lateral mobility of deposited particles observed by many authors [12,13].

For the purpose of this thesis, maintaining the colloidal suspension sufficiently dilute (so that the behaviour is governed by the equilibrium of viscous and electroststic forces) allows to use as a starting point for EPD kinetics the equation known as the Hamacker equation

$$M = \mu C S E t \qquad \text{Eq 3.1}$$

Where M is the deposited mass in g, μ is the electrophoretic mobility (cm^2 / SV), C is the concentration of the colloidal particles (g / cm^3), S is the deposition area (cm^2), E is the electric field intensity (V / cm) and t is the deposition time (sec).

An important assumption in this equation is that the parameters remained unchanged with time, which usually means that it is valid only for short times. Of particular relevance in aqueous solutions is that the effect of electrode reactions are not taken into consideration. Especially when high intensity fields are applied, electrode reactions may occur with multiple effects (local change in ion concentration, pH variation, convection, currents etc). The equation also assumes a homogenous field, therefore edge effects are not accounted, and geometry and positioning of electrodes are of utmost importance. Finally , even in short times, the constancy of the electric field might not be guaranteed where non-conducting particles are deposited.

The electrophoretic mobility defined by $\mu = V / E$, where V is the velocity of the particles under an electric field (cm / sec). Smoluchowski first [25] first addressed the movement of particles under electrophoretic forces and is generally accepted that

$$\mu = \frac{2}{3} \frac{\epsilon_0 \epsilon_r \zeta}{\eta} f(kr) \quad \text{Eq 3.2}$$

Where ϵ_0 is the permittivity of the vacuum, ϵ_r is the relative permittivity of the solvent, η its viscosity and ζ the potential of the slip plane which is equivalent to the zeta potential of the particles that is an experimentally accessible variable. $f(kr)$ is the Henry coefficient which depends on the thickness of the double layer ($1/\kappa$) and the radius of the core (r) of the particle. For rigid spheres and ideally behaved double layer, the Helmholtz- Smoluchowski limit for mobility is usually accepted, i.e

$$\mu = \frac{\epsilon_0 \epsilon_r \zeta}{\eta} \quad \text{Eq 3.3}$$

However, in the case when the core particle is modified by surface polymers it has been suggested that at high energy electrolyte concentrations μ reaches a finite constant value given by

$$\mu = \frac{\rho_0}{\eta \lambda_0^2} \quad \text{Eq 3.4}$$

Where ρ_0 is the nominal charge density of the polyelectrolyte layer and λ_0 has units reciprocal to length, λ_0^{-1} representing the characteristic penetration length of the flow within the “soft” shell of the nanoparticle. ($\lambda_0 = (\kappa_0 / 1/L)^{1/2}$ where κ_0 is the friction coefficient of the polymeric shell with a uniform distribution of segments. In this case, λ_0 and ρ_0 are not easily accessible experimentally.

For the purpose of this thesis recognising for a flat surface $f(kr) = 1$ and that $E = V/L$, where V is the applied voltage and L is the distance between the electrodes, equations 3.1 and 3.2 are combined to yield an expression that is required for interpretation of the results.

$$M = \frac{2}{3} \frac{\epsilon_0 \epsilon_r \zeta}{\eta} \frac{C S V t}{L} \quad (\text{Eq 3.5})$$

Still, it should be noted that in most applications, many authors recognise that the applied voltages should be corrected by the potential drop within the deposited layer which varies with time and is not accessible experimentally.

From equation 3.5, a linear dependence of electrodeposited mass with time is expected. This has been observed for BSA modified particles as shown in the figure 3.3.

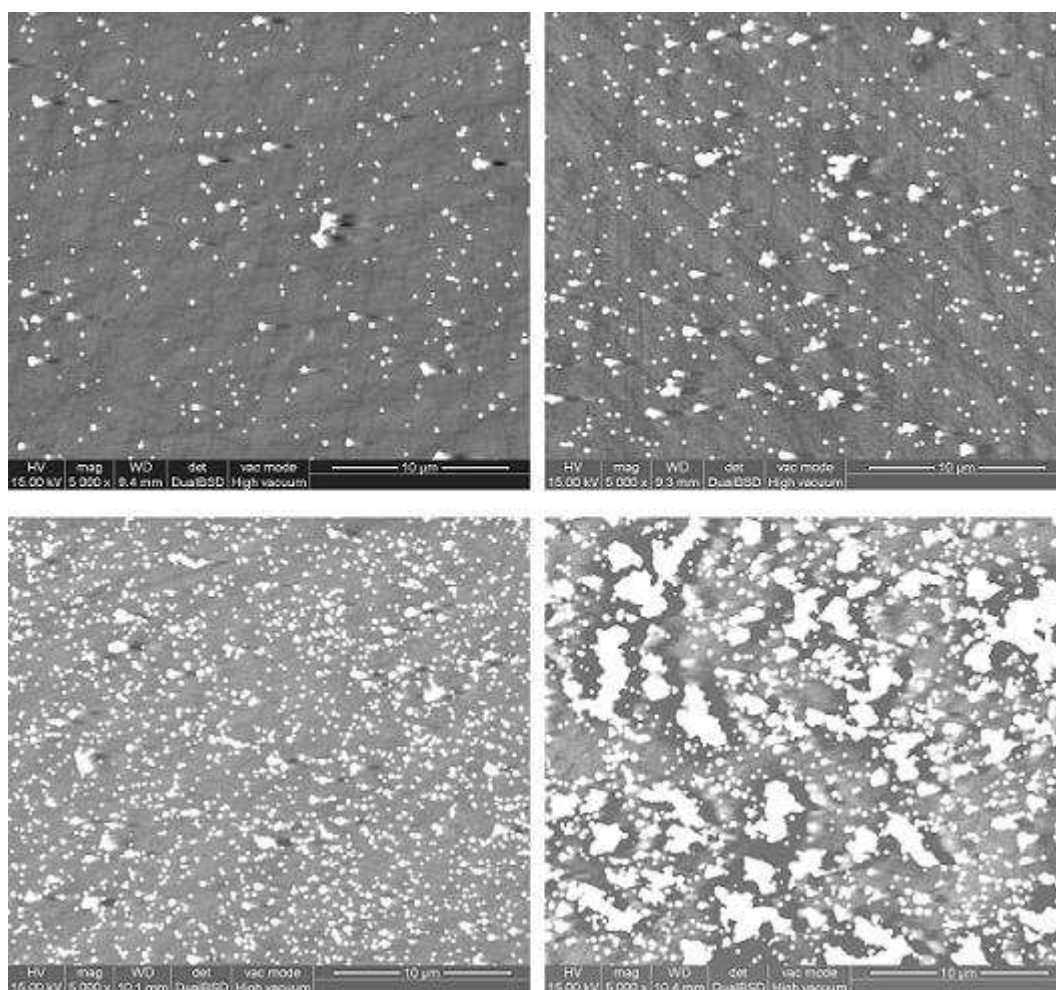


Figure 3.3. SEM images of electrodeposited BSA modified Au nanoparticles on glassy carbon electrode. Images a-d corresponds to different periods of deposition time. (a) 5 (b) 15 (c) 30 (d) 45min. Conditions: Applied potential +1.2 V, Distance between the working and counter electrode 1mm. Particles are suspended in milli Q water (pH 6.7).

Furthermore, in Figure 3,3 a structural overview of the deposits is shown. It can be seen that with increase in the time of deposition, the number of particles deposited increases until a time period of 30min. With further increase in the time period, the number of clusters increases with a concomitant decrease in the number density of the individual particles. The larger cluster formation leads to a very rough electrode surface. Therefore with further increase in the time of electrodeposition, the number of particles deposited increases but the quality of the films decreases due to the formation of clusters. This observation limited to 30 minutes the deposition times used in order to obtain films that are more appropriate for working with biosensors.

Equation 3.5 also predicts a linear dependence of deposition mass with the zeta potential. In figure 3.4, the deposited mass is approximated by the percentage increase of the charge calculated from the integration of the peak characteristic to the gold in the presence of 0.5M H₂SO₄. As shown before with increase in the pH, the zeta potential of BSA modified Au nanoparticles changed from + 25 mV at pH 2.0 to – 20 mV at pH 12.0. Although this is unexpected deposition even when the zeta potential is positive, Figure 3.4 shows a linear increase of the integrated area of gold above the isoelectric point of the particles even though the change in the pH obviously affects more parameters in equation 3.5.

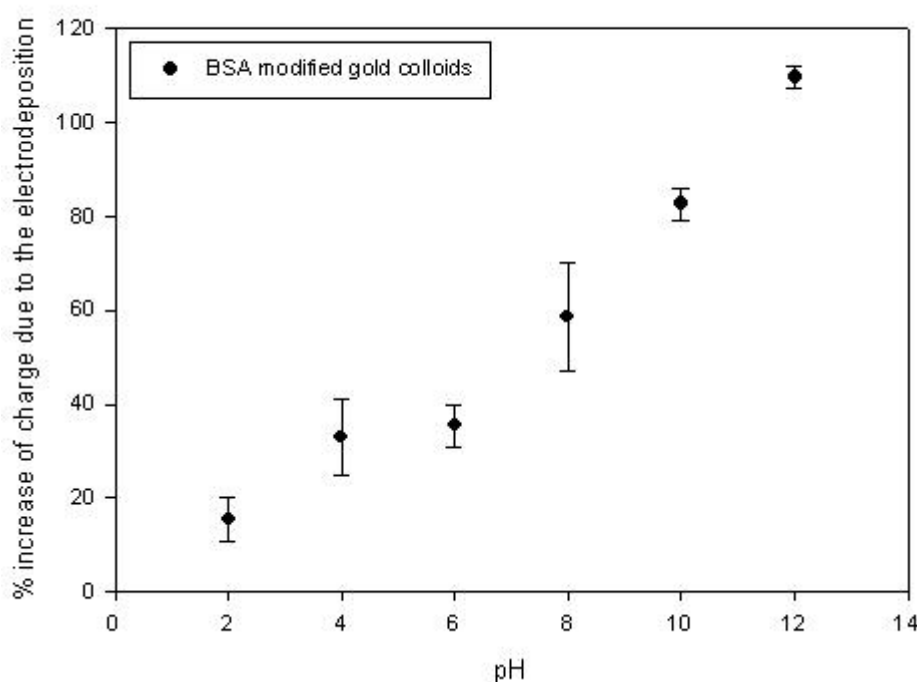


Figure 3.4. Effect of pH on the electrodeposition of BSA modified Au nanoparticles. Conditions: Applied potential +1.2 V for 30 min, Distance between the working and counter electrode is 1mm. Concentration of the particles (2×10^{11} particles mL⁻¹)

Another immediate conclusion of equation 3.5 is that deposition mass should be inversely proportional to interelectrode distance. This effect is observed in Figure 3.6, again assuming that the charge obtained by the integration of reduction peak of the gold oxide in the presence of 0.5M H₂SO₄ scanning from – 0.2 V to + 1.8 V at a rate of 100 mV sec⁻¹ is proportional to the deposited layer mass. In this figure, the distance between the electrodes was varied as explained in the experimental section. Figure 3.5 shows the effect of interelectrode distance on the currents produced

during the deposition of BSA modified gold colloids. From the figure 3.5 it can be observed that the current decreases with increase in the inter electrode distance.

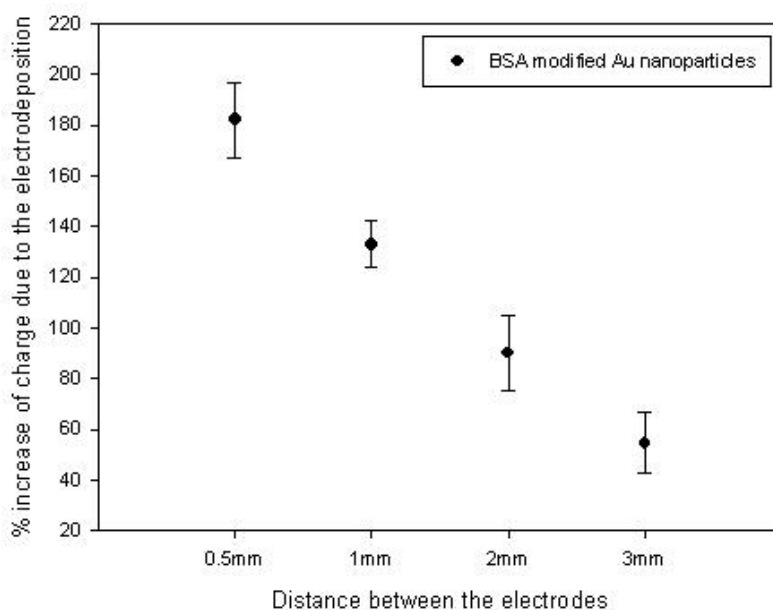


Figure 3.5. Effect of interelectrode distance on the electrodeposition of BSA modified Au nanoparticles. Applied conditions: + 1.2 V for 30 min, BSA modified particles suspended in distilled water (pH 6.7). Concentration of the particles (2×10^{11} particles mL^{-1})

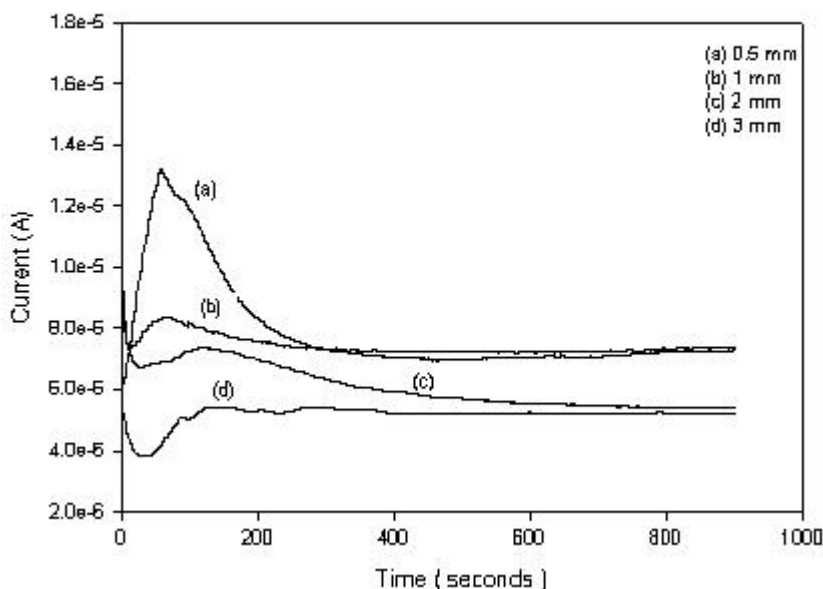


Figure 3.6. Current versus the deposition time for deposition of BSA modified gold nanoparticles for different inter electrode distances (a) 0.5mm (b) 1mm (c) 2mm (d) 3mm.

An interesting observation can be made in this figure is that as the interelectrode distance is diminished an initial peak in the current is observed, a peak that is occurring at shorter times as the distance is diminished. This observation is interesting in that it may mean that in thin layer cells or in microsystems selective electrodeposition on electrodes can be effected within a few minutes. However, further investigation is necessary to identify the origin of these transient peaks.

3.4.3. Electrodeposition of redox polymer modified Au nanoparticles

Despite the fact that the zeta potential of the RP 1 modified Au nanoparticles is positive, the particles are deposited effectively at positive applied potentials. This might be due to the presence of gold core which might be responsible for electrodeposition.

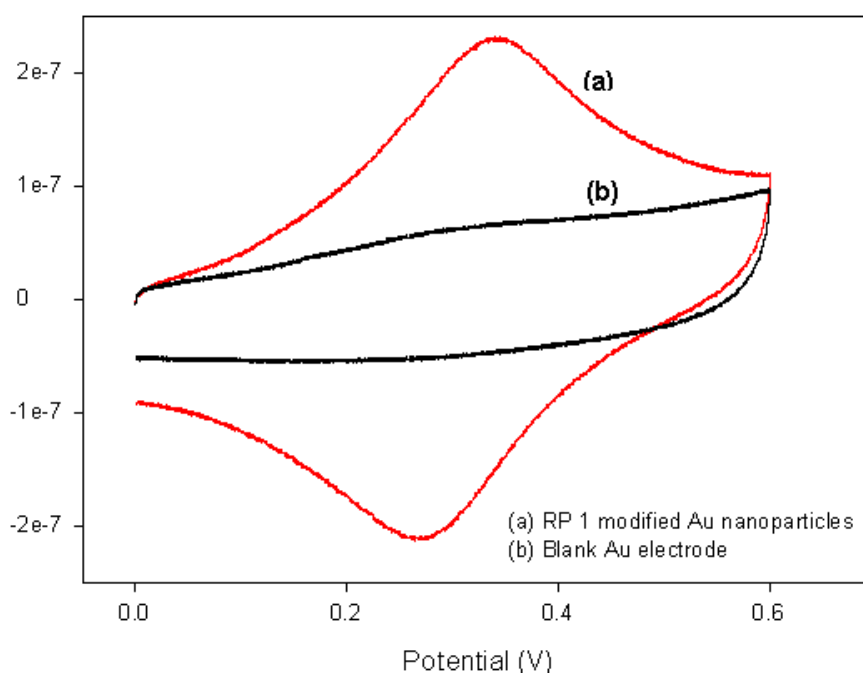


Figure 3.7. Cyclic voltammogram of the gold electrode subjected to EPD of RP 1-modified Au nanoparticles by applying potential of + 1.2 V for 30min with CE 1(a) compared to a bare Au electrode(b). Conditions of the electrolyte: 0.1M PBS pH 7.0 at a scan rate of 100 mV s^{-1} .

As shown before, we used equation 3.5 to observe if the EPD process can show the expected behaviour with RP1 modified Au nanoparticles. Now potential and time were used as variables to observe if the expected behaviour is followed. In addition two

different sizes of gold counter electrodes CE 1 (4 mm^2) and CE 2 (16 mm^2) were used to observe the effect of field line distribution.

Figure 3.7 shows the cyclic voltammogram obtained from the Au electrode after electrophoretic deposition with the RP 1 modified Au nanoparticles. The cyclic voltammogram of the modified electrodes displayed well-defined redox peaks. This clearly shows that the RP 1 modified particles deposited efficiently.

First the effect of potential and time on the electrodeposition of RP 1 modified Au nanoparticles were studied using CE 1. Figure 3.8 shows the charge obtained by integrating the redox peaks of CVs taken from the electrodes modified with potentials + 0.4 V, + 0.8 V, and + 1.2 V for 50min.

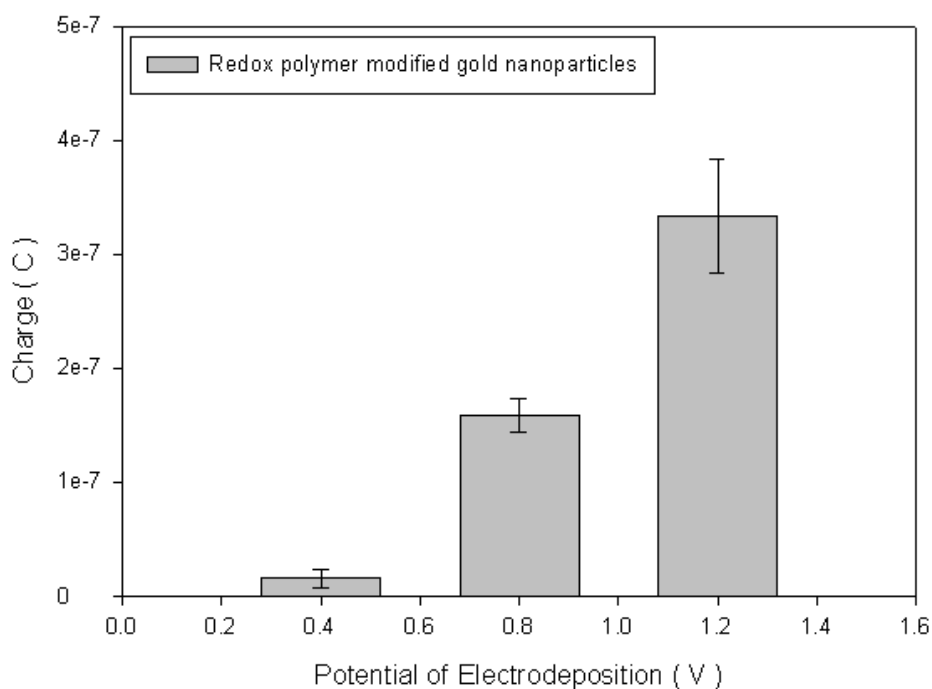


Figure 3.8. Charge calculated from the electrodes subjected to EPD of RP 1 modified gold nanoparticles after application of different electrodeposition potentials using CE 1. Electrolyte : 0.1M PBS pH 7.0 at a scan rate of 100 mV s^{-1} .

It can be observed that in the case of electrodeposition using CE 1, the charge increased with increasing applied potential and that at + 1.2 V there is a maximum charge with well defined redox peaks. Above the potential + 1.2 V, charge decreased which might be due to the loss of redox activity and insulation effect due to the formation of non-

homogenous films which is supported by the loss of redox behaviour. As expected, the deposition of the particles followed Equation 3.5. With increase in the deposition potentials, there is a linear increase in the charge. At higher potentials, there might be a loss of the redox activity and there might be formation of clusters due to the limited time available for the particles which might damage the properties of the thin films.

Figure 3.9 presents the charge under the redox peaks of the CVs obtained from the electrodes subjected to EPD with RP 1 modified Au nanoparticles at various times by applying potentials + 0.8 V and + 1.2 V. From this figure, it can be observed that the increase in the charge with time is lower at + 0.8 V when compared with that at + 1.2 V. With + 1.2 V, the increase in the deposition tends to follow the linear behaviour. This demonstrates that + 1.2 V is a more suitable potential for electrodeposition and for the formation of thin films when compared with lower potentials.

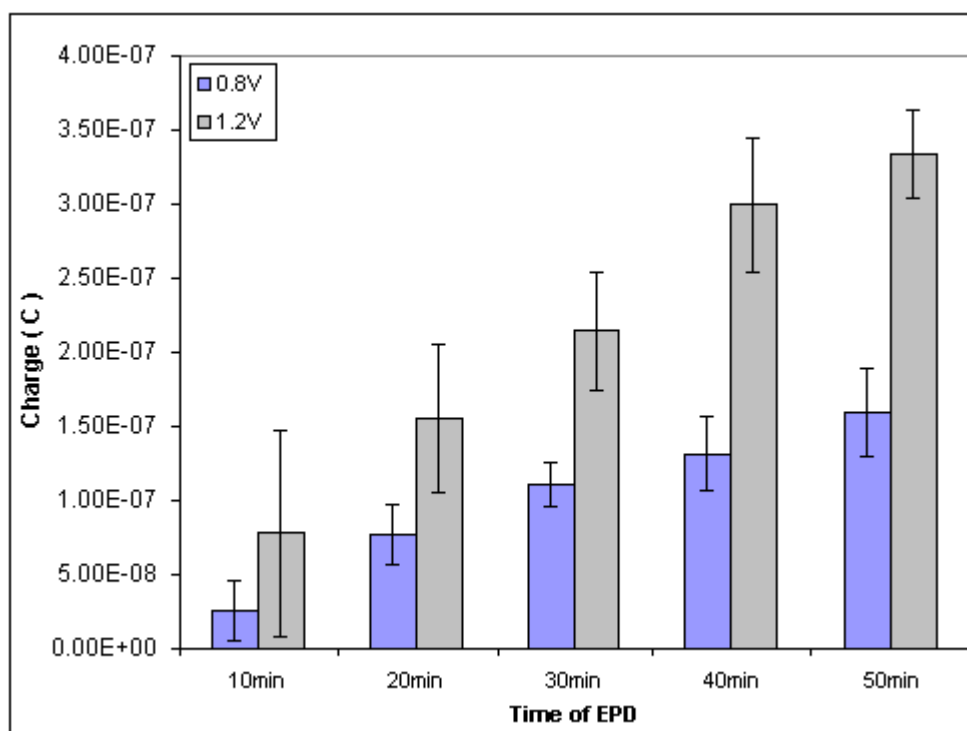


Figure 3.9. Charge calculated from the electrodes subjected to EPD of RP 1 modified gold nanoparticles after application of different times of electrodeposition with CE 1. Electrolyte : 0.1M PBS pH 7.0 at a scan rate of 100 mV s^{-1} . Applied potentials : + 0.8 V and + 1.2 V

The effect of potential and time on the electrodeposition of RP 1 modified Au nanoparticles when using CE2 was studied. Figure 3.10 shows the charge obtained

by integrating the redox peaks of the CVs taken from the electrodes modified at potentials + 0.4 V, + 0.8 V, + 1.2 V and + 1.6 V for 50min. In Figure 3.10, as expected, the charge density increased with increase in the applied potential and at + 0.8 V there is a maximum charge density with well defined redox peaks. Above this potential the charge tends to decrease. This clearly shows that larger counter electrodes might change the equipotential field line distribution leading to the formation of more homogenous films avoiding the presence of edge effects caused by the smaller counter electrodes. Above + 0.8 V the charge decreased which might be due to the insulation effect due to the higher deposition. Higher potentials might damage the redox polymer or there might be insulation due to the deposition of a high number of particles.

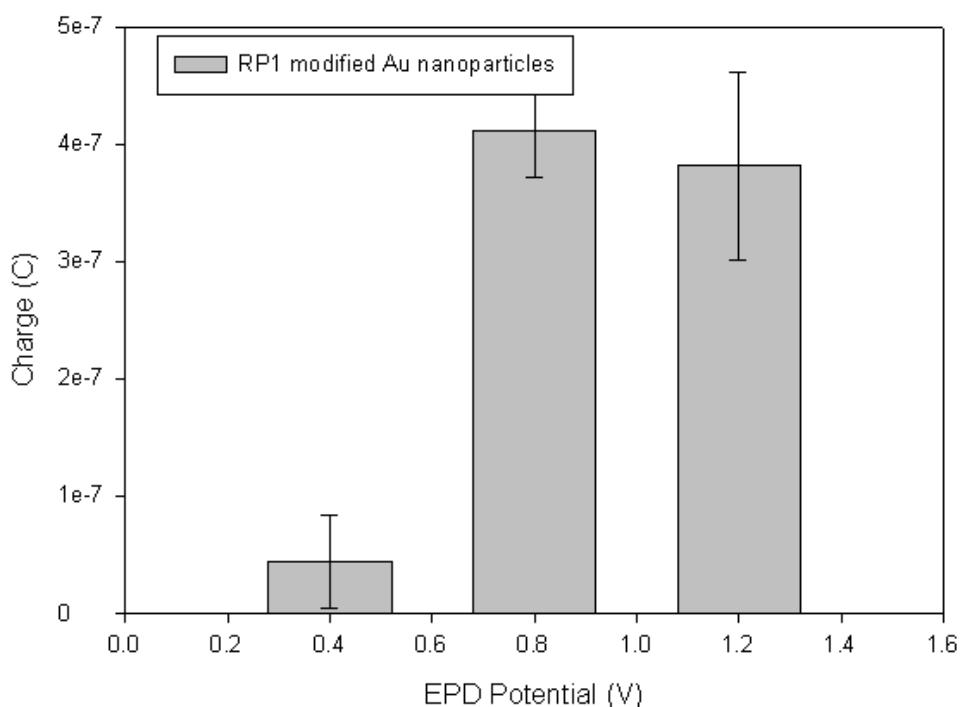


Figure 3.10. Charge calculated from the electrodes subjected to EPD of RP 1 modified gold nanoparticles after application of different electrodeposition potentials using CE 2. Electrolyte: 0.1M PBS pH 7.0 at a scan rate of 100 mV s^{-1} .

Figure 3.11 illustrates the charge calculated from the integration of the redox peaks obtained from the modified electrodes at different times of deposition. From this figure it can be observed that with increase in the size of the counter electrode, at a potential of 0.8 V there is a linear deposition, which is an interesting behaviour when compared with the CE 1. At higher potential of + 1.2 V, the charge from the redox peaks increased linearly at initial times and the increase is higher when compared with that at + 0.8 V. This might be due to the faster electrodeposition of the particles at + 1.2 V. With further increase in the time of deposition, the linear tendency was absent in the case of +1.2 V and the charge became stable which might be due to a saturation deposition of the particles. With + 0.8 V deposition potential, the increase in the charge is linear with time when compared with the + 1.2 V and at longer time periods, the increase in the charge was higher than that at + 1.2 V.

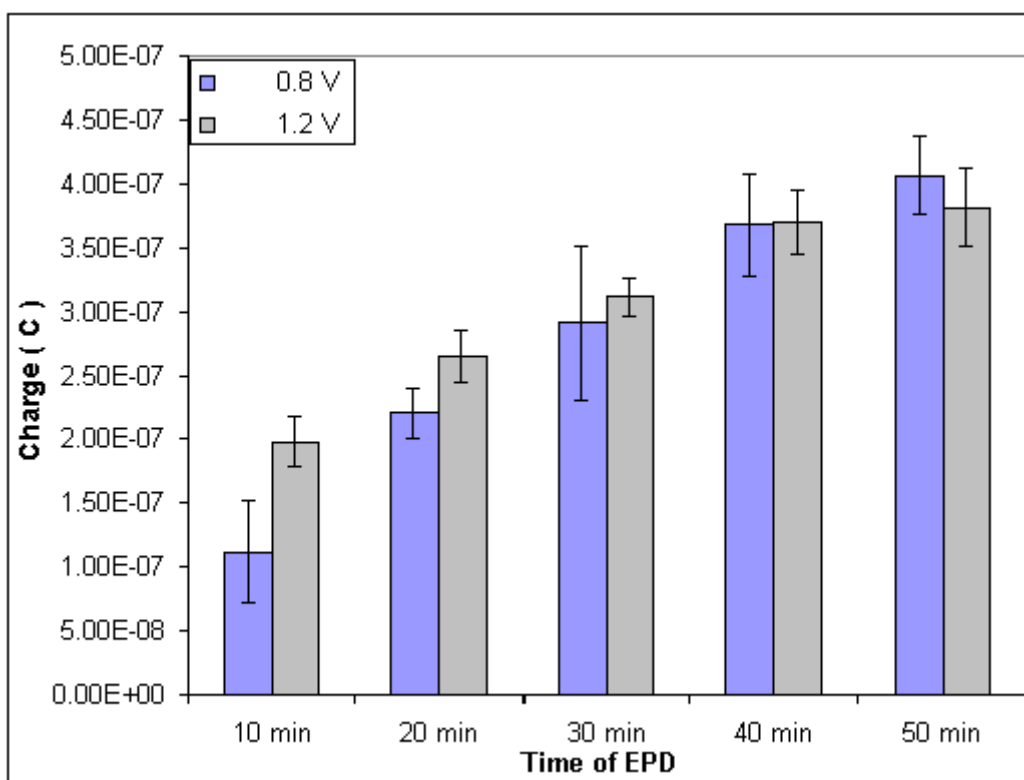


Figure 3.11. Charge under redox peaks obtained from the electrode subjected to EPD of RP 1 modified Au nanoparticles on the gold electrode by applying a potential of + 0.8 V and + 1.2 V for different time periods using CE 2.

Figure 3.12 shows the comparison between the charge obtained from the electrodes modified at + 1.2 V using CE 1 and CE 2. With CE 2, there is a maximum charge due to the deposition of the RP 1 modified Au nanoparticles.

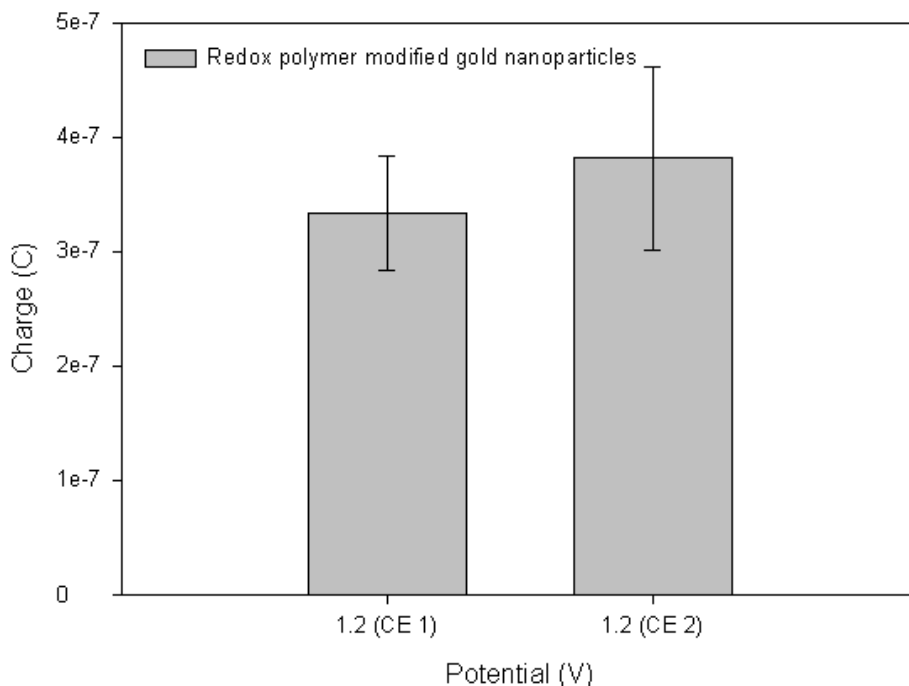


Figure 3.12 . Comparison of the charge calculated from the electrodes modified with redox polymer modified gold nanoparticles by applying electrodeposition potential + 1.2 V for 50 min using two different counter electrodes (1) 4 mm² counter electrode and (2) 16 mm² counter electrode.

This proves that the increase in the counter electrode surface area is having a significant effect on the deposition of the redox polymer modified Au nanoparticles. This may mean that with increase in the size of the counter electrode, there might be more homogenous distribution of equipotential field lines, which makes the particles being deposited in a more homogenous way.

These results are corroborated by a basic study of the electrochemical behaviour of the deposited redox species. In Figure 3.13 a, it can be seen that when CE 1 was used, the deposited redox film shows a marked increase in the peak-to-peak separation with increasing scan rate, indicative of a process that might be counter-ion diffusion limited, however when CE 2 was used; the peak-to-peak separation of the deposited redox film is almost constant with scan rate, which proves that there is

faster electron transfer when a larger counter electrode is used during EPD of the particles, a fact probably explained by a more homogenous deposit. As shown in Figure. 3.13 b, the relationship between the peak current (i_p) and the scan rate (v) shows a linear dependence, an indication of a surface-bound redox species in both cases.

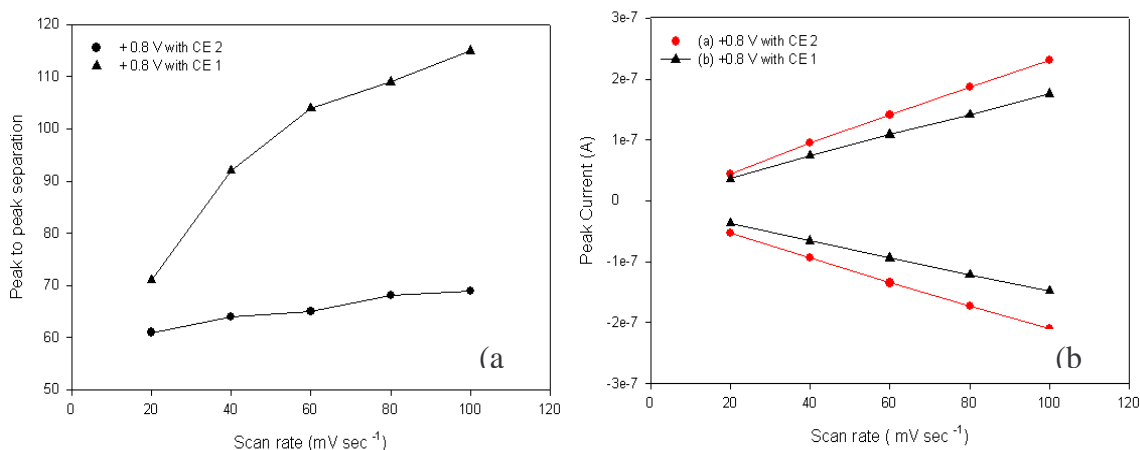


Figure 3.13. Scan rate dependence of the peak-to-peak separation ΔE_p (a) and peak current density i_p (b) of the RP1-Au films obtained at +0.8 V with CE 1 & CE 2 at several scan rates. Applied potential: +0.8V for 50min, Electrolyte: 0.1M PBS pH 7.0

3.4.4. Electrodeposition of enzyme-modified Au nanoparticles

Similar results were observed with enzyme modified Au nanoparticles. Here in an interesting effect was observed which suggests direct electron transfer from enzyme-modified nanoparticles and a significant electroactive area effect on the response of the enzyme electrodes made by electrodeposition. From the Figure 3.13, GOX modified 5nm gold nanoparticles deposited electrode displayed a pair of redox peaks at -480 mV for E_{pc} and -412 mV for E_{pa} at a scan rate of 100 mV s^{-1} with a peak to peak separation of $+76$ mV.

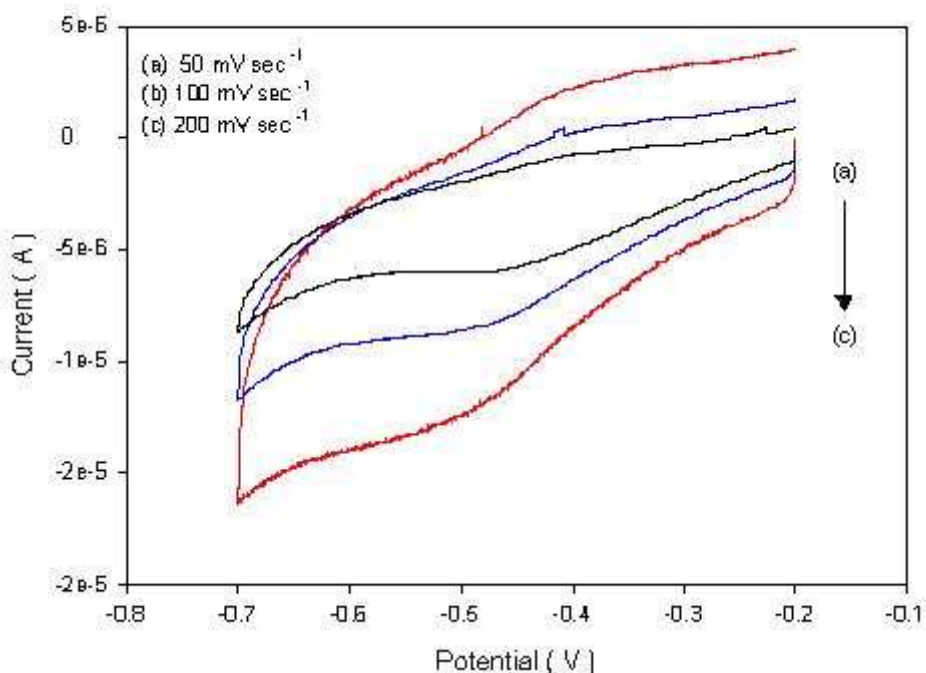


Figure 3.14. Cyclic voltammogram showing the 5nm Au / GOX electrodeposited electrode. Electrolyte : 0.1M PBS pH 5.5.

Current response to glucose from the electrodes. In the case, where the gold electrode was deposited with 20nm gold nanoparticles modified with GOX, there was a max response of around $1.1 \mu\text{A cm}^{-2}$ and for the electrode deposited with 5nm gold nanoparticle modified electrode, the response from the modified electrode was around $4.5 \mu\text{A cm}^{-2}$. This clearly demonstrates that with the smaller nanoparticle size of 5nm, the response to glucose was higher than the electrode modified with 20nm nanoparticle. Deposition of smaller sized particle leads to a greater surface area, which might further enhance the response to glucose.

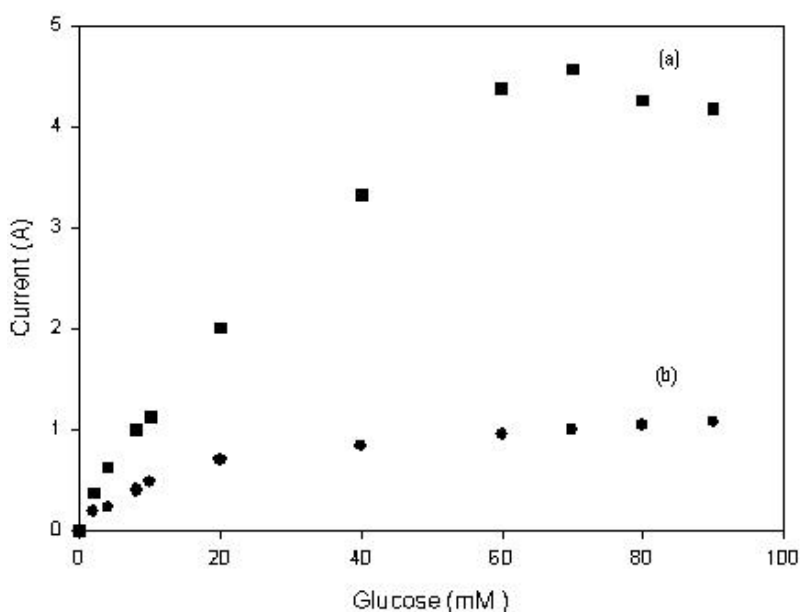


Figure 3.15 . Plot of electrocatalytic current at + 0.6 V (vs. Ag/AgCl) at different glucose concentrations with (a) 5nm Au colloid - GOX deposited electrode.(b) 20nm gold colloid - GOX deposited electrode. Electrolyte : 0.1M PBS at pH 7.0.

Similar effect was observed with HRP-modified Au nanoparticles as seen in Figure 3.15. Amperometric response for different concentrations of peroxide was shown in the figure 3.15 and there was an increase in the reduction current with increasing concentrations of peroxide. Figure 3.15 shows the plot of steady state current vs. peroxide concentration. There was a current response of around $9 \mu\text{A cm}^{-2}$ at a concentration of around 3mM H_2O_2 . If we notice the controls there was a large difference from the experimental electrode. From the above results, we confirmed that the catalytic current was mainly due to the direct electron transfer from the HRP molecules to the bulk electrode. Since Au nanoparticles are distributed through out the electrode surface they allow efficient electron tunnelling and can assist the electron transfer between the redox protein and the bulk electrode surface.

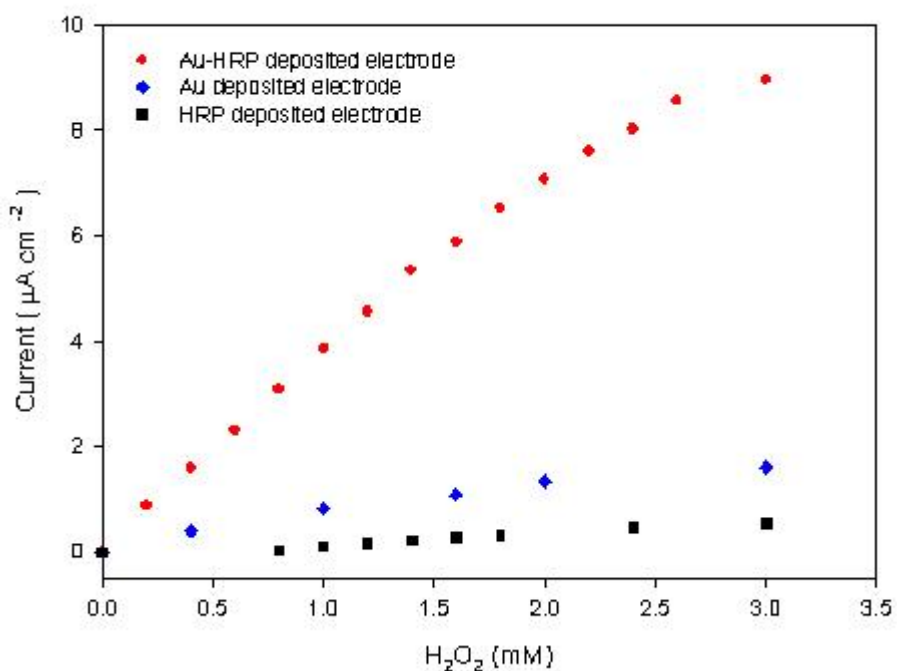


Figure 3.16. Plot of electrocatalytic current at + 0.1 V (vs. Ag/AgCl) for HRP-Au colloid conjugate deposited electrode at different concentrations of peroxide. Electrolyte : 0.1M PBS pH 7.0.

3.5. Conclusions

Electrodeposition principles were tested with the systems at hand comparing the observed behaviour to the Hamacker theory of EPD.

- ✓ BSA modified Au nanoparticles demonstrated the effect of potential, time of deposition, size of the counter electrode, interelectrode distance on the EPD.
- ✓ Redox polymer modified Au nanoparticles demonstrated the effect of potential, time of deposition as well the effect of counter electrode size on the EPD.
- ✓ Finally enzyme modified Au nanoparticles demonstrated the effect of particle size on the response as well as the amplification of the sensor signal in the presence of Au nanoparticles

3.6. Abbreviations

SEM - Scanning Electron Microscopy

TMB - 3,3',5,5'-tetramethyl-benzidine

HRP – Horse Radish Peroxidase

GOX – Glucose oxidase

H₂O₂ – Hydrogen Peroxidase

NaH₂PO₄ – Sodium Hydrogen Phosphate

α-Dig-HRP – Anti-digoxigenin horse radish peroxidase

CV – Cyclic voltammetry

3.7. References

1. Zhitomirsky, I., Gal-Or, L., 1997, *J. Mater. Sci., Mater. Med.*, 8, 213-219.
2. Wang, R., Hu, Y.X., 2003, *J. Biomed. Mat. Res. A*, 67, 270-275.
3. Johnson, K. W., Allen, D.J., Mastrototaro, J.J., Morff, R.J., Nevin, R.S., 1994, *ACS Symp. Ser.*, 556, 84-95.
4. Wang, S. S., Vieth, W.R., 1973, *Biotechnol. Bioeng.*, 15, 93-115.
5. Kim, C. S., Oh, S.M., 1996, *Electrochim. Acta*, 41, 2433-2439.
6. Matsumoto, N., Chen, X., Wilson, G.S., 2002, *Anal. Chem.*, 74, 362-367.
7. Chen, X., Matsumoto, N., Hu, Y., Wilson, G.S., 2002, *Anal. Chem.*, 74, 368-372.
8. Gao, Q., Yang, X., 2004, *Chem. Comm.*, 7, 30-31.
9. Fei, J., Wu, Y., Ji, X., Wang, J., Hu, S., Gao, Z., 2003, *Anal. Sci.*, 19, 1259-1263.
10. Gao, Z., Binyamin, G., Kim, H.H., Barton, S.C., Zhang, Y., Heller, A., 2002, *Angew. Chem. Int. Ed.*, 41, 810-813.
11. Ng, S. Y., Boccaccini, A.R., 2005, *Mat. Sci. Eng. B*, 25, 208-214.
12. Trau, M., Saville, D.A., Aksay, I.A., 1996, *Science*, 272, 706-709.
13. Trau, M., Sankaran, S., Saville, D. A., Aksay, I. A., 2002, *Nature*, 374, 437-439.
14. Hayward, R. C., Saville, D.A., Aksay, I.A., 2000, *Nature*, 404, 56-59.
15. Trau, M., Saville, D.A., Aksay, I.A., 1997, *Langmuir*, 13, 6375-6381.
16. Zhao, J., Wang, X., Li, L., 2006, *Mater. Chem. Phys.*, 99, 350-353.
17. Smoluchowski, M.Z., 1917, *J. Phys. Chem.*, 92, 129

Chapter 4. Selective immobilisation of biofunctionalised Au nanoparticles through selective electrodeposition

4.1. Abstract

The aim of this chapter is to demonstrate selective electrodeposition of biofunctionalised gold nanoparticles for the construction of at least two electrochemical biosensors in close proximity as a proof of principle for patterning of electrochemical biosensors. In order to achieve this, two different enzymes glucose oxidase (GOX) and horse radish peroxidase (HRP) were used as a model biomolecules to modify gold nanoparticles in a layer-by-layer approach. To make the electrodeposition more selective, electrochemical desorption of self-assembled thiol monolayers (SAMs) of triethylene glycol-thioctic acid (TEG-TA) esters present on IDE arrays and further electrodeposition of the biofunctionalised gold nanoparticles on these selectively exposed electrode surfaces was attempted with a 20 μm resolution. Electrochemical impedance spectroscopy (EIS) and cyclic voltammetry (CV) were used to verify the changes on the electrode surface due to the electrochemical desorption which proved that this technique can be used for the selective modification of the IDE array. Suspensions of Au nanoparticles modified with redox polymer and enzymes (GOX, HRP) were used for electrodeposition onto the IDE array. A potential of -1.2 V (vs. Ag / AgCl) for 1 h helped to desorb the thiol SAMs completely. Modified Au nanoparticles were electrodeposited selectively on a gold IDE array by applying $+1.2\text{ V}$ (vs. Ag/AgCl) for 30 min. The selective nature of the modified IDE array was verified by measuring the amperometric response after injecting the glucose and peroxidase. Both the sensors responded selectively for glucose and peroxide with less than 5 % non-specific response. When the nanoparticles were modified externally with RP higher currents were obtained without loss of selectivity.

4.2. Introduction

Biosensors based on an enzyme as a highly specific catalytic recognition element, coupled with electrochemical (amperometric or potentiometric) transduction of

the recognition event, provide a basis for constructing biosensors, biomedical devices and enzymatic bioreactors. Small sample consumption by the analytical system is a must in medical applications and metabolism monitoring in cell cultures. One way to reduce the sample volume is miniaturization of the device; the other possibility is integration of several sensors in a common shared measurement chamber. It is obvious that best results will be obtained by combining both strategies. Compared to parallel single-analyte assays, multianalyte protein assays are important new analytical methods as they allow one to simplify the working procedure, to increase the test throughput, reduce the cost per test, and improve test efficiency [1-13]. Technically demanding applications such as the detection of multiple analytes in vivo require a high density of individual analyte-sensing electrodes, required for miniaturization, which themselves contain large concentrations of enzyme molecules necessary to provide high signal levels. In addition, the fabrication of the sensors must be simple, reliable, reproducible, and at spatially distinct, readily addressable regions on a discrete portion of a surface for designing an electrochemical biosensor. Biosensor development with a priority on spatial orientation and assembly on the nanoscale has thus become an important issue. The area of biomolecule patterning for multianalyte biosensing devices where different biomolecules need to be patterned on the same substrate appears especially challenging. The ability to realize such multi-functional platforms reliably will define the capacity to progress in both the understanding of basic biological and chemical phenomena and the related technological applications.

Two-dimensional arrays of proteins on surfaces are created at micron-level by several arraying techniques. Commonly used protein patterning techniques include microcontact printing [14,15], conventional photolithography [16-22], and photochemistry [23]. Each has its advantages and inherent limitations. Microcontact printing is simple, inexpensive, and effective; however, fails in controlling positions and dimensions of patterned proteins, and the immobilised proteins are nonuniform due to the deformation of elastomeric stamps as patterning masks. Photolithography creates protein patterns on substrates by using chemical linkers to conjugate proteins. The major problem for patterning the substrates with photolithography is high cost need for access to clean rooms, the chemicals involved in the process which can denature protein activity. Photochemical patterning is based on the

selective activation of chemically labile species upon UV irradiation to bind target proteins. The major drawback is UV irradiation can reduce the enzyme activity.

Nanoscale particles offer a variety of interesting properties, and there is growing interest in their assembly into higher ordered structures that can be used in a variety of biosensor applications. Metal and semiconductor nanocrystals have tunable properties (e.g., optical, electronic, and magnetic) that depend on particle size, interparticle spacing, and higher order structure [24-32]. Nanoparticles can display four unique advantages over macroelectrodes when used for electroanalysis: enhancement of mass transport, catalysis, high effective surface area and control over electrode microenvironment. Despic and Pavlovic first time introduced the electrophoretic deposition technique for the deposition of Au nanoparticles on electrode surface [33]. Since then, this technique has been used for the creation of biosensors by modifying the Au nanoparticles with redox enzymes and later electrophoretically depositing them on the electrode surfaces. Crumbliss et al has developed biosensors for peroxide, glucose and xanthine based on this technique [34]. Some fundamental studies of electrodeposition of glucose oxidase have also been reported [35].

Electrodeposition of redox polymers and glucose oxidase has been reported with excellent catalytic activity based on crosslinking. Though in these studies, electrodeposition was used for creating single molecule biosensors, this technique has not been used to address and immobilize these bionanomolecules to specific locations of an array for the development of biosensor arrays. For the first time, selective electrodeposition of oligonucleotide modified Au nanoparticles on an IDE array for the detection of hybridization event successfully using electrochemistry by differentiating the mutated DNA from the complimentary DNA has been reported [36,37]. An electrochemical desorption technique combined with microcontact printing has been used for releasing the patterned cells to the desorbed surfaces [38]. Recently the electrodesorption technique has been used for the controlled removal of proteins from electrode surfaces thus controlling the bioelectrointerfaces. Thus the electrochemical desorption technique has been selected for the patterning of proteins in this chapter.

Multi-analyte biosensors have an increasingly important application in the field of medical diagnostics, especially in low-cost self-care devices. For this application to be feasible, there is a need to develop simplified generic fabrication methods. When

the same principle is used for manufacturing and detection, it is possible to integrate features in the devices that have significant cost lowering effects. A general method was sought that would selectively immobilize proteins with absolute control over orientation and density and that does not require synthetic modification or purification before immobilization. In this chapter, the technical advantage of the electrodeposition technique has been demonstrated for constructing the biosensor array.

In order to realize this, Au nanoparticles were modified with the redox polymer followed by an enzyme molecule (HRP, GOX). Later the modified particles were electrodeposited to specific locations of an IDE array patterned with electrodes using the well known electrodesorption technique. Electrochemical characterisation of the interdigitated array after electrodeposition was done with cyclic voltammetry. Specific response from each enzyme was measured from the electrodes of the interdigitated array by injecting substrates. With this, the generic ability of the electrophoretic deposition technique for the depositing of different biomolecules has been proved.

Also Multifunctional gold nanoparticles were prepared by modifying gold nanoparticles with redox polymer followed by GOX again with redox polymer to produce Au / RP 2 / GOX / RP 2 particles. Later these particles were electrodeposited by just controlling the EPD potentials. Though this strategy has not been demonstrated on the IDE array, the technical advantage of this method has been proven on Au microelectrodes. The proteins are immobilised with absolute control over density and selectivity.

4.3. Experimental

4.3.1. Materials

Glucose oxidase (GOX) was purchased from Biozymes, UK. Horseradish peroxidase (HRP) was purchased from Sigma-Aldrich, Spain. Thiocetic acid was purchased from Acros Organics, Belgium. NaH_2PO_4 from Aldrich. Glucose and hydrogen peroxide was purchased from Sigma-Aldrich, Spain and used as received. All other compounds were purchased from Sigma-Aldrich and used as received. Triethylene glycol was purchased from Sigma-Aldrich Spain. Aqueous solutions

were prepared with Milli Q water (Milli Q system, Millipore). Thioctic esters of triethylene glycol was synthesized as explained in the section 5.3.3.1.

4.3.2. Instrumentation

Electrochemical measurements were carried out using an Autolab PGSTAT10 electrochemical analysis system running GPE management software from Eco Chemie with a conventional three-electrode cell. An Ag/AgCl electrode (BAS, UK) was used as reference electrode and platinum as counter. All solutions were made with purified distilled water obtained from a Milli-Q water system. Interdigitated Array was purchased from ABtech Scientific, Inc. (Richmond, VA). 0.5mm & 50µm gold wire (Advent, Oxford, UK) was resin-sealed (Mercaprex M 42, PRESI, France) within a glass capillary and used as a working electrode.

4.3.2.1. Interdigitated microelectrodes

Indium-tin-oxide (ITO) coated interdigitated gold microelectrodes (IMEs) were obtained from ABtech Scientific, Inc. (Richmond, VA). The IME had 50 electrode pairs with 20 µm of electrode width and space, and the length of the finger electrode was 4,985 µm. Before use, the IMEs were cleaned with acetone, alcohol, and deionised water, and then were dried with a stream of nitrogen.

4.3.3. Methodology

4.3.3.1. Patterning of enzymes by site-selective electrodeposition through electrochemical desorption of thioctic acid esters

Before performing the enzyme patterning on the IDE array, electrodesorption at -1.2 V (vs.Ag/AgCl) was verified with TEG-TA esters immobilised on the gold electrode using the electrochemical impedance spectroscopy. After verification of the electrochemical desorption methodology, Au nanoparticles modified with redox polymer and enzymes (GOX, HRP) were used for the selective electrodeposition on an IDE array.

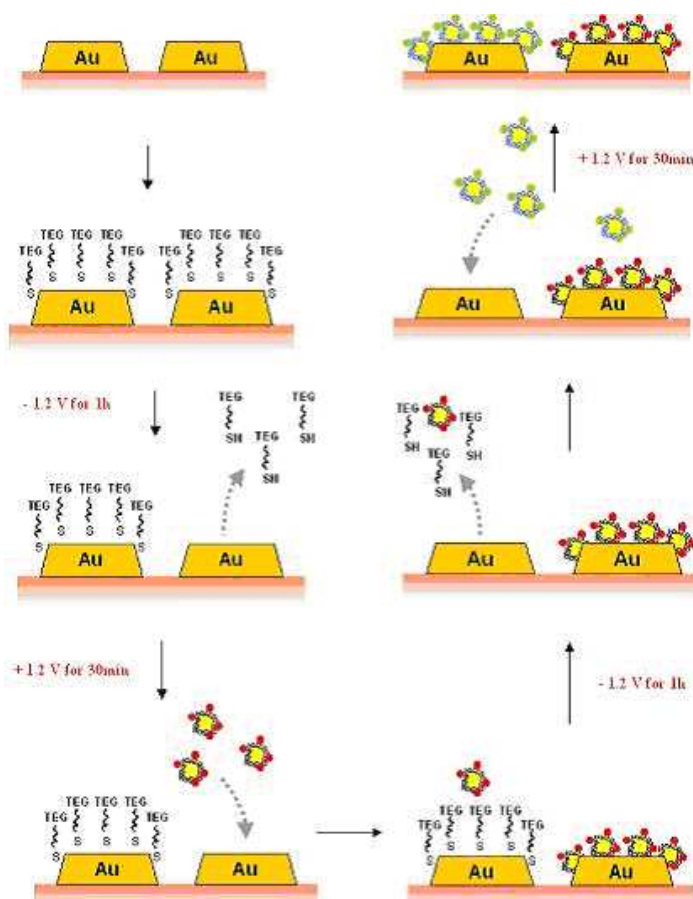
In order to demonstrate the electrochemical desorption of the self assembled TEG-thioctic esters on the gold electrode at cathodic potentials, electrochemical impedance spectroscopy was used as a method for characterization of the changes on the electrode surface. Electrochemical impedance spectroscopy (EIS) was used to characterize the changes in the charge transfer resistance (R_{ct}) offered due to the electrochemical desorption. R_{ct} , the semicircle diameter at higher frequencies in the Nyquist plot of impedance spectroscopy, controls the interfacial electron transfer rate of the redox probe between the solution and the electrode. Experiments were conducted using a three electrode system in the presence of 0.1 M phosphate buffered saline at pH 7.0 as a supporting electrolyte containing 10 mM $K_3 [Fe (CN)_6]$ and 10 mM $K_4 [Fe (CN)_6]$ as a redox probe at the formal potential of the system, $E^0 = 0.227$ V, using AC amplitude of 0.005 V. Impedance measurements were performed in the frequency range from 0.1 Hz to 100 MHz. Initially gold electrode was incubated with 0.1 M TEG-TA esters dissolved in ethanol for 2 h. Later the TEG modified gold electrodes was washed with ethanol followed by distilled water and dried with argon. Next the SAM modified electrode was characterized by impedance spectroscopy. Later a negative potential of -1.2 V (vs. Ag/AgCl) was applied for 15, 30, 45 & 60 min for desorbing the thioctic SAMs. Electrochemical impedance spectroscopy was used to monitor the electrode surface after each time step of electrodesorption.

4.3.3.1.1. Selective electrodeposition of gold nanoparticles modified with enzyme and redox polymer on an interdigitated array

In order to perform these experiments, HRP / RP1 / Au nanoparticles as well as GOX / RP 2 / Au nanoparticles prepared as described in the 2.3.4.3 were used for the experiments. Scheme 4.1 shows the stepwise fabrication process of the Au / RP1 / enzyme particles. First the IDE array was cleaned electrochemically in the presence of 0.5M H_2SO_4 scanning from -0.2 V to 1.6 V at a scan rate of 200 mV sec^{-1} until a constant cyclic voltammogram characteristic of a cleaned Au is obtained. Next the IDE array was immobilised with 0.1M TEG-TA esters dissolved in ethanol for 2 h for forming the self-assembled monolayers. Later the IDE array was cleaned with ethanol followed by distilled water and dried with argon. Next the first set of electrodes (IDE 1) was applied a potential of -1.2 V (vs.Ag/AgCl) for

1h to desorb the TEG-TA esters. Later the IDE array is washed with distilled water and dried with argon. Next 50 μL of the HRP / RP1 / Au particles (2×10^{11} particles mL^{-1}) solution was placed on the IDE array and the IDE 1 was connected to the potentiostat and applied a potential of + 1.2 V (vs. Ag/AgCl) for 30 min.

After electrodeposition, IDE array was washed with distilled water and dried with argon. Next the IDE 2 was connected to the potentiostat and applied a potential of - 1.2 V (vs. Ag/AgCl) for 1 h to desorb the TEG-TA SAMs from the gold surface. After washing, 50 μL of GOX / RP 2 / Au particles (2×10^{11} particles mL^{-1}) solution was placed on the IDE array and applied a potential of + 1.2 V (vs. Ag / AgCl) for 30 min to the IDE 2. After electrodeposition, IDE array was washed with distilled water and dried with nitrogen.



Scheme 4.1. Scheme of the selective electrodeposition of enzyme / redox polymer modified Au nanoparticles on an interdigitated array.

4.3.3.1.2. Electrochemical Characterisation of the IDE array

After electrodeposition of HRP / RP1 /Au particles on the IDE 1 , cyclic voltammogram of the IDE array was taken scanning from 0V to 0.6V at a scan rate of 100 mV sec⁻¹ to characterise the quasireversible behaviour of the redox polymer due to the specific deposition on the IDE 1 and non-specific deposition on the IDE 2. After electrodesorption of the TEG-TA esters from the IDE 2, CV was taken again to check the behaviour of the electrode surface for comparison with the CV before desorption. Finally after electrodeposition of the GOX / RP 2 / Au particles on the IDE 1 , CV was taken to characterize the quasireversible behaviour of the RP 2 due to the specific deposition on the IDE 2 as well as non-specific deposition on the IDE 1 where HRP modified particles were deposited already. The charge under the redox peaks was calculated in order to estimate the percentage of non-specific adsorption.

4.3.3.1.3. Amperometric measurements of the IDE array

After modifying the IDE array with HRP deposited on the IDE 1 and GOX deposited on the IDE 2, amperometric measurements were taken first for the HRP using chronoamperometry at a potential of 0V(vs. Ag/AgCl) by injecting hydrogen peroxide into the cell while stirring to check substrate specific response from the IDE 1. Next amperometric measurements were taken for the GOX by injecting glucose into the cell with continuous stirring at a potential of +0.5V (vs. Ag/AgCl) under nitrogen to check the substrate specific response from the IDE 2. Response due to the non-specific adsorption was estimated from the current produced by the IDE array.

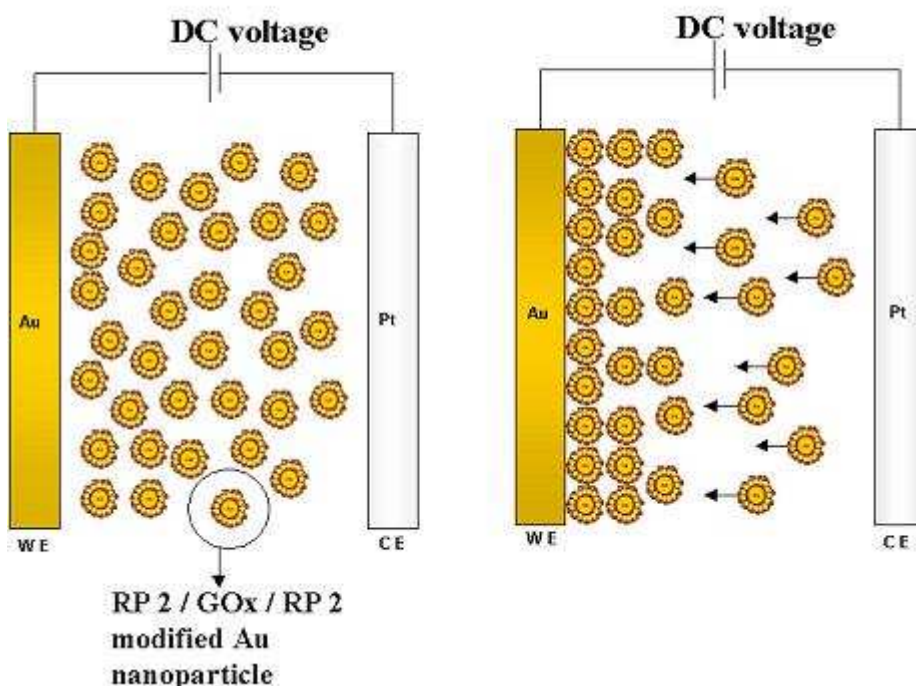
4.3.3.2. Controlled electrodeposition of layer-by-layer modified Au nanoparticles with redox polymer and enzyme and redox polymer.

In this strategy, multifunctional gold nanoparticles prepared by modifying particles layer-by-layer with redox polymer (RP 2) followed by GOX and again with redox polymer (RP 2) as explained in the 2.3.4.3. These modified Au nanoparticles were used for electrodeposition to create glucose sensor. Different optimisation steps

were presented and finally these particles were electrodeposited on a microelectrode to prove the technical advantage of this methodology for creating microarray.

4.3.3.2.1. Electrochemical conditions

The RP 2 / GOX / RP 2 modified Au nanoparticles were electrodeposited by applying potential using a two electrode system with Pt as a counter electrode and Au as working electrode and maintaining a distance of 1mm in between the two electrodes as shown in the scheme 4.2. After electrodeposition, the electrodes were washed and dried under argon. For current measurements from the modified electrodes for glucose, a constant potential of + 0.4 V was applied to the deposited electrode to measure the amperometric response due to the electro-oxidation of H₂O₂ produced enzymatically. The base line was allowed to stabilize in a blank buffer solution of working pH. Aliquotes of the glucose stock solution in PBS were added to the electrochemical cell, under constant stirring and the correspondence increase in the current was recorded. These steady-state background current values, from which the baseline was subtracted, were used to construct calibration graphs. After electrodeposition, characterisation of the modified electrodes was carried out by cyclic voltammetry in 0.1 M pH 7.0 PBS solutions scanning from 0V to + 0.6V at a scan rate of 100mV sec⁻¹ to check the quasi-reversible behaviour of the RP 2 functionality present on the deposited particles.



Scheme 4.2. Schematic representation of the electrodeposition of Au nanoparticles modified layer-by-layer with RP 2 followed by GOX and finally with RP 2

4.3.3.2.2. Influence of electrodeposition potential on the glucose response

Effect of electrodeposition potential on the glucose response was studied in order to optimise the best potential which provides a stable and maximum glucose response from the Au / RP2 / GOX / RP 2 deposited electrodes. In this study, the Au / RP 2 / GOX / RP 2 particles were electrodeposited on the Au electrodes by applying four different potentials 0 V, + 0.8 V, + 1.2 V & + 1.6 V for 15 min using the electrodeposition conditions as explained above. Application of 0 V potential served as a control for this experiments. After modification and washing, electrodes were characterized by cyclic voltammogram and the glucose response was measured from the modified electrodes by using the conditions explained above.

4.3.3.2.3. Influence of time on the glucose response

In order to see the effect of electrodeposition time on the glucose response, experiments were conducted to electrodeposit RP 2 / GOX / RP 2 modified Au nanoparticles on electrode by applying an optimized anodic potential optimized from the 4.2.4.4 for 15min, 30min and 60min.

4.3.3.2.4. Influence of outer redox layering on the glucose response

In order to see the difference in the glucose response from the biosensor after electrodeposition of the modified gold nanoparticles with and without the outer redox polymer layer, experiments were done by electrodeposition of GOX / RP2 / Au as well as RP2 / GOX / RP2 / Au nanoparticles on different electrode surfaces by applying + 1.2 V for 30 min on both the electrodes. After washing, response to glucose was measured from the modified electrodes.

4.3.3.2.5. Influence of type of potential on the glucose response

In this experiment, two different potentials + 1.2 V and - 1.2 V were applied for 15 min in order to study the effect of negative and positive potentials on the electrodeposition and on the glucose response. After washing, glucose response was measured from the modified electrodes.

4.3.3.2.6. Influence of electrode geometry on glucose response

Glucose response was measured from the electrodes with two different geometries electrodeposited with RP 2 / GOX / RP 2 modified Au nanoparticles for 15 minutes at + 1.2 V in order to study the the effect of miniutarisation of electrode surface on the glucose response. In this case electrode with two geometries 50 μ m and 0.5mm were used for study.

4.4. Results & Discussion

In this chapter an effort is made to prove the thesis that using EPD, an enzyme biosensor can be manufactured as proof of principle for the construction of multianalyte sensors. In the first part, techniques to improve the selectivity of directed depositions are discussed while in the second, methods to optimise and modulate the response of enzymatic amperometric sensors made through EPD are discussed.

4.4.1. Patterning of enzymes by site-selective electrodeposition

In principle, one would expect closely spaced electrodes could be selectively modified by direct EPD at different electrode sites. However initial experiments showed that electrodes on which modification was not intended were modified by non-specific adsorption of colloidal nanoparticles. In order to avoid this, a protection technique was developed that was summarised in scheme 4.1. This section describes the application of this technique for the selective immobilisation by EPD of nanobiomolecules that show selective response to two different substrates. First the efficiency of the electrochemical desorption of the protective TEG-thioctic esters from the electrode surface is demonstrated. Figure 4.1 are the Nyquist plots of EIS performed with electrode exposed at different times of electrodesorption of the TEG-TA esters. The EIS is done in the presence of $\text{Fe}(\text{CN})_6$ and it can be seen that in the beginning they demonstrate high charge transfer resistance since the SAMs act as insulators to the ferro/ferri redox couple reaction. Figure 4.1 also shows that after 30min no significant decrease in the charge transfer resistance is observed and the behaviour is almost the same as blank Au electrode. These results demonstrate that electrochemical desorption effectively removes the TEG-TA SAMs and therefore it can be used to improve the selectivity of directed EPD when the two-enzyme sensors are created.

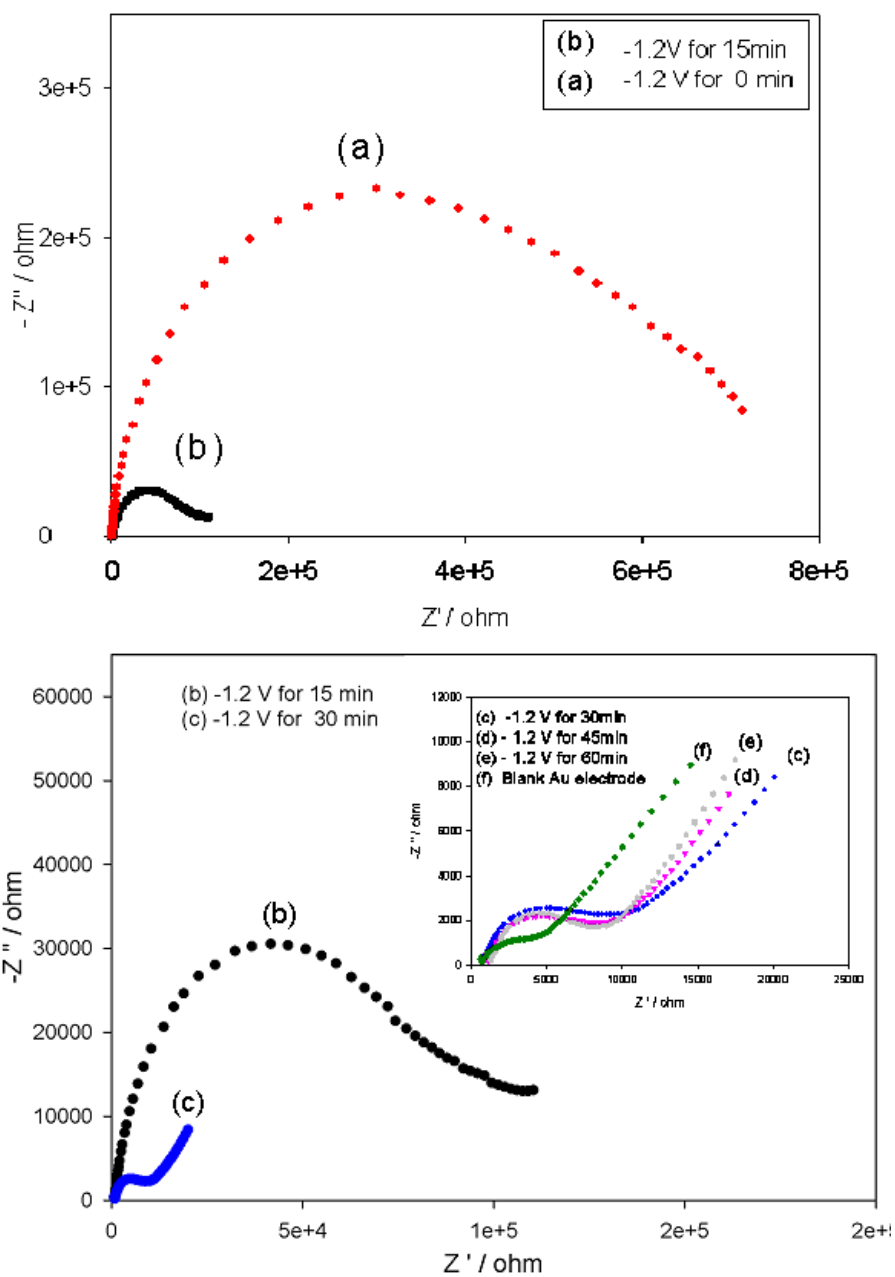


Figure 4.1. Electrodesorption of TEG-thioctic acid esters after applying a cathodic potential of -1.2 V (vs. Ag/AgCl) for (1) 15min (2) 30min (3) 45min, 60min in the presence of 0.1M PBS pH 7.0 containing 10 mM $K_3[Fe(CN)_6]$ and 10 mM $K_4[Fe(CN)_6]$ a) $E_0 = 0.227$ V and frequency range 0.1Hz to 100mHz., amplitude 5mV

The proof of principle that EPD can be used as an arraying method for multianalyte enzyme biosensor was undertaken on an IDE array using bionanomodules modified with two different enzymes (HRP and GOX) and two different polymers (RP 1 with

E_0 of 0.312 V and RP 2 with E_0 of 0.18 V respectively) to facilitate the detection of non-specific phenomenon. The IDE array was first modified with the TEG-thioctic esters as described in the experimental section. At first, the IDE 1 was deprotected and the whole array was exposed to a solution of Au / RP 1/ HRP nanomolecules. Potential of + 1.2 V for 30min was applied to IDE 1.

Figure 4.2 shows CVs taken from the IDE array after the electrodeposition of the Au / RP 1 / HRP nanoparticles. It can be observed that IDE 1 showed well-defined redox peaks of the Os^{2+} / Os^{3+} couple with a formal potential of + 312.5 mV. Thus the Au / RP 1 / HRP nanoparticles were electrodeposited successfully on the IDE 1. However, CVs from the IDE 2 also showed quasi-reversible redox peaks characteristic of RP1 which presumably is due to the non-specific deposition of the HRP / RP1 / Au particles. The peaks are not well defined from the IDE 2 when compared to the IDE 1 and peak currents were lower. The charge under the redox peaks was used to estimate the non-specific adsorption of the HRP / RP 1 modified Au nanoparticles on the IDE 2 compared to the IDE 1, and it was estimated that a non-specific adsorption of 34% was present on the IDE 2.

However, after applying a negative potential of - 1.2 V (vs. Ag / AgCl) for 1h, the redox peaks characteristic to the osmium polymer disappeared completely from the IDE 2 and the behaviour became almost the same as that of the blank IDE 2. This clearly proves that the electrochemical desorption of the thiols is successful in removing the non-specific adsorption. This shows the advantage of the electrochemical desorption technique

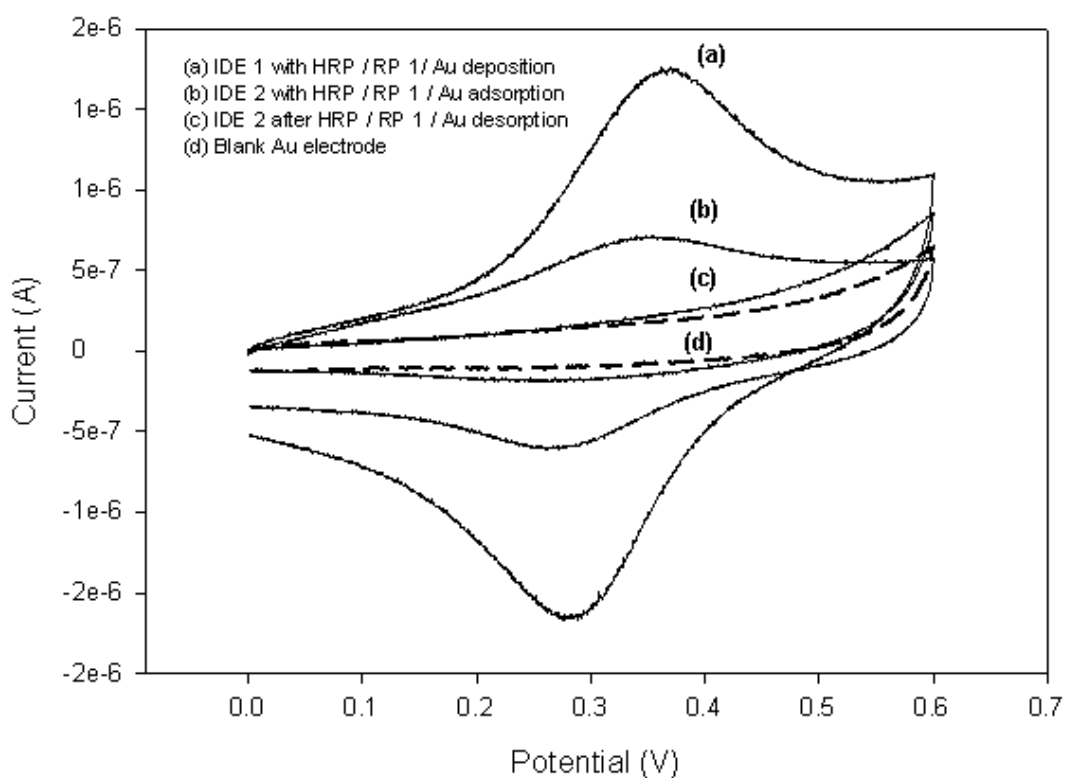


Figure 4.2. Cyclic voltammograms of the IDE array after the electrodeposition of 50 μL of Au / RP1 / HRP particles (2×10^{11} particles mL^{-1}) on the IDE 1. Applied potential : + 1.2 V for 30 min , Supporting electrolyte : 0.1M PBS pH 7.0, Scan rate : 50 mV s^{-1} .

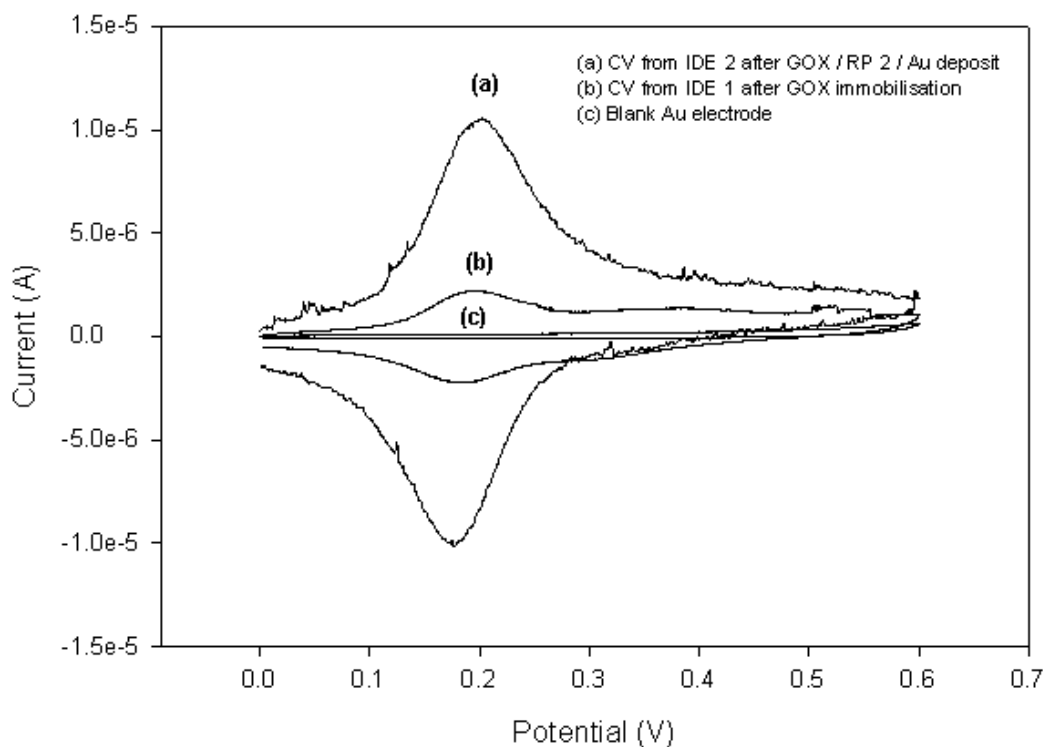


Figure 4.3. Cyclic voltammograms of the IDE array after the electrodeposition of 50 μL of Au / RP2 / GOX particles (2×10^{11} particles mL^{-1}) on the IDE 2. Applied potential : + 1.2 V (vs. Ag / AgCl) for 30 min. Supporting electrolyte : 0.1M PBS pH 7.0, Scan rate: 50 mV s^{-1}

Subsequently, the IDE array was exposed to a solution of Au / RP 2 / GOX nanoparticles and the same EPD conditions as for the HRP electrodes were applied for IDE 2. Figure 4.3 shows the corresponding CV s after the electrochemical deposition of the Au / RP 2 / GOX particles on the IDE 2. The well-defined redox peaks characteristic to RP 2 with a redox potential of + 181.5 mV at IDE 2. This clearly shows that the IDE 2 was effectively modified by the GOX / RP 2 /Au nanoparticles. However , CVs from the IDE 1 displayed peaks corresponding to the RP 2 as well as the redox peaks corresponding to the RP 1. This shows that there is still non-specific adsorption on the IDE 1. Integration of the charge under the redox peaks showed that the non-specific adsorption is around 12.3 %.

The presence of non-specifically adsorbed nanoparticles is only part of the non-specific phenomenon. The most important piece of data is if these nanomodules give a significant non-specific amperometric response. To quantify this, the IDE array was probed. Figure 4.4 displays the typical steady-state catalytic response with

successive additions of H_2O_2 solution to the electrochemical cell at an applied potential of 0V. With increase in the peroxide concentration, there is an increase in the reduction current from the IDE 1.

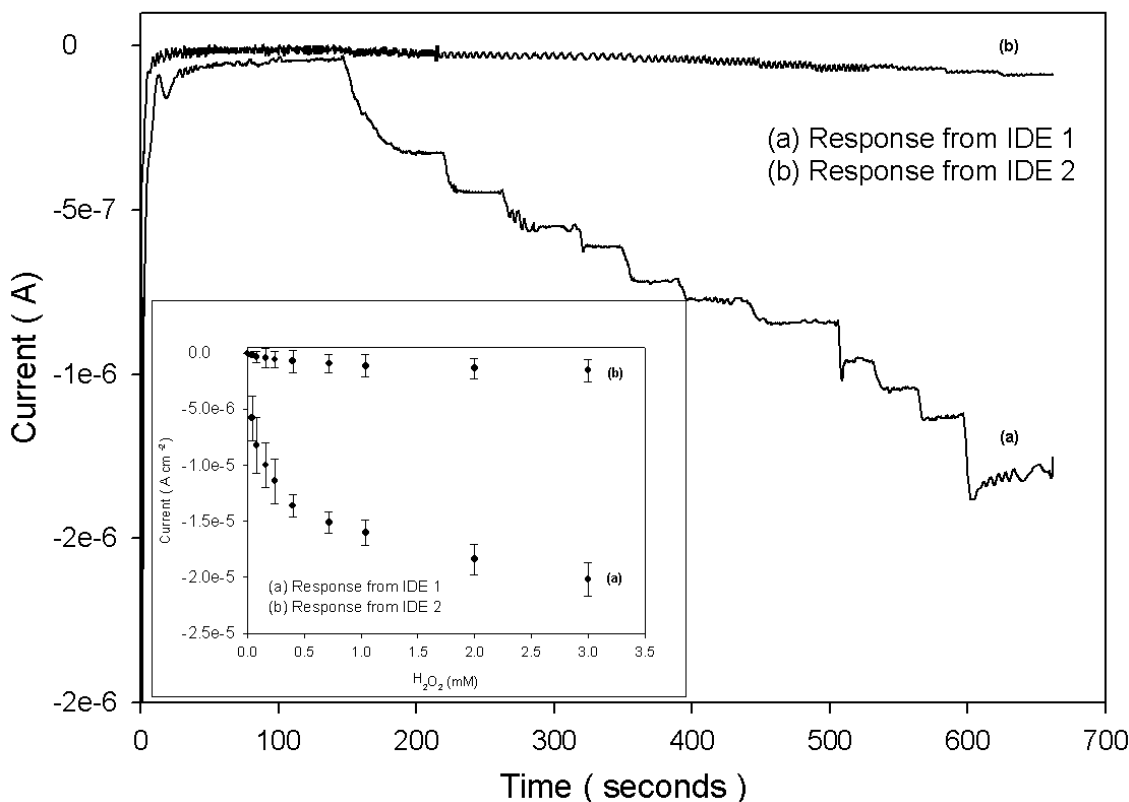


Figure 4.4. Typical steady-state current response of the biosensor electrodeposited with the Au / RP 1 / HRP particles on the IDE 1 for successive injection of H_2O_2 into stirring PBS. Applied potential : 0V, supporting electrolyte : 0.1M PBS pH 7.0. Inset : Calibration plot of the currents produced due to the increasing H_2O_2 concentrations from the IDE array after immobilization of Au / RP 1 / HRP on the IDE 1

The response from the IDE 2 was minimal. The inset shows the calibration curve of the array for H_2O_2 . From the inset of figure 4.5, it can be seen that for example at 3mM H_2O_2 , there was a response of $20 \mu A cm^{-2}$ from the IDE 1 whereas from the IDE 2 the current response due to the peroxide is $0.5 \mu A cm^{-2}$. Thus the non-specific response to the H_2O_2 from the IDE 2 is about 2.5% when compared to the response from the IDE 1. It is therefore obvious that the desorption scheme gurantees selectivity during patterning.

In order however to ascertain that EPD is efficient as patterning method, it should be secured that the IDE 1 modified with Au / RP 1/ HRP nanoparticles do not respond in the presence of glucose. Figure 4.5 shows the response of the IDE array to different concentrations of glucose. There is an increase in the oxidation current response from the IDE 2. Although there is a response from the IDE 1 due to the glucose injections, this response is minimal when compared to the IDE 2. When currents are plotted against concentration (inset Figure 4.5), at 80mM glucose, there was a response of 0.8 mA cm^{-2} from the IDE 2 whereas as the response from IDE 1 is 0.04 mA cm^{-2} . Thus the response to glucose produced from the non-specific adsorption of the GOX / RP 2 / Au nanoparticles on the already HRP / RP 1 / Au nanoparticles electrodeposited IDE 1 is around 5%.

From the figure 4.3 about 12 % of non-specific adsorption of Au / RP 2 / GOX nanoparticles was observed on IDE 1, however this only resulted to about 5% non-specific response. This means although nanoparticles are present, the enzyme they contain is not efficiently “wired” to the electrode. This IDE array can obviously be used with acceptable reliability to measure simultaneously the two analytes.

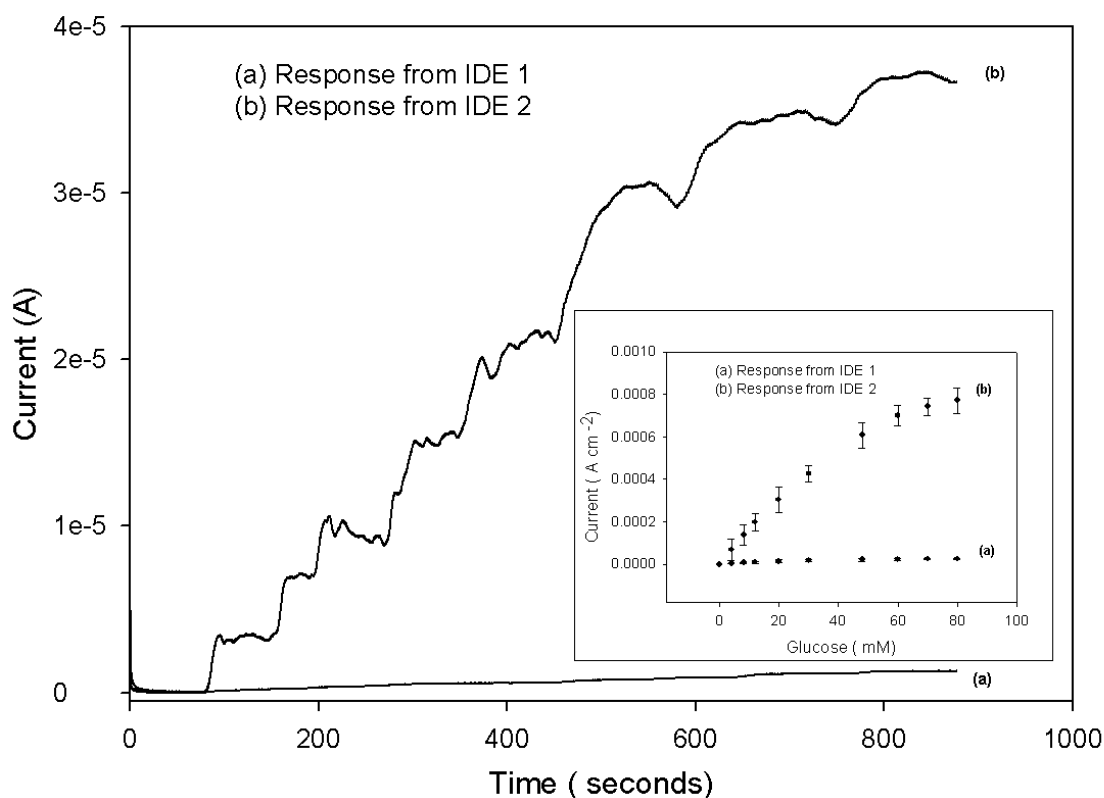


Figure 4.5. Typical steady-state current response of the biosensor electrodeposited with the Au / COPOs / GOX particles on the IDE 2 for successive injection of glucose into stirring PBS. Inset : Calibration plot of the currents produced due to the increasing glucose concentrations from the IDE array after immobilization of Au / RP 2 / GOX on the IDE 2 . Applied potential : + 0.4V (vs. Ag / AgCl), supporting electrolyte: 0.1M PBS pH 7.0.

4.4.2. Optimisation of electrode construction and transduction

In the previous section the proof of concept of patterning with EPD was demonstrated. The EPD parameters used were those optimised in chapter 3 (+1.2V for 30min with a larger counter electrode) . In this section, an effort was made to further optimise these conditions in order to achieve higher current densities. The first parameter to be examined was the magnitude of the electric field during EPD. Figure 4.6 shows the effect of the applied EPD potential on the resulting electrocatalytic current from the modified electrodes. It can be observed that the electrodeposition potential has a profound effect on the glucose dependent catalytic currents. It appears that this effect follows a step function with threshold between 0.8 and 1.2V. At the deposition potential of + 0.8 V, the response to glucose was $27 \mu\text{A cm}^{-2}$ and the response at + 1.2 V is

$225 \mu\text{A cm}^{-2}$. At $+1.6\text{V}$ the response was around $194 \mu\text{A cm}^{-2}$. However if we try to calculate the apparent K_m and the I_{max} for each EPD potential. We obtain the following results.

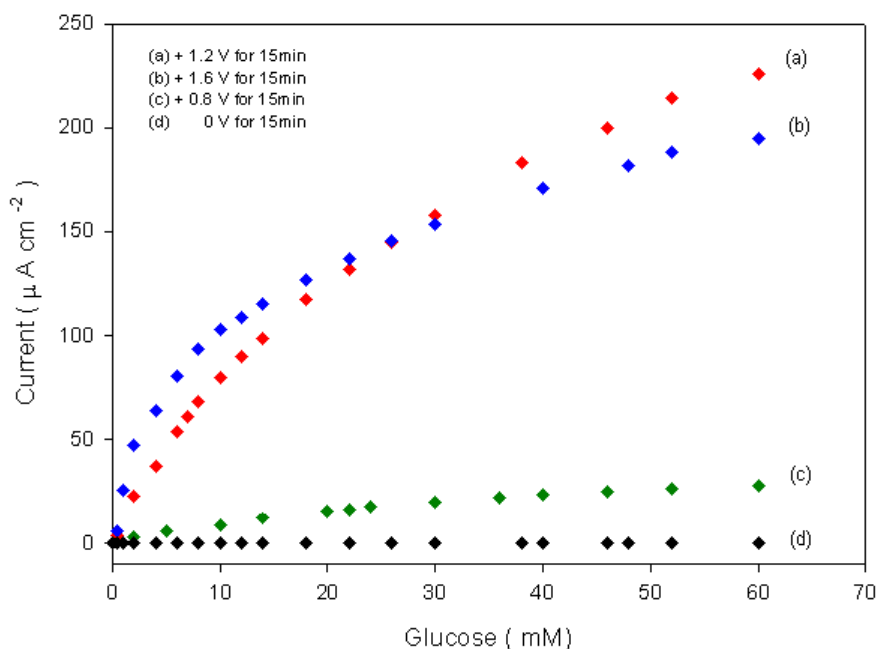


Figure 4.6. Steady-state amperometric responses to the glucose from the electrode deposited with RP2/GOX/RP2/Au nanoparticles by applying different electrodeposition potentials. Applied Potential for amperometric response: $+0.4\text{V}$ (vs Ag / Ag Cl) ; supporting electrolyte: 2mL of 0.1M PBS pH 7.0 with stirring.

It is not necessary to explain these results. The apparent I_{max} is proportional to the “wired” enzyme amount deposited, while the K_m app is an indicator of the combined kinetic / mass transport resistance for the sensor. Increased mass transport resistance would increase the value of K_m app giving also I_{max} corresponding to lower “wired” enzyme than there really is on the modified electrode. The electrodes made by the application of $+1.6\text{V}$ for EPD showed the lower K_m app values but also lower I_{max} than those exposed to $+1.2\text{V}$ during EPD. This observations contradicts the microscopic findings in chapter 3 (that showed clustering and therefore the possibility of severe intensified mass transport limitations). From the data at hand, it can only be speculated that the response from $+1.6\text{V}$ exposed electrodes comes from those parts of the nanoparticles that from

thin deposits, while the clustered parts are essentially disconnected from the electrode. It was therefore that + 1.2 V was the optimal EPD potential.

EPD potential (V)	$I_{\max \text{ app}}$ ($\mu\text{A cm}^{-2}$)	$K_m \text{ app}$ (mM)
0	0	0
+ 0.8	44.6	37.9
+ 1.2	225	23.08
+ 1.6	194	5.7

Table 4.1 . Kinetic parameters I_{\max} (maximum current) and $K_m \text{ app}$ (Michaelis Menten constant) from the glucose sensors made by EPD of RP 2/ GOX / RP 2 / Au nanoparticles by applying different potentials. Electrodeposition for 15min.

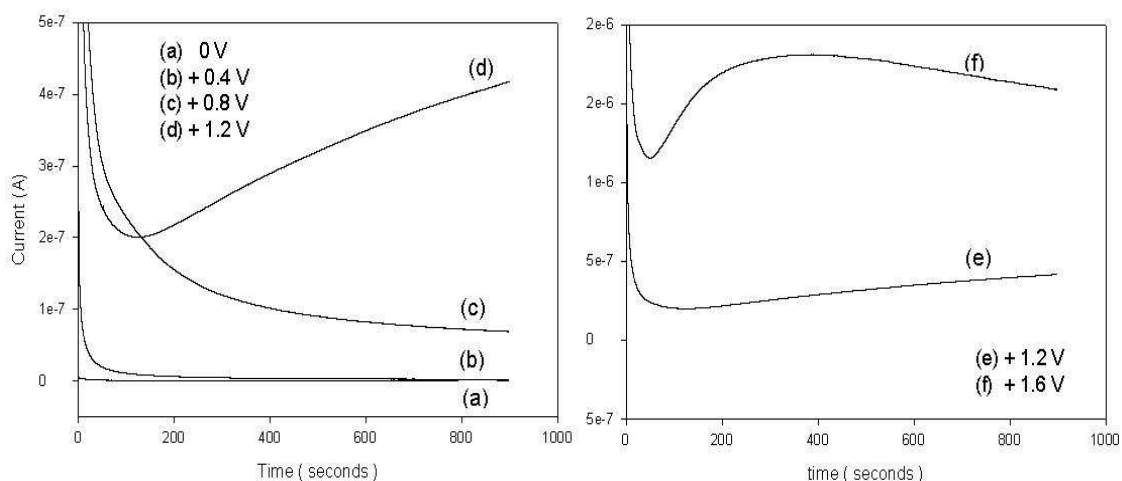


Figure 4.7. (a) Current produced during the electrodeposition of RP 2 / GOX / RP 2 modified Au nanoparticles by applying electrodeposition potentials 0V (curve a), + 0.4 V (curve b), + 0.8 V (curve c) and +1.2V (curve d) for 15min. (b) Currents produced for +1.2 V(curve e) and +1.6 V (curve f) for 15min.

Another explanation however for the observation is that at the applied potential, electrode reactions might denature the enzyme directly or indirectly or affect the redox behaviour of the polymer. Some additional data on the issue of the influence of EPD on the response can be obtained by monitoring the current obtained during EPD in real time. This current may not result solely from the mass of electrodeposited particles but also from parasitic electrode reactions. However it is clear from Figure 4.7 that a marked change in behaviour is observed between 0.8 and + 1.2 V. At + 1.2 V the current increased linearly with time as expected by equation 3.5. However at + 0.8 V, there is what looks like a diffusion dependent decay. As discussed in chapter 3, one has to remember that these hybrid particles have both anionic and cationic character. It is therefore likely that a threshold potential is necessary to provide enough electrokinetic force for deposition. On the other hand comparison of the response at + 1.2 V and + 1.6 V shows that in the latter case, after an initial Hamaker like behaviour a decrease in deposition rate is observed. This might be due to the clustering and the increased resistivity of the clustered substrates which decrease the electrophoretic efficiency of the electrode.

The second parameter to be examined was the time of EPD. From equation 3.5, increased time should result to higher nanoparticle mass deposited and higher response. Figure 4.8 shows the response to glucose from the electrodes modified with Au colloids modified with RP 2 / GOX / RP 2 at different times of deposition). At 60mM glucose, the maximum response was around $225.6\mu\text{A cm}^{-2}$ at 15min of deposition. After increase in the time of electrodeposition from 15min to 30min, the glucose response increases to $337.5\mu\text{A cm}^{-2}$. Finally after 60min of electrodeposition, the glucose response is $207\mu\text{A cm}^{-2}$, which is 61.3 % of the response found from 30min to EPD. This explanation can be supplemented by the information obtained from the electrodeposition of BSA modified Au nanoparticles at different times of deposition (Figure 3.3). The current decrease observed at 1h of electrodeposition in Figure 4.8 probably is a result of the loss of enzyme activity suffered from exposure to low local pH conditions for an extended time, or loss of redox functionality of the polymer (at higher potential ligand substitution is formed).

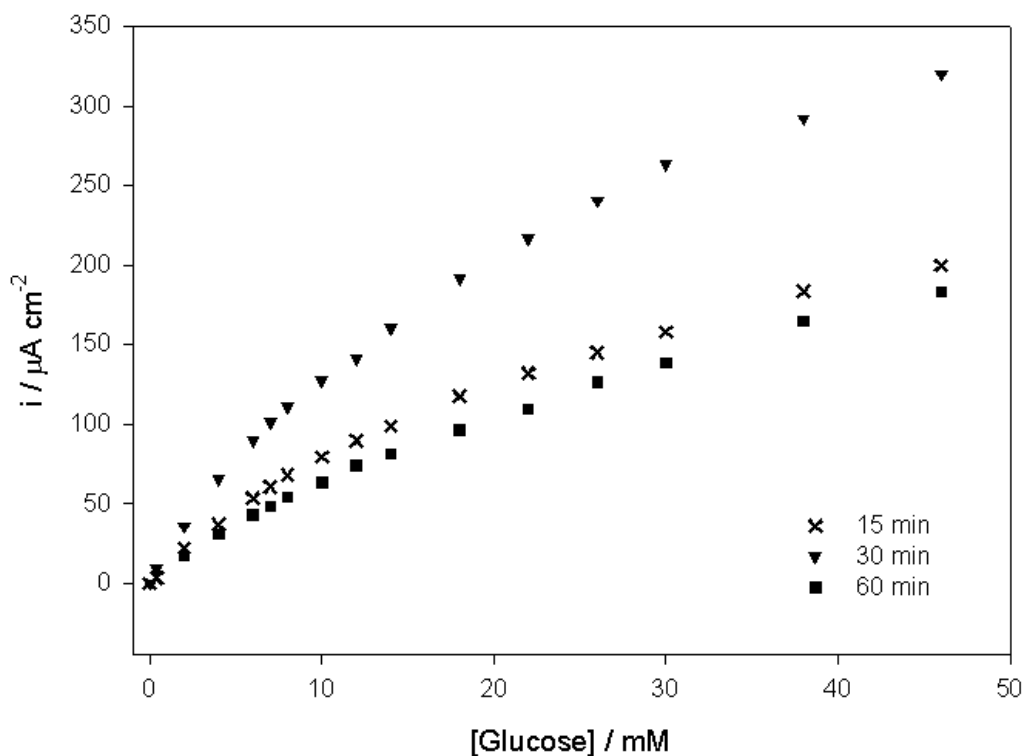


Figure 4.8. Steady-state amperometric responses of the biosensor with different electrodeposition at +1.2V for 15, 30, 60min to the oxidation of glucose in stirring PBS. Applied Potential for amperometric response: + 0.4V (vs Ag / Ag Cl) ; supporting electrolyte: 2mL of 0.1M PBS pH 7.0 with stirring.

The results in figure 4.9 seem to support this second explanation: the effect of electrodeposition time on the redox functionality of the modified is shown. Electrodes deposited at + 1.2 V showed well defined redox peaks in voltammograms obtained after 15, 30 and 60min deposition. CV s at 15 and 30min taken after electrodeposition of the modified gold nanoparticles showed the oxidation and reduction peaks at + 0.24 V & + 0.19 V characteristic of the redox polymer with a redox potential of + 0.21 V. However electrodes subjected to EPD for 60min lost some definition in their redox behaviour.

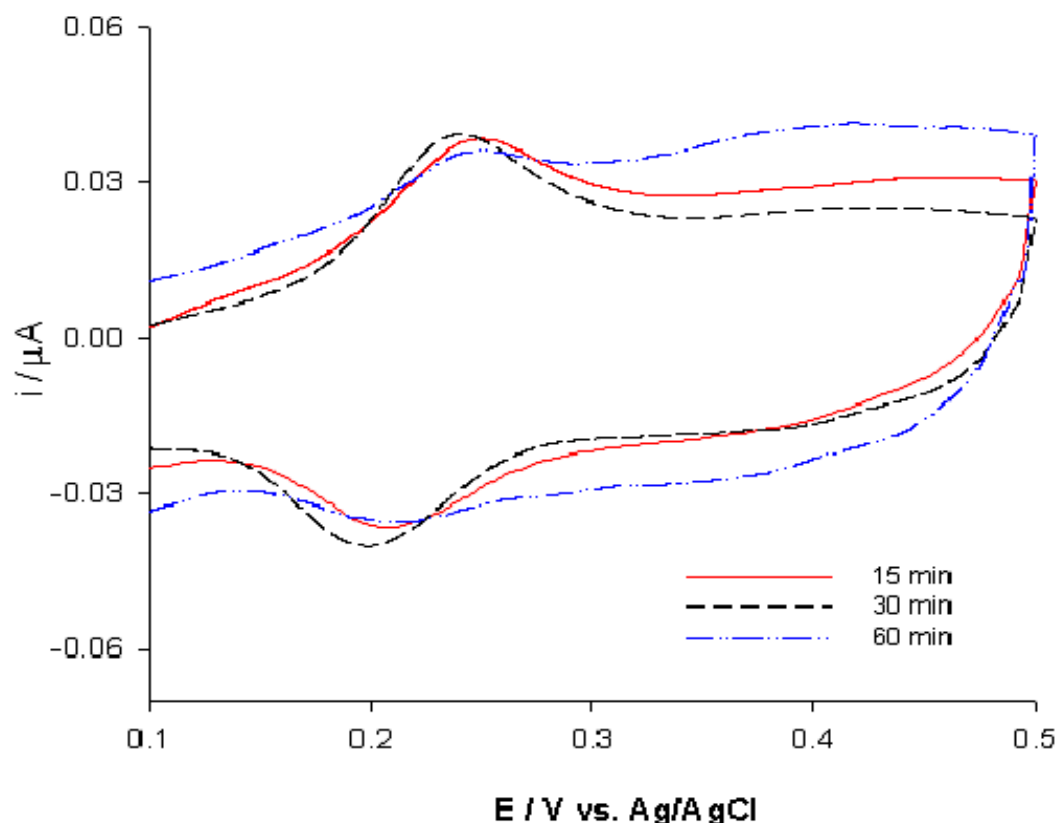


Figure 4.9. Cyclic voltammogram of the electrodes deposited at different deposition times (15,30 and 60min) with gold nanoparticles modified L-b-L with RP 2 and GOX and RP 2. Electrodeposition conditions : + 1.2 V for 15, 30 and 60 min, Scan rate : 100 m V sec⁻¹. Supporting electrolyte : 2mL of 0.1M PBS pH 7.0.

Finally the nature of colloidal nanoparticles was altered in the hope of observing higher currents. It was thought that by including outer redox polymer layer, electron transfer would be faster and therefore current densities are higher. Unfortunately, due to the precipitation, this second layer of redox polymer could not be added to the HRP-modified electrodes. For this reason in what follows only GOX-modified nanoparticles were used. From Figure 4.10, the electrode with particles having the outer redox polymer layer produced a current response of 153 $\mu\text{A cm}^{-2}$ whereas the electrodes without the outer redox polymer produced a current response of 73 $\mu\text{A cm}^{-2}$ at 50mM glucose concentration. Amperometric measurements showed that the redox polymer on the outer surface of the modified gold nanoparticles almost doubled the glucose response when compared to the particles without the outer

redox layer. Several phenomena were considered contributing factors for this greater amperometric response observed from gold nanoparticles containing two redox polymer layers.

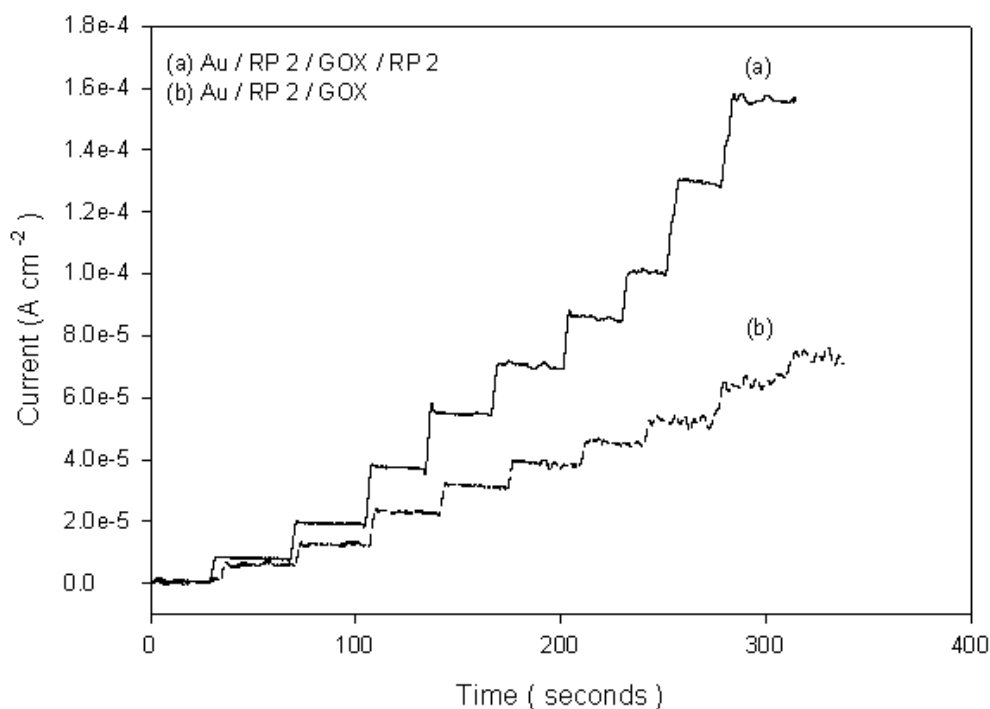


Figure 4.10. Typical steady state chronoamperometric response of the biosensor on successive injections of glucose from the electrodes modified with Au / RP 2 / GOX / RP 2 & Au / RP 2 / GOX. Inset : currents plotted against the concentration of glucose. Applied Potential for amperometric response: + 0.4V (vs Ag / Ag Cl) ; supporting electrolyte: 2mL of 0.1M PBS pH 7.0 with stirring.

Presence of an extra redox polymer layer may enhance the electron transfer between the enzyme and the electrode and also between the adjacent particles showing a better response at the electrode. Finally it is also thought that an outer redox polymer layer stabilises the glucose oxidase as well as protecting it from a loss of the activity due to the direct contact with the electrode surface. As expected from the behaviour of the microelectrodes, when a 50mm diameter gold electrode was used instead of a 0.5mm electrode the current was increased eight fold (0.3 mA cm⁻² to 2.3 mA cm⁻², results not shown)

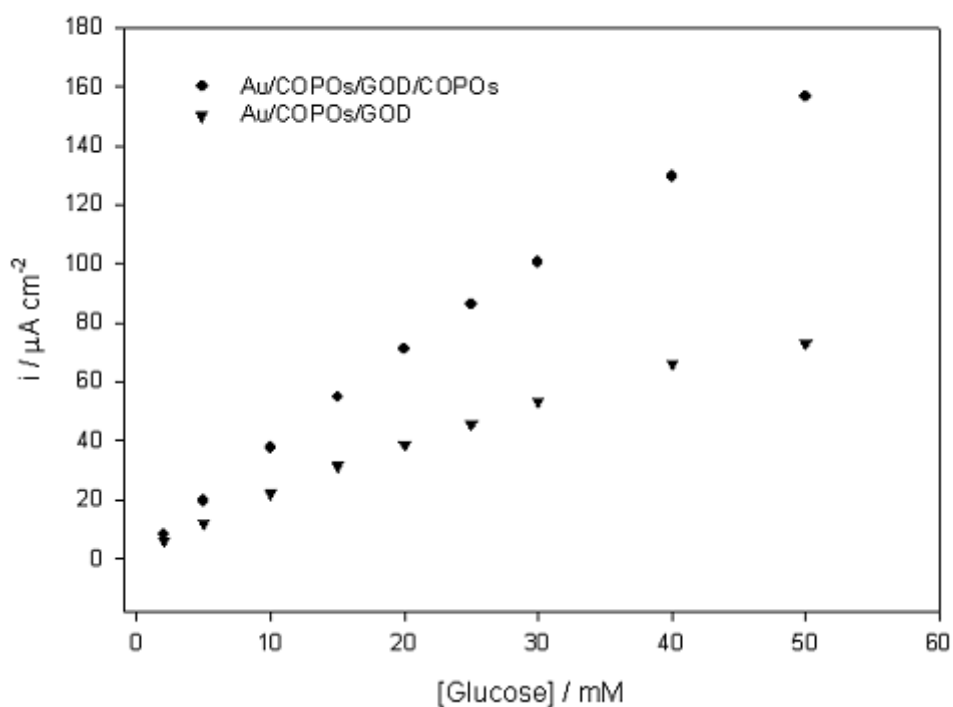


Figure 4.11. Calibration curve of the currents produced from the biosensor on successive injections of glucose from the electrodes modified with Au / RP 2 / GOX / RP 2 & Au / RP 2 / GOX. Applied Potential for amperometric response: + 0.4V (vs Ag / Ag Cl) ; supporting electrolyte: 2mL of 0.1M PBS pH 7.0 with stirring.

When the outer layer is redox polymer, it was observed in chapter 2 that the zeta potential is positive. Despite the fact that EPD was achieved with positive applied potentials, intuition and theory dictate that a negative EPD could result to higher efficiency. For this reason potentials of + 1.2 V and - 1.2 V were applied for 30 min using the same number of particles in solution.

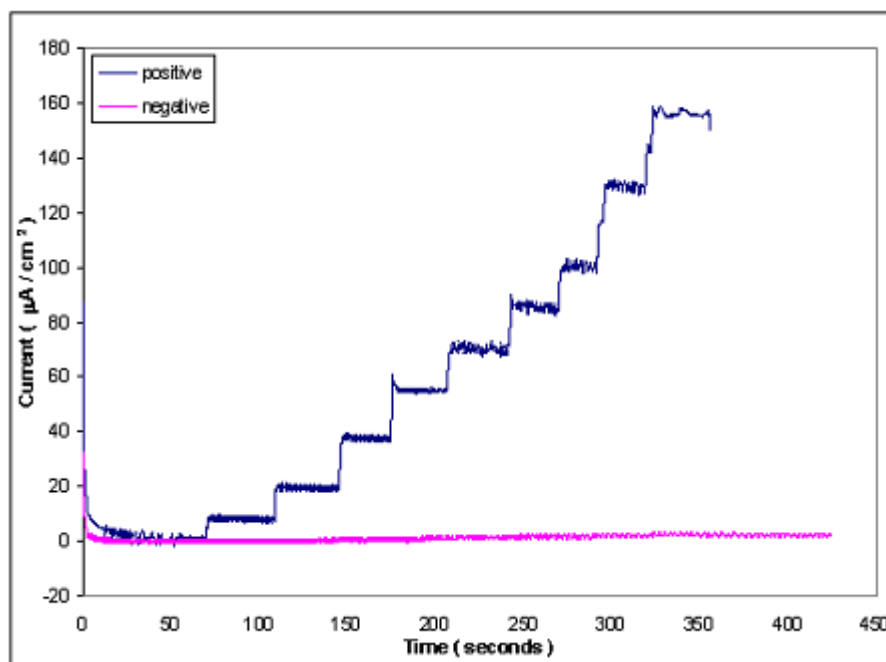


Figure 4.12. Typical steady state chronoamperometric response of the biosensor on successive injections of glucose from the electrodes modified with Au / RP 2 / GOX / RP 2 by the application of electrodeposition potential of +1.2 V and – 1.2 V for 15 min. Applied Potential for amperometric response: + 0.4V (vs Ag / Ag Cl) ; supporting electrolyte: 2mL of 0.1M PBS pH 7.0 with stirring.

From Figure 4.12, at 50mM glucose with + 1.2 V, there was a response of $153 \mu\text{A cm}^{-2}$ to the glucose whereas the electrodes subjected at EPD at – 1.2 V produced only $2.36 \mu\text{A cm}^{-2}$ which is of 1.54 % of the response produced from the electrodes deposited with + 1.2 V. This shows as discussed in chapter 3, the gold core of the nanoparticles plays a major role during electrodeposition and stabilization.

That the deposition of the nanoparticles with an outer redox polymer layer is selective could not be shown with the use of second enzyme. For this reason the magnitude of the non-specific phenomenon was quantified versus an electrode where EPD potential was applied. Figure 4.13 shows the chronoamperometric response from the electrodes modified with Au colloid / RP 2 / GOX / RP 2 particles at two different potentials. Initially when the electrodes are deposited with the modified particles by applying a potential of 0 V for 30 min, the response to glucose from the electrodes after

modification is completely absent. On the same electrode after applying a potential of + 1.2 V for 30 min with the same number of modified particles, there was a stable and quick response to different concentrations of glucose. This clearly demonstrates that at 0V, the response to glucose was completely absent which clearly proves that this type of particles can also be used for producing closely spaced multienzyme sensors.

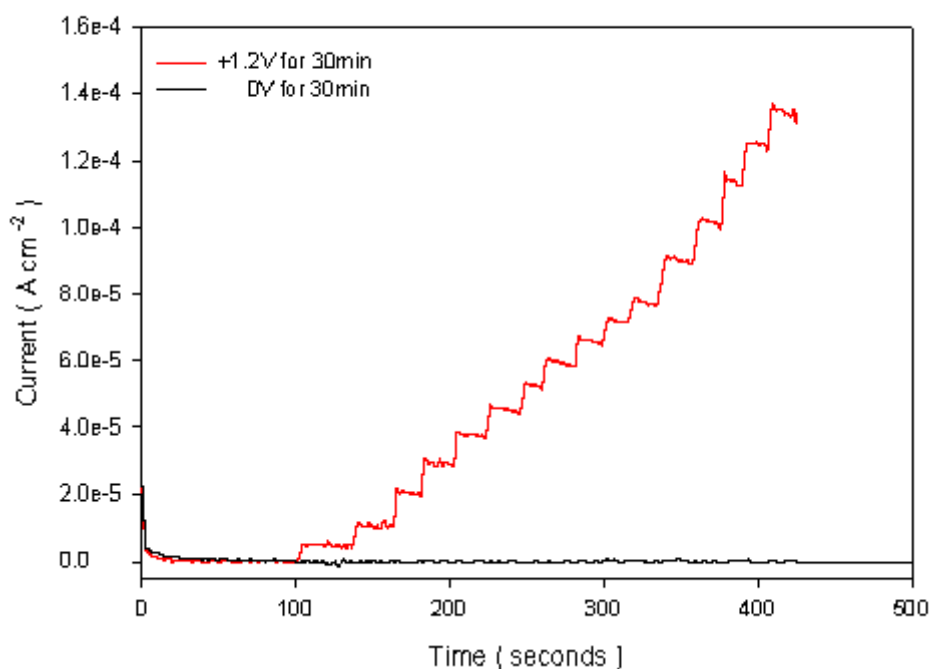


Figure 4.13. Typical steady state chronoamperometric response of the biosensor on successive injections of glucose from the same electrode modified with Au / RP 2 / GOX / RP 2 by applying 0 V for 30 min first followed by + 1.2V for 30 min. Applied Potential for amperometric response: + 0.4V (vs Ag / Ag Cl) ; supporting electrolyte: 2mL of 0.1M PBS pH 7.0 with stirring.

4.5. Conclusions

In this work a novel method for fabrication of a biosensor array based on the combination of electrodesorption of TEG-TA esters and electrodeposition of enzyme functionalised redox polymer modified Au nanoparticles. The Au nanoparticles modified with redox polymer and enzymes were successfully electrodeposited on the microelectrodes. In addition, closely spaced sensors with different enzymes exhibited faster and specific response with minimal non-specificity. The osmium complex in the resulting enzyme/redox polymer / Au

nanoparticle modified films effectively mediates the electron transfer from the enzymes to the substrate. The advantage of this methodology is that it is very simple, with good catalytic response and could be applicable to other biomolecules like antibodies, oligonucleotides. Au nanoparticles were modified initially with redox polymer followed by the enzymes in a layer-by-layer approach. The main advantage of using electrodesorption technique is that it can be used for removing the already non-specifically adsorbed particles from the electrode surface, which makes this approach suitable for creating the successful biosensor array. Using the redox polymer on the Au nanoparticles outer layer also resulted in better electrocatalytic response due to electrical wiring of enzymes. The in situ deposition of these generic nanomolecules in microsystems can be possible as far as such devices are equipped with microelectrodes with the corresponding contacts. The overall advantage of this technique is that the described method uses the same technique (electrochemistry) to both manufacture the multi-sensoric platform and detect the (bio) recognition event. With both arraying and measurement by electrochemical methods, overall fabrication costs should be minimized.

4.6. Abbreviations

Au - gold

GOX - Glucose oxidase

HRP - Horse radish peroxidase

RP 1- redox POs

RP 2 – Redox Co polymer

TEG – Triethylene glycol

TA- Thioctic acid

4.7. References

1. Albers, J., Grunwald, T., Nebling, E., Piechotta, G., Hintsche, R., *Anal. Bioanal. Chem.*, 2003, 377, 521-527.
2. Brian, G.H., Lin, Li., David, R.W., *Biosens. Bioelectron.*, 1997, 12, 521-529.
3. Brecht, A., *Anal. Bioanal. Chem.*, 2005, 381, 1025-1026.
4. Ding, Y., Zhou, L.P., Halsall, H.B., Heineman, W.R., *J. Pharm Biomed Anal.*, 1999, 19, 153-161.
5. Jia, N.Q., Zhang, Z.R., Zhu, J.Z., *Chin. J. Chem.*, 2004, 22, 908-912.
6. Maestre, E., Katakis, I., Narvaez, A., Dominguez, E., *Biosens. Bioelectron.*, 2005, 21, 774-781.
7. Wittstock, G., *Anal. Bioanal. Chem.*, 2002, 372, 16-17.
8. Stefan, R.I., van Staden, J.F., Aboul-Enein, H.Y., *Crit. Rev. Anal. Chem.*, 1999, 29, 133-153.
9. Wilson, M.S., Nie, W.Y., *Anal. Chem.*, 2006, 78, 2507-2513.
10. Zen, J.M., Lai, Y., Yang, H.H., Kumar, A.S., *Sens. Act. B.*, 2002, 84, 237-244.
11. Zhi, Z.L., Murakami, Y., Morita, Y., Hasan, Q., Tamiya, E., *Anal. Biochem.*, 2003, 318, 236 - 243.
12. Zhu, J., Tian, C., Wu, W., Wu, J., Zhang, H., Lu, D., Zhang, G., *Biosens. Bioelectron.*, 1994, 295- 300.
13. Cho, E.J., Tao, Z., Tehan, E.C., Bright, F.V., *Anal. Chem.*, 2002, 74, 6177 - 6184.
14. Bernard, A., R.J., Michel, B., Bosshard, H.R., Delamarche, E., *Adv. Mat.*, 2000, 12, 1067-1070.
15. James, C.D., D.R., Kam, L., Craighead, H.G., Isaacson, M., Turner, J.N., Shain, W., *Langmuir*, 1998, 14, 741 -744.
16. Flounders, A.W., Brandon, D.L., Bates, A.H., *Biosens. Bioelectron.*, 1997, 12, 447-456.
17. Lee, K.N., Shin, D.S., Lee, Y.S., Kim, Y.K., *J. Micromech. Microeng.*, 2003, 13: p. 18-25.
18. Kostecky, R., Song, X.Y., Kinoshita, K., *J. Electrochem. Soc.*, 2000, 147: p. 1878-1881.
19. Iwasaki, Y., Morita, M., *Current Separations*, 1995, 14, 2-8.
20. Dobson, P.J., Jiang, L., Leigh, P.A., Hill, H.A.O., Kaneko, S., *Adv. Mat. Opt. Electron.*, 1992, 1, 133 - 138.
21. Shin, D.S., Lee, K.N., Jang, K.H., Kim, J.K., Chung, W.J., Kim, Y.K., Lee, Y.S., *Biosens. Bioelectron.*, 2003, 19, 485-494.
22. Sorribas, H., Padeste, C., Tiefenauer, L., *Biomaterials*, 2002, 23, 893-900.
23. Blawas, A.S., Reichert, W.M., *Biomaterials*, 1998, 19, 595-609.
24. Jena, B.K., Raj, C.R., *Anal. Chem.*, 2006, 78, 6332-6339.

25. Endo, T., Kerman, K., Nagatani, N., Hiepa, H.M., Kim, D.K., Yonezawa, Y., Nakano, K., Tamiya, E., *Anal. Chem.*, 2006, 78, 6465-6475.
26. Peng, H., Soeller, C., Cannell, M.B., Bowmaker, G.A., Cooney, R.P., Travas-Sejdic, J., *Biosens. Bioelectron.*, 2005, 21, 1727-1736.
27. Liu, G.L., Rodriguez, V.B., Lee, L.P., *J. Nanosci. Nanotech.*, 2005, 5, 1933-1937.
28. Liu, S.F., Li, Y.F., Li, J.R., Jiang, L., *Biosens. Bioelectron.*, 2006, 21, 1727-1736.
29. Chu, X., Fu, X., Chen, K., Shen, G.L., Yu, R.Q., *Biosens. Bioelectron.*, 2005, 20, 1805-1812.
30. Li, M., Lin, Y.C., Su, K.C., Wang, Y.T., Chang, T.C., Lin, H.P., *Biosens. Bioelectron.*, 2006, 21, 451-456.
31. Luo, X.L., Killard, A.J., Smyth, M.R., *Electroanalysis*, 2006, 18, 1131-1134.
32. Agui, L., Manso, J., Yanez-Sedeno, P., Pingarron, J.M., *Sens. Act. B*, 2006, 113, 272-280.
33. Despic, A.R., Pavlovic, M.G., *Electroanal. Chem.*, 1984, 180: p. 31-40.
34. Crumbliss, A.L., Perine, S.C., Stonehuerner, J., Tubergen, K.R., Zhao, J., Henkens, R.W., O'Daly, J.P., *Biotechnol. Bioeng.*, 1992, 40, 483-490.
35. Matsumoto, N., Chen, X., Wilson, G.S., *Anal. Chem.*, 2002, 74, 362-367.
36. Campàs, M., Katakis, I., *Anal. Chim. Acta*, 2006, 556, 306-312.
37. Campàs, M., Katakis, I., *Sens. Act. B*, 2006, 114, 897-902.
38. Jiang, X., Ferrigno, R., Mrksich, M., Whitesides, G.M., *J. Am. Chem. Soc.*, 2003, 125, 2366-2367.

Chapter 5. Site-directed immobilisation of proteins through electrochemical deprotection on electroactive self-assembled monolayers

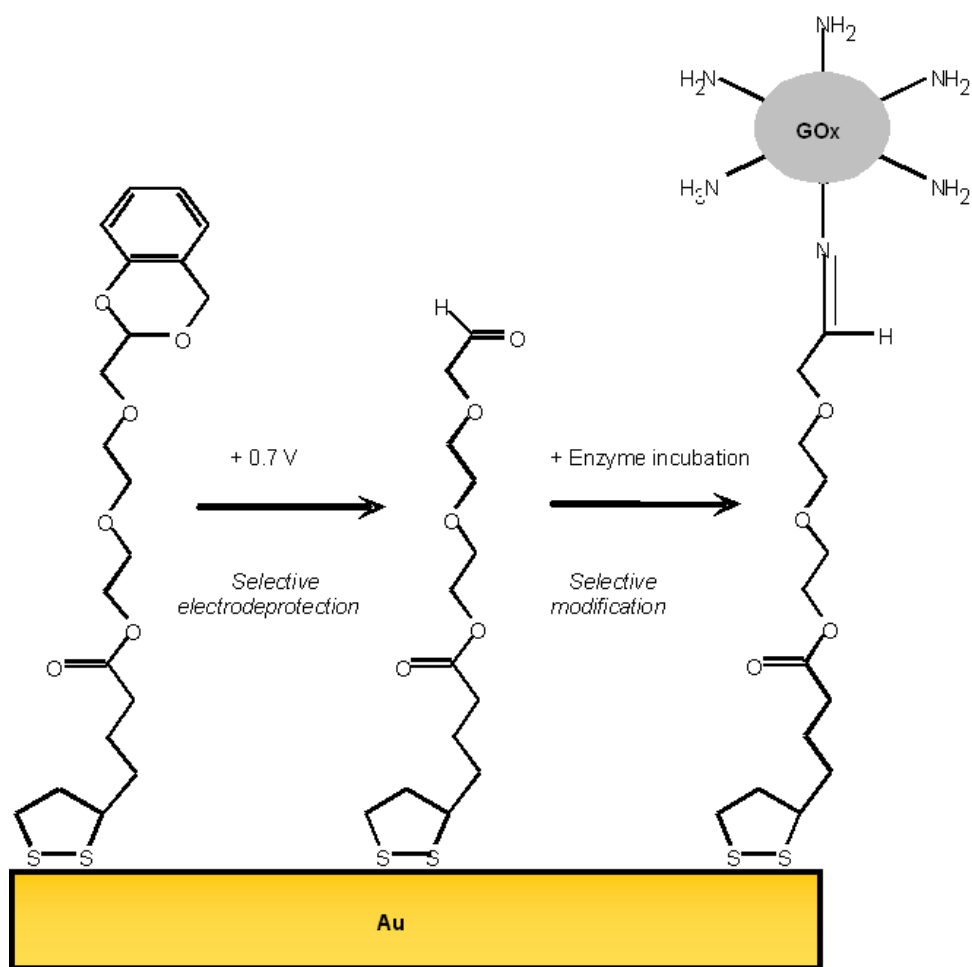
5.1. Abstract

Self-assembled monolayers were obtained on gold electrodes using thioctic esters of benzo [1,3] dioxinol. These SAMs present a group that can be electroactivated selectively and was used for the directed, reagentless, covalent patterning of proteins. The advantage of this moiety is that it allows electroactivation at low potentials increasing selectivity and reliability. In this study, the efficiency of this patterning system is examined. Cyclic voltammetry (CV) was used to confirm the electroactive nature of SAM modified electrodes, showing fast and complete electrochemical deprotection with one scan. The enzymes glucose oxidase (GOX) and horseradish peroxidase (HRP) were patterned on the SAM-modified electrode through Schiff's base formation after electrochemical deprotection, confirming the selective nature of the electroactive substrate. Amperometric response was measured after the GOX immobilisation showing high selective response. Real time monitoring is shown by immobilisation of HRP on the SAM modified surface using electrochemical surface plasmon resonance (ESPR) after electrochemical deprotection, again showing high selective response when compared to the protected control.

5.2. Introduction

The controlled patterning of biomolecules (proteins or oligonucleotides) or cells on solid substrates is a crucial step in the successful fabrication of defined arrays for the fabrication of biosensors, biochips, or intelligent implants and hybrid materials ^[1,2]. Reliable and selective patterning is required to achieve the reliability, sensitivity and reproducibility that are required for such devices. Depending on the application, selective patterning needs to achieve varied resolution limits. Several methods for the patterning of proteins onto solid surfaces have been reported such as microcontact printing, photolithography, pin or ink deposition, and surface

chemistry [3,4]. The use of electrochemistry (electrical fields or selective surface activation) as an alternative provides the advantage of employing the final devices in the format that it will be used and a method (electrochemistry) that is the same that is employed many times for transduction and actuation [5-7]. In previous chapters it was shown that using bio/nanomodules and electric field as driving force relatively interference-free arrays can be constructed [5,6]. Alternative methods for patterning include those of deprotection or activation of preformed immobilisation spots such as photodeprotection ^[9,10] or acid/base treatment ^[11], but the limitations in the quantification of the deprotection and the complex treatments associated, that can imply severe changes in the physico-chemical conditions inducing degradation of the biomolecules, make the electrochemical a more suitable deprotection/activation method. In this sense, the use of protecting groups for specific binding sites that can be subsequently deprotected electrochemically can be employed for patterning [12-14]. Such methods have been developed for the patterning of biomolecules, offering new frontiers for the design of advanced intelligent materials [15-17]. Dynamic SAM presenting ligands that can be switched from an inert (where the ligand is protected) to an active state (where the ligand is deprotected or activated and ready for the binding of a specific biomolecule) has been developed for the selective immobilisation of biomolecules [12]. These substrates offer real time control over the presentation of ligands to attach biomolecules, allowing the modulation of the ligand activity and biomolecule immobilisation. The utilisation of different potentials to induce the protection/deprotection of specific binding sites of SAMs has been reported as an efficient method to tune the binding biomolecules [12-14]. In this chapter for the first time is described a dynamic electroactive substrate presenting benzo [1,3] dioxinol SAM for the selective patterning of biomolecules. The strategy for the selective patterning of biomolecules using the self-assembled monolayers presenting the electroactive substrate is illustrated in scheme 5.1. The advantage of this moiety is the lower activation potential that allows for more selectivity and avoids the possible desorption of thiols. In addition, the electroactivation creates an aldehyde group that allows the direct coupling with amines on biomolecules without the need to add other coupling reagents, presumably increasing also the efficiency of patterning.



Scheme 5.1. Schematic representation of the generation of the aldehyde group by electrochemical deprotection/activation of SAM containing thioctic esters presenting benzo1,3 dioxinol substrate and subsequent covalent coupling of aldehyde with amine containing enzymes.

This efficiency and selectivity are studied by ESPR, cyclic voltammetry using glucose oxidase and horseradish peroxidase, as a model system.

5.3. Experimental

5.3.1. Materials

Thioctic acid (Acros Organics, Spain) was used immediately as received. Triethylene glycol (Acros Organics, Spain) was dried over drierite for one week and distilled under vacuum (114°C/0.1 mm Hg) before using. Chloroform was distilled from calcium chloride. Dichloromethane was dried by distillation from phosphorous pentoxide. Chromium oxide (Sigma-Aldrich, Spain) was dried over P₂O₅; pyridine was distilled over KOH prior to use. Glucose oxidase (GOX) was purchased from Biozymes, UK. All other compounds were purchased from Sigma-Aldrich and used as received. Glucose and HRP were purchased from Sigma-Aldrich and used as received.

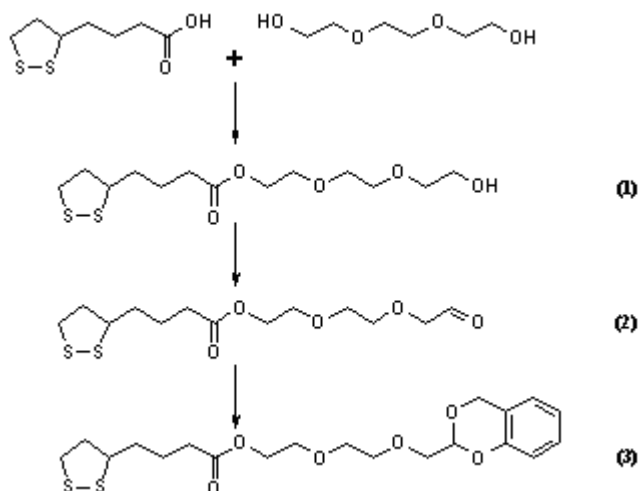
5.3.2. Instrumentation

Electrochemical experiments were performed using an AUTOLAB PGSTAT10 potentiostat (Eco Chemie, Netherlands) in a conventional three-electrode cell. A Ag/AgCl electrode (BAS, UK) was used as reference electrode and platinum wire as counter. 0.5 mm diameter gold wire (Advent, Oxford, UK) was resin-sealed (Mecaprex M42, PRESI, France) within a glass capillary and used as working electrode. All solutions were made with purified distilled water obtained from a Milli-Q water system. ESPR measurements were carried out with a ESPRIT instrument (Eco Chemie, Netherlands). ¹H NMR spectra were recorded using standard conditions on a Varian Gemini 300 spectrometer. Flash chromatography was performed using silica gel 60 (230-400 mesh).

5.3.3. Methods

5.3.3.1. Synthesis of electroactive thioctic acid esters

The steps for the synthesis of the electroactive substrate are shown in scheme 5.2.



Scheme 5. 2. Steps for the synthesis of benzo (1,3) dioxinol thioctic ester

Compound 1[15]. Triethylene glycol (12 g, 0.08 mol), dicyclohexylcarbodiimide (4.94, 0.024 mol) and 4,4-dimethylaminopyridine (0.244, 0.002 mol) were added to a solution of thioctic acid (4.12 g, 0.02 mol) in chloroform (50 mL). After 24 h at room temperature chloroform was removed under reduced pressure and the mixture extracted with diethyl ether. The organic solution was washed with brine, dried over MgSO₄ and concentrated. Flash chromatography with THF-hexane (1:1) afforded 3.27 g of pure yellow oil. Yield: 37 %.

¹H NMR (400 MHz, CDCl₃) δ4.24-4.28 (t, 1H, J=2.22 Hz), 3.59-3.75 (m, 12H), 3.51-3.61 (m, 1H), 3.15-3.19 (m, 2H), 2.42-2.60 (m, 1H), 2.37-2.40 (t, 2H), 1.92-1.95 (m, 1H), 1.67-1.74 (m, 4H), 1.49-1.55 (m, 2H).

Compound 2. Pyridine (4.21 g, 0.054 mol) in dichloromethane (15 mL) was added dropwise to a suspension formed by chromium oxide (2.66 g, 0.026 mol) and dichloromethane (20 mL). The mixture was kept under argon at room temperature and protected from light for 90 min. Then, a solution of ester (1.5 g, 4.6 mmol) in

dichloromethane (25 mL) was added dropwise for 15 min and 90 min later the mixture was filtered very slowly through glass wool. The mixture was concentrated, dissolved in ethanol, filtered through celite and concentrated again. Yield: 57%

^1H NMR (400 MHz, CDCl_3) δ 9.75 (t, 1H), 3.49-3.76 (m, 11H), 3.15-3.19 (m, 2H), 2.42-2.60 (m, 1H), 2.37-2.40 (t, 2H), 1.92-1.95 (m, 1H), 1.67-1.74 (m, 4H), 1.49-1.55 (m, 2H).

Compound 3. 2-hydroxybenzyl alcohol (0.194 g, 1.6 mmol) and aldehyde compound (0.49 g, 1.5 mmol) were refluxed in anhydrous dioxane (5 mL), concentrated sulphuric acid (150 μL) and anhydrous magnesium sulphate (0.5 g) for 3 h. The mixture was filtered and concentrated. The product was selectively isolated from hexane:acetone (1:2). Yield: 26%

^1H NMR (400 MHz, CDCl_3) δ 7.20 (d, 1H), 7.00 (d, 1H), 6.80 (dd, 2H), 4.65 (s, 2H), 3.59-3.75 (m, 11H), 3.51-3.61 (m, 1H), 3.14-3.19 (m, 2H), 2.42-2.61 (m, 1H), 2.37-2.40 (t, 2H), 1.92-1.95 (m, 1H), 1.67-1.74 (m, 4H), 1.49-1.55 (m, 2H).

5.3.3.2. Preparation of the electrode

0.5mm gold disk electrodes were successively polished with 6, 3, 1, 0.5 and 0.1 μm diamond paste (Buehler) and sonicated in water for 1 min after each polishing step. Later the electrode was electrochemically cleaned by scanning from -0.2 to $+1.8$ V (vs. Ag/AgCl) at a scan rate of 0.2 V s^{-1} in a 2 M H_2SO_4 solution until a constant cleaned gold voltammogram was obtained [18]. Next the electrode was rinsed with distilled water and dried with nitrogen. Self assembled monolayers were prepared by incubating the gold electrode with ethanolic solutions of the thioctic acid esters presenting benzo [1,3] dioxinol for *ca.* 12 h . Finally the electrodes were rinsed with ethanol and dried with nitrogen.

5.3.3.3. Characterisation of the benzo 1,3 dioxinol modified electrode

Electrochemical characterisation of the modified electrode was done by performing cyclic voltammetry in 10 mM phosphate buffered saline with 150 mM NaCl pH 7.0, scanning from +0.4 V to +1.0 V (vs. Ag/AgCl) at a rate of 0.1 V s⁻¹.

5.3.3.4. Electrochemical impedance spectroscopy

Electrochemical impedance spectroscopy (EIS) was used to characterize the changes in the charge transfer resistance (R_{ct}) offered due to the electrochemical deprotection. R_{ct} , the semicircle diameter at higher frequencies in the Nyquist plot of impedance spectroscopy, controls the interfacial electron transfer rate of the redox probe between the solution and the electrode. Experiments were conducted using a three electrode system in the presence of 0.1M phosphate buffered saline at pH 7.0 as a supporting electrolyte containing 10mM $K_3[Fe(CN)_6]$ and 10mM $K_4[Fe(CN)_6]$ as a redox probe at the formal potential of the system, $E^{\circ} = 0.227V$, using AC amplitude of 0.005V. Impedance measurements were performed in the frequency range from 0.1 Hz to 100MHz. Experiments were also conducted using a three electrode system in the presence of 0.1M phosphate buffered saline at pH 7.0 as a supporting electrolyte containing 10mM $Ru(NH_3)_6^{3+}$ as a redox probe at the formal potential of the system, $E^{\circ} = -0.225V$, using AC amplitude of 0.005V. Impedance measurements were performed in the frequency range from 0.1 Hz to 100MHz.

Finally EIS was used to demonstrate the electrodesorption of thioctic acid esters self-assembled on gold electrode at +0.8V(vs Ag/AgCl) after 15 and 30min. Initially EIS of the blank Au electrode was taken in the presence of 0.1M phosphate buffered saline at pH 7.0 as a supporting electrolyte containing 10mM $K_3[Fe(CN)_6]$ and 10mM $K_4[Fe(CN)_6]$ as a redox probe at the formal potential of the system, $E^{\circ} = 0.208 V$, using AC amplitude of 0.005V. For this, a gold electrode was incubated with 1mM TEG-thioctic acid esters dissolved in ethanol for 2hr. Later the Au electrode was washed with ethanol and dried under argon. After washing, electrodes were kept in 0.1M PBS pH 7.0 and a potential of 0.8V (vs.Ag/AgCl) for 15 and 30min. After each potential step EIS was taken to

see the changes in the charge transfer resistance (R_{ct}) offered due to the electrochemical desorption.

5.3.3.5. Electrochemical surface plasmon resonance (ESPR) measurements

In order to determine the efficiency and selectivity of patterning of proteins on the activated SAMs the electrochemical surface plasmon resonance (ESPR) technique was used so that efficiency of patterning and function of the immobilized proteins could be studied separately. The modified benzo [1,3] dioxinol electrode was activated as the SPR measurement was taken by applying + 0.7 V (vs. Ag/AgCl) for 120 s. Next a pH 7.0, 0.01M PBS solution with 0.15 M NaCl was used to wash the activated electrode surface in a flow setup, until a constant baseline was observed which is the starting point in Figure 5.7. Next the horseradish peroxidase (HRP, 10 $\mu\text{g mL}^{-1}$) dissolved in 0.01 M pH 7.0 PBS was left in contact with the electrode for a period of 300 s, after which it was washed with a similar PBS solution until reaching a new value of resonance angle. The difference between the initial and final values is indicative of the immobilisation of HRP on the electrochemically-activated electrode. To quantify the non-specific adsorption control experiments were performed exposing the non-activated electrode surface to similar HRP concentration followed by the same washing steps.

5.4. Results and discussion

5.4.1. Electrochemical activation of SAMs

As shown in figure 5.1, an irreversible anodic peak around + 0.6 V was observed during the first scan, which rapidly disappeared in subsequent scans, behaviour indicative of fast, nearly complete, (93% after the first scan as evidenced by integration of the charge passed) (98.5% after the second scan) activation after three scans.

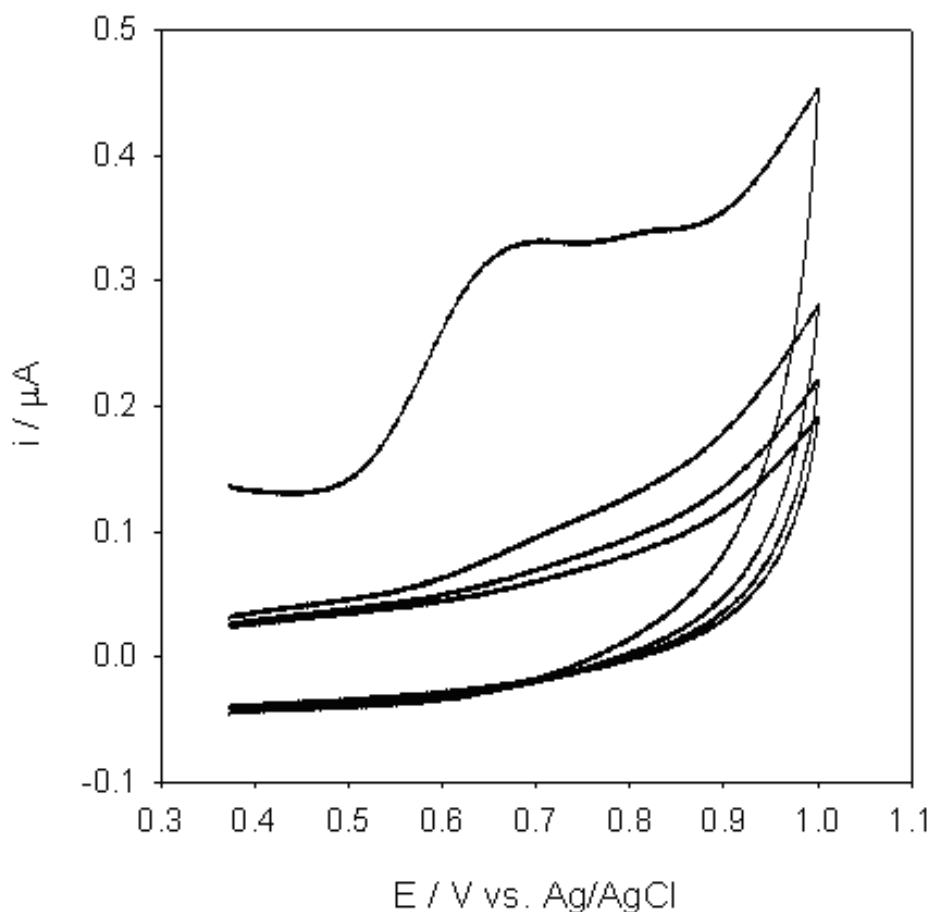


Figure 5.1. Cyclic voltammetry of benzo 1,3 dioxinol functionalised SAMs in 10 mM phosphate buffered with 0.15 M NaCl pH 7.0 at 0.1 V s^{-1}

The progressively decreasing electrochemical activity shows the electroinactive nature of the created aldehyde groups as expected. Further cyclic voltammograms were performed to the aldehyde-presenting SAM modified electrode confirming the lack of any electrochemical activity.

5.4.2. Electrochemical anodic desorption of TEG-thioctic acid esters

Figure 5.1 shows that electrochemical activation of the dioxinol moiety can occur at the interval 0.6 to 0.7 V (Ag/AgCl). As mentioned, alternative chemistries have appeared in the literature to bring about the same effect, but applying higher potentials. To demonstrate the advantage of the method used here, TEG-thioctic acid esters were used as SAM models to demonstrate that at these higher potentials

significant desorption of thiol-based SAMs occurs, therefore diminishing the presentation of active ligands to the solution.

Figure 5.2 shows the electrochemical impedance spectroscopy characterisation of the electrodesorption at such higher potentials of TEG-thioctic acid esters immobilized on the gold electrode surface. It is shown that, there is semi-circle formation in the case of gold electrodes modified with TEG-thioctic esters which is presumably due to the charge transfer resistance offered by the thioctic ester monolayers self assembled on the gold electrode.

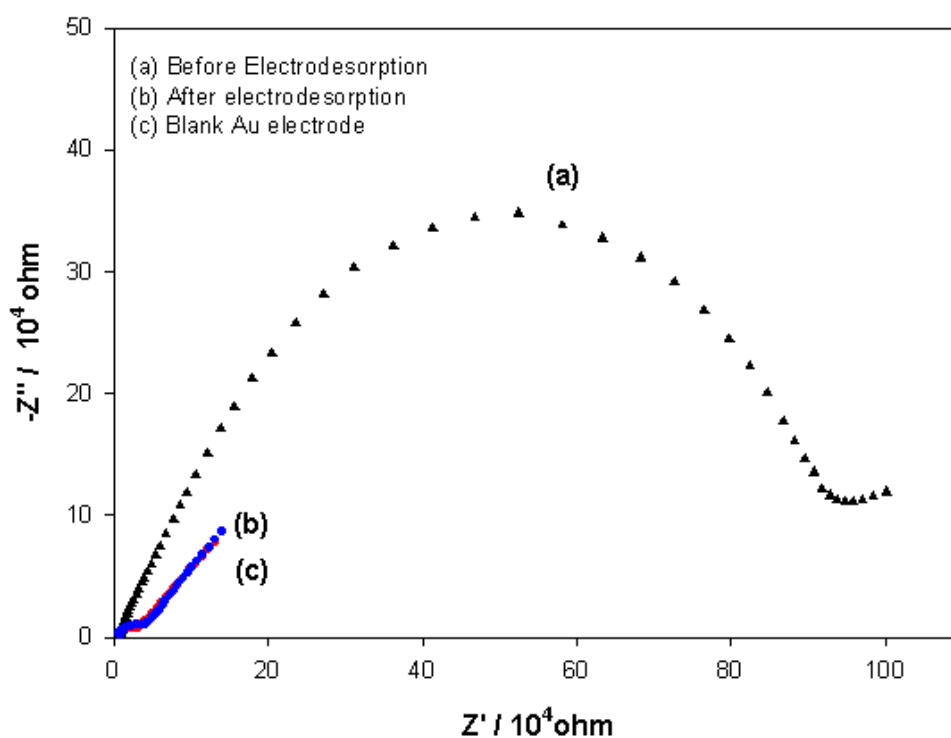


Figure 5.2. Nyquist plot Impedance response in 0.1M pH 7.0 PBS in the presence of 10 mM $K_3[Fe(CN)_6]$ and 10 mM $K_4[Fe(CN)_6]$. Conditions: $E_0 = 0.205$ V and frequency range 0.1Hz to 100mHz., amplitude 5mV .

After 15 min of applying the potential + 0.8 V (vs.Ag/AgCl), there is a decrease in the semi circle formation which was presumably due to the removal of the SAMs from the gold electrode surface. The impedance behaviour is the same as that of the blank gold electrode. This clearly shows the possible advantage of using lower potentials for electrochemical deprotection as there can be electrodesorption at higher potentials while working with gold electrode, which was demonstrated from the above experiments.

5.4.3. Electrochemical properties of modified electrodes

SAM formation and the effects of SAM and activation on the electrochemical behavior of the electrodes could be observed and studied with impedance spectroscopy and cyclic voltammetry of a solution electroactive species.

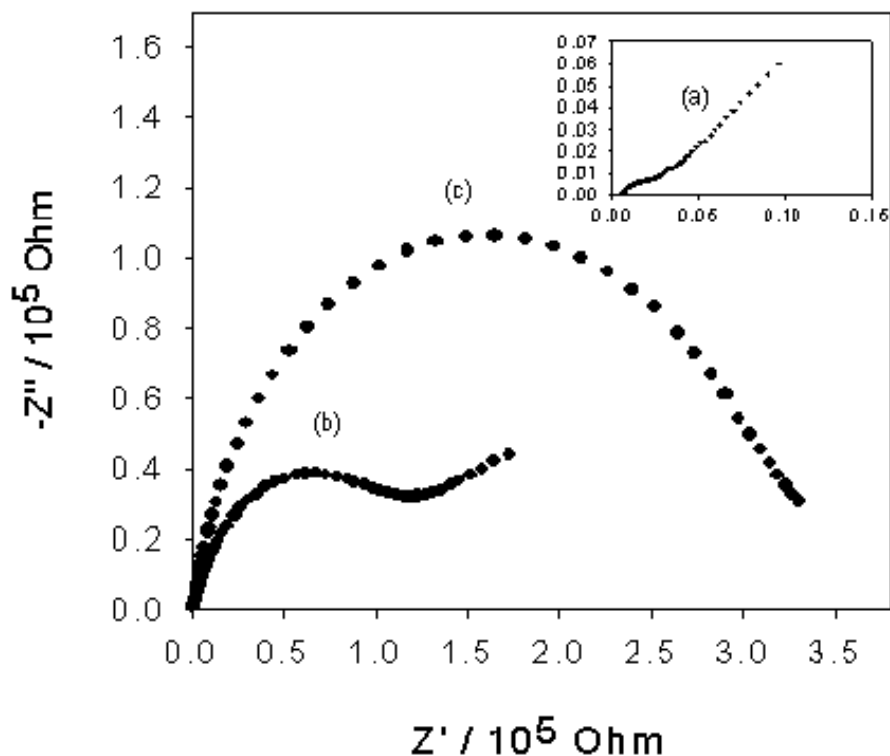


Figure 5.3. Nyquist plot Impedance response in 0.1M pH 7.0 PBS in the presence of 10 mM $K_3[Fe(CN)_6]$ and 10 mM $K_4[Fe(CN)_6]$ a) $E_0 = 0.227 \text{ V}$ and frequency range 0.1Hz to 100 mHz. b) 0.05 V s^{-1} . (a) Blank electrode, (b) non activated and (c) activated

As observed in Figure 5.3(a) and 5.4(a) the bare electrode showed the facile kinetics behavior of the reversible $Fe(CN)_6^{3/4-}$ couple with an almost imperceptible semicircle formation in the Nyquist plot and reversible cyclic voltammetry.

However, after the formation of the electroactive SAM before activation (plot b in both Figures) the behavior of the system changed considerably: the peak-to-peak separation of the CV did not change significantly, but the peak height decreased dramatically.

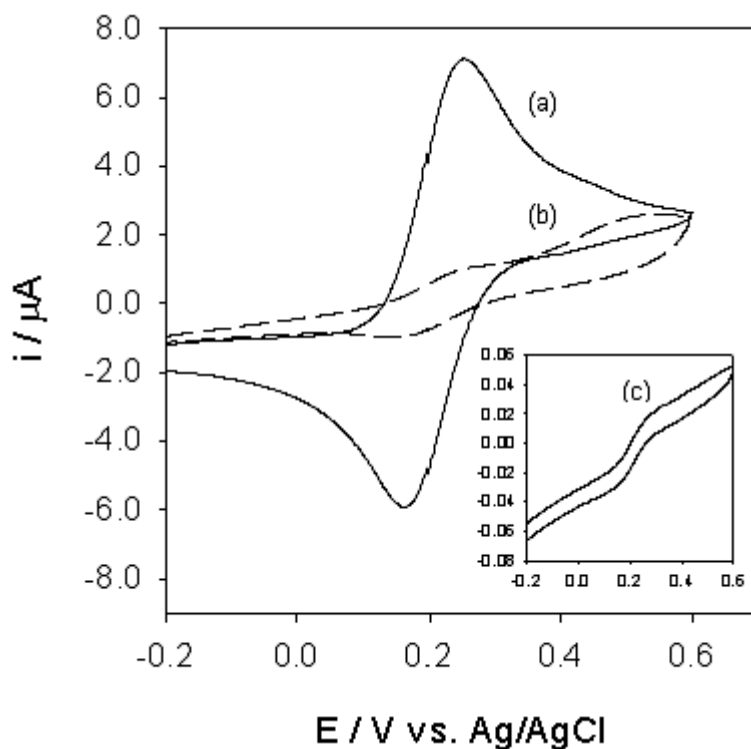


Figure 5.4. Cyclic voltammety response in 0.1M pH 7.0 PBS in the presence of 10 mM $K_3[Fe(CN)_6]$ and 10 mM $K_4[Fe(CN)_6]$ at 0.05 V s^{-1} . (a) blank electrode, (b) non activated and (c) activated

The Nyquist plot showed a considerable increase in the diameter of the semicircle at the high frequency range indicative of a higher charge transfer resistance. The behavior of the system changed further when the SAM layer was activated (plot c in both Figures): the diameter of the semicircle increased making impossible to perceive a linear part even at the lowest frequency range in the Nyquist plot, and cyclic voltammety indicated a further attenuation of the peak current. To explain these observations it is postulated that the closely packed SAM acts as a “passivator” of the electrode.

However, the structure presented to the solution (that of benzodioxinol) is not perfectly packed and allows some partition of the electroactive species. It is also possible that this structure causes a slight resonance effect which disappears after activation. However, after activation it is postulated that the free aldehyde groups are rapidly reacting with water forming carboxylic acids that present an anionic surface to solution. In addition, the $Fe(CN)_6^{3/4-}$ couple can oxidize the aldehyde group to an acidic group. This further inhibits the permeation of the anionic ferri/ferro cyanide couple, a fact that demonstrates itself as a further attenuation of

the peak height in cyclic voltammetry and as an apparent increase of charge transfer resistance.

To further probe the physiochemical properties of the SAM-modified electrodes $\text{Ru}(\text{NH}_3)_6^+$ (a cationic species) was used to repeat the same experiments. After electrochemical deprotection by activation the electron transfer increases which is due to the removal of aromatic benzene rings from the electrode surface. Figure 5.5 shows the cyclic voltammogram of the changes occurring on the gold electrode surface due to the electrochemical deprotection. As observed in Figure 5.5, the blank Au electrode displayed redox peaks at -0.246 V and -0.166 V with a peak to peak separation of 80 mV . After immobilization of the thioctic acid esters presenting 1,3 dioxinol on the gold electrode, the peak currents decrease with peak potentials -0.240 V and -0.160 V .

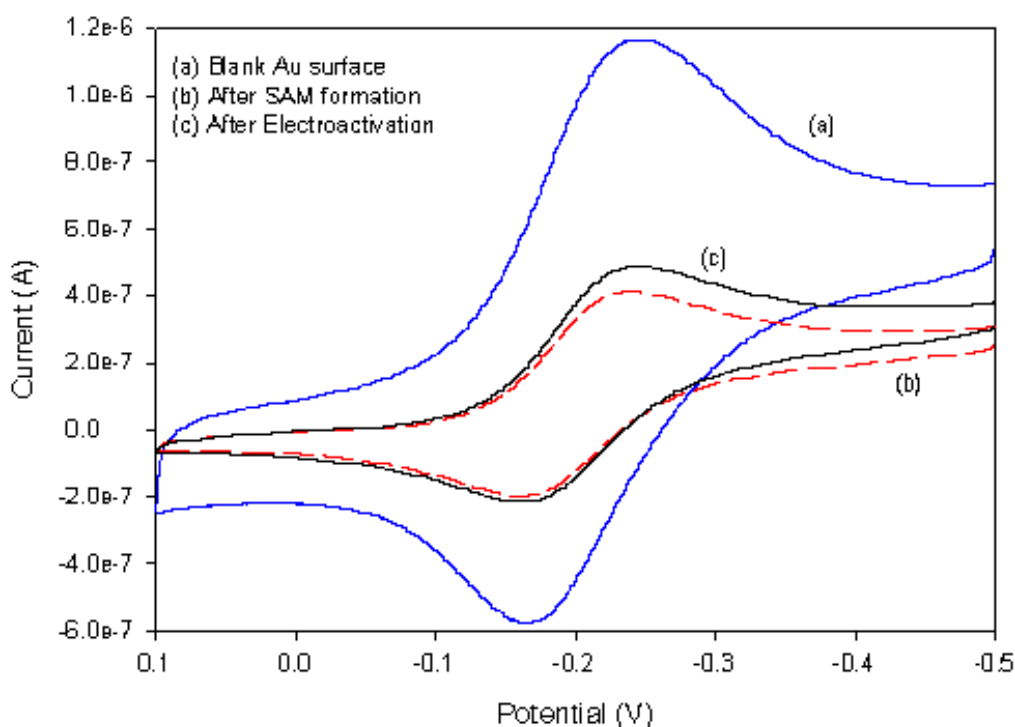


Figure 5. 5. Cyclic voltammetry response of the changes on the gold electrode in 0.1 M pH 7.0 PBS in the presence of 10 mM $\text{Ru}(\text{NH}_3)_6^+$, scan rate 50 mV sec^{-1}

This might be due to the change in the electrode surface due to the formation of self assembled monolayer of the electroactive substrate. Finally after the electroactivation, there is a slight increase in the peak currents, but definitely not the drastic decrease observed in Figure 5.4 with $\text{Fe}(\text{CN})_6^{3/4-}$. These results clearly demonstrates that the

electron transfer of $\text{Ru}(\text{NH}_3)_6^+$ couple showed distinctly different behaviour from the ferri/ferro cyanide couple after electroactivation. From the above observations, it seems that the electrostatic effect indeed was the cause of the change in behavior by using ruthenium hexaamine in solution, instead of the ferricyanide couple.

It therefore remained to examine if this apparent passivation inhibited the electron transfer from species immobilised on the activated SAM and therefore in close proximity to the surface, because such an eventuality would render the patterning methods useless for electrochemical biosensors.

5.4.4. Patterning efficiency verification through surface plasmon resonance measurements

Figure 5.6 shows the SPR monitoring of HRP immobilization on the electroactivated 1,3 benzene dioxinol self assembled gold electrodes. The shift of SPR angle is used to evaluate the amount of the HRP immobilized successfully on the modified gold electrode surface.

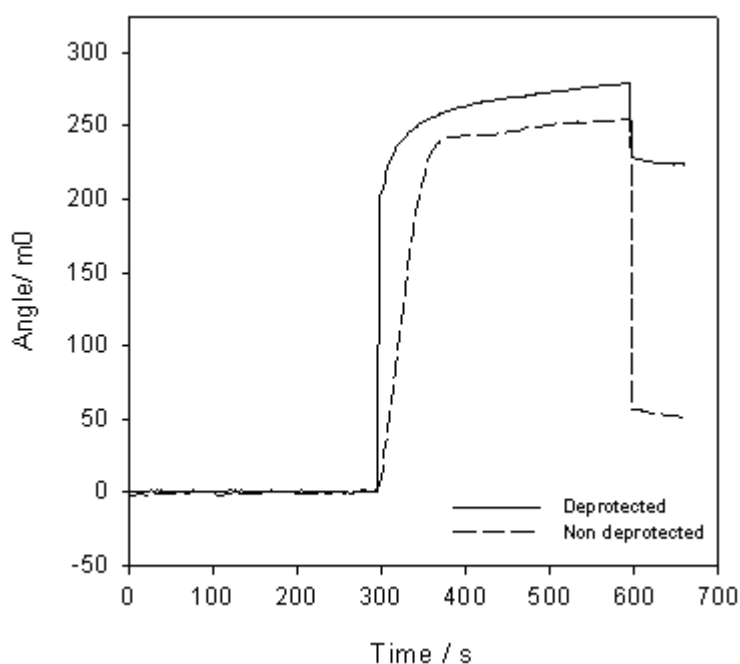


Figure 5.6. ESPR measurement of the HRP immobilisation on electroactive SAM modified electrode after and before electrochemical activation. 10 mM pH 7.0 PBS with 0.15 M NaCl and $10\mu\text{g mL}^{-1}$ HRP.

The amount of HRP immobilized on the activated surface was calculated to be 1.9 ng mm^{-2} using the manufacturer's approximation that about 120 m° of resonance angle change correspond to 1 ng mm^{-2} of protein on the surface. In surface modification experiments, there is always the possibility that non-specific forces develop leading to non-specific adsorption of proteins.

The measured change in resonance angle allows the estimation of non-specific adsorption of the HRP and was estimated to be about 19% . From the value of about 50 m° that was measured for the specific phenomena, it was calculated that the amount of HRP non-specifically immobilized corresponds to significantly lower than monolayer surface coverage (about $10^{-13} \text{ mol cm}^{-2}$). It is therefore concluded that although it is not possible to avoid totally non-specific adsorption, the method can be used for patterning selectively proteins onto electrodes through electrochemical activation of the benzodioxinol SAMs.

5.4.5. Functionality of patterned proteins

In order to verify the functionality of the patterned proteins glucose oxidase (GOX) was used as the model protein since its functionality could be verified by measuring H_2O_2 production directly amperometrically.

For this reason GOX was patterned on gold electrodes in a setup similar to that described previously for HRP, on electrodes activated by applying $+ 0.7 \text{ V}$ (vs. Ag/AgCl) for 120 s, followed by incubation in a, $10 \text{ } \mu\text{g mL}^{-1}$ GOX solution in pH 7.0 0.01 M PBS solution with 0.15 M NaCl for a period of 30 minutes. 0.02M Sodium borohydride was added after activation for the reduction of the Schiff base. The electrodes were then rinsed with distilled water and ried with argon. The response to glucose was measured in 0.1 M PBS, pH 7.0 amperometrically by applying 0.7 V vs. Ag/AgCl. Control experiments to quantify the amperometric response due to the non-specific adsorption of GOX were made using the non-activated SAM-modified electrodes. The results are compared in Figure 5.7. Figures 5.7 a) and 5.7 b) show the amperometric response to glucose of activated and non-activated electrodes. There was an average current increase of $0.015 \text{ } \mu\text{A}$ per 10 mM of glucose added for the specifically activated and modified electrode, whereas only 7 % of this response was observed when GOX was applied on the non-activated electrodes.

Some preliminary experiments (results not shown) were performed using a diffusional mediator in solution (osmium bipyridine) to transduce the electrons from the oxidation of glucose at + 0.5 V vs Ag/AgCl. The results showed a tenfold amplification of the currents recorded, making more noticeable the current increase in the presence of glucose and decreased the relative response from the non specifically modified electrode.

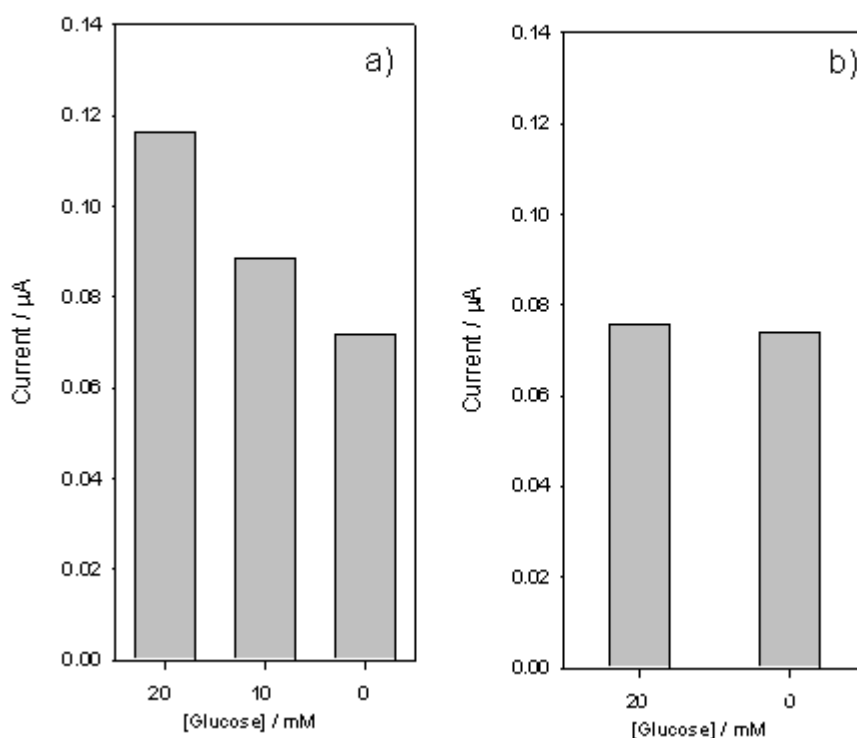


Figure 5.7. Amperometric response of electrodes exposed to GOX in 0.1 M pH 7.0 PBS, at a) at 0.7 V vs Ag/AgCl showing the response 0, 10 and 20 mM concentrations of glucose on a) activated electrode b) non-activated electrode

These results taken together demonstrate that the patterned proteins are functional after immobilization and that the observed “passivation” of the surface due to the SAM does not prohibit the collection of current from the immobilised protein layer. In Figure 5.8 the results of ESPR and amperometric detection are compared, clarifying the effect of non-specific phenomena as observed with the two techniques.

It can be seen that SPR shows an about 20% non-specifically adsorbed protein on the non-activated electrodes, whereas only about 10% of non-specific current is observed in the amperometric response to glucose. This difference is significant within experimental error and might be due to the fact that non-specifically adsorbed protein is less efficient in transferring electrons due to orientation or other phenomena. Still, it is obvious that this patterning method could not be used for extensive arrays, but it might be suitable for 8-10 analyte devices.

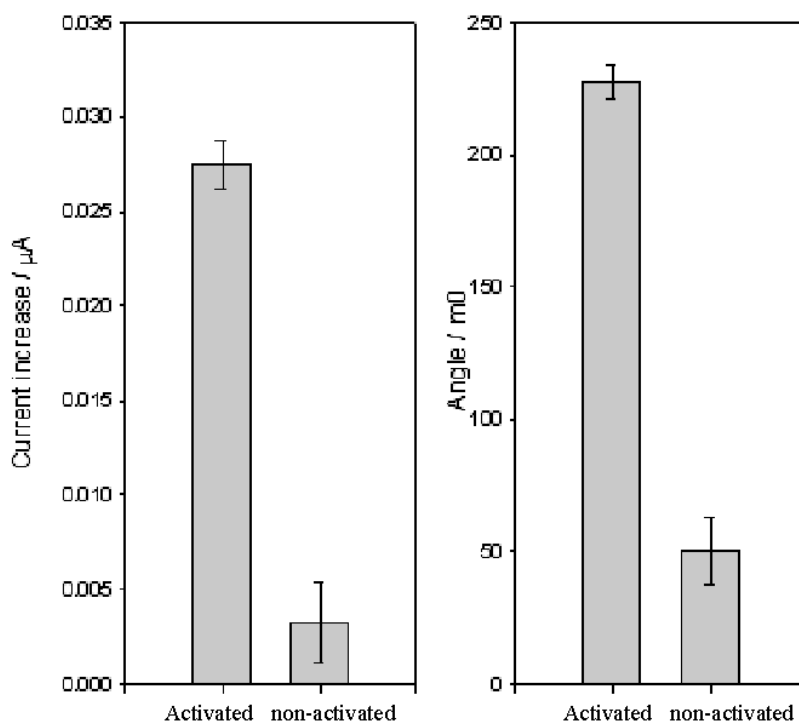


Figure 5.8. (a) Comparison of amperometric response due to selective patterning vs. non-specific adsorption of GOX. (b) Comparison of HRP patterned vs. HRP non-specifically adsorbed as evidenced by ESPR. Data taken from Figures 5.7 and 5.8 respectively.

For this reason, further optimisation to avoid the non-specific adsorption of proteins is necessary.

5.5. Conclusions

It was described in this chapter that the site directed immobilisation of proteins by electrochemical activation of acetal-containing SAMs is another possible selective protein patterning method. Thioctic esters presenting benzo (1,3) dioxinol were synthesized and characterized successfully. It was found that electrochemical

activation is fast and can be achieved at relatively low electrochemical potentials. The active SAMs provide a reagentless method for patterning proteins but non-specific adsorption is significant. However, we believe that by optimising the system to avoid the non-specific phenomena either kinetically or by verifying their source the technique can be used to produce low-number multianalyte sensor arrays or fuel cells with insitu modification and micro or submicrometric resolution.

5.6. Abbreviations

CV - cyclic voltammetry
ESPR - electrochemical surface plasmon resonance
EIS - electrochemical impedance spectroscopy
GOX - glucose oxidase
HRP - horse radish peroxidase
PBS - phosphate buffered saline
SAM - self assembled monolayer
TEG - triethylene glycol

5.7. References

- 1) Pirrung, M.C, *Chemical Reviews*, 1997, 97, 473-478
- 2) Whitesides, G.M., Ostuni, E., Takayama, S., Jiang, X., Ingber, D.E, *Annual Review of Biomed.Eng*, 2001,3,335-373
- 3) Blawas, A.S., Reichert, W.M, *Biomaterials*, 1998,7, 595-609
- 4) Lee, C.S., Lee, S.H., Park, S.S., Kim, Y.K., Kim, B.G, *Biosens. Bioelectron*, 2003, 18, 437-444
- 5) Campàs, M., and Katakis, I., *Sens.Act.. B: Chemical*, 2006,114, 897-902
- 6) Campàs, M., and Katakis, I. *Analytica Chimica Acta*,. 2006, 556, 306-312
- 7) Wang, J., Jiang, M., Kawde, A.M., Polsky, R, *Langmuir*, 2000, 16, 9687-9689.
- 8) Matsue, T., Turyan, I., Mandler, D, *Anal. chem*, 2000, 72, 34321-3435
- 9) Fodor, S.P.A., Read, J.L., Pirrung, M.C., Stryer, L., Lu, A.T., Solas, D, *Science*, 1991, 251, 767-773

- 10) Yang, Z., Frey, W., Chilkoti, A., Oliver, T, *Langmuir*, 2000, 16 ,1751-1758
- 11) Frutos, A.G., Brockman, J.M., Corn, R.M, *Langmuir*, 2000, 16 , 2192-2197
- 12) Russell, T.P, *Science*, 2002, 297 ,964-967
- 13) Blonder, R., Katz, E., Willner, I., Wray, V., Bückmann, A.F. *J. Am. Chem. Soc*, 1997, 119 , 11747-11757.
- 14) Yeo, W.S., Mrksich, M., *Adv. Mater*, 2004, 16, 1352-1356
- 15) Kim, K., Yang, H., Jon, S., Kim, E., Kwak, J., *J. Am. Chem. Soc*, 2004, 126, 15368-15369
- 16) Kim, K., Yang, H., Kim, E., Han, Y. B., Kim, Y. T., Kang, S. H., Kwak, J., *Langmuir*; 2002,18, 1460-1462
- 17) Veiseh, M., Zareie, M.H., Zhang, M., *Langmuir*, 2002, 18, 6671-6678
- 18) Angerstein-Kozłowska, H., Conway, B.E; Hamelin, A., Stoicoviciu, L. *Electrochim.Acta*, 1986, 31 ,1051-1057
- 19) Bhosale, R.S., Bhosale, S.V., Bhosale, S.V., Solanke, K.S., Pawar, R.P., Chougule, H.S., Dongare, M.K., *Synth . Comm*, 2006,36, 659-663
- 20) Wiles, C., Watts, P., Haswell, S.J. *Tetrahedron*, 2005, 61, 5209-5217
- 21) Ranu, B.C., Jana, R., Samanta, S. *Adv. Synth.Catal*, 2004, 346, 446-450
- 22) Srilakshmi Krishnaveni, N., Surendra, K., Arjun Reddy, M., Nageswar, Y.V.D., Rama Rao, K. *J. Org. Chem*, 2003 68, 2018-2019
- 23) Kantam, M.L., Neeraja, V., Sreekanth, P. *Catal.Comm*, 2, 301-304

Chapter 6 : Selective Electrodeposition of Viologen Functionalised Biomolecules

6.1. Abstract

The aim of this chapter is to prove the principle of yet another electrochemical patterning of proteins on individually addressable electrodes. In this case, the proof of principle did not include two different enzyme electrodes but only a modified electrode and a control to assess non-specific phenomenon. This method consists selectively depositing enzymes using N-methyl-N'-(ω -carboxy pentyl)-4,4'-bipyridinium as an immobilization vehicle. Initially, 4,4'-bipyridyl carboxylic acid derivative was synthesized and characterised electrochemically. Cyclic voltammetry of the carboxylic acid derivative of the 4,4'-bipyridinium showed an active electrochemical signal. Later the carboxylic acid functionality was used for attaching HRP through carbodiimide chemistry. HRP conjugated viologen derivative was characterised by UV-Vis spectroscopy as well as electrochemistry successfully. Next the HRP was deposited by using the carboxylic acid functionalised viologen derivative as an immobilizing vehicle. Two different approaches were used in this experiment. In the first strategy, HRP was immobilised in two steps with initial electrodeposition of carboxylic acid viologen derivative followed by the immobilization of the HRP. In the second strategy, HRP was deposited in a single step by electrodepositing HRP conjugated 4,4'-bipyridyl derivative on the electrode surface. Both the approaches showed a good selectivity with the single step deposition method showing comparatively higher selectivity. Electrochemical quartz crystal microbalance (EQCM) experiments were used to see the deposition behaviour of the HRP functionalised viologen derivative at different potentials and proved that at a potential of -0.85 V (vs. Ag/AgCl), there is a maximum deposition with higher selectivity.

6.2 . Introduction

New methods for protein immobilization should have several characteristics to make them well suited to the preparation of protein arrays [1-7]. First, the substrates that are used for immobilization must be inert to the nonspecific adsorption of protein.

Inert substrates are necessary to prevent denaturation of immobilised proteins and unwanted adsorption of proteins in assays (which leads to both false positive and negative responses in assays and large background signals that limit sensitivity). Secondly, the reactions that covalently link the protein to the substrates should be selective, so the need to rigorously purify the protein is avoided and the protein is immobilised in a defined orientation. Thirdly, the reaction should be rapid so that only small amounts of protein are necessary, and that problems associated with solvent evaporation are minimized. Fourthly, the method should provide control over the density of immobilised protein, to ease steric interactions of neighboring proteins and to ensure that the amount of immobilised protein is reproducible. Finally, the resulting substrate should be compatible with several of the important detection technologies used in reading protein microarrays, fluorescence, surface plasmon resonance (SPR) and mass spectrometry.

Recently electrochemical deposition of Au particles functionalised bipyridinium adical cation has been used for biocatalytic applications[8]. The electroswitchable and the biocatalytic/electrochemical switchable interfacial properties of a 4,4'-bipyridinium monolayer associated with a Au surface are described. N-methyl-N'-(carboxyalkyl)-4,4'-bipyridinium has been self assembled on the gold electrode and used for coupling proteins towards the application of electrochemical biosensors[9,10]. Based on the free radical linking to the electrode surface, biomolecules were immobilised on the electrode surface by reduction of the diazonium salts where the biomolecule is conjugated to the aniline molecule and further these aniline derivatives were diazonated to form diazonium derivatives[11-12]. Later these diazonium derivatives are reduced to aryl free radical. Consecutive and reversible reductions of bipyridinium dication to the corresponding radical cation and neutral species has been shown with each reaction having different redox potentials [13]. Electrochromic properties of N,N'-disubstituted-4,4'-bipyridinium dication have been studied with the reduction of the dication of viologens to a highly colored cation radical [14].

Two different approaches were used for the selective immobilization of HRP on the Au electrode using carboxylic acid functionalised 4,4'-bipyridinium derivative for optimizing the best immobilization strategy which produces a selective response. In the first approach shown in scheme 6.2, two-step immobilization was used for patterning of HRP. In this case, 4,4'-bipyridinium derivative was initially deposited

on the Au electrode followed by HRP immobilization in the second step. The second approach is a single step immobilization procedure as shown in the scheme 6.3, where HRP was conjugated initially to the carboxylic acid functionalised 4,4'-bipyridinium derivative and later electrodeposited in a single step on the Au electrode.

6.3. Experimental

6.3.1. Instrumentation

Electrochemical experiments were performed using an AUTOLAB PGSTAT10 potentiostat (Eco Chemie, Netherlands) in a conventional three-electrode cell. A Ag/AgCl electrode (BAS) was used as reference electrode and platinum wire as counter electrode. 0.5 mm diameter gold wire (Advent) was resin-sealed (Mecaprex M42, PRESI, France) within a glass capillary and used as working electrode. All solutions were made with purified distilled water obtained from a milli-Q water system. ¹H NMR spectra were recorded using standard conditions on a Varian Gemini 300 spectrometer. Flash chromatography was performed using silica gel 60 (230-400 mesh). Electrochemical Quartz Crystal Microbalance (EQCM) measurements were conducted with a CHI 440 electrochemical workstation (CH Instruments, Austin, TX). The quartz crystal working electrode has a fundamental frequency of 7.995 MHz and is coated with thin gold films on both sides.

6.3.2. Reagents

4,4'-bipyridyl, iodomethane, DMF, diethyl ether and methyl 5-bromovalerate were purchased from Sigma-Aldrich, Spain and were used as received. Freshly distilled benzene over Sodium was used. Horse Radish Peroxidase (HRP) was purchased from Sigma-Aldrich, Spain. 3,3',5,5'-Tetramethyl benzidine liquid substrate (TMB) (T0440) was purchased from sigma-adrich,spain. Aqueous solutions were prepared with Milli Q water (Milli Q system, Millipore). All other chemicals were of analytical grade.

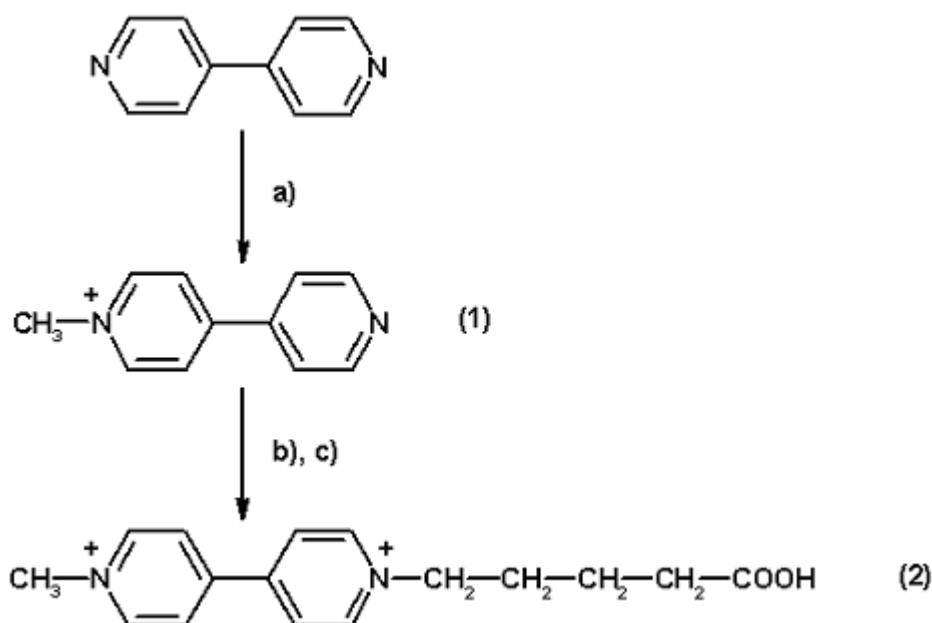
6.3.3. Preparation of the electrode

Gold disk electrodes were successively polished with 6, 3, 1, 0.5 and 0.1 μm diamond paste (Buehler) and sonicated in water for 1 min after each polishing step. Later the electrode was electrochemically cleaned by scanning from -0.2 to 1.8 V (vs. Ag/AgCl) at a scan rate of 0.1 V s^{-1} in a $0.5 \text{ M H}_2\text{SO}_4$. EQCM crystal was cleaned electrochemically.

6.3.4. Synthesis of 4,4'-bipyridinium derivatives

Steps for the synthesis of carboxylic acid functionalised 4,4'-bipyridinium derivative was shown in scheme 6.1. The synthesis involves in total three steps. In the first step, 4,4'-bipyridyl was quarternized with methyl iodide to form N-methyl-4-(4'-pyridyl)pyridinium iodide derivative.

In the second step, N-methyl-4-(4'-pyridyl)pyridinium iodide derivative was quarternized on the other side with and methyl 5-bromovalerate. Finally in the third step, hydrolysis of methyl valerate derivative of N-methyl-4-(4'-pyridyl)pyridinium iodide gives us a carboxylic acid functionalised 4,4' bipyridinium derivative.



Scheme 6.1. Steps in synthesis of a) CH_3I , benzene, room Temperature, 48h; b) methyl 5-bromovalerate, DMF, 110°C , 20h; c) H_2O , 16 % HCl

6.3.4.1. N-methyl-4-(4'-pyridyl)pyridinium iodide (1).

Iodomethane (0.710 g, 5 mmol) was added to a solution of 4,4'-bipyridyl (0.950 g, 6 mmol) in benzene (10 mL). The mixture was left for 48 h at room temperature. The orange precipitate was filtered, washed with diethyl ether and dried under vacuum to afford the pure pyridinium iodide (yield: 88 %).

^1H NMR (400 MHz, DMSO- d_6) δ 9.16 (d, 2H), 8.85 (d, 2H), 8.04 (d, 2H), 4.41 (s, 3H).

^{13}C NMR (400 MHz, DMSO- d_6) δ 148.55 (1C, arom.), 144.09 (1C, arom.), 138.75 (2C, arom.), 122.89 (1C, arom.), 119.82 (1C, arom.), 45.60 ($\underline{\text{C}}\text{H}_3$).

6.3.4.2. N-methyl-N'-(ω -carboxypentyl)-4,4'-bipyridinium saltⁱ (2).

N-methyl-4-(4'-pyridyl)pyridinium iodide (0.298g, 1mmol) and methyl 5-bromovalerate (0.293 g, 1.5 mmol) in DMF (5 mL) were heated to 110 °C for 20 h. After cooling to room temperature the mixture was filtered and washed with small volumes of DMF followed by diethyl ether. Finally the product was hydrolysed in 16% aqueous HCl solution. The solution was evaporated and the orange product was dried. Yield (98%).

^1H NMR (400 MHz, DMSO- d_6) δ 9.48 (d, 2H), 9.36 (d, 2H), 8.86 (dd, 4H), 4.77 (t, 2H), 4.50 (s, 3H), 2.34 (t, 2H), 2.06-2.02 (m, 2H), 1.65-1.55 (m, 2H).

^{13}C NMR (400 MHz, DMSO- d_6) δ 174.02 ($-\underline{\text{C}}\text{OOH}$), 148.55 (1C, arom.), 148.11 (1C, arom.), 146.62 (2C, arom.), 145.80 (2C, arom.), 126.60 (2C, arom.), 126.11 (2C, arom.), 60.45 ($-\underline{\text{C}}\text{H}_2\text{-N}$), 47.99 ($\underline{\text{C}}\text{H}_3\text{-N}$), 32.87 ($-\underline{\text{C}}\text{H}_2\text{-CH}_2\text{-N}$), 30.15 ($-\underline{\text{C}}\text{H}_2\text{-COOH}$), 20.86 ($-\underline{\text{C}}\text{H}_2\text{-CH}_2\text{-COOH}$)

6.3.5. Electrochemical Characterisation of 4,4'-bipyridinium carboxylic acid

Electrochemical characterization of the N-methyl-N'-(ω -carboxypentyl)-4,4'-bipyridinium was done by cyclic voltammetry in the presence of the compound dissolved in 0.1M phosphate buffered saline (PBS) scanning from - 0.3 V to - 0.9 V

(vs.Ag/AgCl) at scan rates 0.1, 0.3, 0.5, 1, 2 V sec⁻¹. The redox behaviour of the derivative was studied at different scan rates.

6.3.6. Conjugation of HRP to 4,4'-bipyridinium carboxylic acid

In order to conjugate HRP to the 4,4'-bipyridinium carboxylic acid derivative, EDC carbodiimide coupling was used for linking primary amine groups of the HRP and carboxylic acid functionality of the viologen derivative. 5 mg mL⁻¹ of the methyl 4,4'-bipyridinium carboxylic acid was dissolved in 0.1M PBS pH 7.0. To this solution, 0.1 M EDC + 5 mM sulfo-NHS was added along with 20mg mL⁻¹ HRP and left to react for 30min. After reaction, the mixture was purified using G-25 sephadex column with 0.1M PBS pH 7.0. Finally HRP functionalised 4,4'-bipyridinium carboxylic acid was separated.

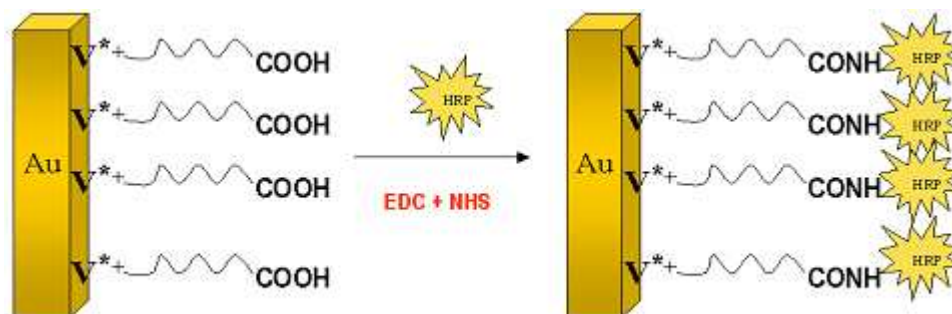
6.3.7. UV-Visible spectroscopy and electrochemical characterization of HRP functionalised 4,4'-bipyridinium carboxylic acid

UV-Visible spectroscopy was used to characterize the HRP conjugated derivative to observe the characteristic peaks of 4,4'-bipyridinium at 260nm as well as the heme peak of HRP at 405nm. Electrochemical characterization of the HRP functionalised 4,4'-bipyridinium derivative was done by cyclic voltammetry in the presence of the compound dissolved in 0.1M phosphate buffered saline (PBS) scanning from -0.3V to -0.9 V (vs.Ag/AgCl) at scan rates 0.1, 0.3, 0.5, 1, 2 V sec⁻¹ to check whether the HRP functionalised derivative retains the characteristic redox properties.

6.3.8. Selectivity of HRP immobilization on Au electrodes

Selectivity of carboxylic acid functionalised viologen derivative immobilised Au electrode surfaces was studied by electroactivation. Cleaned gold electrodes were kept in 2mg mL⁻¹ viologen derivative and applied a potential of -0.85 V (vs. Ag/AgCl) for 10min. In continuation, the electrode was washed and incubated with EDC (2M) + NHS (0.05M) dissolved in 0.01M HEPES buffer pH 7.5 mixture for 20 min. Subsequently the electrode was washed and incubated with different

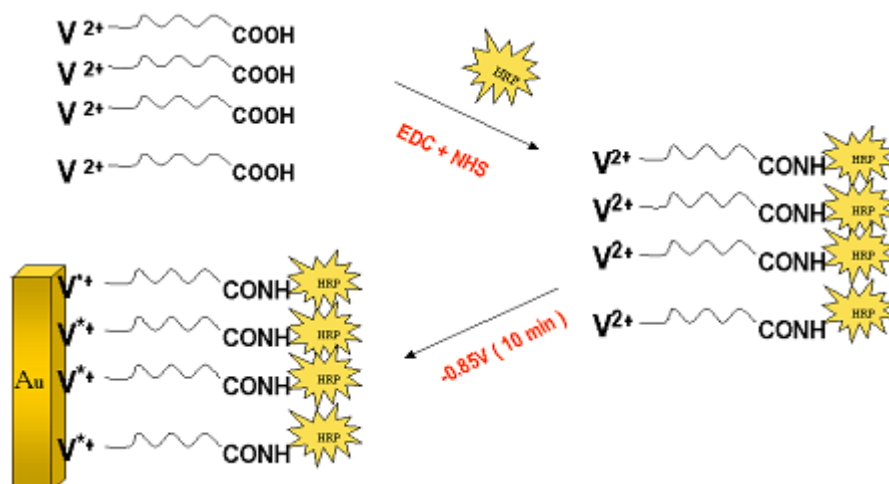
concentrations of HRP (1 mg mL^{-1} , 0.1 mg mL^{-1} , $10\ \mu\text{g mL}^{-1}$) in 0.1 M PBS pH 7.0 for 10min to optimise the best concentration which gives a high specific response.



Scheme 6.2. Double step immobilisation of HRP functionalised viologen derivative.

Colorimetric substrate TMB was added and incubated after washing the electrodes for two min. Finally absorption measurements were taken at 650nm. Control experiments were performed on the Au electrode by keeping the viologen derivative for 10min by applying 0V potential.

In the second approach, $10\ \mu\text{g mL}^{-1}$ of the HRP functionalised viologen derivative electrodeposited by applying a potential of -0.85 V (vs.Ag/AgCl) for 10 min.



Scheme 6.3. Single step immobilisation of HRP on the gold electrode.

Control experiments were performed on the Au electrode by keeping the HRP-viologen derivative for 10min by applying 0V potential. .

6.3.9. Electrochemical Quartz Crystal Microbalance (EQCM) studies

EQCM studies were used to monitor the real time changes on the electrode surface at different potentials. 4mL of the 0.1M PBS pH 7.0 containing $10\mu\text{g mL}^{-1}$ of HRP functionalised viologen derivative was placed on the EQCM crystal and a potential of -0.85 V (vs. Ag/ AgCl) was applied for 10 min. Frequency change was monitored during this deposition period. The control experiment was performed with the electrode poised at 0V (vs. Ag / AgCl) in order to see the frequency change due to the non-specific adsorption. Next in order to monitor the changes on the electrode surface within the same solution, first a potential of -0.85 V (vs.Ag/AgCl) was applied for 10 min. Next within the same solution, a potential of -0.4 V (vs. Ag/AgCl) was applied for 10 min. This potential step experiments were repeated for total two times. Subsequently to the same cell, a positive potential of $+0.1\text{ V}$ (vs. Ag / AgCl) was applied for 10min to check whether the positive potential can produce different frequency changes when compared to the above mentioned potentials.

6.4. Results and Discussion

6.4.1. Characterisation of electroactivable immobilisation vehicles

Figure 6.1 shows cyclic voltammetry in the presence of N-methyl-N'-(ω -carboxypentyl)-4,4'-bipyridinium . Two consecutive and reversible one-electron redox waves are observed. The first redox wave is characteristic of the reduction of dicationic viologen (V^{2+}) to radical cation (V^{+*}). The second redox wave is characteristic of reduction of radical cation (V^{+*}) to neutral species (V^0). The reduction of bipyridinium cations to a monocation free radical (V^{+*}) produced a violet coloured film on the electrode surface indicating the adhesion of the radical

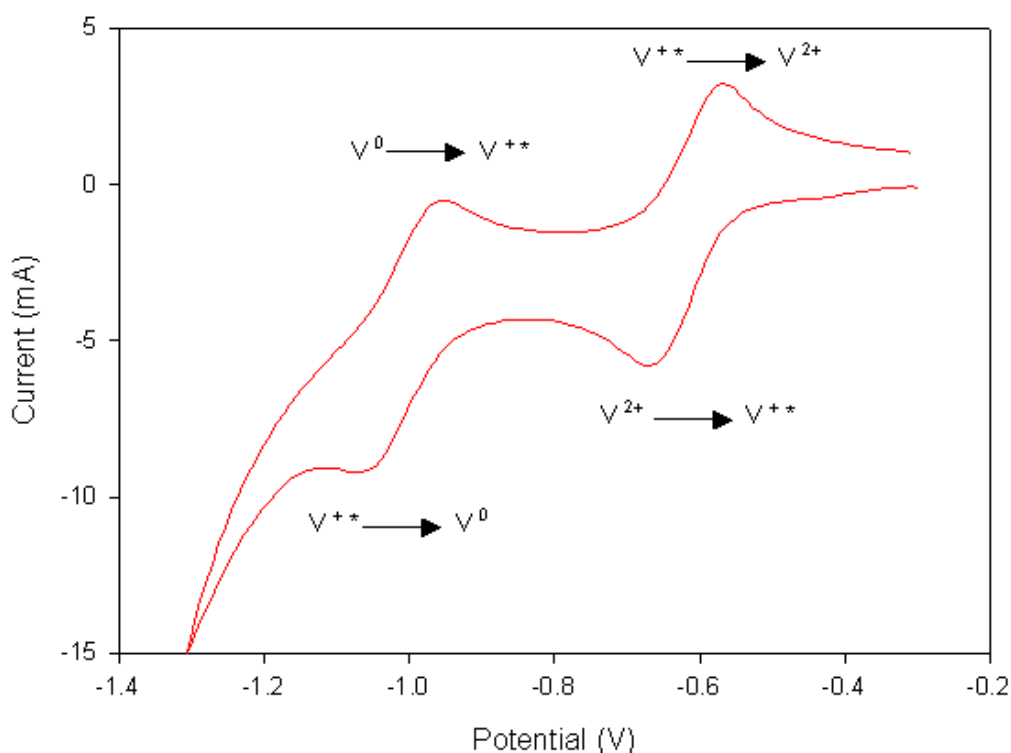


Figure 6.1. Cyclic voltammogram of the carboxylic acid functionalised viologen derivative recorded . Background electrolyte solution composed of phosphate buffer 0.1M, pH 7.0, under argon. Scan rate 1 V s^{-1} , working electrode area (16 mm^2), Reference electrode : Ag / AgCl.

cation viologen derivative. Since the free radicals are attached to the electrode surface, subsequent experiments were performed in a window more positive than -0.85 V for electrodeposition to make sure that the free radical cation is not reduced completely to neutral species. Figure 6.2 shows the cyclic voltammograms in the presence of N-methyl-N'-(ω -carboxypentyl)-4,4'-bipyridinium at different scan rates. It displayed electrochemical behaviour typical to the 4,4'-bipyridinium units with a quasi-reversible one electron reduction (V^{2+} to V^{1+*}) behaviour showing well formed redox peaks with a redox potential of -0.68 V and peak to peak separation of 100 mV . This clearly demonstrates the electrochemical functionality of the N-methyl-N'-(ω -carboxypentyl)-4,4'-bipyridinium derivative, and is also indicative that the functionalisation was successful since its CV shows a better peak definition and a substantial peak shift compared to the starting material.

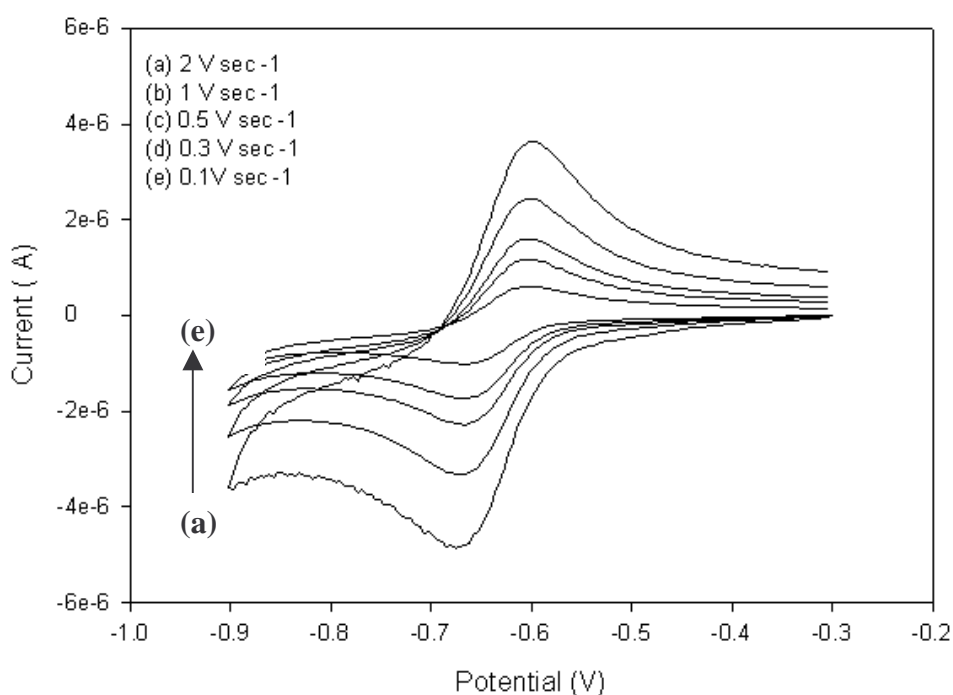


Figure 6.2. Cyclic voltammogram of the gold electrode in the presence of carboxylic acid functionalised viologen derivative dissolved in phosphate buffer 0.1M, pH 7.0, under argon recorded at different scan rates. Working electrode area : 4 mm^2

Figure 6.3 shows the UV-Visible spectroscopic characterization of HRP functionalised N-methyl-N'-(ω -carboxypentyl)-4,4'-bipyridinium. The characteristic heme peak at 405nm and the N-methyl-N'-(ω -carboxypentyl)-4,4'-bipyridinium characteristic peak at 260nm can be simultaneously observed in the purified product. These peaks correspond to the peak of viologen at 260nm and HRP peak at 405nm.

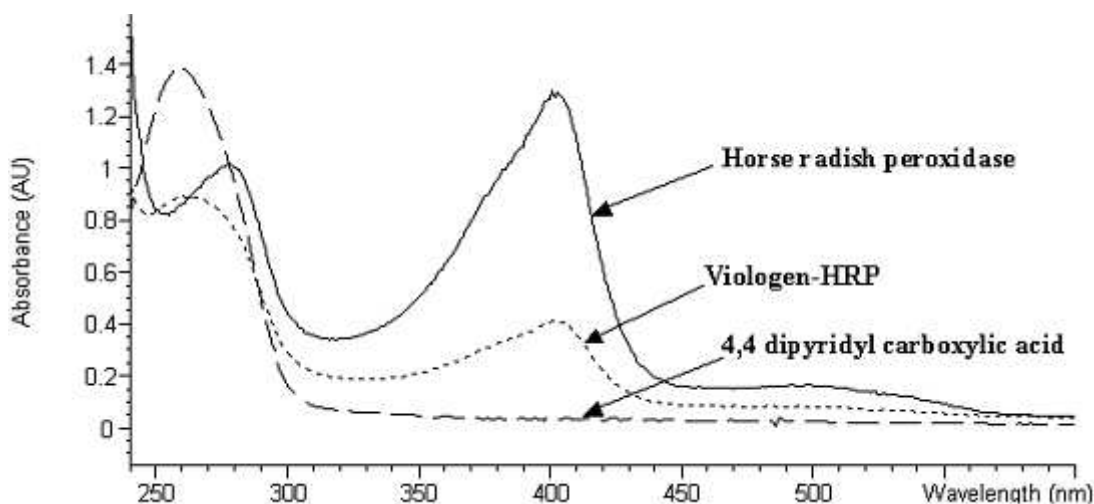


Figure 6.3. UV-Vis spectroscopy of HRP-conjugated 4,4'-bipyridinium derivative. Electrolyte: 0.1M PBS pH 7.0, concentrations : 4,4 dipyridyl carboxylic acid ($20\mu\text{g mL}^{-1}$), HRP ($500\mu\text{g mL}^{-1}$).

Figure 6.4 shows the electrochemical behaviour of the HRP functionalised the N-methyl-N'-(ω -carboxypentyl)-4,4'-bipyridinium. The cyclic voltammogram of the HRP-functionalised viologen derivative displayed electrochemical behaviour typical of the 4,4'-bipyridinium product, with well formed redox peaks indicative of the quasi-reversible one electron reduction ($[\text{viologen}]^{2+/+}$) $E^0 = -0.68\text{V}$, peak-to-peak separation $\Delta E = 105\text{mV}$ (at a potential scan rate of 1 V s^{-1}), similar to the values obtained for the starting material. Therefore the 4,4'-bipyridinium after conjugation to HRP retains its electrochemical functionality.

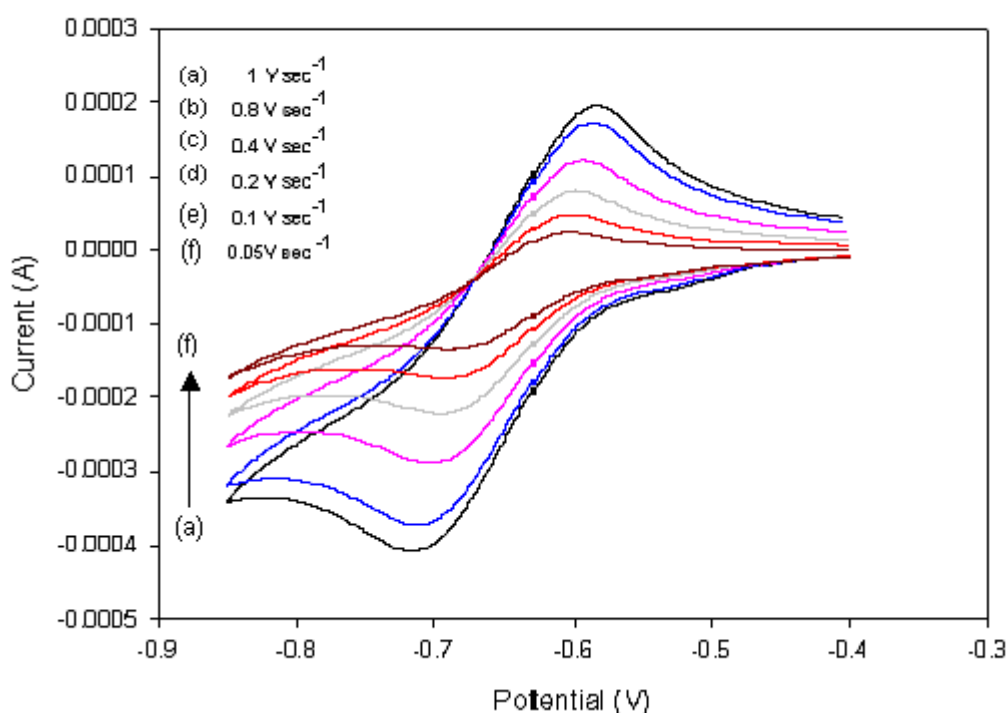


Figure 6.4. Cyclic voltammogram of the gold electrode in the presence of HRP conjugated viologen derivative dissolved in phosphate buffer 0.1M, pH 7.0, under argon recorded at different scan rates. Working electrode area 4 mm²

6.4.2. Directed electrode modification of 4,4'-bipyridinium carboxylic acid and HRP patterning

The first method for the directed HRP patterning was to selectively modify electrodes with the 4,4'-bipyridyl carboxylic acid and molecule reacting it afterwards with HRP through EDC activation. Since the NHS ester of carboxylic acid can be deactivated by water different concentrations of HRP were used to obtain the most efficient surface modification with minimum non-specific adsorption. The amount of HRP immobilised was first evaluated by a colourimetric assay.

Figure 6.5 shows the colourimetric response obtained after immobilization of different concentrations of HRP on the N-methyl-N'-(ω -carboxypentyl)-4,4'-bipyridinium modified gold electrode after application of at - 0.85 V and 0 V (control) . The absorbance values obtained from the electrodes showed that

with decreasing concentration of HRP from 1 mg mL^{-1} to $10\ \mu\text{g mL}^{-1}$, there is a decrease in the non-specific absorbance with higher specific response. Thus HRP concentration of $10\ \mu\text{g mL}^{-1}$ was chosen for further studies.

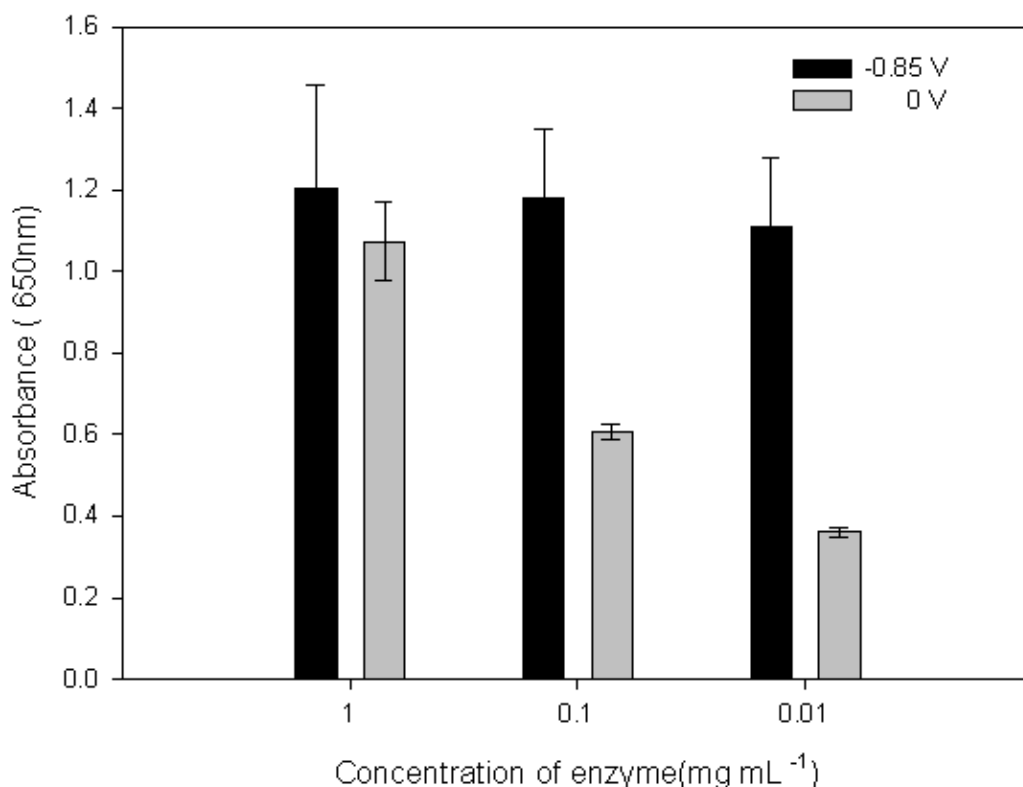


Figure 6.5. Absorbance at 650nm from the colourimetric reaction of the electrode immobilised with different concentrations of HRP on 4,4'-bipyridine modified Au electrode at -0.85 V for 10min. and 0V as control for 10min. Working electrode : gold electrodes (4 mm^2).

The same colourimetric method was used to assess the potential for bipyridine carboxylate immobilisation. Figure 6.6 shows the colourimetric response obtained after HRP immobilization on the N-methyl-N'-(ω -carboxypentyl)-4,4'-bipyridinium electromodified gold electrode after application of different potentials. The response is higher from the electrodes modified at a potential of -0.85 V (vs. Ag/AgCl). Electrodes modified with the viologen derivative at 0V (vs. Ag / AgCl) showed a non-specific response of 35%. This shows some selective capability for the immobilisation of HRP. From the Figure 6.5, it can be observed that by applying a potential of -0.4 V (vs. Ag/AgCl), there is a decrease in the absorbance and is about 60% of that obtained from the electrodes modified at -0.85 V . At -0.85 V

(vs. Ag/AgCl), the V^{2+} is reduced to V^{1+*} . The formation of free radical helps in the attachment of the viologen derivative to the Au electrode and this explains the higher efficiency of immobilisation at that potential. At - 0.4 V (vs. Ag/AgCl), the free radical containing viologen derivative V^{1+*} is oxidized back to V^{2+} which makes the viologen derivative desorb from the gold electrode surface.

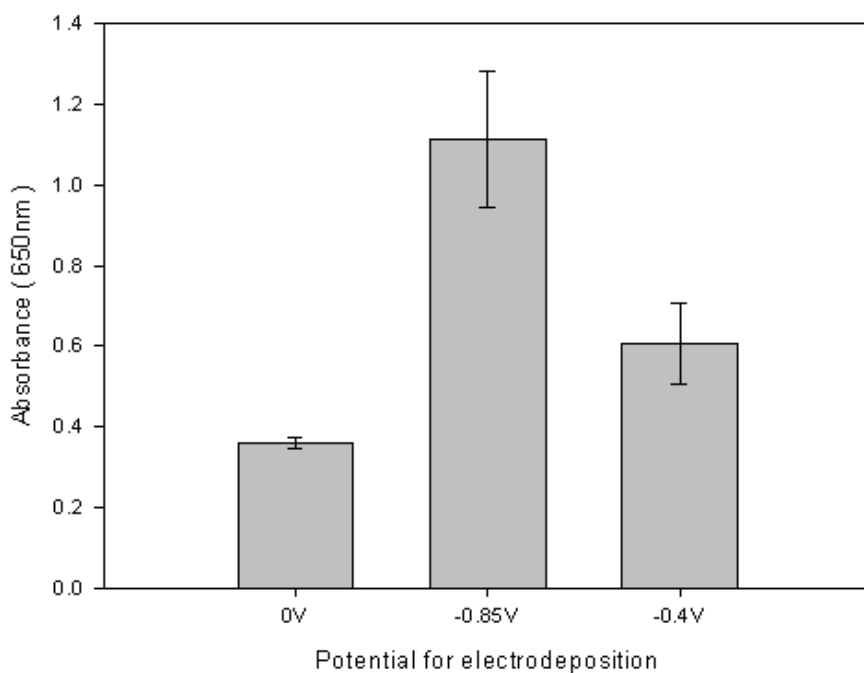


Figure 6.6. Colourimetric response of the electrode immobilised with HRP on 4,4'-bipyridine modified Au electrode at - 0.85 V and later applying - 0.4 V for 10min. Colorimetric detection was performed after 10min incubation with TMB and the colored product is detected at 650nm. Electrodeposition conditions : - 0.85V for 10min (experiment) and 0V for 10min (blank).

The second method of selective HRP patterning avoided this two step process for the directed immobilisation of HRP by using directly the HRP-viologen derivative in solution. Figure 6.7 compares the two methods by the colourimetric assay of electrodes modified with HRP-4,4'-bipyridinium as shown in the scheme 6.3 using a single step. As shown in the figure the absorbance from the electrode modified by applying potential of -0.85V showed a higher value when compared to the control. Electrodes deposited by applying 0V produced an absorbance value of around 15% of the value produced by the experiment. These results demonstrate the advantage of one step deposition when compared to the two step procedure.

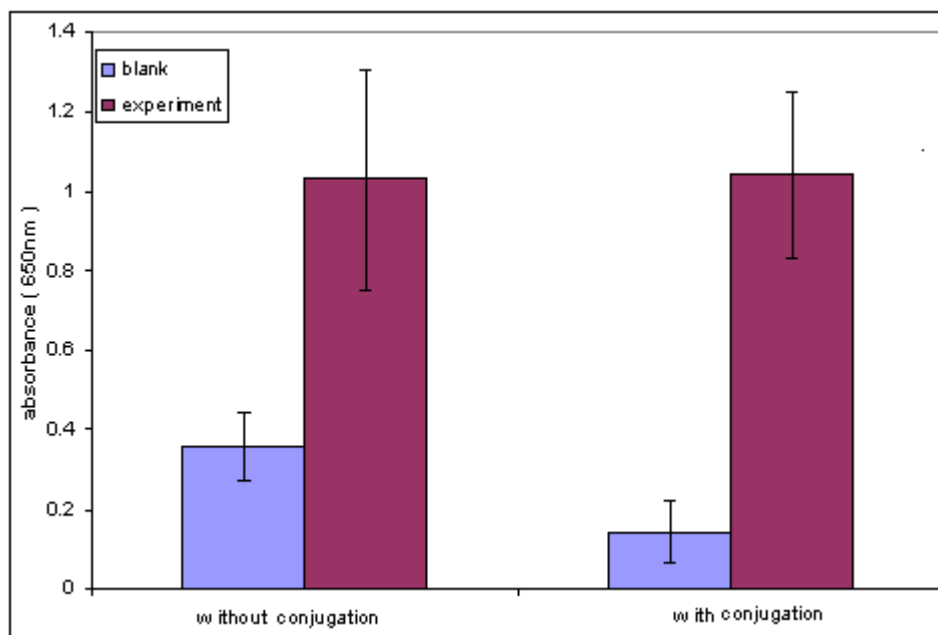


Figure 6.7. Colourimetric assay response of the electrodes modified by HRP with and without conjugating to the carboxylic acid functionalised 4,4'-bipyridinium prior to the immobilization on the electrode. Colorimetric detection was performed after 10min incubation with TMB and the colored product is detected at 650nm. Electrodeposition conditions : - 0.85V for 10min (experiment) and 0V for 10min (blank).

6.4.3. EQCM measurement of the HRP-4,4'-bipyridinium deposition

The selectivity of the modification technique can be verified by independent methods. One of them is EQCM that combines the possibility of electrochemical manipulation with microgravimetric detection. Figure 6.8 shows the frequency changes on the quartz crystal during the deposition of HRP functionalised viologen derivative at - 0.85 V, - 0.4 V and 0V for 10 min. It can be noticed that at - 0.85 V, the frequency change is higher and the amount of mass deposited calculated from the frequency variation was 10.42 η g. At - 0.4 V the amount of mass deposited is 4.85 η g. At 0V, the amount of mass deposited was calculated to be 1.96 η g. From these observations it can be demonstrated although the conversion of free radical to dication by applying a potential of - 0.4 V can desorb the viologen biomolecules, the non-specificity of adsorption to the Au surface cannot be minimised completely.

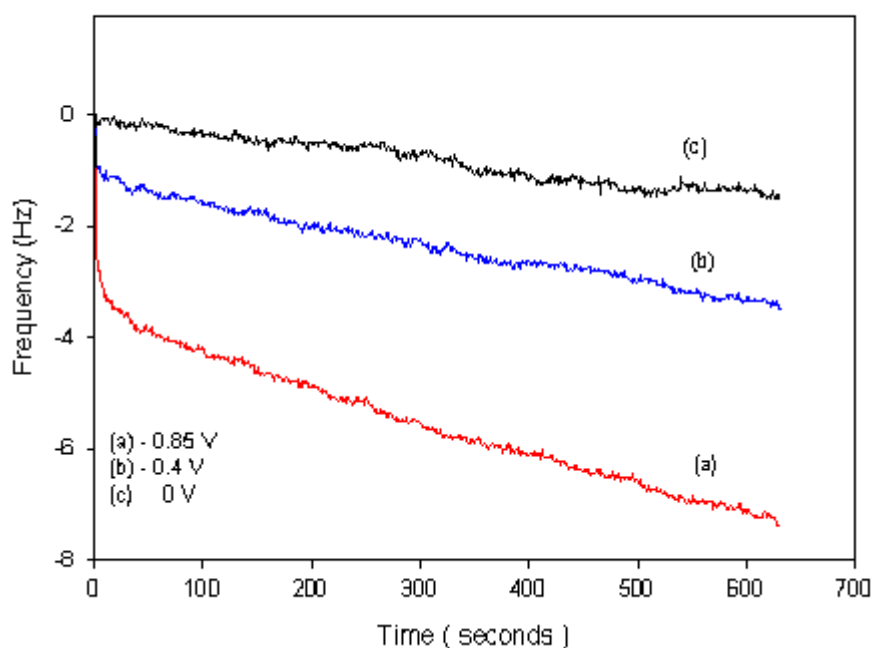


Figure 6.8. Frequency variation during the immobilization of HRP functionalised viologen derivative dissolved in 0.1M PBS pH 7.0 by applying different potentials. Conditions:(a) Electrodeposition potentials -0.85 V (vs Ag/AgCl) for 10 min (b) -0.4 V (Ag/AgCl) for 10 min and (c) $+0.1$ V for 10min. Surface area of the quartz crystal 0.196 cm². Electrolyte : 0.1M PBS pH 7.0 under argon.

Figure 6.9 shows the frequency changes on the electrode surface due to electrochemical deposition and dissolution of the bipyridinium radical cation by switching the potentials from -0.85 V to -0.4 V and vice versa on the same substrate. It can be observed that upon reduction of bipyridinium-HRP conjugate at -0.85 V the frequency change is around -10 Hz . Upon application of the -0.4 V potential that oxidizes the bipyridinium radical cation attached to the quartz crystal, there is an increase in the frequency. This might be due to the desorption caused by the conversion of a free radical which is formed at -0.85 V to a positive charge.

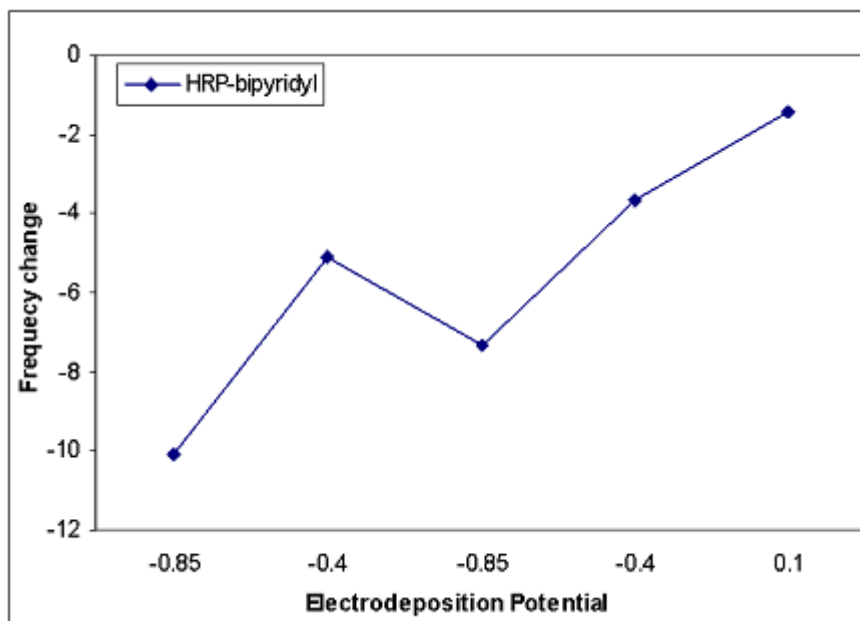


Figure 6.9. Variation in the frequency of the quartz crystal modified with HRP functionalised 4,4-bipyridyl molecules with switching the potential. Conditions : Electrodeposition potential s – 0.85 V (vs Ag/AgCl) for 10 min followed by - 0.4 V (Ag/AgCl) for 10 min and finally + 0.1V for 10min. Surface area of the quartz crystal 0.196 cm²). Electrolyte : 0.1M PBS pH 7.0 under argon.

For the second round of reduction potential, there is decrease in the frequency again although the value did not reach the original value. Finally when a potential of + 0.1 V was applied to the electrodes, the increase in the frequency is more than the frequency observed with – 0.4 V. This clearly proves that although there is a desorption at –0.4 V, at more positive potentials the non-specific adsorption can be minimised.

6.5. Conclusions

This study has demonstrated a novel way of electrochemically controlled patterning of biomolecules using 4,4-bipyridinium as an immobilization vehicle. HRP was immobilised on the electrode surface by taking advantage of the free radical metallic bonding. Selectivity was demonstrated by the colourimetric detection of the immobilised HRP on the electrode surface. Still there is significant non-specific adsorption with this technique which could be optimised by improving the electrochemical desorption from electrodes that is not desired to be modified. An

interesting observation is that reversible switching of the dication to a free radical is possible permitting real time modification of surface functionalities.

6.6. Abbreviations

EQCM – Electrochemical quartz crystal microbalance

HRP – Horse radish peroxidase

PBS-Phosphate buffered saline

TMB - 3,3',5,5'-Tetramethyl benzidine liquid substrate

6.7. References

1. Albers, J., Grunwald, T., Nebling, E., Piechotta, G., Hintsche, R., *Anal. Bioanal. Chem.*, 2003, 377, 521-527.
2. Brian, G.H., Lin, L., David, R.W., *Biosens. Bioelectron.*, 1997, 12, 521-529.
3. Brecht, A., *Anal. Bioanal. Chem.*, 2005, 381, 1025-1026.
4. Ding, Y., Zhou, L.P., Halsall, H.B., Heineman, W.R., *J. Pharm Biomed Anal.*, 1999, 19, 153-161.
5. Jia, N.Q., Zhang, Z.R., Zhu, J.Z., *Chin. J. Chem.*, 2004, 22, 908-912.
6. Maestre, E., Katakis, I., Narvaez, A., Dominguez, E., *Biosens. Bioelectron.*, 2005, 21, 774-781.
7. Wittstock, G., *Anal. Bioanal. Chem.*, 2002, 372, 16-17.
8. Zayats, M., Pogorelova, S.P., Kharitonov, A.B., Lioubashevski, O., Katz, E., Willner, I., *Chemistry*, 2003, 9, 6108-6114.
9. Katz, E., Itzhack, N., Willner, I., *Langmuir*, 1993, 1392-1396.
10. Willner, I., Katz, E., Riklin, A., Kashier, R., *J. Am. Chem. Soc.*, 1992, 114, 10965-10966.
11. Corgier, B.P., Marquette, C.A., Blum, L.J., *J. Am. Chem. Soc.*, 2005, 27, 18328-18332.
12. Corgier, B.P., Marquette, C.A., Blum, L.J., *Biosens. Bioelectron.*, 2006: p. in press.
13. Raymo, F. M., Alvarado, R.J., *Chem. Rec.*, 2004, 4, 204-218.
14. Sung, H. K., Jin, S.B., Seok, H.H., Tae, S.G., Myung, K.D., *Dyes. Pigm.*, 1997, 33, 167-172.

Chapter 7. Selective Microscale Protein Patterning through Photolithography

7.1. Abstract

A novel method for patterning proteins on microscale dimensions has been developed. This produced an interference and cross-talk free dual electrode amperometric biosensor integrated with a polyelectrolyte multilayer spacing for monitoring glucose and sarcosine simultaneously. Using a novel biocompatible resist process, two different redox enzymes glucose oxidase (GOX) and sarcosine oxidase (SOX) were patterned in successive lithographic steps to cover the appropriate areas of the corresponding electrodes in an interdigitated (IDE) array. In the first experiment, one side of the biocompatible photoresist over the first set of electrodes of the interdigitated array (IDE 1) was opened and deposited first enzyme along with redox polymer. Before depositing the second enzyme on the other set of electrodes (IDE 2), self deposited polyelectrolyte multilayer spacing done by layer-by-layer approach using cationic polyvinyl pyridine (PVP) and anionic polystyrene sulfonate (PSS) on the IDE 1 was used as a blocking step in order to reduce the non-specific adsorption from the second enzyme. Finally using a flat exposure, the biocompatible resist is removed from the IDE 2 in order to deposit the second enzyme second enzyme along with redox polymer. When tested electrochemically, glucose and sarcosine sensors exhibited analyte sensitivities of $1.5\mu\text{A cm}^{-2}$, $1\mu\text{A cm}^{-2}$ respectively. Moreover there was no cross-talk interference between each other and the redox enzymes were fabricated successfully.

7.2. Introduction

There is an increasing demand of multianalyte sensing devices having potential applications in biomedical, biotechnological, industrial and environmental fields. Multianalyte protein assays are important new analytical methods as they allow one to simplify the working procedure, to increase the test throughput, reduce the cost per test, and improve test efficiency as compared to parallel single-analyte assays [1-13]. Various assay formats have been designed to realize multianalyte assays. The most successful assay is a sensing system utilizing a microfabricated substrate

with dimensions in the micrometer to millimetre range in which many biofunctional molecules are integrated in their individual addresses using a technique photolithography. Photolithography is the process by which microelectrodes can be fabricated on the wafers with complex and arbitrary shapes and sizes with excellent reproducibility. Modern photolithography techniques permit the production of transducer arrays with very small dimensions, often in the same range as those of microelectrodes [14-20]. One of the most prominent examples of this type of electrode is an interdigitated microelectrode array.

Interdigitated array (IDA) electrodes have been used as highly sensitive detectors because of their inherent features, such as larger currents, high sensitivity, and rapid current rise to a steady state [21-32]. IDA consists of many parallel bands of electrodes, each separated by a small insulating gap.

The area of biomolecule patterning for multianalyte biosensing devices where different biomolecules need to be patterned on the same substrate appears especially challenging. A good spatial control during enzyme deposition step is strictly necessary; each enzyme has to be precisely deposited on the surface of the relevant sensor (e.g. an amperometric transducer), avoiding mixing that can compromise the biosensor specificity. Apart from this, the enzyme needs to retain the activity. Wired enzyme electrode has been widely used as the method for producing stable glucose currents by using cationic osmium redox polymers electrostatically linked to the anionic glucose oxidase [33]. However, both the study and application of proteins have been challenged by the inherent difficulties associated with positioning these tiny objects.

With the development of microelectrodes and enzyme deposition techniques possessing improved special control, the possibility of producing miniaturized multianalyte sensors combining closely spaced enzyme microelectrodes is becoming feasible. Until now such devices typically contained sensing elements separated by distances greater than the diffusion layer of soluble reactants, the individual microelectrodes behaved independently of each other and displayed only a little reciprocal influence. However as the separation distance decreases, this is no longer the case since diffusion layers overlap. This phenomenon can lead to a number of effects such as shielding, recycling and cross talk.

Cross talk occurs when there are freely diffusing species detectable at adjacent (enzyme) microelectrodes [34-40]. The simplest case of cross talk originates when

the enzymatic reactions produce a common detectable species, e.g., H_2O_2 in the case of oxidase enzymes. The H_2O_2 generated at one microsensor can diffuse to a neighbouring array element causing a signal eventhough the corresponding element is not present. In order to avoid this problem, different approaches have been developed like using of interference- suppressing enzyme layers (eg., containing catalase to decompose H_2O_2), electrolysis of the interference-causing compound at band electrodes placed between the individual sensors [41].

A primary enabling technology is the ability to precisely immobilize biomolecules in well-defined patterns while retaining their native functionality. Towards achieving this goal, in this chapter, first a methodology for the enzyme immobilization has been optimized on the macroelectrode by depositing the cationic osmium redox polymer and enzyme. Next, during the deposition of two enzymes on the IDE array, there is a problem of the non-specific adsorption while patterning the second enzyme on the IDE 2. It should be noted that during the immobilization of enzymes + redox polymer, the deposition mixture is placed over the both sets of electrodes in the IDE and the second enzyme can be non-specifically adsorbed over the first enzyme already immobilized on the IDE 1 and can produce an unwanted response. In order to avoid this, the response due to the non-specific adsorption should be blocked. To simulate the above problem that we can find during the enzymes immobilization on the patterned photolithographic array, different reagents were tried for blocking the non-specific response from the second enzyme. The main objective of these blocking experiments is first to avoid the non-specific adsorption of the second enzyme or second even if there is non-specific adsorption the response produced by this should be minimized. For this, we measured in a single electrode the response from the electrode after immobilization of the first layer of one enzyme and later the response from the same electrode after immobilization of the second layer of the another enzyme over the first enzyme, and we tested different blockings between two layers of enzymes to avoid the unwanted response from the second enzyme. The best solution for this problem was found by optimizing the blocking step. Later the optimized bioimmobilization procedure combined with the blocking step was applied on the IDE array. Next the biosensor response of the modified IDE was tested by injecting the substrates to check the cross-talk. Finally this chapter described an interference and cross-talk free dual

electrode amperometric biosensor integrated with a blocking agent for simultaneous monitoring of glucose and sarcosine. The integrated device showed high sensitivity, wide linear ranges of response, total absence of cross-talk effects, and complete suppression of electroactive interferences. If the current densities remain high along with the absence of cross talk, the possibility of creating a sensor that is competitive with current market technology will be obtained.

7.3. Experimental

7.3.1. Materials

The enzymes glucose oxidase (EC 1.1.3.4, GOX, 200U mg⁻¹) from *Aspergillus Niger* and sarcosine oxidase (EC 1.5.3.1, SOX, 20U mg⁻¹) from recombinant *E.Coli* were purchased from Biozyme laboratories, UK. Glucose, sarcosine, polyvinyl pyridine (PVP), thioctic acid, N-succinimidyl ester dithio dithiopropionic acid (DTSP), 3-mercapto-1-propane-sulfonic acid (MPSA) was purchased from Sigma Chemical Co (St.Louis, MO, USA). The poly (styrene sulfonic acid) (PSS) (MW 70000, Polyscience) was used as received. The polycationic redox polymer, poly [(vinyl pyridine) Os (bpy)₂ Cl] was synthesized according to a procedure described previously [42]. The positively charged polyelectrolyte was prepared by partial quarternization of PVP with bromoethylamine and has the same structure as redox polymer except that no Os redox centres are present [43]. Aqueous solutions were prepared with Milli Q water (Milli Q system, Millipore, Japan). All other chemicals are of analytical grade. The glucose stock solution was at least allowed to mutarotate for at least 24h before use.

7.3.2. Instrumentation

Electrochemical measurements were monitored using an Autolab bipotentiostat PGSTAT10 electrochemical analysis system and GPE management software from Eco Chemie. MG 1410 mask aligner from SET France, Laurel WS-400B spin coater for coating the photoresist, 4-inch silicon wafer was used for photolithography. An Ag / AgCl as reference electrode and platinum as a counter electrode were used for all the experiments.

For optimisation studies, gold electrodes were prepared by cutting a 2mm diameter gold wire and soldering electrically with copper wire. Later this soldered gold wire was kept in hollow cylindrical tubes. Resin of Cold mounting resin mercaptes MA2 (100 w/w) and Hardener Mercapex MA2 (12 w/w) was prepared in order to fix the gold wires inside the tubes. Gold wires were inserted into the hollow cylindrical tubes. Resin prepared was poured into the tubes and left to stand overnight at room temperature in order to firmly fix the gold wires. Later the gold wire sealed tubes were polished on sand paper to remove any resin attached to it and later polished with 3grades of alumina and left for sonication for 20 min. All the gold electrodes were cleaned electrochemically by scanning from -0.2 V to 1.8 V (vs. Ag /AgCl) at a scan rate of 0.2 V s^{-1} in a 0.5 M H_2SO_4 solution until a constant cleaned gold voltammogram was obtained. Next the electrode was rinsed with distilled water and dried with nitrogen.

7.3.3. Methodology

7.3.3.1. Optimisation of protein patterning method on macroelectrodes

In order to optimize an immobilization strategy that produces a stable and better analytical response, different methods were tried to immobilize GOX and SOX on the gold electrodes. Along with the enzyme, osmium redox polymer as shown in the figure 7.1 was used for the immobilization to have better electron transfer capability and to have better analytical response. For all the experiments, $40\mu\text{l}$ containing 2000 U ml^{-1} GOX & 10 mg ml^{-1} redox polymer was used for the immobilization.

In the first method, GOX was modified by introducing sulfhydryl groups on the native structure using N-Succinimidyl-S-acetylthioacetate (SATA) [44]. Later the electrodes were incubated with a mixture containing GOX + redox polymer on the gold electrode. After incubation, electrodes were washed with distilled water and dried with argon. The objective of this immobilization strategy is to attach the proteins by taking advantage of strong gold-thiol chemistry.

In the second method, self-assembled monolayer was formed by modifying the gold electrode with 0.1 M thiocetic acid dissolved in 1:1 ethanol and water for 1h. Later

the modified electrodes were incubated with 0.6 mg N- (3-Dimethylaminopropyl)-N'-ethylcarbodiimide (EDC) for 30min to activate the carboxyl groups of the thioctic acid followed by the immobilization of a mixture containing GOX and redox polymer for 2h. After modification, electrodes were washed with distilled water and dried with argon. The objective of this experiment is form an amide bond between the activated carboxyl groups and primary amines of the protein as well as the enzyme [45-48].

In the third method, self-assembled monolayer was formed on the gold electrode by incubating with 6 μ l of 0.25 M 3-mercapto-1-propane-sulfonic acid (MPSA) for 1h. Later the electrode was washed with distilled water and incubated with a mixture containing GOX and redox polymer for 2h. After modification with enzyme-redox mixture, electrode was washed with distilled water and dried under argon. The objective of this experiment is to immobilize the cationic osmium polymer on the negatively charged MPSA surface of the electrode [49-51].

In the fourth method, enzyme-polymer mixture was immobilized by covalent linkage on Di N-succinimidyl ester dithio-dithiopropionic acid (DTSP) SAMs formed on gold electrode. In this case, self-assembled monolayer was formed by incubating the gold electrode with 20mM of DTSP for 1h. After washing, the electrodes were incubated with a mixture containing GOX and redox polymer for 2h. After modifying with enzyme-redox mixture, electrode was washed with distilled water and dried under argon [52-54].

Finally, GOX was immobilized by direct adsorption of a mixture containing GOX and redox polymer for 2h on the gold electrode. After modifying with enzyme-redox mixture, electrode was washed with distilled water and dried under argon.

All the above experiments were also repeated by substituting the GOX with the second enzyme SOX with the same activity. After each modification, amperometric response of the enzyme-modified electrodes was measured by injecting their respective substrates.

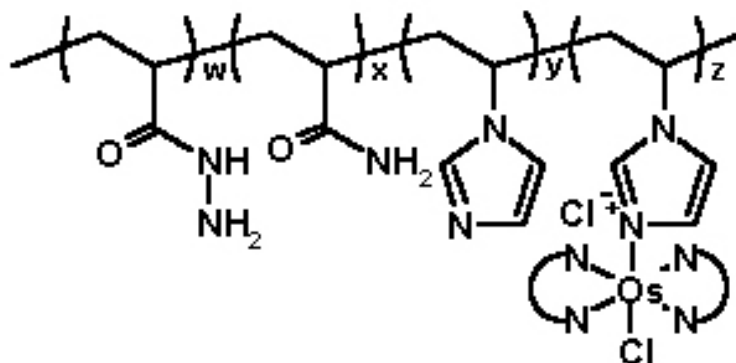


Figure 7.1. Structure of osmium redox polymer used in the patterning of enzymes.

7.3.3.2. Optimisation of non-specific response

For all the following experiments, 40 μ l containing 2000 U ml⁻¹ enzyme & 10 mg ml⁻¹ redox polymer was used for the immobilization.

In the first experiment, Au electrode was incubated with GOX + redox polymer mixture for 2h. After incubation, electrode was washed with distilled water, and later the modified Au electrode was incubated with SOX + redox polymer for 2h. Amperometric measurements were taken by injecting glucose and sarcosine separately.

In the second experiment, electrode was incubated with GOX + redox polymer for 2h. After washing with distilled water, the modified Au electrode was incubated with 100Mm Triton X-100 as a blocking agent for 1h [55,56]. Next after washing the electrode, the modified electrode was incubated with SOX + redox polymer for 2h. Amperometric measurements were taken by injecting glucose and sarcosine separately.

In the third experiment, electrode was incubated with GOX + redox polymer for 2h. After washing with distilled water, the modified Au electrode was incubated with 1% BSA as a blocking agent for 1h [57,58]. Next after washing the electrode, the

modified electrode was incubated with SOX + redox polymer for 2h. Amperometric measurements were taken by injecting glucose and sarcosine separately.

In the fourth experiment, electrode was incubated with GOX + redox polymer for 2h. After washing with distilled water, the modified Au electrode was incubated with 10% BSA as a blocking agent for 1h. Next after washing the electrode, the modified electrode was incubated with SOX + redox polymer for 2h. Amperometric measurements were taken by injecting glucose and sarcosine separately.

In the fifth experiment, electrode was incubated with GOX + redox polymer for 2h. After washing with distilled water, the modified Au electrode was incubated with 100mM milk as a blocking agent for 1h [59-61]. Next after washing the electrode, the modified electrode was incubated with SOX + redox polymer for 2h. Amperometric measurements were taken by injecting glucose and sarcosine separately.

Finally, electrode was incubated with GOX + redox polymer for 2h. After washing with distilled water, the modified Au electrode was incubated with self-deposited multilayers by sequential deposition of different polyelectrolytes [43]. Initially the modified electrodes were adsorbed with 50 mg L⁻¹ of anionic polyelectrolyte polystyrene sulfonic acid (PSS) for 30min followed by the adsorption of 20 mg L⁻¹ of cationic quaterised polyelectrolyte PVP for 1hour. Alternative steps of PSS and PVP adsorption was repeated in order to make sure that there is formation of at least three layers of each. All the polyelectrolytes were dissolved in pure water. The concentrations of the polyelectrolyte solutions were relatively high in order to make sure that a maximum number of charged groups remain exposed to the solution, and thus, the surface charge was effectively reversed. The idea behind the polyelectrolyte adsorption step is to make sure that the second enzyme is far enough so that it do not produce any non-specific response. Next after washing the electrode, the modified electrode was incubated with SOX + redox polymer for 2h. Amperometric measurements were taken by injecting glucose and sarcosine separately.

All the experiments were repeated by reversing the enzyme positions with SOX + redox polymer first followed by GOX + redox polymer.

7.3.3.3. Patterning of proteins on interdigitated array

The gold IDE array consisted of two sets of 50 microelectrodes with 20 μ m gapwidth and bandwidth (Figure 7.2).

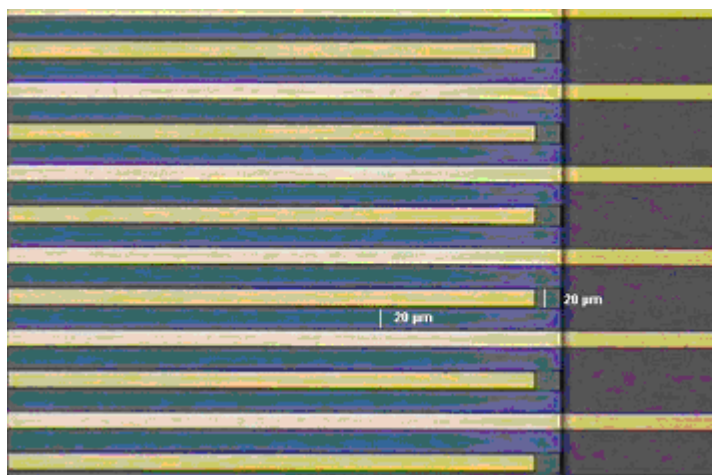


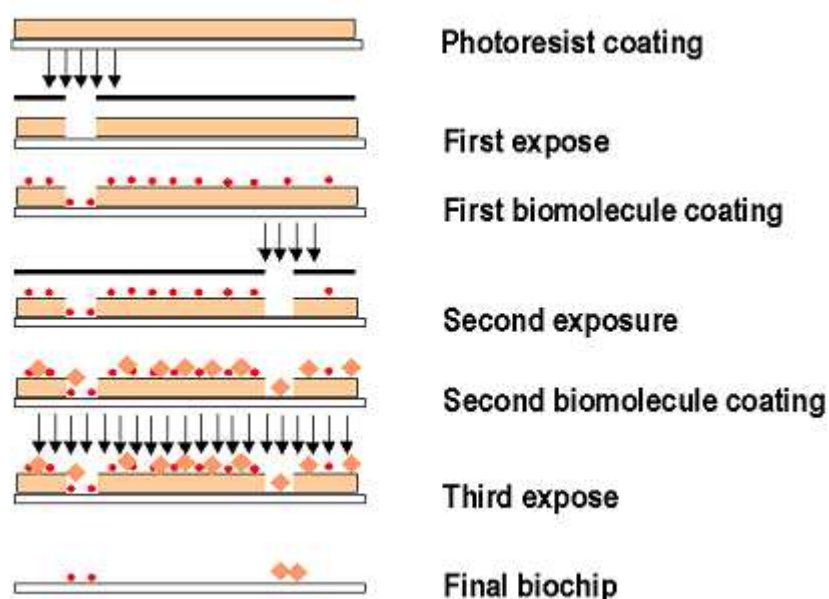
Figure 7.2. Gold interdigitated electrodes array image. Each set of electrodes consists 50 microelectrodes with a width of 20 μ m and a distance between electrodes of 20 μ m.

Gold electrode arrays were left uncut as a wafer. A layer of a special biocompatible photoresist as developed by NSCR Demokritos was spin coated for 30 seconds at 7000 RPM on top of the wafer.

The general lithographic scheme used for the patterning of proteins with a resist based process was shown in scheme 7.1[62,63]. The steps followed during the process are

- The coating of the radiation sensitive biocompatible photoresist on the substrate
- The exposure of selected areas of the coating to the radiation of 320nm wavelength
- Dissolution of the exposed areas with a selected suitable developer 1mM of tetramethylammonium hydroxide (TMAH).

- The deposition of the first protein on the substrate but also probably on the surface of the remaining radiation sensitive photoresist.
- The exposure of the remaining resist areas to radiation of 320nm wavelength
- The removal of these exposed areas with a suitable developer 1mM of tetramethylammonium hydroxide (TMAH).
- The deposition of the second protein on the substrate of the remaining radiation sensitive photoresist
- The exposure of the remaining resist areas to radiation of 320nm wavelength and the removal of these exposed areas with a suitable developer 1mM of tetramethylammonium hydroxide (TMAH).



Scheme 7.1. Lithographic scheme for the patterning of proteins

Figure 7.3 shows the bienzyme patterning of interdigitated array using photolithography with two enzymes (GOX, SOX) immobilized on different sets of electrodes. As shown in the scheme 7.1, IDE 1 was exposed to UV light at 320nm and later developed with 1mM of tetramethylammonium hydroxide (TMAH). This left the IDE 1 unprotected while the IDE 2 remained protected by the polymer. Initially the IDE 1 was incubated with 40 μL of 2000 U mL^{-1} of GOX and 10 mg mL^{-1} of RP mixture dissolved in milliQ water for 2h. At the end of this period, the electrode was carefully rinsed with distilled water and dried with argon. Before removing the photoresist from the IDE 2, we used self deposited polyelectrolyte

multilayer as a blocking step in order to reduce the non-specific adsorption from the SOX over GOX as described above. After blocking with the polyelectrolytes, IDE array was washed with distilled water and dried with argon. Later the IDE 2 was exposed to UV-light at 320nm and developed with 1mM of TMAH. The IDE 2 were incubated with 40 μL of 2000 U mL^{-1} of SOX and 10 mg mL^{-1} of RP mixture dissolved in milliQ water for 2h.. This produced gold electrode arrays fabricated with two different redox enzymes. This experiment was also repeated with SOX on the IDE 1 and GOX on the IDE 2.

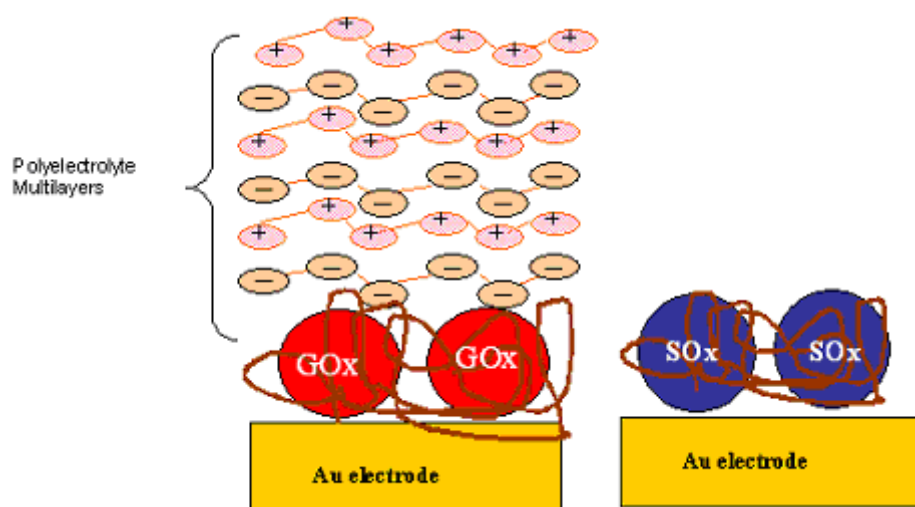


Figure 7. 3. Scheme of patterning of enzymes (GOX, SOX) on two sets of electrodes within the IDA electrodes

7.3.3.4. Electrochemical characterization of the IDE array

Cyclic voltammogram of IDE array was performed at a scan rate of 30mV sec^{-1} from 0 to 600mV (vs Ag / AgCl) in the presence of 0.1 M PBS pH 7 to characterize the RP adsorption during different steps of the protein fabrication on IDE array. This gives the information regarding the electrochemical behaviour of the immobilization of redox polymer + enzymes on the IDE array. All experiments were performed at room temperature (25°C).

7.3.3.5. Amperometric measurements of modified IDE array

Amperometric measurements of the modified electrodes were performed at + 500 mV potential vs Ag/AgCl in unstirred solutions. All the measurements were performed at 25 °C. Several additions of the substrate were made. In order to check the substrate specific response, initially the response to glucose was checked from the IDE in order to make sure that the enzyme GOX was functional even after the self-deposition of polyelectrolyte multilayers on the IDE 1. Later, the response to sarcosine was checked from the IDE after the immobilization of SOX + redox polymer on the IDE 2. Finally simultaneous response to sarcosine and glucose was monitored from the IDE in the same cell by injecting sarcosine initially followed by glucose for cross-talk assessment.

7.4. Results and Discussion

7.4.1. Optimisation of enzyme immobilization strategy

Sensor response for the glucose and sarcosine from the electrodes immobilized with GOX and SOX using different immobilization strategies was shown in the table 7.1. Among all the strategies, as shown in the table 7.1, in the case of direct adsorption of the enzymes (GOX, SOX), there was a stable response from both enzymes with higher currents. In the case of first strategy, with the thiolation of GOX & SOX there was a stable response for glucose from the GOX modified electrodes where as the response for sarcosine from the SOX modified electrode was completely absent. This might be due to the loss of SOX enzyme activity while modification.

Immobilization strategy	Response to GOX ($\mu\text{A cm}^{-2}$)	Response to SOX ($\mu\text{A cm}^{-2}$)
Thiolation of the enzymes	6.3	No Response
Thioctic acid SAMs	3.8	No response
3-mercapto-1-propane-sulfonic acid (MPSA) SAMs	4.7	1.59
Di N-succinimidyl ester dithio dithiopropionic acid (DTSP) SAMs	14.77	0.95
Direct adsorption of the redox enzymes	20.71	5.7

Table 7.1. Summary of biosensor response using different strategies for the immobilization of the GOX + redox polymer & SOX + redox polymer on the gold electrode

In the case of Au electrodes self assembled with thioctic acid, there was complete absence of sarcosine response from the SOX modified electrodes where as the response for the glucose was very less from the GOX modified electrodes. This might be due to the lack of perfect covalent linkage between the redox polymer-enzyme mixture and the thioctic acid surface.

In the third strategy, where the Au electrodes were self-assembled with MPSA, there is a stable but less response from both the enzyme modified electrodes to their respective substrates. In this case, since the both the oxidases are negative at the pH 7, there might be an electrostatic repulsion between the enzymes and the negative charged MPSA surface.

With DTSP SAMs on the Au electrodes, the response was higher in the case of GOX and the response is low and unstable with SOX. Table 7.1 shows the electrocatalytic response of the GOX and SOX modified electrodes in the presence of glucose and sarcosine. Finally direct adsorption strategy was chosen for the patterning of enzymes. GOX with RP was immobilized on the IDE 1 and SOX with the same polymer was patterned on the IDE 2 by biocompatible photolithography.

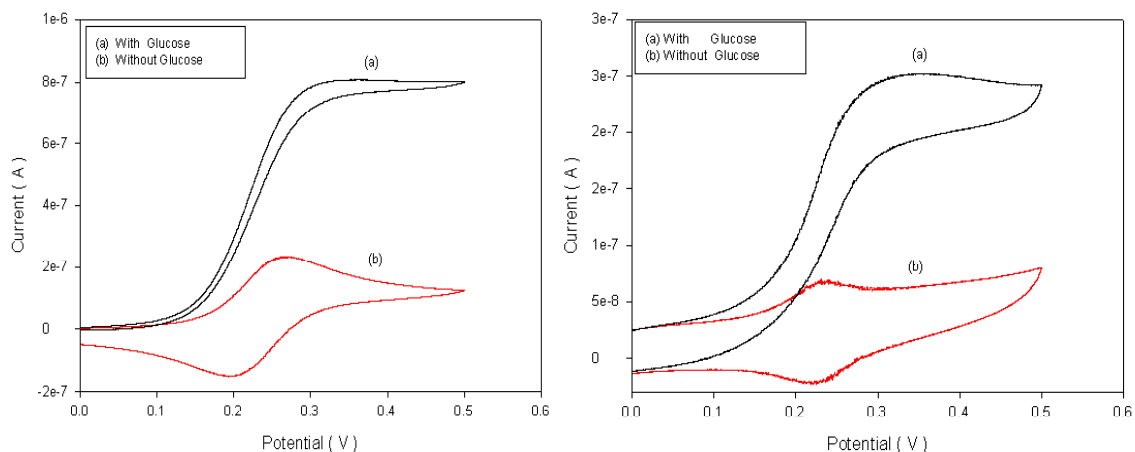


Figure 7.4. (a) Dependence of the steady-state-D-glucose catalytic oxidation current density on electrode potential for a GOX / redox polymer immobilised on electrode through direct adsorption in 100 mM PBS buffer of pH 7.0, 50mM glucose at 2 mV s⁻¹; (b) Dependence of the steady-state-D-sarcosine catalytic oxidation current density on electrode potential for a SOX / redox polymer immobilised on electrode through direct adsorption in 100 mM PBS buffer of pH 7.0, 50 mM sarcosine at 2 mV s⁻¹.

7.4.2. Optimisation of non-specific response

From the figure 7.5, the current response obtained from the electrodes modified with GOX + redox polymer followed by a spacer and finally with SOX + redox polymer showed that polyelectrolyte spacing gave the best and specific response when compared to other blocking agents as spacers. In the first case, where the electrodes were immobilized with GOX followed by second layer of SOX without spacer, the response for the glucose was stable but there is a 25% unwanted response for sarcosine.

In the case of triton X-100 as a spacer, there is a huge unwanted response from the electrode. This might be due to the detergent nature of triton X-100 that might remove some of the GOX attached to the electrode during washing.

In the case of 1% BSA there is huge decrease in the current response from the glucose electrode and also there is presence of unwanted sarcosine response from the same electrode. With increase in the concentration of BSA from 1% to 10%, there is complete absence of current response from the glucose electrode. So BSA as a spacer was avoided due to its complete blocking of not only the unwanted response for sarcosine but also the response for glucose.

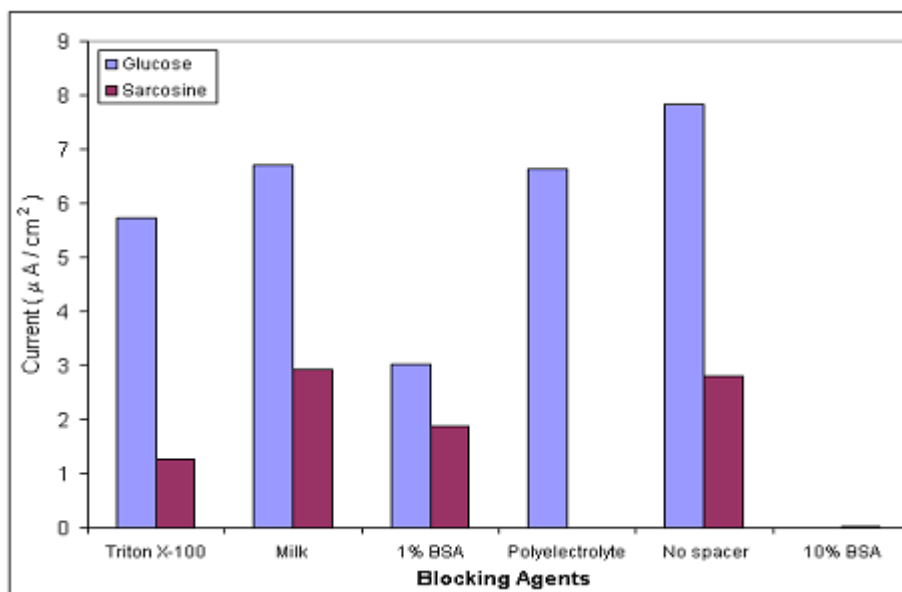


Figure 7.5. Current response to the glucose and sarcosine from the electrodes immobilised in the order GOX + redox polymer / spacer / SOX + redox polymer using different types of blocking agents as spacers

With milk as an agent for preventing unwanted response, there is a stable response from the GOX modified electrode for glucose and 40% of unwanted response from sarcosine.

But in the case of polyelectrolyte layers as spacer, the response from the GOX modified electrodes was stable and specific with complete absence of unwanted response from the sarcosine.

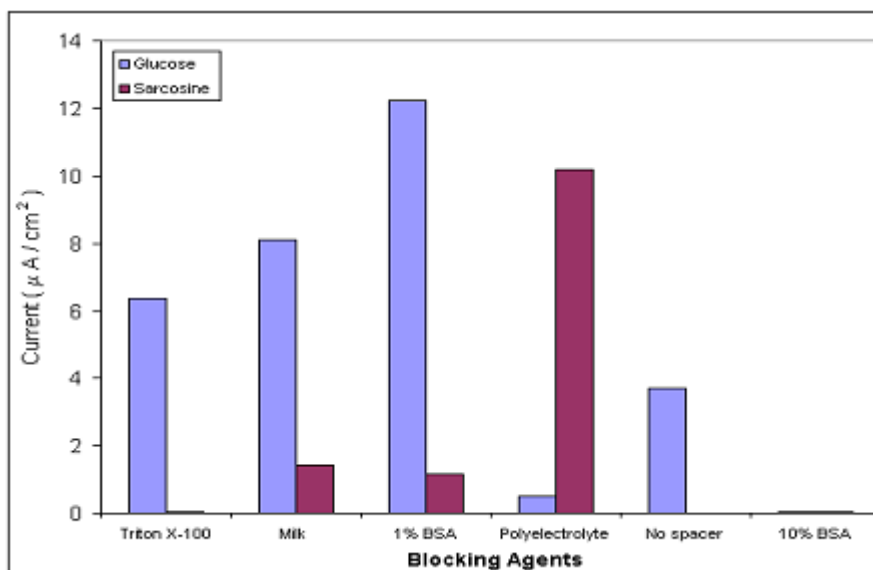


Figure 7.6. Current response to the glucose and sarcosine from the electrodes immobilized in the order SOX + redox polymer / spacer / GOX + redox polymer using different types of blocking agents as spacers

The current response from the electrodes modified with SOX + redox polymer followed by a spacer and finally with GOX + redox polymer was shown in the figure 7.6. Among all the spacers used as blocking agents, polyelectrolyte spacing gave the best, specific and selective response to sarcosine. This clearly shows that self-assembled polyelectrolyte multilayering as a blocking step in between the wanted enzyme and the unwanted enzyme can be used in experiments for avoiding for avoiding the cross talk.

7.4.3. Electrochemical characterisation of the modified IDE array after GOX + RP immobilization on the IDE 1

Figure 7.7 shows the cyclic voltammogram obtained from the IDE array after the immobilization of GOX + RP on the IDE1. The CV of the IDE 1 showed a quasi-reversible behaviour with a well-defined anodic and cathodic redox peaks characteristic of the surface confined redox polymer at + 275mV & + 190mV with a redox potential of + 227.5mV. There was a noisy response from the IDE 2. This demonstrated successfull deposition of the redox polymer on the IDE 1.

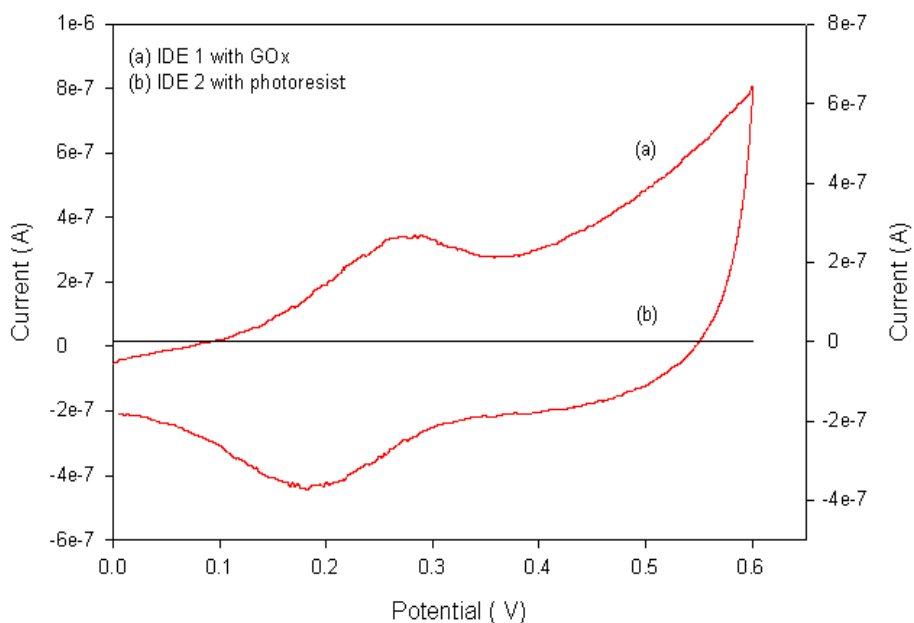


Figure 7.7. Voltammetric response of the IDE array after GOX + redox polymer mixture immobilized on the IDE 1 (redox CV), before the exposure of photoresist polymer on the IDE 2 (noisy).

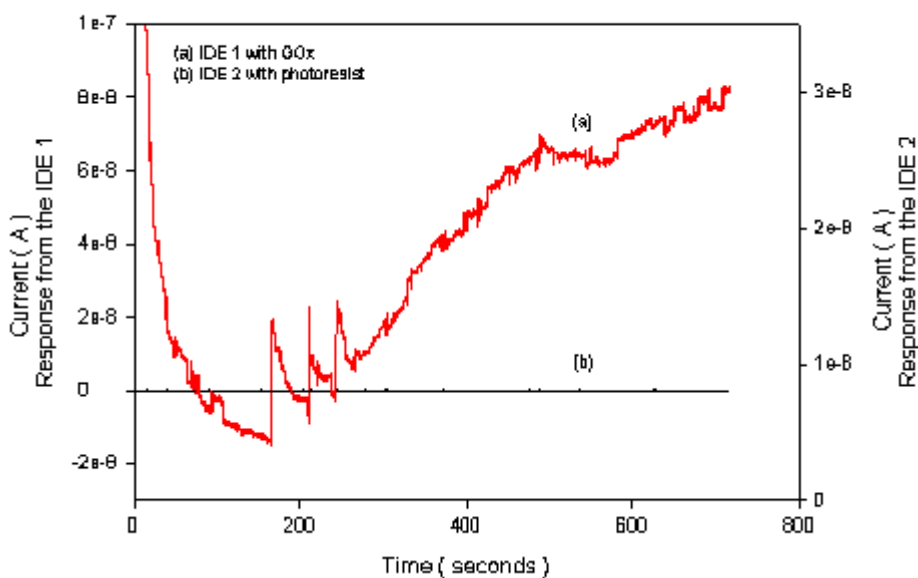


Figure 7.8. Chronoamperometric response of IDE array after the deposition of GOX + redox polymer followed by polyelectrolyte multilayer on the IDE1 and before exposure of the photoresist on the IDE 2 at + 500mV (vs. Ag / Ag Cl) in 0.1M phosphate buffer pH 7 during successive injection of glucose.

From the figure 7.8, there was a stable oxidation current response with glucose injection from the IDE 1 and the response from the IDE 2 was completely absent. This clearly demonstrated that GOX immobilized along with redox polymer was stable and responded to the glucose very well whereas the response from the IDE 2 was completely absent which indicates that biocompatible polymer was functional and is able to protect the IDE 2 from the unwanted response due to the non-specific adsorption of the GOX + redox polymer mixture.

7.4.4. Electrochemical characterization of the IDE after polyelectrolyte self-assembling on the IDE 1

After the immobilization of GOX + redox polymer on the IDE 1 followed by the self-assembling of PE multilayer and before exposing the photoresist on the IDE 2,

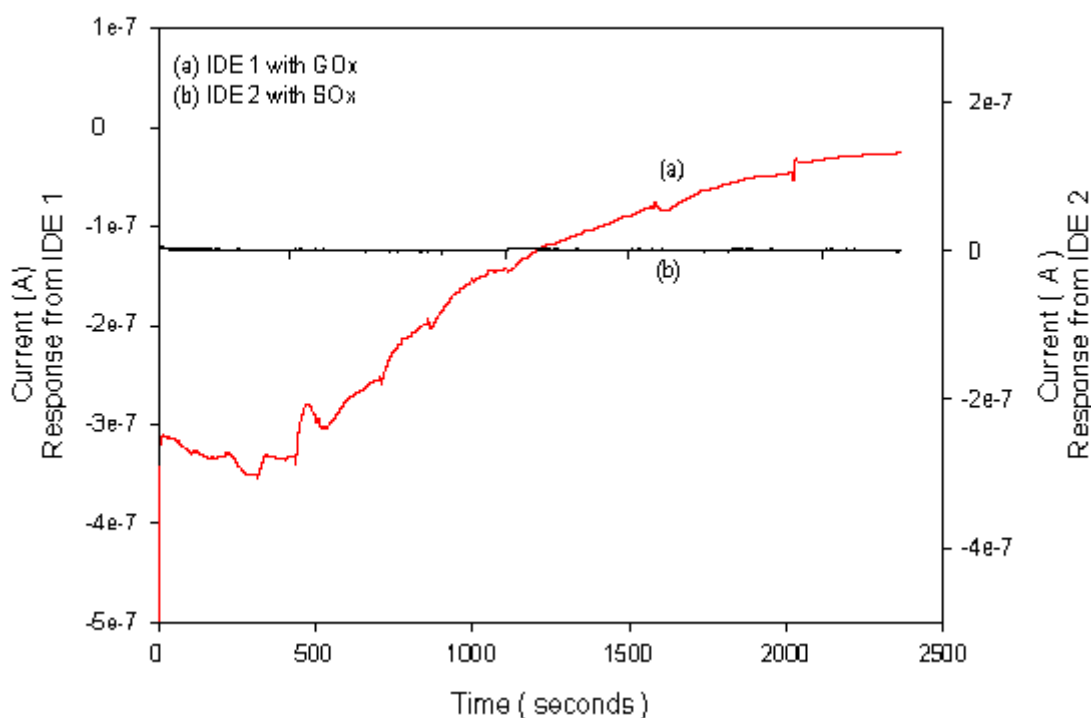


Figure 7.9. Chronoamperometric response of IDE array after the deposition of SOX + redox polymer followed UV-Vis exposure on the IDE 2 at +500mV (vs Ag / Ag Cl) in 0.1M phosphate buffer pH 7 during successive injection of glucose.

amperometric response was taken from the IDE to check the functionality of the GOX immobilized on the IDE 1. From the figure 7.9, with each injection of glucose

into the cell, there is an increasing oxidation current response from the IDE 1 where GOX was immobilized and the response from the IDE 2 was completely absent. Anodic currents were plotted against the glucose concentration and from the figure 7.10; there was a current response maximum of around $3.23 \mu\text{A cm}^{-2}$ with 60mM glucose from the IDE 1 where GOX was immobilized and the response from the IDE 2 was completely absent. This clearly demonstrates that the GOX has retained its activity even after blocking with the polyelectrolyte multilayer on the IDE 1.

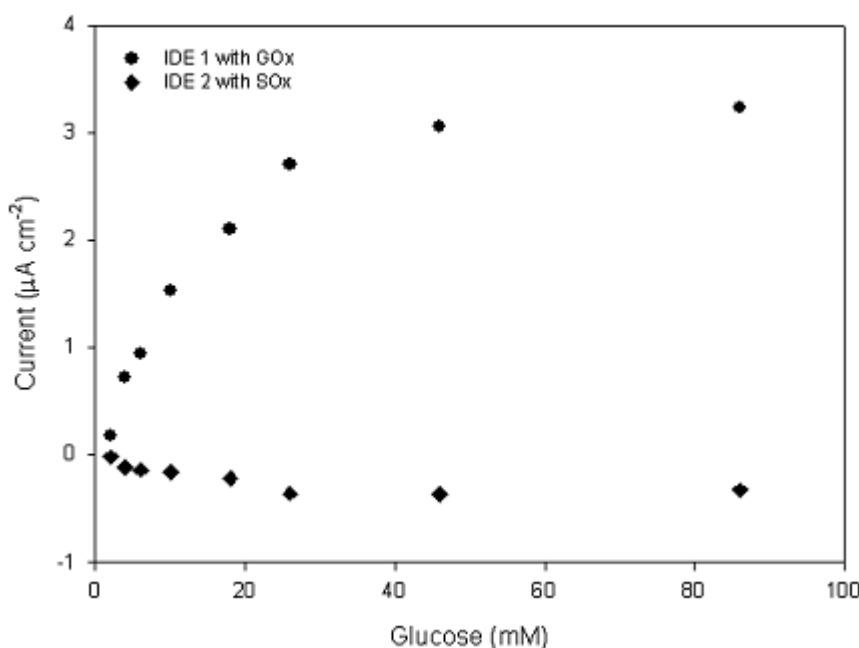
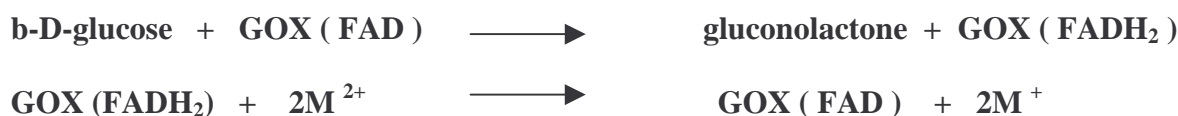


Figure 7.10. Steady state response for glucose from the IDE after polyelectrolyte multilayer formation over the IDE 1 after GOX + redox polymer mixture immobilization

The oxidase catalyzed reaction scheme with Os sites on the redox polymer serving as electron relays between enzyme and electrode surface may be expressed as follows



Where GOX (FAD) and GOX (FADH₂) represent the oxidized and reduced forms, respectively of the enzyme's cofactor – flavin adenine dinucleotide (FAD) and M



represents an Os redox site of the polymer in its oxidized (2^+) and reduced (1^+) forms. Electrons are thus transferred from the enzyme to the redox polymer, shuttled between the redox sites in a self-exchange reaction until being transferred to an electrode surface that is poised positive of the polymer.

As a result, a current that is proportional to substrate concentration is created. As seen from the reaction mechanism presented above, sensors incorporating redox polymers such as those used here should be less dependent on oxygen than those based on hydrogen peroxide oxidation. This fact is important for in vivo application of a sensor, since oxygen concentration in tissue can vary.

7.4.5. Electrochemical Characterization of the IDE array after SOX + redox polymer immobilization on the IDE 2

Figure 7.11 shows the cyclic voltammogram of the IDE array after immobilization of the SOX + redox polymer on the IDE 2.

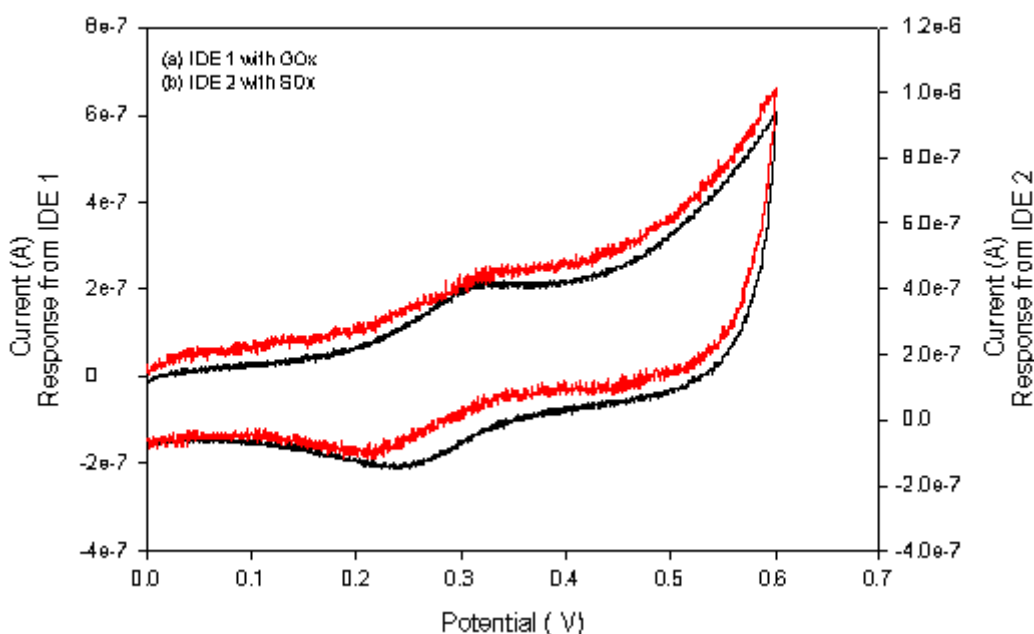


Figure 7.11. Cyclic voltammetry of the IDE array after the exposure of the photoresist polymer and SOX + RP mixture immobilization on the IDE 2 (black)

CV showed a quasi-reversible behaviour characteristic of the redox polymer from the both the sets of electrodes. This clearly says that IDE array is successfully immobilized with the two enzymes. The redox peaks are not well defined in the case of IDE 1, which might be due to the polyelectrolyte multilayering over the IDE 1. From these above experiments it was clear that both the enzymes were immobilized successfully on the IDE array

S arcosine sensor was characterized independently by taking the amperometric measurements from both the sets of electrodes of the IDE array with the addition of the sarcosine after the immobilization of SOX along with redox polymer on the IDE 2. From the figure 7.12, there was an oxidation current response maximum of around $2\mu\text{A cm}^{-2}$ with 20 mM sarcosine from the IDE 2 with complete absence of response from the IDE 1.

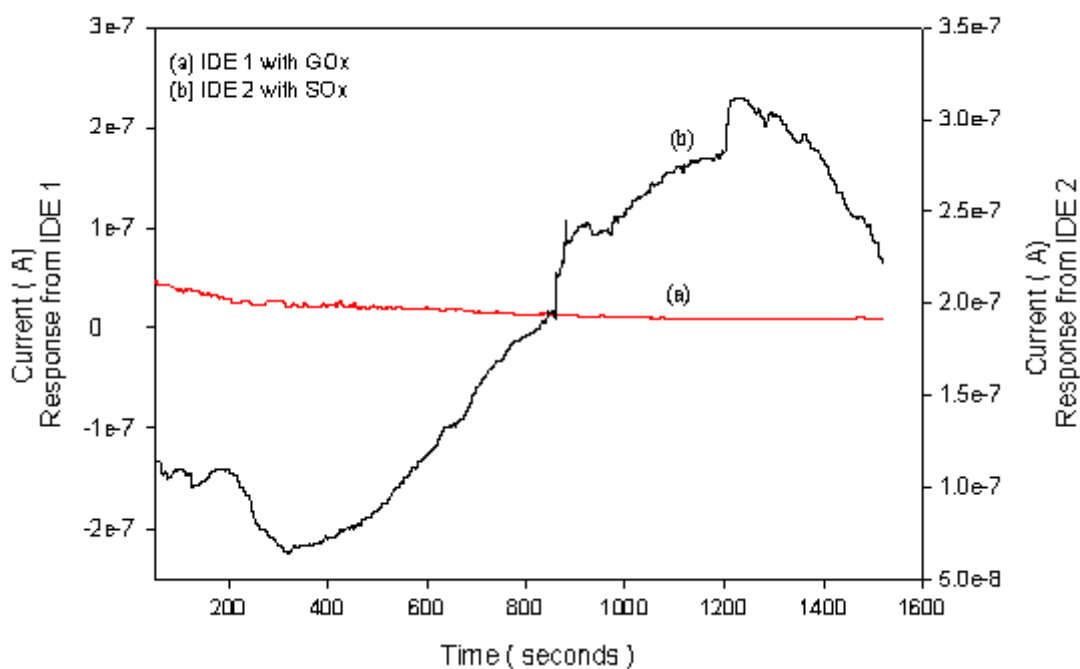


Figure 7.12. Chronoamperometric response of IDE array after the deposition of SOX + redox polymer followed UV-Vis exposure on the IDE 2 at + 500mV (vs. Ag / Ag Cl) in 0.1M phosphate buffer pH 7 during successive injection of sarcosine.

7.4.6. Protein patterning with SOX + redox polymer on the IDE 1 and GOX + redox polymer on the IDE 2

In this experiment, IDE array was deposited with SOX + redox polymer on the IDE 1 and GOX + redox polymer on the IDE 2. Amperometric measurements were taken from both the IDE array to check the substrate specific current response.

7.4.6.1. Amperometric response from the IDE array after immobilization of the enzymes

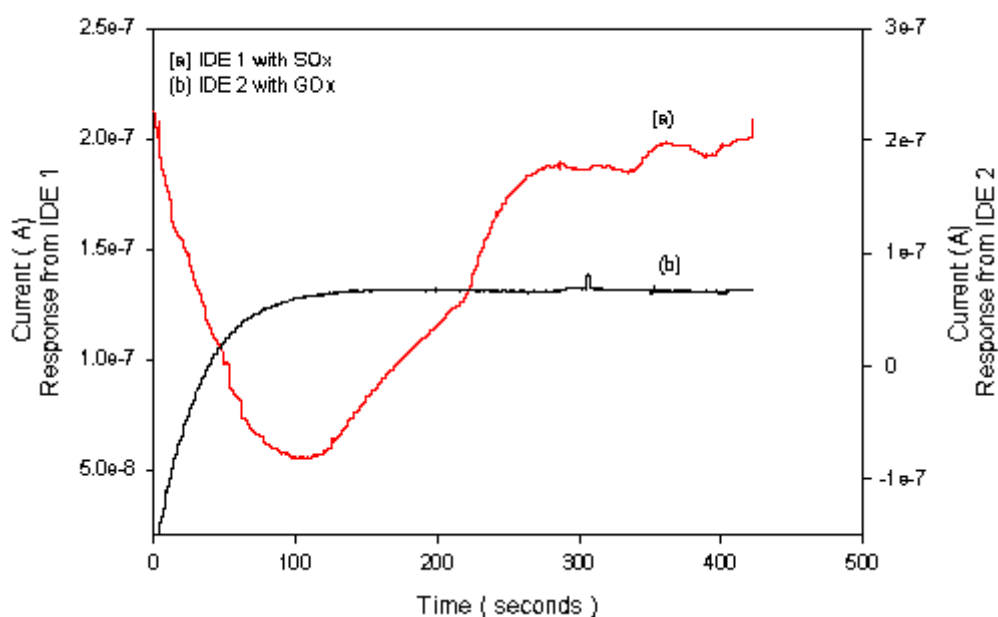


Figure 7.13. Chronoamperometric response of IDE array modified with SOX + redox polymer on the IDE 1 and GOX + redox polymer on the IDE 2 at +500mV (vs Ag / Ag Cl) in 0.1M phosphate buffer pH 7 during successive injection of sarcosine.

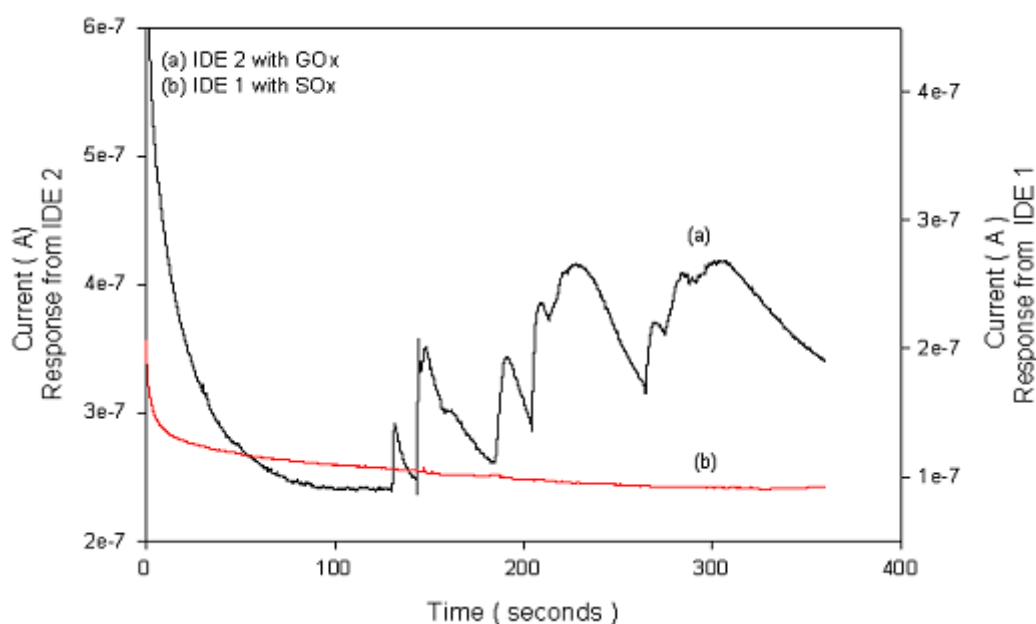


Figure 7.14. Chronoamperometric response of IDE array modified with SOX + redox polymer on the IDE 1 and GOX + redox polymer on the IDE 2 at +500mV (vs Ag / Ag Cl) in 0.1M phosphate buffer pH 7 during successive injection of glucose.

From the figure 7.13, there was increase in the oxidation current response with the addition of sarcosine from the IDE 1 where SOX was immobilised initially followed by blocking with polyelectrolyte multilayers and the response was almost absent from the IDE 2 where GOX was immobilized. This shows that the SOX is functional after polyelectrolyte layering & after GOX immobilization on the IDE 2. From the figure 7.14, when amperometric response measurements were taken for glucose from the IDE array, there was an increasing oxidation current response from the IDE 2 where GOX was immobilized and the response from the IDE 1 was absent.

This clearly shows that the unwanted response for glucose from the SOX immobilized IDE 1 after the protein patterning on the IDE array was completely absent. Finally layer-by-layer approach of polyelectrolytes has proven to be an excellent cross talk and interference reducing method.

7.4.7. Assessment of cross talk

Finally amperometric response was measured from the IDE array immobilized with GOX + redox polymer on IDE 1 and SOX + redox polymer on IDE 2 by injecting sarcosine and glucose simultaneously one after another within the same buffer to see whether there is any cross talk. From the figure 7.15, initially experiment was started with the addition of sarcosine and after some additions, glucose was injected into the same cell. Response was measured initially with sarcosine by injecting different concentrations of sarcosine into the cell. From the IDE 2 where SOX was immobilized, there was an increase in the oxidation current response and finally a maximum current response of around $1\mu\text{A cm}^{-2}$ at a concentration of around 10mM sarcosine was detected and reached a steady state with no increase in the current for further addition of sarcosine and the response from the IDE 1 was completely absent. Later when glucose was injected, there was an increase in the oxidation current response maximum of around $1.5\mu\text{A cm}^{-2}$ at 40mM glucose from the IDE 1 and response to glucose was completely absent from the IDE 2. These results demonstrate that there is substrate specific response from both the sets of electrodes with complete absence of unwanted response. This also proves that polyelectrolyte multilayering step has proven to be successful blocking step in preventing the unwanted response from both the electrodes.

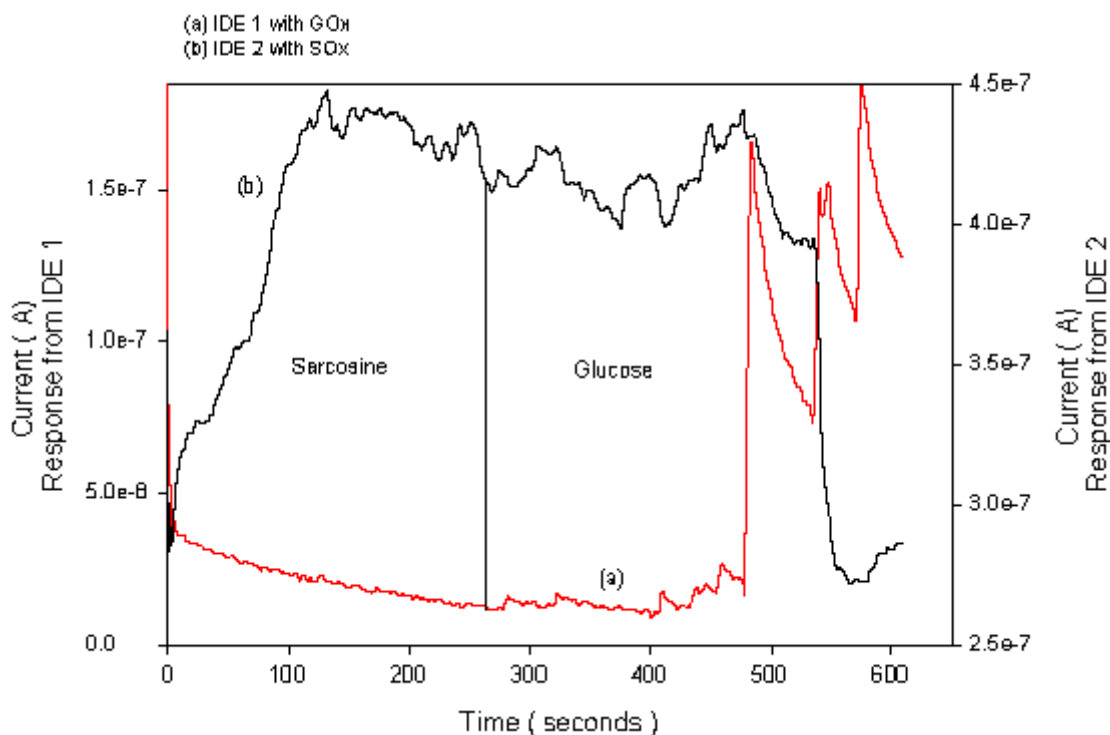


Figure 7.15. The signal independence of the sarcosine and glucose sensors within the IDE microarray at + 500 mV (vs. Ag / Ag Cl) in 0.1M phosphate buffer pH 7.0 during successive injection of sarcosine followed by glucose.

There might be either of the following two reasons behind this. Since the last polyelectrolyte used in these experiments forming the polyelectrolyte multilayers is quarternised PVP, which possess the dense positive charges and if there is any non-specific adsorption of the SOX with redox polymer which also possess excess positive charge there might be electrostatic repulsion between each other which prevents the unwanted response.

The other reason might be that polyelectrolyte multilayer is forming an insulating layer and even though there is non-specific adsorption of the SOX along with the redox polymer, the response might be completely prevented due to insulating properties of polyelectrolyte multilayers [43,64]. Even at higher substrate concentrations the response was completely absent due to the substrate of the other enzyme, indicating that the non-specific adsorption, which results in cross talk did not occur and can be used for the fabrication of multi-analyte sensors.

7.5. Conclusions

An interference and cross-talk free dual biosensor was developed for simultaneous monitoring of glucose and sarcosine. Among the different immobilization strategies tried for the optimisation of the best method, direct adsorption of enzymes along with the redox polymer gave good results with very stable currents when compared to the other strategies. Among the different blocking agents tried to reduce the unwanted response from the second enzyme during the enzyme patterning on the IDE array, polyelectrolyte multilayering as a blocking step was successful and is able to remove the unwanted response completely. When the optimised system was applied on photolithographically patterned microelectrodes with 20 μ m resolution, there was a successfully detection of glucose and sarcosine simultaneously from their respective electrodes. Both the sensors gave very good currents with out any cross talk. So finally an optimised system integrated with polyelectrolyte multilayer spacing for avoiding cross-talk interference was developed, which makes a way for multianalyte biosensing.

7.6. Abbreviations

GOX - Glucose Oxidase

SOX - Sarcosine Oxidase

PVP - Polyvinyl Pyridine

PSS - Polystyrene Sulfonate

DTSP - Di N-succinimidyl ester dithio-dithiopropionic acid

MPSA - 3-Mercapto-1-propane-sulfonic acid

SATA - N-Succinimidyl-S-acetylthioacetate

EDC - N-(3-Dimethylaminopropyl)-N'-ethylcarbodiimide

IDE - Interdigitated electrode

IDE 1 - First set of electrodes

IDE 2 - Second set of electrodes

TMAH - Tetramethyl ammonium hydroxide

PBS - Phosphate Buffered Saline

7.7. References

1. Albers, J., Grunwald,T., Nebling,E., Piechotta,G., Hintsche,R, *Anal.Bioanal.Chem*, 2003. 377: p. 521-527.
2. Bian, G.H., Lin,Li., David,R.W, *Biosens.Bioelectron*, 1997. 12: p. 521-529.
3. Maestre, E., Katakis,I., Narvaez,A., Dominguez,E, *Biosen.Bioelectron*, 2005, 1,774-781.
4. Ding, Y., Zhou,L.P., Halsall,H.B.,Heineman,W.R, *J. Pharm Biomed Anal*, 1999,19, 153-161.
5. Jia, N.Q., Zhang,Z.R., Zhu,J.Z, *Chin.J.Chem*, 2004. 22: p. 908-912.
6. Wittstock, G., *Anal.Bioanal.Chem*, 2002. 372: p. 16-17.
7. Brecht, A., *Anal.Bioanal.Chem*, 2005. 381: p. 1025-1026.
8. Stefan, R.I., van Staden,J.F., Aboul-Enein,H.Y, *Crit.Rev.Anal.Chem*, 1999. 29: p. 133-153.
9. Wilson, M.S., Nie,W.Y, *Anal.Chem*, 2006. 78: p. 2507-2513.
10. Zen, J.M., Lai,Y.,Yang,H.H., Kumar,A.S, *Sens.Act.B*, 2002. 84: p. 237-244.
11. Cho, E.J., Tao,Z.,Tehan,E.C., Bright,F.V, *Anal.Chem*, 2002. 74: p. 6177 - 6184.
12. Taitt, C.R., Anderson,C.P., Lingerfelt,B.M., Feldstein,M.J, *Anal.Chem*, 2002. 74: p. 6114 - 6120.
13. Zhi, Z.L., Murakami,Y.,Morita,Y., Hasan,Q., Tamiya,E, *Anal. Biochem*, 2003. 318(2): p. 236-243.
14. Flounders, A.W., Brandon,D.L., Bates,A.H, *Biosens. Bioelectron*, 1997. 12: p. 447-456.
15. Lee, K.N., Shin,D.S., Lee,Y.S., Kim,Y.K, *J. Micromech. Microeng*, 2003. 13: p. 18-25.
16. Kostecki, R., Song,X.Y., Kinoshita,K, *J.Electrochem.Soc*, 2000. 147: p. 1878-1881.
17. Iwasaki, Y., Morita,M, *Current Separations*, 1995. 14: p. 2-8.
18. Dobson, P.J., Jiang,L., Leigh,P.A., Hill,H.A.O., Kaneko,S, *Adv. Mat. Optic. Electron*, 1992. 1: p. 133 - 138.
19. Shin, D.S., Lee,K.N., Jang,K.H., Kim,J.K., Chung,W.J., Kim,Y.K., Lee,Y.S, *Biosens Bioelectron*, 2003. 19: p. 485-494.
20. Sorribas, H., Padeste,C., Tiefenauer,L, *Biomaterials*, 2002. 23: p. 893-900.
21. Padeste, C., Steiger,B., Grubelnik,A., Tiefenauer,L, *Biosens.Bioelectron*, 2004. 20: p. 545-552.
22. Cohen, A.E., Kunz,R.R, *Sens. Act. B*, 2000. 62: p. 23-29.

23. Postlethwaite, T.A., Hutchison, J.E., Murray, R., Fosset, B., Amatore, C., *Anal. Chem.*, 1996. 68: p. 2951-2958.
24. Radke, S.A., Alocilja, E.C., *Biosens. Bioelectron.*, 2005. 20: p. 1662-1667.
25. Hintsche, R., Paeschke, M., Wollenberger, U., Schnakenberg, U., Wagner, B., Lise, T., *Biosens. Bioelectron.*, 1994. 9: p. 697-705.
26. Zhu, J., Tian, C., Wu, W., Wu, J., Zhang, H., Lu, D., Zhang, G., *Biosens. Bioelectron.*, 1994. 9: p. 295-300.
27. Min, J., Baeumner, A.J., *Electroanalysis*, 2004. 16: p. 724-729.
28. Jin, P., Yamaguchi, A., Oi, F.A., Matsuo, S., Tan, J., Misawa, H., *Analytical Sciences*, 2001. 17: p. 841-846.
29. Zhang, S., Zhao, H., John, R., *Anal. Chim. Acta*, 2000. 419: p. 175-187.
30. Wang, J., Chen, Q., *Anal. Chem.*, 1994. 66: p. 1007-1011.
31. Sandison, M.E., Anicet, N., Glidle, A., Cooper, J.M., *Anal. Chem.*, 2002. 74: p. 5717 - 5725.
32. Pearce, T.M., Wilson, J.A., Oakes, S.G., Chiu, S.Y., Williams, J.C., *Lab. Chip*, 2005. 5: p. 97-101.
33. Heller, A., *J. Phy. Chem.*, 1992. 96: p. 3579-3587.
34. Frebel, H., Chemnitz, G.C., Cammann, K., Kakerow, R., Rospert, M., Mokwa, W., *Sens. Act. B*, 1997. 43: p. 87-93.
35. Strike, D.J., Rooij, N.F., Koudelka, M., *Biosens. Bioelectron.*, 1995. 10: p. 61-66
36. Smistrup, K., Kjeldsen, B.G., Reimers, J.L., Dufva, M., Petersen, J., Hansen, M.F., *Lab. Chip*, 2005. 5: p. 1315-1319.
37. Yu, P.G., Wilson, G.S., *Faraday. Disc.*, 2000. 116: p. 305-317.
38. Yu, X., Lv, R., Ma, Z., Liu, Z., Hao, Y., Li, Q., Xu, D., *Analyst*, 2006. 131: p. 745-750.
39. Kojima, K., Hiratsuka, A., Suzuki, H., Yano, K., Ikebukuro, K., Karube, I., *Anal. Chem.*, 2003. 75: p. 1116 -1122.
40. Quinto, M., Koudelka-Hep, M., Palmisano, F., *Analyst*, 2001. 126: p. 1068-1072.
41. Gregg, B.A., Heller, A., *J. Phys. Chem.*, 1991. 95: p. 5970-5975.
42. Cobellis, G.L.M., Scarpa, D., Izzo, G., Fienga, G., Meccariello, R., Pierantoni, R., Fasano, S., *Biol. Reprod.*, 2005. 72: p. 1101-1108.
43. Narváez, A., Suárez, G., Popescu, I.C., Katakis, I., Domínguez, E., *Biosens. Bioelectron.*, 2000. 15: p. 43-52.
44. Weiser, H., S.W., Belitz, H.D., *J. Cereal. Sci.*, 1994. 19: p. 149-155.
45. Chow, E., H.D., Gooding, J.J., *Anal. Chim. Acta*, 2005. 543: p. 167-176.
46. Pei, R.J., C.Z., Wang, E.K., Yang, X.R., *Biosens. Bioelectron.*, 2001. 16: p. 355-361.
47. Susmel, S., G.G., O'Sullivan, C.K., *Biosens. Bioelectron.*, 2003. 18: p. 881-889.

48. Ball.JC, P.L., Bachas.LG, *Anal.Chem*, 2003. 75: p. 6932 -6937.
49. Rosca, V., Popescu,I.C, *Electrochem. Comm*, 2002. 4: p. 904-911.
50. Zhao, H.T., Ju,H.X, *Anal. Biochem*, 2006. 350: p. 138-144.
51. Calvo, E.J., Etchenique,R., Pietrasanta,L., Wolosiuk,A., Danilowicz,C, *Anal.Chem*, 2001. 73: p. 1161-1168.
52. Darder, M., Takada,K., Pariente,F., Lorenzo,E., Abruna,H.D, *Anal. Chem*, 1999. 71: p. 5530-5537.
53. Parra, A., Casero,E., Vazquez,L., Jin,J., Pariente,F., Lorenzo,E.A, *Langmuir*, 2006. 75: p. 5443 - 5450.
54. Mena, M.L., Carralero,V., Gonzalez-Cortes,A., Yanez-Sedeno,P., Pingarron,J.M, *Electroanalysis*, 2005. 17: p. 2147 - 2155.
55. Bakker, A.J., *Clin.Chem*, 1988. 34: p. 82-86.
56. Bakker, A.J., Jellema,B, *Ann.Clin.Biochem*, 1999. 36: p. 163-167.
57. Dunlop.LC, S.M., Bendall.LJ, Favalaro.EJ, Castaldi.PA, Gorman.JJ, Gamble.JR, Vadas.MA, Berndt.MC, *J.Exp.Med*, 1992. 175: p. 1147-1150.
58. Tsutsui.S, S.J., Noorbakhsh.F, Henry.S, Yong.VW, Winston.BW, Warren.K, Power.C, *J Neurosci*, 2004. 24: p. 1521-1529.
59. Chung.JW, B.R., Pyun.JC, *J.Immunol.Methods*, 2006. 311: p. 178-188.
60. Lasne.F, *J.Immunol.Methods*, 2001. 253: p. 125-131.
61. Narváez.A, S.G., Popescu.IC, Katakis.I, Domínguez.E, *Biosens. Bioelectron*, 2000. 15: p. 43-52.
62. Douvas.A, Argitis.P., Diakoumakos.CD, Misiakos.K, Dimotikali.D, Kakabakos.SE, *J.Vac. Sci. Tech. B*, 2001. 19: p. 2820-2824.
63. Douvas.A, Argitis.P., Misiakos.K, Dimotikali.D, Petrou.PS, Kakabakos.SE, *Biosens. Bioelectron*, 2002. 17: p. 269-278.
64. Liu.A, A.J.-I., *Langmuir*, 2003. 19: p. 4043 - 4046.

Chapter 8. Conclusions and Future work

In this thesis, different types of patterning methods for the selective immobilization of enzymes for the construction of biosensor arrays were discussed. The first three methods are electrochemically controlled patterning methods and the final method is based on the photolithography. The most important findings from each chapter are described.

Regarding patterning through selective electrodeposition of biofunctionalized biomolecules

Au nanoparticles of different diameters were synthesized and characterized successfully by different methods.

Enzymes were conjugated to the gold colloids by using chemical conjugation based on gold-thiol dative bonding, electrostatic interactions and also direct adsorption. Stability of the biofunctionalized Au nanoparticles was verified by zeta potential, UV-Vis spectroscopy and optical methods.

Fundamental studies of the electrodeposition of Au nanoparticles modified with BSA as a model protein were done to see the behaviour of different parameters on the electrodeposition. Fundamental studies with the redox polymer modified Au nanoparticles were done to see the behaviour of electrodeposition changing different parameters.

Electrocatalytic behaviour studies of the redox enzymes on the Au nanoparticle modified electrodes showed the presence of direct electron transfer of the enzyme to the electrode via Au nanoparticles without any mediator.

Selective patterning of enzymes was done on an IDE array by selective electrodeposition of enzyme modified Au nanoparticles on the gold electrode after selective electrochemical desorption of thioctic ester SAMs. Able to produce substrate specific response with complete absence of non-specific response.

Controlled electrodeposition of Au nanoparticles modified layer-by-layer with redox polymer, gold nanoparticles followed by redox polymer has been proved on the gold electrode has been demonstrated successfully. Technical advantage of using microelectrodes for biosensor design over the macroelectrode has been demonstrated.

Regarding patterning through electrochemical deprotection of electroactive self assembled monolayers

Site directed immobilisation of proteins by electrochemical activation of acetal-containing SAMs has been proved. Thiocctic esters presenting benzo (1,3) dioxinol were synthesized and characterized successfully.

It was found that electrochemical activation for the deprotection of acetal to aldehyde is fast and can be achieved at relatively low electrochemical potentials.

The active SAMs provide a reagentless method for patterning proteins with a significant non-specific adsorption

Regarding patterning through electrochemical deposition of biofunctionalized 4,4-bipyridyl

Carboxylic acid functionalised 4,4 bipyridyl has been synthesized and characterized successfully by electrochemistry. 4,4 bipyridyl derivative showed an excellent redox chemistry.

HRP functionalized 4,4 bipyridyl derivative was synthesized and characterized successfully with electrochemistry, UV-Vis spectroscopy.

Single step HRP functionalised 4,4 bipyridyl electrodeposition on the gold electrode gave a good selective response when compared to the double step strategy where carboxylic acid functionalised 4,4 bipyridyl was electrodeposited first followed by HRP immobilization.

Regarding selective microscale protein patterning

Direct adsorption of redox enzymes along with redox polymer gave a better and stable response to both glucose and sarcosine from the GOX and SOX modified Au electrodes when compared to the different methods of immobilization of enzymes.

Polyelectrolyte multilayering as a spacer was successful on macroelectrodes to prevent the cross talk due to non-specific adsorption when compared to other spacers tried.

Both GOX and SOX were immobilized successfully on an IDE array fabricated through photolithography with complete absence of crosstalk.

Summarizing all, four different selective patterning methods were demonstrated for the immobilization of enzymes. All the four methods were able to pattern the enzymes selectively. Although there needs a further investigations to be done in order to make sure this patterning methods can be used for creation of multianalyte biosensing devices, by improving generic capability trying with DNA, antibodies and other biomolecules apart from enzymes but the work presented here can be taken as an advantage for improving.

Future Work- Extensions

Selective electrodeposition should be performed with antibodies, aptamers, peptides and other biomolecules to prove the generic capability of this technique.

Label free techniques like EQCM, ESPR should be used to improve the versatility of the electrodeposition technique.

Selective electrodeposition should be performed on a multianalyte array to prove the technical advantage of this methodology. In order to make this technique marketable, analyte detection should be performed on the multianalyte array.

Sensitivity of the analyte detection should be improved by optimising the electrodeposition conditions, using different nanoparticle sizes, functionalities.

Though in this thesis multifunctional nanoparticles have been created by using layer-by-layer approach through electrostatic interactions, this approach might not be suitable for the other biomolecules like antibodies, oligonucleotides due to their random orientation while adsorbing electrostatically. Efforts should be made in order to prepare particles which can be used for functionalising any biomolecule.

In the case of selective immobilisation using electroactive substrates, the still present non-specific adsorption should be avoided. This might be possible by using mixed monolayers of TEG functionalised thiols along with electroactive thiols.

Synthesis procedure of the electroactive substrate should be optimised for obtaining better quantity of the final product.

Efforts should be made in order to improve the versatility of the electrochemical deprotection technique for the selective immobilisation different biomolecules like DNA, antibodies, peptides, aptamers etc.

Signal amplification of the biomolecule detection in the case of selective immobilization of the viologen can be improved by functionalizing gold nanoparticles with 4,4-bipyridinium and biomolecule. Later these multifunctional viologen derivatives can be selectively deposited on the electrode surface as explained in this thesis.

Label free techniques like EQCM, ESPR should be optimized to improve the versatility of the viologen based selective immobilization technique. Though in this thesis, some efforts have been performed with the piezoelectric detection, the experimental set up should be optimised.

Viologen based selective immobilization should be tested with other biomolecules to prove the technical advantage of creating multianalyte biosensor arrays.

Though selective patterning of the biomolecules on an interdigitated array through photolithography have been demonstrated by using polyelectrolyte multilayers as a blocking step, this might not be possible while patterning proteins on multiple array. Efforts should be made in order to have a technique where it can improve the efficiency as well as the reliability without disturbing the native functionality of the immobilised biomolecule.

Curriculum Vitae

Name : Dondapati Srujan Kumar
Nationality : Indian
Date of birth : 04th May, 1976
Present Address : Dondapati Srujan Kumar,
Baron de 1V Torres,
12-B, 1 C, Tarragona,
43002, Spain

EDUCATIONAL QUALIFICATIONS

- A) M.Sc in Medical Microbiology (1997-2000)
Kasturba Medical College, Manipal Academy Of Higher Education,
- B) DEA (2002-2004) **Chemical & Process Engineering**, Universitat Rovira I
Virgili, Tarragona, SPAIN. (Specialisation in Bioelectrochemistry)

PROJECTS DONE

- 1) Patterning methods for biosensor arrays (DEA project)
- 2) Antibacterial activity of *Holarrhena Antidysenterica* [kurchi] against the enteric pathogens (MSc project)

PUBLICATIONS

- 1) Electronic 'off-on' Molecular Switch for Rapid Detection of Thrombin, Josep Lluís Acero Sanchez, Eva Baldrich, Abd El-Gawad Radi, Srujan Dondapati, Pablo Lozano Sanchez, Ioanis Katakis, Ciara K.O'Sullivan , **Electroanalysis**, Vol.18, 1879-1884, 2006.
- 2) Site-Directed Immobilization of Proteins Through Electrochemical Deprotection

- on Electroactive Self-Assembled Monolayers, Srujan Kumar Dondapati, Josep Maria Montornes, Pablo Lozano Sanchez, Abd Radi, Josep Lluís Acero Sanchez, Ciara O'Sullivan, Ioanis Katakis, **Electroanalysis**, Vol 18, 1957-1962, 2006.
- 3) Controlled electrodeposition of multifunctional nanommodules for electrochemical biosensor, Dondapati Srujan Kumar, Sanchez Lozano Pablo, Katakis Ioannis (under submission)
 - 4) Electrochemical detection of biomolecules patterned on microarray by biocompatible photolithography. Mònica Mir, **Srujan Kumar Dondapati**, Maria Viviana Duate, Margarita Chatzichristid, Panagiotis Argitis, Ioanis Katakis (under submission)
 - 5) Two New Bromotyrosine-Derived Metabolites from the Sponge *Psammaphysilla Purpurea* T.V.Goud, Vanimireddy Lakshimi Narasimha Reddy, Adelli Vijender Reddy, Tadikamalla Prabhakar Rao, **Dondapati Srujan Kumar**, Upadhyayula Suryanarayana Murty, and Yenamandra Venkateswarlu, **Chemical & Pharmaceutical Bulletin**, Vol.51, 2003, 990.
 - 6) Two New Macrocyclic Diaryl Ether Heptanoids from *Boswellia ovalifoliolata* Vanimireddy Lakshimi Narasimha Reddy, Kodela Ravinder, Masuna Srinivasulu, T.V.Goud, S.M.Reddy, **Dondapati Srujan Kumar**, Tadikamalla Prabhakar Rao, Upadhyayula Suryanarayana Murty, and Yenamandra Venkateswarlu, **Chemical & Pharmaceutical Bulletin**, Vol.51,2003,1081.
 - 7) Antibacterial activity of *Holarrhena Antidysenterica* [kurchi] against the enteric Pathogens: M. Ballal, **D. Srujan**, K.K. Bhat, A. Shirwaikar, P.G. Shivananda, **Indian Journal Of Pharmacology**, Vol 32, 2001, 392-393.

CONFERENCE COMMUNICATIONS

- A) Has Presented a poster on "Antibacterial activity of Holarrehena Antidysenterica a medicinal plant" in the XXII national congress of IAMM held at PGIMER, Chandigarh.
- B) "Site Directed Immobilisation of Biorecognition Nanomodules for Multianalyte Biosensing Devices". (Oral Presentation) **S. Dondapati**, I. Katakis, M. Campàs at Second International Workshop on Multianalyte Biosensing Devices, Tarragona, Spain 2004.
- C) "Functionalised Au nanoparticles for electrochemical biosensors" **S.dondapati**, I. Katakis(Poster presentation) Second International Workshop on Multianalyte Biosensing Devices, Tarragona, Spain 2004.
- D) "Fundamental Investigations on Au colloids: Methods for the characterisation of electrodeposition and surface coverage of biomolecules" **S.Dondapati**, I.Katakis(Poster presentation) V111 Transfrontier Meeting about Sensors and Biosensors, CERET, France August 2003
- E) "Electrodeposition of Au nanoparticles as a method to construct a third generation- enzyme biosensor" **S. Dondapati**, I. Katakis(Oral Presentation) 1X Transfrontier Meeting about Sensors and Biosensors, September 2004, Tarragona,SPAIN
- F) "Amperometric Evaluation of Protein and DNA patterning with Biocompatible Photoresist Polymer" - **S.Dondapati**, M.Mir, I. Katakis, M. Chatzichristidi, P. Argitis(Oral presentation) 1X Transfrontier Meeting about Sensors and Biosensors, September 2004, Tarragona,SPAIN
- G) "Nanobiotechnology in the Bioelectronic Interface: Towards Molecular Biofuel Cells" P. Pescador, **S.K. Dondapati**, J.M. Montornés, F.J. Hernández, J.M. Orellana, I.Katakis(Oral Presentation) at thecongress of the national society for biotechnology

- H) “Electroactive platform for the selective immobilisation of biomolecules for electrochemical biosensors” Josep.M. Montornes, **S. Dondapati** and I. Katakis (oral presentation) at XVII International Symposium on Bioelectrochemistry and Bioenergetics June 2005, Coimbra, Portugal.
- I) “Selective immobilization of bionanomodules by electrochemical desorption of thioctic acid monolayers” **S. Dondapati** and I. Katakis (poster presentation) at XVII International Symposium on Bioelectrochemistry and Bioenergetics June 2005, Coimbra, Portugal.

RESEARCH INTERESTS

Biosensors and Bioelectronics, Biological Fuel cells, Molecular biology, Proteomics
